

University of Alberta

**Carbon-Hydrogen and Carbon-Fluorine Bond Activation
Promoted by Adjacent Metal Centres**

by

Michael Eric Slaney

A thesis submitted to the Faculty of Graduate Studies and Research
in partial fulfillment of the requirements for the degree of

Doctor of Philosophy

Department of Chemistry

©Michael Eric Slaney

Spring 2012

Edmonton, Alberta

Permission is hereby granted to the University of Alberta Libraries to reproduce single copies of this thesis and to lend or sell such copies for private, scholarly or scientific research purposes only. Where the thesis is converted to, or otherwise made available in digital form, the University of Alberta will advise potential users of the thesis of these terms.

The author reserves all other publication and other rights in association with the copyright in the thesis and, except as herein before provided, neither the thesis nor any substantial portion thereof may be printed or otherwise reproduced in any material form whatsoever without the author's prior written permission.

Abstract

The facile cleavage of relatively inert chemical bonds followed by their functionalization into value-added products is an important goal in chemistry. Although monometallic complexes are effective at both the cleavage of inert bonds and the subsequent functionalization of the activated substrates, it is intriguing to consider the influence a second metal can have in promoting reactivity not commonly observed in monometallic systems.

This dissertation explores the roles that metal-metal cooperativity and ancillary diphosphine ligands play in the selective C–H bond activation of α -olefins and C–F bond activation of fluoroolefins. Two unique bimetallic systems, bridged by *bis*(diphosphine) ligands, are the focal point for this study, with the first system containing the *bis*(diphenylphosphino)methane (dppm) ligand (Chapters 2 and 3), while the second uses the smaller, more basic *bis*(diethylphosphino)methane (depdm) ligand (Chapters 4 and 5). We compare both ligand systems, emphasizing the steric and electronic factors, and how they influence the C–H bond activation of α -olefins and the C–F bond activation of fluoroolefins.

In Chapter 2, methods for the selective C–F activation of trifluoroethylene when bridging two metal centres are reported under a variety of conditions followed by functionalization of the activated fluorocarbyl fragments through fluorine replacement by either hydrogen or a methyl group. Chapter 3 explores the different methods for fluoride-ion abstraction from bridging 1,1-difluoroethylene and tetrafluoroethylene units and the subsequent

functionalization of the fluorocarbyl units produced. The different reactivities of the three fluoroolefins are described.

Chapter 4 outlines the syntheses of depm-bridged complexes of Ir₂, Rh₂ and IrRh and initial reactivity studies involving these complexes, highlighted by the facile activation of both geminal C–H bonds of α -olefins by one compound. Finally, Chapter 5 describes the reactivity of fluoroolefins (vinyl fluoride, 1,1-difluoro-, trifluoro- and tetrafluoroethylene) with a depm-bridged Ir₂ complex, with emphasis on the role of water in the activation processes, the difference in reactivity between the fluoroolefins studied, and the differences of complexes having either dppm or depm as an ancillary ligand.

Acknowledgements

I find it ironic that when I started as a graduate student in 2006, all I could think about was the amount of work that must be done to complete a Ph.D. while now, looking back on this project, all I can think about is the amount of work that others have contributed to make it possible. I am truly amazed and thankful for all the help, guidance and understanding that so many people have given me.

At the cornerstone of all projects is the supervisor who can guide you through the rough patches while also being just as excited as you when the results come ‘pouring in’. Marty, you have certainly been this and much more for me. I am grateful for the numerous hours you have spent reading my manuscripts (I believe Gail should also receive many thanks here), for all the helpful discussions and most importantly, for teaching me. Although there were inevitable patches where it seemed like there weren’t enough red pens in the world, I hope you can look back at those moments when retirement seems ‘slow’ and remember exactly why you were so excited to retire in the first place.

I would also like to thank all my *friends* with whom I have shared the lab over the years, including Jim, Wiggy, Stevie-T, Matthias, Jason, R-man, K-dawg, the Hounje, Zamz, the Tizz, and Mo. Jason: Thank you for the numerous chemistry discussions and for teaching me ‘the ways of the lab’. You truly are meant to be a teacher!! R-man: Thanks for the many helpful chemistry discussions and for all the hockey talks, even though they may have revolved around the Canucks a bit more than my fancy. K-dawg: Thanks for working all those late nights in the lab, and for keeping things interesting with your unique ‘Alberta-isms’; there was never a dull moment. The Hounje: I am still amazed at how you seem to know something about every topic in chemistry. Thank you for all our impromptu ‘chalktalks’, they always seemed to help. Zamz: I couldn’t have asked for a better person to travel across the world with for ICOMC. Considering we outlasted the Germans and the British, I think we did it right! The Tizz: I am amazed that even after spending 40+ hours a week with me in the same lab, you have managed to keep your cool and not kill me. Thank you for all

the discussions, suggestions, patience, and most importantly, all the coffee breaks!!! Mo: Thanks for all the knowledge you shared about literature and for all those comical “Ohhhhhhh my goodness” moments.

This project would have never come close to completion without the help of the extensive support staff in the Chemistry Department, including the NMR staff, Analytical Services staff and Mass Spectrometry staff. I would also like to extend my appreciation to Bob McDonald and Mike Ferguson at Camp X-Ray for all their help with solving crystal structures. Although many ‘sea-urchins’ were brought over, you still gave them an honest effort (even though we all knew they were flat out ugly).

Another important aspect of graduate school is learning how to become an effective teaching assistant, and for that I owe thanks to Dr. Norman Gee and Dr. Jason Cooke. I especially want to thank Dr. Cooke for going above and beyond to accommodate my difficult schedule, especially during my bout with pneumonia and for listening to me vent some frustrations about students.

Finally, I want to thank all my friends and family who have been there for me during the last few years. Joel, Tiara and Ridley – thank you all for the amazing weekends and holidays together, especially Disney! Robert, Ivy and Jane – thanks for understanding our schedule and especially for treating me like a son/brother. Uncle Bruce and Aunt Peggy – thank you for your constant support. Patrick and Alice – thank you both for always listening, offering advice, and playing games with me. Nan – you inspire me to be the best person I can be, thank you! Mom and Dad – thank you for all the guidance and support, you both made this process much easier for me. Last but not least, I want to thank my beautiful wife, Anne. You have seen me during the lows and have always found ways to make things better!

Thank you,

Mike

Table of Contents

| | |
|--|-----------|
| Chapter 1 – Introduction to Carbon-Hydrogen and Carbon-Fluorine Bond Activation | 1 |
| Section 1.1 – Carbon-Atom Bond Activation | 1 |
| Section 1.2 – Carbon-Hydrogen Bond Activation..... | 3 |
| 1.2.1 – Carbon-hydrogen bond properties | 3 |
| 1.2.2 – Methods of C–H activation..... | 4 |
| 1.2.3 – Single and Geminal C–H Activation of Olefins | 7 |
| Section 1.3 – Carbon–Fluorine Bond Activation | 16 |
| 1.3.1 – Carbon-Fluorine Bond Properties..... | 16 |
| 1.3.2 – Intermolecular Activation..... | 19 |
| 1.3.3 – Intramolecular Activation..... | 22 |
| 1.3.4 – C–F Activation of Fluoroolefins..... | 24 |
| Section 1.4 – References | 32 |
| | |
| Chapter 2 – The Bridged Binding Mode as a New, Versatile Template for the Selective Activation of Carbon–Fluorine Bonds in Fluoroolefins: Activation of Trifluoroethylene | 40 |
| Section 2.1 – Introduction | 40 |
| Section 2.2 – Results | 43 |
| 2.2.1 – Trifluoroethylene Coordination | 43 |
| 2.2.2 – C–F Bond Activation..... | 47 |
| 2.2.2.1 – Activation by Strong Lewis Acids..... | 47 |
| 2.2.2.2 – Removal of a Second Fluoride Ion | 51 |
| 2.2.2.3 – Activation by Water..... | 52 |
| 2.2.2.4 – [1,2]-Fluoride Shift | 55 |
| 2.2.3 – Fluorocarbyl Group Functionalization | 57 |
| 2.2.3.1 – Hydrogenolysis | 57 |
| 2.2.3.2 – Reductive Elimination of Difluoropropenes... | 60 |
| 2.2.3.3 – Protonation..... | 63 |
| Section 2.3 – Discussion | 66 |
| 2.3.1 – Olefin Binding | 66 |
| 2.3.2 – C–F Activation..... | 66 |
| 2.3.3 – Fluoroolefin Functionalization | 69 |
| Section 2.4 – Conclusions | 71 |
| Section 2.5 – Experimental..... | 71 |

| | |
|--|-----------|
| 2.5.1 – General Comments | 71 |
| 2.5.2 – Preparation of Compounds | 72 |
| 2.5.3 – X-ray Structure Determinations..... | 79 |
| 2.5.3.1 – General..... | 79 |
| 2.5.3.2 – Special Refinement Conditions..... | 79 |
| Section 2.6 – Acknowledgements | 80 |
| Section 2.7 – References | 82 |

Chapter 3 – Facile Carbon-Fluorine Bond Activation and Subsequent Functionalization of 1,1-Difluoroethylene and Tetrafluoroethylene Promoted by Adjacent Metal Centers 88

| | |
|---|------------|
| Section 3.1 – Introduction | 88 |
| Section 3.2 – Results | 90 |
| 3.2.1 – C–F Bond Activation by Lewis Acids..... | 90 |
| 3.2.1.1 – Tetrafluoroethylene..... | 90 |
| 3.2.1.2 – 1,1-Difluoroethylene..... | 96 |
| 3.2.2 – C–F Activation Promoted by Co Addition | 98 |
| 3.2.2.1 – Tetrafluoroethylene..... | 98 |
| 3.2.2.2 – 1,1-Difluoroethylene..... | 100 |
| 3.2.3 – C–F Activation Promoted by H ₂ O Addition..... | 102 |
| 3.2.4 – Fluorovinyl Group Functionalization | 104 |
| 3.2.4.1 – Reactions with H ₂ | 105 |
| 3.2.4.2 – Reactions with CO | 107 |
| Section 3.3 – Conclusions | 108 |
| Section 3.4 – Experimental..... | 110 |
| 3.4.1 – General Comments | 110 |
| 3.4.2 – Preparation of Compounds | 111 |
| 3.4.3 – X-ray Structure Determinations..... | 119 |
| 3.4.3.1 – General..... | 119 |
| 3.4.3.2 – Special Refinement Conditions..... | 120 |
| Section 3.5 – Acknowledgements..... | 122 |
| Section 3.6 – References | 123 |

| | | |
|--|---|------------|
| Chapter 4 – | <i>Bis</i>(diethylphosphino)methane as a Bridging Ligand in Complexes of Ir₂, Rh₂ and IrRh: Geminal C–H Activation of α-Olefins | 129 |
| Section 4.1 – Introduction | | 129 |
| Section 4.2 – Results | | 130 |
| 4.2.1 – Synthesis of Diiridium Complexes | | 130 |
| 4.2.2 – Synthesis of Dirhodium Complexes | | 138 |
| 4.2.3 – Synthesis of Iridium/Rhodium Complexes | | 143 |
| 4.2.4 – Geminal C–H Activation of Olefins | | 146 |
| Section 4.3 – Discussion | | 150 |
| Section 4.4 – Experimental | | 153 |
| 4.4.1 – General Comments | | 153 |
| 4.4.2 – Preparation of Compounds | | 154 |
| 4.4.3 – X-ray Structure Determination | | 172 |
| 4.4.3.1 – General | | 172 |
| 4.4.3.2 – Special Refinement Conditions | | 173 |
| Section 4.5 – Acknowledgements | | 174 |
| Section 4.5 – References | | 175 |
| | | |
| Chapter 5 – | Tandem C–F and C–H Bond Activation of Fluoroolefins Promoted by a <i>Bis</i>(diethylphosphino)methane-Bridged Diiridium Complex: Role of Water in the Activation Processes | 180 |
| Section 5.1 – Introduction | | 180 |
| Section 5.2 – Results | | 182 |
| 5.2.1 – Activation of Vinyl Fluoride | | 182 |
| 5.2.2 – Activation of 1,1-Difluoroethylene | | 185 |
| 5.2.3 – Activation of Trifluoroethylene | | 189 |
| 5.2.4 – Activation of Tetrafluoroethylene | | 195 |
| Section 5.3 – Discussion | | 197 |
| 5.3.1 – Trifluoroethylene Activation | | 197 |
| 5.3.2 – 1,1-Difluoroethylene Activation | | 201 |
| 5.3.3 – Tetrafluoroethylene Activation | | 202 |
| 5.3.4 – Vinyl Fluoride Activation | | 203 |
| Section 5.4 – Experimental | | 204 |
| 5.4.1 – General Comments | | 204 |
| 5.4.2 – Preparation of Compounds | | 205 |

| | |
|---|------------|
| 5.4.3 – X-ray Structure Determination | 210 |
| 5.4.3.1 – General | 210 |
| 5.4.3.2 – Special Refinement Conditions..... | 210 |
| Section 5.5 – Acknowledgements | 211 |
| Section 5.6 – References | 212 |
| | |
| Chapter 6 – Conclusions..... | 217 |
| Section 6.1 – Project Motivation | 217 |
| Section 6.2 – Synthesis of Depm Precursors | 217 |
| Section 6.3 – Carbon-Hydrogen Bond Activation..... | 219 |
| Section 6.4 – Carbon-Fluorine Bond Activation | 220 |
| Section 6.5 – Final Remarks and Future Directions | 226 |
| Section 6.6 – References | 228 |
| | |
| Appendices | 229 |
| Appendix I – Contributions from Co-Authors..... | 230 |
| Appendix II – Drying Agents for Solvents..... | 231 |
| Appendix III – Crystallographic Experimental Details | 232 |
| Appendix IV – Crystallographic Data | 251 |

List of Charts

Chapter 1

- Chart 1.1** – Concerted C–H bond cleavage of an alkane by a metal complex 6
- Chart 1.2** – Mechanism for geminal activation of olefins in multimetallic systems 12
- Chart 1.3** – Proposed mechanism for geminal activation of 1,3-butadiene by $[\text{Ir}_2(\text{CH}_3)(\text{CO})_2(\text{dppm})_2][\text{OTf}]$ 14
- Chart 1.4** – Bond lengths, bond strengths and partial charges as fluorine substitution increases 18
- Chart 1.5** – π -Back donation from the metal d-orbital into the carbon-fluorine σ^* -orbital 23
- Chart 1.6** – The analogy between a bridging fluoroolefin and two metal fluoroalkyl groups 29

Chapter 2

- Chart 2.1** – How a bridging fluoroolefin is analogous to two substituted fluoroalkyl ligands 42
- Chart 2.2** – Proposed mechanism for fluoride-ion abstraction to produce a *cis*-difluorovinyl unit 67
- Chart 2.3** – Proposed mechanism for the activation of **2** by water 68

Chapter 4

- Chart 4.1** – Proposed mechanism for geminal C–H activation of an olefin by a bimetallic complex 152

Chapter 5

- Chart 5.1** – Proposed mechanism for C–F bond activation by water 203

List of Figures

Chapter 2

| | | |
|---------------------|---|-----------|
| Figure 2.1 – | $^{31}\text{P}\{^1\text{H}\}$ NMR spectrum of compound 3 , displaying the large trans-phosphine couplings of an ABCD spin-system..... | 48 |
| Figure 2.2 – | ^1H NMR spectrum of compound 3 , displaying four unique methylene proton resonances, confirming the loss of ‘front/back’ and ‘top/bottom’ symmetry..... | 49 |
| Figure 2.3 – | ORTEP diagram of compound 3 | 51 |
| Figure 2.4 – | ORTEP diagram of compound 5 | 55 |
| Figure 2.5 – | Observed and simulated ^{19}F spectra of <i>cis</i> -difluoropropene (left two spectra) and 2,3-difluoropropene (right two spectra)..... | 61 |
| Figure 2.6 – | ORTEP diagram of compound 13 | 65 |
| Figure 2.7 – | ^{19}F NMR spectrum of 1,1,1-trifluoroethane (left) and 1,1,1-trifluoro-2-deuteroethane | 65 |

Chapter 3

| | | |
|---------------------|--|------------|
| Figure 3.1 – | ORTEP diagram of compound 14 | 94 |
| Figure 3.2 – | ORTEP diagram of compound 16 | 95 |
| Figure 3.3 – | ORTEP diagram of compound 21 | 100 |
| Figure 3.4 – | ORTEP diagram of compound 22 | 102 |
| Figure 3.5 – | NMR chemical shifts and coupling constants for 2-fluoropropene..... | 104 |
| Figure 3.6 – | ORTEP diagram of compound 16 , showing the disorder of the trifluorovinyl ligand..... | 121 |

Chapter 4

| | | |
|---------------------|--|------------|
| Figure 4.1 – | ORTEP diagram of compound 26 | 132 |
| Figure 4.2 – | ORTEP diagram of compound 29 | 135 |
| Figure 4.3 – | ORTEP diagram of compound 41 | 141 |
| Figure 4.4 – | ORTEP diagram of compound 43 | 143 |
| Figure 4.5 – | ORTEP diagram of compound 47 | 146 |
| Figure 4.6 – | ORTEP diagram of compound 47 , showing the disordered IrRhMe(CO) ₃ fragment | 174 |

Chapter 5

| | | |
|---------------------|--|------------|
| Figure 5.1 – | ORTEP diagram of compound 58 | 184 |
| Figure 5.2 – | The ¹⁹ F { ³¹ P} NMR spectrum of a mixture of compounds 60a and 60b | 187 |
| Figure 5.3 – | ORTEP diagram of compound 63 | 192 |

List of Schemes

Chapter 1

| | | |
|----------------------|---|----|
| Scheme 1.1 – | Oxidative addition of alkanes reported by Janowicz and Bergman (top) and Hoyano and Graham (bottom) | 7 |
| Scheme 1.2 – | Single C–H activation of ethylene reported by Perutz <i>et al.</i> (top) and Crabtree (bottom)..... | 8 |
| Scheme 1.3 – | Thermal C–H activation of ethylene reported by Graham ... | 9 |
| Scheme 1.4 – | Jones proposal for η^2 -arene coordination prior to C–H activation | 9 |
| Scheme 1.5 – | Bergman proposal for σ -interaction with olefinic hydrogen of ethylene | 10 |
| Scheme 1.6 – | Photolytic activation of ethylene | 11 |
| Scheme 1.7 – | Geminal activation of ethylene by $[M_3(CO)_{12}]$ (M =Ru, Os) | 12 |
| Scheme 1.8 – | Geminal activation of ethylene by $[FeCl_2(tms)]$ | 13 |
| Scheme 1.9 – | Geminal activation of ethylene by $[Ru(Cp^*)_2(\mu-H)_4]$ | 13 |
| Scheme 1.10 – | Geminal activation of 1,3-butadiene by $[Ir_2(CH_3)(CO)_2(dppm)_2][OTf]$ | 14 |
| Scheme 1.11 – | C–H and C–F bond activation of 1,2,4,5-tetrafluorobenzene | 21 |
| Scheme 1.12 – | Proposed mechanism for [1,2]-fluoride shift of trifluoroethylene | 25 |
| Scheme 1.13 – | Hydrolysis of tetrafluoroethylene to carbon monoxide..... | 27 |
| Scheme 1.14 – | Proposed mechanism for the hydrodefluorination of 1,1,1-trifluoropropene | 28 |
| Scheme 1.15 – | Mechanism for the selective hydrodefluorination of 1,1,1-trifluoropropene | 29 |

Chapter 2

| | | |
|---------------------|--|-----------|
| Scheme 2.1 – | Coordination of trifluoroethylene to compound 1 | 44 |
| Scheme 2.2 – | C–F bond activation of the bridging trifluoroethylene moiety by Me ₃ SiOTf and/or HOTf | 47 |
| Scheme 2.3 – | C–F bond activation of the bridging trifluoroethylene moiety by water | 53 |
| Scheme 2.4 – | The addition of carbon monoxide to compound 2 , producing a bridging 2,2,2-trifluoroethylidene ligand (7) | 56 |
| Scheme 2.5 – | Functionalization of the <i>cis</i> -difluorovinyl ligand with H ₂ , resulting in the elimination of <i>cis</i> -difluoroethylene | 58 |
| Scheme 2.6 – | Functionalization of the <i>cis</i> -difluorovinyl unit with CO, resulting in the reductive elimination of two difluoropropene isomers..... | 60 |
| Scheme 2.7 – | Functionalization of the bridging 2,2,2-trifluoroethylidene moiety by triflic acid. | 64 |

Chapter 3

| | | |
|---------------------|--|------------|
| Scheme 3.1 – | Coordination of tetrafluoroethylene to [Ir ₂ (CH ₃)(CO) ₂ -(dppm) ₂][OTf] (1) and subsequent C–F bond activations..... | 91 |
| Scheme 3.2 – | Two isomers of [Ir ₂ (CH ₃)(CO) ₂ (C ₂ F ₂ H ₂)(dppm) ₂][OTf] (18) and fluoride abstraction from 18a | 97 |
| Scheme 3.3 – | Sequential reaction of compound 14 with CO and BF ₃ in attempts to induce a 1,2-fluoride shift..... | 99 |
| Scheme 3.4 – | Unprecedented loss of 2 equivalents of HF from 1,1-difluoroethylene | 101 |
| Scheme 3.5 – | C–F activation of compound 18a with water, yielding [Ir ₂ (CO) ₂ (μ–OH)(dppm) ₂][OTf] and 2-fluoropropene. Carbon-13 enrichment of the methyl ligand yields the two isotopomers (A and B) shown | 103 |
| Scheme 3.6 – | H ₂ addition to compound 16 at –20 °C and subsequent hydrogenolysis upon warming | 105 |

| | | |
|---------------------|---|------------|
| Scheme 3.7 – | Addition of carbon monoxide to compound 15 | 107 |
|---------------------|---|------------|

Chapter 4

| | | |
|---------------------|---|------------|
| Scheme 4.1 – | Synthesis of diiridium <i>bis</i> (diethylphosphino)methane complexes..... | 131 |
| Scheme 4.2 – | Addition of carbon monoxide to compounds 27 , 37 and 45 | 133 |
| Scheme 4.3 – | Sequential carbon monoxide uptake by compound 29 | 136 |
| Scheme 4.4 – | Addition of carbon monoxide to compound 34 | 137 |
| Scheme 4.5 – | Synthesis of dirhodium <i>bis</i> (diethylphosphino)methane complexes..... | 138 |
| Scheme 4.6 – | Addition of excess acid to compound 41 | 142 |
| Scheme 4.7 – | Synthesis of mixed-metal rhodium/iridium <i>bis</i> (diethylphosphino)methane complexes | 144 |
| Scheme 4.8 – | Geminal C–H bond activation of α -olefins by compound 34 | 147 |

Chapter 5

| | | |
|---------------------|--|------------|
| Scheme 5.1 – | Reaction of compound 34 with vinyl fluoride | 182 |
| Scheme 5.2 – | Reaction of compound 34 with 1,1-difluoroethylene at -10 °C..... | 186 |
| Scheme 5.3 – | The addition of trifluoroethylene to compound 34 at -30 °C | 189 |
| Scheme 5.4 – | Warming compounds 62a and 62b to form a mixture of 63 and 64 | 191 |
| Scheme 5.5 – | Deuterium labeling of 62a and 62b and subsequent warming to form 63 | 193 |
| Scheme 5.6 – | Reaction of compound 64 with a second equivalent of trifluoroethylene | 195 |

| | | |
|---------------------|--|------------|
| Scheme 5.7 – | Reaction of compound 34 with tetrafluoroethylene | 196 |
| Scheme 5.8 – | Proposed mechanism for C–F bond activation of trifluoroethylene in 62a by water | 199 |
| Scheme 5.9 – | Proposed mechanism for C–F bond activation of a second equivalent of trifluoroethylene to form 64 | 201 |

Chapter 6

| | | |
|---------------------|---|------------|
| Scheme 6.1 – | A comparison of the three different dppm fluorovinyl binding modes upon C–F activation of the respective fluoroolefin-bridged adducts | 221 |
| Scheme 6.2 – | A comparison of the reactivities of the three different fluoroolefin-bridged dppm adducts with water | 222 |
| Scheme 6.3 – | A comparison of the reactivities of the three different fluoroolefin-bridged dppm adducts with carbon monoxide .. | 223 |

List of Tables

Chapter 1

| | | |
|--------------------|---|-----------|
| Table 1.1 – | Bond dissociation energies for common H–R molecules | 4 |
| Table 1.2 – | Methods for C–H activation..... | 5 |
| Table 1.3 – | F–R bond dissociation energies..... | 17 |
| Table 1.4 – | Intermolecular C–F activation processes | 20 |
| Table 1.5 – | Intramolecular C–F activation processes | 22 |

Chapter 2

| | | |
|--------------------|---|-----------|
| Table 2.1 – | Derived coupling constants for <i>cis</i> -difluoropropene and 2,3-difluoropropene..... | 63 |
|--------------------|---|-----------|

Appendices

| | | |
|---------------------|--|------------|
| Table A.1 – | Crystallographic experimental details for compound 3 | 232 |
| Table A.2 – | Crystallographic experimental details for compound 5 | 233 |
| Table A.3 – | Crystallographic experimental details for compound 13 | 234 |
| Table A.4 – | Crystallographic experimental details for compound 14 | 235 |
| Table A.5 – | Crystallographic experimental details for compound 16 | 237 |
| Table A.6 – | Crystallographic experimental details for compound 21 | 238 |
| Table A.7 – | Crystallographic experimental details for compound 22 | 240 |
| Table A.8 – | Crystallographic experimental details for compound 26 | 241 |
| Table A.9 – | Crystallographic experimental details for compound 29 | 242 |
| Table A.10 – | Crystallographic experimental details for compound 36 | 244 |
| Table A.11 – | Crystallographic experimental details for compound 41 | 245 |
| Table A.12 – | Crystallographic experimental details for compound 43 | 246 |

| | | | |
|-------------------|---|--|------------|
| Table A.13 | – | Crystallographic experimental details for compound 47 | 247 |
| Table A.14 | – | Crystallographic experimental details for compound 58 | 248 |
| Table A.15 | – | Crystallographic experimental details for compound 63 | 249 |
| Table A.16 | – | Crystallographic identification codes..... | 251 |

List of Abbreviations and Their Meanings

| Symbol | Meaning |
|-------------------------------|--|
| {X} | decoupled-nucleus X |
| ‡ | transition state |
| 1D | one-dimensional |
| 2D | two-dimensional |
| Å | Angström |
| APT | attached proton test |
| b.p. | boiling point |
| BAr ^F ₄ | [B[3,5-(CF ₃) ₂ C ₆ H ₃] ₄] ⁻ |
| BDE | bond dissociation energy |
| ca. | approximately |
| cm | centimetre |
| COD | 1,5-cyclooctadiene or $\eta^2:\eta^2$ -1,5-cyclooctadiene in a metal complex |
| Cp | cyclopentadiene |
| Cp* | pentamethylcyclopentadiene |
| dcm | dichloromethane |
| dep _m | <i>bis</i> (diethylphosphino)methane |
| dmf | dimethylformamide |
| dmp _m | <i>bis</i> (dimethylphosphino)methane |
| dms _o | dimethylsulfoxide |
| dp _{pe} | 1,2- <i>bis</i> (diphenylphosphino)ethane |
| dpp _m | <i>bis</i> (diphenylphosphino)methane |
| EI | electron impact |
| ESI | electrospray ionization |
| Et | ethyl |
| eV | electronvolt |
| FT | Fourier transform |
| FWHM | full width at half-maximum |
| g | gram |

| | |
|------------------------------|---|
| gCOSY | gradient-enhanced correlation spectroscopy |
| gHMBC | gradient heteronuclear multiple bond correlation |
| gHMQC | gradient heteronuclear multiple quantum coherence |
| gHSQC | gradient heteronuclear single quantum coherence |
| h | hour(s) |
| HOMO | highest occupied molecular orbital |
| HRMS | high resolution mass spectrometry |
| Hz | hertz |
| ipa | <i>iso</i> -propyl alcohol |
| ⁱ Pr | <i>iso</i> -propyl |
| IR | infrared |
| K | Kelvin |
| kg | kilogram |
| kJ | kiloJoule |
| L | litre |
| LUMO | lowest unoccupied molecular orbital |
| m | metre |
| <i>m/z</i> | mass to charge ratio |
| M ⁺ | molecular ion |
| Me | methyl |
| <i>meta</i> - | 1,3- |
| mg | milligram |
| MHz | megahertz |
| min | minute |
| mL | millilitre |
| mm | millimetre |
| mmol | millimole |
| mol | mole |
| MS | mass spectrometry |
| n/a | not applicable |
| ⁿ J _{AB} | n-bond AB coupling constant |

| | |
|----------------------------|---|
| NMR | nuclear magnetic resonance |
| NOE | nuclear Overhauser effect |
| η^x | hapticity of x contiguous atoms |
| Oac | acetate |
| $^{\circ}\text{C}$ | degree Celcius |
| ORTEP | Oak Ridge Thermal Ellipsoid Plot |
| <i>ortho-</i> | 1,2- |
| OTf | triflate |
| <i>para-</i> | 1,4- |
| Ph | phenyl |
| pK_a | logarithmic reciprocal of K_a |
| pK_b | logarithmic reciprocal of K_b |
| ppm | parts per million |
| Pr | propyl |
| RT | room temperature (22 $^{\circ}\text{C}$) |
| $r_{\text{vdw}}(\text{A})$ | van der Waals radius of atom A |
| s | second |
| $t_{1/2}$ | half-life |
| ^tBu | <i>tert</i> -butyl |
| <i>tert</i> | tertiary |
| thf | tetrahydrofuran |
| TMS | tetramethylsilane |
| TOCSY | total correlation spectroscopy |
| TOF | time of flight |
| Tol | tolyl, $\text{C}_6\text{H}_5\text{CH}_3$ |
| TROESY | transverse rotating-frame Overhauser enhancement spectroscopy |
| vs. | versus |
| Z_{eff} | effective nuclear charge |
| δ | partial charge or chemical shift in ppm |
| Δ | difference |
| ΔG^{\ddagger} | Gibbs energy of transition state (activation energy) |

| | |
|--------------|--|
| κ^n-A | ligated by atom(s) A by n sites |
| μ | micro |
| $\mu-$ | bridging |
| ν_{A-B} | A-B bond stretching frequency (cm^{-1}) |
| χ | Pauling electronegativity |
| χ_{AR} | Allred-Rochow electronegativity |

Chapter 1 – Introduction to Carbon-Hydrogen and Carbon-Fluorine Bond Activation

1.1 Carbon-Atom Bond Activation. All chemical transformations involving the conversion of one molecule to another occur by the breaking and making of chemical bonds. Therefore, understanding the nature of these chemical bonds is paramount if we, as chemists, are to bring about the rational conversion of commonly available starting materials into useful products. One major challenge that face chemists regarding the cleavage of carbon-containing bonds, in particular, is performing the bond activation in a *selective* manner, whereby preference for cleavage of a specific bond is exhibited. For example, the activation of a variety of chemical bonds such as carbon-hydrogen,¹⁻⁶ carbon-chlorine,^{7,8} carbon-oxygen,^{9,10} carbon-fluorine,¹¹⁻¹⁷ and even carbon-carbon bonds can lead to increasingly reactive intermediates, which can be further transformed under mild conditions to generate specific materials. Unfortunately, performing these transformations in a selective manner is often not trivial.¹⁸⁻²⁰ Therefore, being able to access new transformations through the selective cleavage of these inert bonds has the potential to open up new pathways, as well as lower production costs, for the formation of targeted products. For example, carbon-hydrogen cleavage is fundamental to the dehydrogenation of paraffins, a process that is crucial for the development of more useful chemical feedstocks, including styrene – a molecule used for the synthesis of polymers and plastics.²¹ The cleavage of the very strong carbon-oxygen bond in carbon monoxide is a key step during the initial stages of Fischer-Tropsch reaction, which is achieved over a number of metal surfaces and finds subsequent use for the conversion of syngas ($\text{CO} + \text{H}_2$) to a variety of useful organic products including alkenes, alkanes, alcohols, aldehydes, ketones and acids.²² Carbon-chlorine bond activation gives access to carbon-carbon cross coupling reactions, which has become an important chemical transformation for the production of pharmaceuticals.²³ Carbon-fluorine bond activation is showing potential as an effective method for the degradation of chlorofluorocarbons (CFC's) that are retained in the atmosphere for hundreds of

years and display ozone depleting properties.²⁴⁻²⁷ Finally, carbon-carbon bond activation is accomplished by a variety of processes, including olefin metathesis, which is important in polymerization catalysis, specifically ring-opening metathesis polymerization (ROMP).²⁸

In all of the above transformations, transition-metal complexes can provide convenient routes for cleaving inert bonds, rendering the reaction kinetically favourable by lowering the activation energy for breaking the strong chemical bond. Another advantage that transition metal complexes have provided is the ability to perform these transformations in a selective manner, allowing for regio- and stereoselective control over the products, without which many of the products would not be accessible.

Two of the bond-activation processes described above, namely the cleavage of carbon-hydrogen and carbon-fluorine bonds, will be the focal points for this thesis. As will be noted in what follows, the strategies for both types of bond activations are very different, although in this study very similar metal complexes will be used in both cases. What ties these two themes together within this thesis is the strategy of using a *pair* of adjacent metals in a cooperative manner to activate otherwise unreactive bonds. Furthermore, I will be investigating substrates containing *both* C–H and C–F bonds, and in work to be described later in this thesis, I will consider factors that favour one activation process over the other.

The following two sections will introduce the properties of carbon-hydrogen and carbon-fluorine bonds, and in particular, will discuss the factors that influence the nature of each of these bonds. Each section will describe the classes of reactions that are successful for cleaving C–H and C–F bonds, with specific examples to aid in understanding the fundamental differences between C–H and C–F bond activation. Finally, attention will be drawn to the cleavage of these bonds within olefins; in particular I will address the geminal activation of C–H bonds within olefins and the cleavage of C–F bonds in fluoroolefins, and how pairs of adjacent metals can play a role in these activation processes.

1.2 Carbon-Hydrogen Bond Activation

1.2.1 Carbon-Hydrogen Bond Properties. Carbon-hydrogen bond activation refers to the cleavage of typically inert C–H bonds. In order to tailor transition-metal complexes to enhance their ability to undergo C–H activation, it is necessary to have an understanding of the fundamental properties of a C–H bond and what contributes to its relative inertness.

Electronegativity (χ), defined by Pauling as “*the power of an atom in a molecule to attract electrons to itself*”,²⁹ is a property of atoms that helps explain the nature of chemical bonds involving these atoms. Allred and Rochow expanded upon the concept presented by Pauling and defined electronegativity (χ_{AR}) as being proportional to the effective nuclear charge (Z_{eff}) felt by the valence electrons and inversely proportional to the radius (r ; Å) of the atom squared, as shown in Equation 1.1.³⁰ It is evident from this equation that a higher Z_{eff} or a smaller radius leads to an increase in the electronegativity of an atom.

$$\chi_{\text{AR}} = 0.359 \frac{Z_{\text{eff}}}{r^2} + 0.744 \quad (\text{Eq. 1.1})$$

The difference in electronegativity values between two bonded atoms is useful for rationalizing the type of bonding interaction involved. Two mutually bonded atoms with comparable electronegativity values ($\Delta\chi < 0.5$) will share electrons near equally, producing a *covalent bond*.³¹ Conversely, when there is a large difference in electronegativity between the atoms the bond becomes *ionic* ($\Delta\chi > 2.0$), with the electronegative atom essentially becoming a negative point charge and the electropositive atom becoming a positive point charge.³¹ Between these two extremes is a *polar covalent bond*, in which there is a noticeable difference between the electronegativity values of the two atoms ($0.5 < \Delta\chi < 2.0$), producing a polarized bonding interaction with the majority of the bonding electron density being associated with the more electronegative atom.³¹

A carbon-hydrogen bond is predominately covalent, owing to the small difference in electronegativity between carbon ($\chi_{\text{AR}} = 2.5$) and hydrogen ($\chi_{\text{AR}} = 2.2$).³⁰ Although this suggests that all C–H bonds have the same degree of

covalency, there are variations in the electronegativity values for carbon that are dependent upon hybridization, resulting from the increase in s -character as the hybridization of carbon changes from sp^3 to sp . Since s -orbitals are lower in energy, owing to their better penetration of the core electron density and subsequent poorer shielding from the nucleus, they have a larger Z_{eff} and therefore a larger electronegativity value. For example, the electronegativity for an sp^3 -hybridized carbon is given as 2.5, while an sp^2 -hybridized carbon has an electronegativity value of 2.7 (now comparable to sulfur) and an sp -hybridized carbon atom has a calculated electronegativity value of 3.3 (comparable to chlorine and oxygen), leading to C–H bonding interactions that become more polar as the amount of s -character on carbon increases.³² In part,[†] the increased polarity of the covalent bonds between carbon and hydrogen leads to an increase in their bond dissociation energies (BDE), with the BDE for methane being 438 kJ/mol, compared to 444 kJ/mol for ethylene and 552 kJ/mol for acetylene, as shown in Table 1.1.³³

Table 1.1 – Bond dissociation energies for common H–R molecules.

| H–R Bond | BDE (kJ/mol) | H–R Bond | BDE (kJ/mol) |
|---------------------------------|--------------|---------------------------------|--------------|
| H–H | 436 | H–F | 570 |
| H–CH ₃ | 439 | H–CF ₃ | 450 |
| H–C ₆ H ₅ | 450 | H–C ₆ F ₅ | 477 |
| H–SiR ₃ | 477 | H–C ₂ H ₅ | 438 |
| H–C ₂ H ₃ | 444 | H–C ₂ H | 552 |

1.2.2 Methods of C–H Activation. A wide range of strategies that do not utilize metals have been used for the cleavage of C–H bonds, including homolytic cleavage of alkanes to produce R₃C• and H• radicals and combustion of hydrocarbons to give H₂O and CO₂.⁴ Although both of these reactions are important and widely used, radicals have minimal selectivity, often resulting in a mixture of products, while combustion results in the indiscriminate cleavage of all

[†] A second factor that contributes to the increased bond dissociation energies of C–H bonds as s -character increases is the directionality of the bonding orbitals, in which the orbital overlap between carbon and hydrogen increases as the s -character of carbon increases.

(or essentially all) bonds in the molecule, giving products that are not considered to be "value added".

Transition metal complexes have provided a way to activate C–H bonds in a manner that provides a variety of new reactions that can be stereo- and/or regioselective, which in principle can result in the selective replacement of one or more hydrogen atoms in hydrocarbons by other elements or groups, generating value-added products. Transition-metal assisted C–H activation can be divided into 5 classes of reactions: (i) oxidative addition, (ii) σ -bond metathesis, (iii) metalloradical activation, (iv) 1,2-addition and (v) electrophilic activation,⁴ as outlined in Table 1.2.

Table 1.2 – *Methods of C–H activation.*

| Reaction | Example |
|---|--|
| (i) Oxidative addition | $L_nM^{(x)} + R-H \longrightarrow L_nM^{(x+2)} \begin{array}{c} H \\ \\ R \end{array}$ |
| (ii) σ-bond metathesis | $L_nM^{(x)}-R' + R-H \rightleftharpoons L_nM^{(x)}-R + R'-H$ |
| (iii) Metalloradical activation | $2 L_nM^{(x)} + R-H \rightleftharpoons L_nM^{(x+1)}R + L_nM^{(x+1)}H$ |
| (iv) 1,2-Addition | $L_nM^{(x)}\equiv L + R-H \longrightarrow L_nM^{(x)}-L(H) \begin{array}{c} \\ R \end{array}$ |
| (v) Electrophilic activation | $L_nM^{(x+2)}X_2 + R-H \longrightarrow L_nM^{(x)} + R-X + H-X$ |

Early transition-metals typically undergo σ -bond metathesis, particularly for d^0 systems for which oxidative addition is prohibited, while late transition-metals in low oxidation states, having ample electrons, preferentially undergo oxidative addition. Metalloradical activation and electrophilic addition are not

metal specific, and usually occur without the observation of any metal-containing intermediates, while [1,2]-additions involve the addition of an alkane across a metal-heteroatom double bond, and although this typically occurs for early and middle transition-metals, its potential for alkane functionalization is still unclear.⁴ The majority of reported C–H activation reactions involve the insertion of a transition-metal complex into the C–H bond via oxidative addition,^{1-6,34-36} particularly for arenes, although examples of alkane C–H oxidative addition are now prevalent, as described below. Interestingly, both kinetic and thermodynamic factors play a role in the proclivity for C–H activation of arenes versus alkanes, although the exact nature of the preference is under dispute.³⁷ The transition states for both arene and alkane C–H bond activation involve coordination of the substrate, the former by an η^2 -coordination mode involving the π -system, while alkanes form a σ -interaction between the metal and the C–H bond, which involves the donation of electron density from the C–H bonding orbital to the metal in conjunction with electron donation from the metal to the C–H antibonding orbitals, as shown in Chart 1.1. However, arenes have less steric encumbrance due to the greater C–C–H bond angles and lower orbital directionality compared to alkanes (trigonal planar versus tetrahedral), both of which allow for easier access to the C–H bond, effectively lowering the transition state energy for arene activation relative to alkane activation.³⁷ The thermodynamic driving force favouring arene over alkane C–H bond activation stems from the difference between metal-aryl and metal-alkyl bond strengths being greater than the difference between arene C–H and alkane C–H bond strengths.³⁸

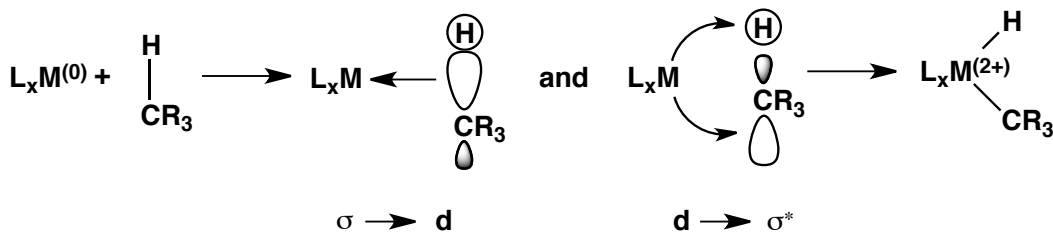
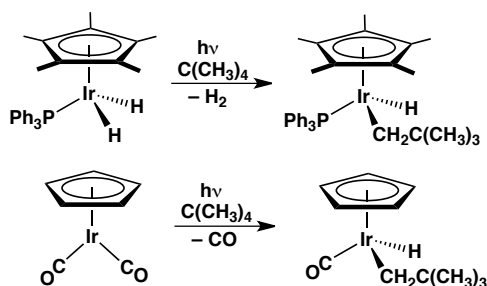


Chart 1.1 – *Concerted C–H bond cleavage of an alkane by a metal complex.*

The first example of oxidative addition of a C–H bond by a transition-metal complex was reported by Chatt and Davidson in 1965, when they described aromatic C–H activation of a variety of arenes (benzene, naphthalene, anthracene and penanthrene) with ‘Ru(dmpe)₂’, formed from the reduction of *trans*-[RuCl₂(dmpe)₂] by the corresponding sodium arene salt, to produce the hydrido-aryl complex *cis*-[RuH(aryl)(dppe)₂].³⁹

The first examples of oxidative addition of alkane C–H bonds were reported in rapid succession by Janowicz and Bergman in late 1981⁴⁰ and Hoyano and Graham in early 1982.⁴¹ Bergman found that photolysis of [(Cp*)Ir(H)₂(PPh₃)] (Cp*⁻ = pentamethylcyclopentadienyl, C₅(CH₃)₅⁻) led to the highly reactive intermediate, [(Cp*)Ir(PPh₃)], which readily reacts with neopentane to give the oxidative addition product, [(Cp*)Ir(H)(CH₂C(CH₃)₃)(PPh₃)], while Graham reported that photolysis of [(Cp)Ir(CO)₂] (Cp⁻ = cyclopentadienyl, C₅H₅⁻) results in loss of CO to produce the reactive intermediate [(Cp)Ir(CO)], which undergoes oxidative addition of neopentane to give [(Cp)Ir(H)(CH₂C(CH₃)₃)(CO)]. These two reactions, shown in Scheme 1.1, played a critical role in improving our understanding of how oxidative addition occurs, and led to an explosion of reports on C–H activation.^{1-6,34-36}

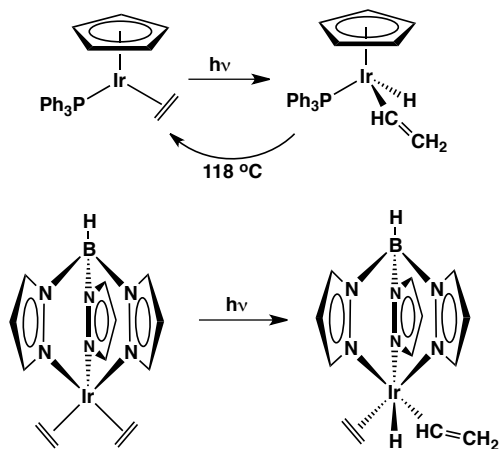


Scheme 1.1 – Oxidative addition of alkanes reported by Janowicz and Bergman (top) and Hoyano and Graham (bottom).

1.2.3 Single and Geminal C–H Activation of Olefins. A variety of examples have been reported showing the C–H activation of olefins, whereby the olefin undergoes either single C–H oxidative addition to produce a vinyl hydride

product,⁴²⁻⁴⁹ or double activation of either vicinal⁵⁰⁻⁵⁴ or geminal pairs⁵⁵⁻⁶³ of C–H bonds. Single C–H activation of olefins commonly occurs with late transition metal complexes analogous to the Bergman and Graham systems for alkane C–H activation, (for example, [(Cp)Ir(L)_x]⁴²⁻⁴⁷ and the isolobal analogue [(Tp)IrL_x] (Tp[−] = *tris*(pyrazolyl)borate, [HB(C₃N₂R₂)₃][−]),^{48,49} while vicinal and geminal activation are much less common, being observed in the few known examples, for bimetallic and cluster complexes,^{50-54,56-63} with only one example known for a monometallic complex, involving the geminal activation of ethylene,⁵⁵ as outlined in the following section.

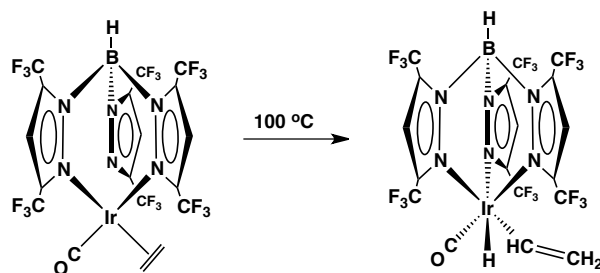
As shown in Scheme 1.2, [(Cp)Ir(PPh₃)(η^2 -C₂H₄)]⁴⁷ and [(Tp)Ir(η^2 -C₂H₄)₂]⁴⁸ both undergo similar reactions with ethylene under photolytic conditions, giving the respective vinyl hydride compounds, although in the case of the top reaction, the process is reversed under thermolysis conditions, reverting to the η^2 -ethylene adduct. In both examples, the authors describe the η^2 -ethylene compounds as the thermodynamically preferred species rather than the vinyl hydride complexes.



Scheme 1.2 – Single C–H activation of ethylene reported by Perutz et al. (top) and Crabtree (bottom).

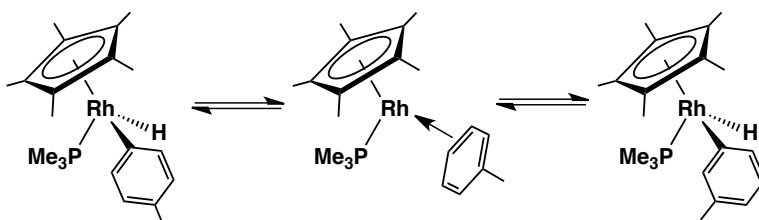
The opposite thermodynamic preference was reported by Graham and co-workers, in which the vinyl hydride complex, [(Tp^{(CF₃)₂)Ir(H)(C₂H₃)(CO)], is preferred at higher temperatures over its η^2 -ethylene counterpart, [(Tp^{(CF₃)₂)Ir(η^2 -}}

$\text{C}_2\text{H}_4)(\text{CO})]$ (Scheme 1.3).⁶⁴ The trifluoromethyl substitution at the 3- and 5-positions of the Tp ligand is responsible for this “opposite” thermodynamic preference, with the trifluoromethyl substituted complex performing C–H activation, while the proteo-analogue coordinates ethylene to form an adduct.⁶⁵ Although the reasons for the preference for η^2 -coordination versus C–H activation are still unclear, another important question is *how* the C–H activation of olefins occurs.



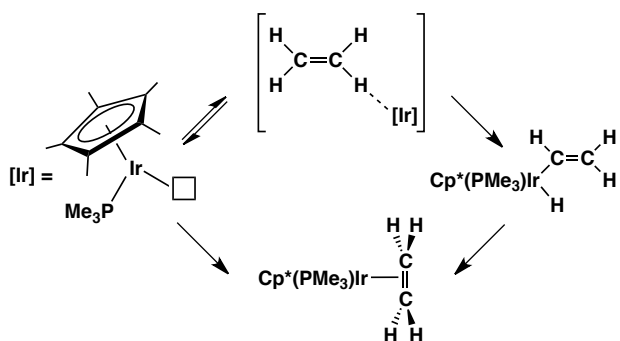
Scheme 1.3 – Thermal C–H activation of ethylene reported by Graham.

The greater tendency for C–H activation of unsaturated versus saturated substrates was rationalized on the basis that η^2 -coordination of the substrate (bound via a C=C bond) led to a favourable transition state, lowering the activation barrier for C–H cleavage. Certainly this result was found by Feher and Jones, in a study that examined the reversible reductive elimination and oxidative addition of a *para*-tolyl hydride complex in the presence of benzene, as outlined in Scheme 1.4.^{66,67} Labelling experiments and variable temperature NMR studies show no exchange with benzene, rather exclusive isomerization of the *para*-tolyl group to the *meta*-isomer, indicating that the intermediate after reductive elimination but prior to oxidative addition is an η^2 -arene adduct, leading to the proposal that, in this case, coordination of the π -bond facilitates oxidative addition.



Scheme 1.4 – Jones proposal for η^2 -arene coordination prior to C–H activation.

However, Bergman *et al.* reported that the C–H activation of ethylene by the ‘Cp*IrPMe₃’ fragment occurs to give a vinyl hydride/ η^2 -ethylene mixture, and increasing the temperature gives complete conversion of the vinyl hydride complex to the η^2 -ethylene adduct, shown in Scheme 1.5.^{42,44} This indicates that the vinyl hydride complex is the kinetic product while the η^2 -ethylene adduct is the thermodynamic product showing that ethylene coordination *cannot* be an intermediate in the formation of the vinyl hydride complex. The authors proposed as an alternative mechanism a metal/C–H σ -complex, the interaction of which is not described, as the transition state leading to activation of the C–H bond.

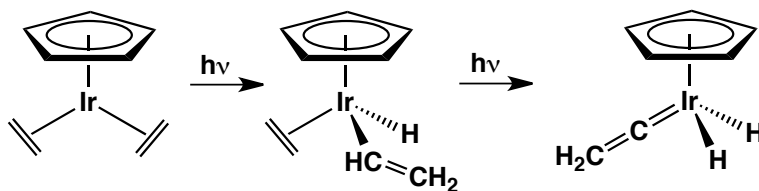


Scheme 1.5 – Bergman proposal for σ -interaction with olefinic hydrogen of ethylene.

As observed from the above examples, single C–H activation of olefins is typically a thermodynamically less favourable process, with the η^2 -ethylene complex usually being preferred over the vinyl hydride isomer.⁶⁸ Extension to the geminal activation of olefins (double C–H activation) becomes even less favourable, due to necessary increase in oxidation state of 4 in this double oxidative addition, thus making the second C–H activation difficult. Vinylidene complexes, the products resulting from geminal C–H activation of olefins, are certainly well known but are typically generated from their alkyne tautomer, whereby the thermodynamically favourable primary alkyne can spontaneously transform to the vinylidene tautomer in the presence of transition-metals.³² In the absence of transition-metals the tautomerization process becomes thermodynamically unfavourable (+180 kJ/mol for acetylene).³²

The synthesis of vinylidene complexes by the geminal activation of olefins is exceedingly rare, particularly for the monometallic case, for which there is only

one report, by Perutz and coworkers in 1990, in which $[\text{Ir}(\text{Cp})(\eta^2\text{-C}_2\text{H}_2)_2]$ was found to activate the geminal C–H bonds of ethylene under photolytic conditions to produce $[\text{Ir}(\text{Cp})(\text{H})_2(\text{CCH}_2)]$, as shown in Scheme 1.6.⁵⁵ In this example, photolysis ($\lambda > 360$ nm) in an argon or neon matrix at 198 K first produced a vinyl hydride intermediate, observed by IR spectroscopy, followed by secondary photolysis ($\lambda > 280$ nm), producing the vinylidene dihydride product. To confirm that the product is a result of geminal activation and not vicinal activation followed by a 1,2-hydride shift, 1,1-deuteroethylene was used, and the exclusive formation of $[\text{Ir}(\text{Cp})(\text{H})_2(\text{CCD}_2)]$ and $[\text{Ir}(\text{Cp})(\text{D})_2(\text{CCH}_2)]$ with no mixed H/D products, confirmed the geminal activation pathway.⁵⁵



Scheme 1.6 – Photolytic activation of ethylene.

One method for overcoming the unfavourable thermodynamics for geminal activation and facilitating double C–H activation of olefins is to use multimetallic systems, whereby a second metal can potentially aid in activation of the second C–H bond, possibly by a mechanism similar to that suggested in Chart 1.2, while also facilitating a larger variety of coordination modes for the vinylidene moiety, such as symmetrically or unsymmetrically bridging.^{69,70} Although, as noted by Bergman *et al.*, prior olefin coordination is not a necessary condition for its C–H activation, binuclear complexes, having adjacent metals, can potentially act cooperatively, possibly involving coordination of the olefin at one metal which can align the olefin in an orientation suitable for C–H activation by the adjacent metal.⁷¹ Subsequently, the metal adjacent to the resulting vinyl group is in a position that is favourable for the second C–H activation step.

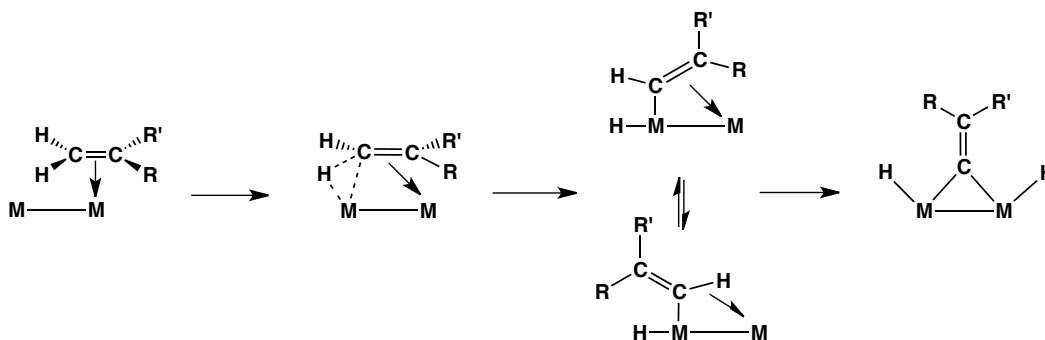
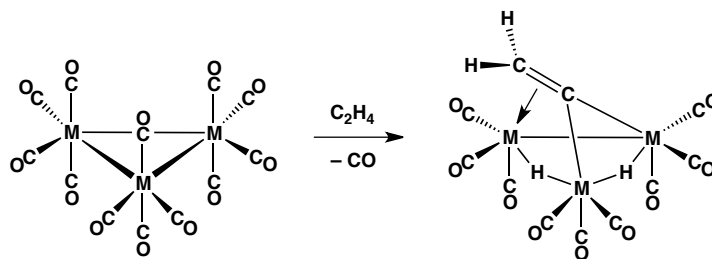


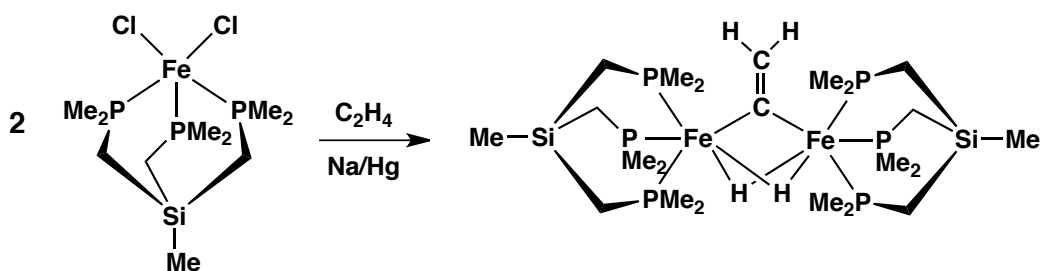
Chart 1.2 – Mechanism for geminal activation of olefins in multimetallic systems.

To our knowledge, there are only four reports in which geminal activation of olefins has occurred in multimetallic systems.⁵⁶⁻⁶³ The first example was reported by Deeming *et al.*, in which they demonstrated that the trimetallic clusters $[M_3(CO)_{12}]$ ($M = Ru$ or Os) react with ethylene in refluxing octane to yield $[M_3(H)_2(CO)_9(\mu-\kappa^1:\kappa^1:\eta^2-CCH_2)]$, as shown in Scheme 1.7.⁵⁸⁻⁶¹ In this example the vinylidene unit adopts a bridging coordination mode, σ -bound to two of the metals while π -bound to the third metal.



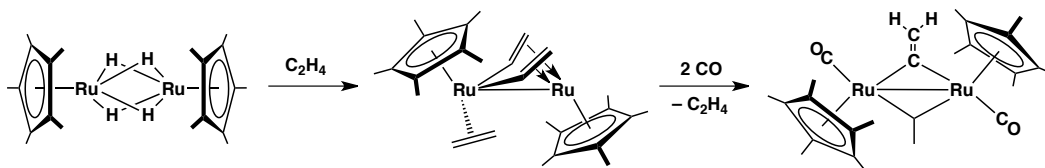
Scheme 1.7 – Geminal activation of ethylene by $[M_3(CO)_{12}]$ ($M = Ru, Os$).

Ten years later Green and coworkers reported that two equivalents of $[FeCl_2(tms)]$ ($tms = MeSi(CH_2PMe_2)_3$) react with ethylene (2 atm, 22 °C) in the presence of Na/Hg to give the binuclear, vinylidene-bridged complex $[(tms)_2Fe_2(\mu-H)_2(\mu-CCH_2)]$ (Scheme 1.8).^{56,57} Alternatively, reacting $[Fe(\eta^4-C_6H_6)(tms)]$ with ethylene (7 atm, 50 °C, 12 h)^{56,57} generated the same vinylidene-bridged product. In both cases, the starting transition-metal complex is monometallic, forming the vinylidene-bridged binuclear product upon reacting with ethylene; however, no mechanistic information was supplied.



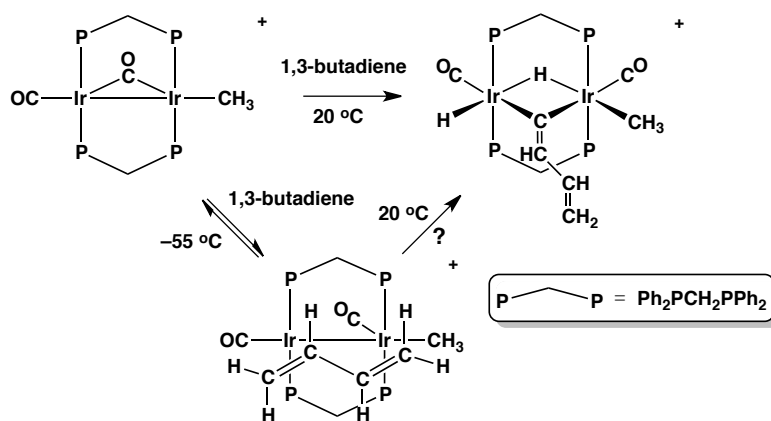
Scheme 1.8 – Geminal activation of ethylene by $[FeCl_2(tms)]$.

The third example was reported by Suzuki and coworkers in 1993, in which the binuclear complex $[Ru_2(Cp^*)_2(\mu-H)_4]$ reacts with 2 equivalents of ethylene to produce a *bis*($\kappa^1:\eta^2$)-vinyl ethylene complex, followed by a second C–H activation upon the addition of CO, giving a vinylidene- and ethylidene-bridged product (Scheme 1.9).⁶³ The authors describe the second activation as occurring readily in the presence of carbon monoxide to give an intermediate containing vinyl, vinylidene and hydride ligands, followed by insertion of the vinyl and hydride groups to give a bridging ethylidene group, as shown.



Scheme 1.9 – Geminal activation of ethylene by $[Ru_2(Cp^*)(\mu-H)_4]$.

The most recent example was reported by our group in 2000, and is the first reported example of geminal activation of an olefin other than ethylene.⁶² The diiridium complex, $[Ir_2(CH_3)(CO)_2(dppm)_2][OTf]$ (dppm = *bis*(diphenylphosphino)methane, $Ph_2PCH_2PPh_2$), was found to react at ambient temperature with 1,3-butadiene in a saturated CH_2Cl_2 solution over 48 h to give $[Ir_2(CH_3)(H)(CO)_2(\mu-H)(\mu-C=C(H)C(H)CH_2)(dppm)_2][OTf]$, as outlined in Scheme 1.10.⁶² Low temperature NMR investigations allowed the detection of a *transoid*-butadiene adduct, leading the authors to propose its possible intermediacy in the formation of the final product.



Scheme 1.10 – Geminal activation of 1,3-butadiene by $[\text{Ir}_2(\text{CH}_3)(\text{CO})_2(\text{dppm})_2][\text{OTf}]$.

A mechanism of activation was also proposed whereby single C–H activation initially occurs, giving a vinyl-containing, hydride-bridged intermediate, followed by rotation about the metal-phosphine axes, resulting in the hydride migrating between the two metals to the opposite face, bringing the vinyl moiety into close proximity to the second metal, promoting the second C–H activation (Chart 1.3). This mechanism helped rationalize the mutually trans arrangement of hydride ligands on opposite faces of the "Ir₂P₄" core. Although this system is able to activate 1,3-butadiene, the C–H activation of other olefins was not observed.⁷²

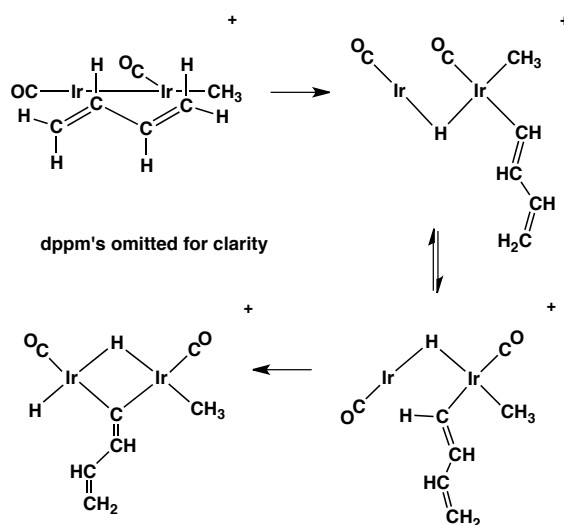


Chart 1.3 – Proposed mechanism for geminal activation of 1,3-butadiene by $[\text{Ir}_2(\text{CH}_3)(\text{CO})_2(\text{dppm})_2][\text{OTf}]$.

I was interested in following up this study with two goals in mind. First, I was interested in obtaining additional mechanistic information on the double C–H activation of 1,3-butadiene, described above. In particular, I was interested in determining the role (if any) of the "double π -adduct" in the activation process. Since this adduct is extremely labile, with reversible butadiene loss even at -80 °C, and no adduct observed at ambient temperature, it was unclear whether the π -adduct preceded C–H activation or represented a non-productive resting state. The stability of the π -adduct could presumably be increased by decreasing the congestion at the metals by the use of less bulky diphosphine ligands, while more basic diphosphines would also result in more π -back donation, also helping to bind the diolefin. At the same time more basic diphosphines would also favour the C–H activation steps, allowing these to be more conveniently studied. Both of these modifications to the diphosphines could be achieved by substituting the phenyl substituents by smaller alkyl groups. In addition, I was interested in increasing the scope of geminal C–H activation of olefins by increasing the reactivity of the diiridium complex towards a variety of olefins. The above strategy of substituting dppm by a more basic diphosphine also seemed capable of achieving this goal.

The obvious choice of alkyldiphosphine was the smallest such diphosphine containing methyl substituents, namely *bis*(dimethylphosphino)methane (dmpm, $\text{Me}_2\text{PCH}_2\text{PMe}_2$). The synthesis of the related diiridium system, $[\text{Ir}_2(\text{CH}_3)(\text{CO})_2(\text{dmpm})_2]^+$ was reported and appeared to be the obvious candidate for the comparison to the dppm analogue.⁷³⁻⁷⁵ However, I was unable to reproduce the results from this report and found that the chemistry involving dmpm significantly deviated from the dppm chemistry in unpredictable ways.

I subsequently turned to the related *bis*(diethylphosphino)methane (depm, $\text{Et}_2\text{PCH}_2\text{PEt}_2$) ligand, which was much better behaved than dmpm, displaying chemistry analogous to its dppm congeners.⁷⁶ This chemistry was initiated by Dr. Dusan Ristic-Petrovic and Dr. Jason Anderson in our group and followed up by myself. Due to the increased basicity of the ethyl groups relative to the phenyl substituents, in conjunction with the smaller size compared to the phenyl rings,

the depm systems display increased reactivity relative to the analogous dppm complexes.

Chapter 4 will describe the synthesis and characterization of all the depm precursors, including the diiridium complexes synthesized initially by Jason Anderson and subsequently (many times) by me, the dirhodium complexes initiated by Jason and completed by me, and finally the mixed-metal iridium/rhodium complexes – work started during my summer NSERC USRA grant in 2005 and completed during my tenure as a Ph.D. student. Chapter 4 also outlines the initial reactivity studies of $[\text{Ir}_2(\text{CO})_3(\mu\text{-H})(\text{depm})_2]^+$ with a variety of α -olefins, with the goal of determining whether the increased basicity, and the smaller size of the diphosphines can facilitate C–H activation of a wider variety of olefins than found with a related dppm complex.

1.3. Carbon-Fluorine Bond Activation

1.3.1 Carbon-Fluorine Bond Properties. Carbon-fluorine bond activation involves the scission of carbon-fluorine bonds in organofluorine substrates. It is noticeably different from carbon-hydrogen bond activation due to several electronic differences between hydrogen and fluorine that result in increased inertness, higher thermal stability, and increased resistance to chemical attack of carbon-fluorine bonds compared to carbon-hydrogen bonds.⁷⁷ Note that while the electronic properties of C–F bonds are much different than C–H bonds, steric differences are subsidiary, with the van der Waals radius of fluorine (150 – 160 pm) being only slightly larger than that of hydrogen (120 – 145 pm).²⁹ This means the substitution of hydrogen by fluorine in organic molecules, which is an area of great interest for the generation of pharmaceuticals,⁷⁸⁻⁸² refrigerants,^{25,83} surfactants,⁸⁴⁻⁸⁶ and polymers,^{24,87} has relatively minor steric consequences, leaving the molecule relatively unperturbed from this perspective (although substantially different electronically).

A list of bond dissociation energies of F–X bonds is outlined in Table 1.3 (for comparison to H–X bond dissociation energies, refer to Table 1.1).^{15,88} The strength of the carbon-fluorine bond stems from the higher effective nuclear charge felt by the valence electrons of fluorine relative to carbon, leading to a

Table 1.3 – F–R bond dissociation energies.

| F–R Bond | BDE (kJ/mol) | F–R Bond | BDE (kJ/mol) |
|-------------------------------------|---------------------|-------------------------------------|---------------------|
| F–H | 570 | F–F | 159 |
| F–CH₃ | 472 | F–CF₃ | 547 |
| F–C₆H₅ | 533 | F–C₆F₅ | 487 |
| F–SiR₃ | 565 | | |

higher electronegativity for fluorine ($\chi_{\text{AR}} = 4.1$) relative to carbon ($\chi_{\text{AR}} = 2.5$), resulting in a C–F bond that is highly polarized. This is accompanied by an increase in ionic character as a consequence of the bonding electron density being concentrated towards fluorine ($\Delta\chi_{\text{AR}} = 1.6$). Increasing the number of fluorine atoms bonded to carbon further increases the polar nature of the C–F bonds, leading to an increase in carbon-fluorine bond strength as the number of fluorine substituents increase. This is demonstrated by observing the change in bond length, bond enthalpy and partial charges of carbon and fluorine as fluorine substitution increases from fluoromethane to tetrafluoromethane (Chart 1.4). The C–F bond *lengths* steadily decrease with increasing fluorine substitution, as the incorporation of additional electronegative fluorines withdraws increasing amounts of electron density from carbon, creating a stronger bond with increasing ionic character – an effect that is amplified as substitution increases. This is also reflected in the increased C–F bond *strengths* as fluorine substitution increases, culminating in a C–F bond strength of 547 kJ/mol for tetrafluoromethane, which is 75 kJ/mol stronger than observed in fluoromethane. Furthermore, as fluorine substitution increases the partial charge distribution on both carbon and fluorine also increases, with carbon showing a dramatic increase in partial positive charge while fluorine shows a minor decrease in partial negative charge, reiterating the increase in polar covalent nature of C–F bonds.

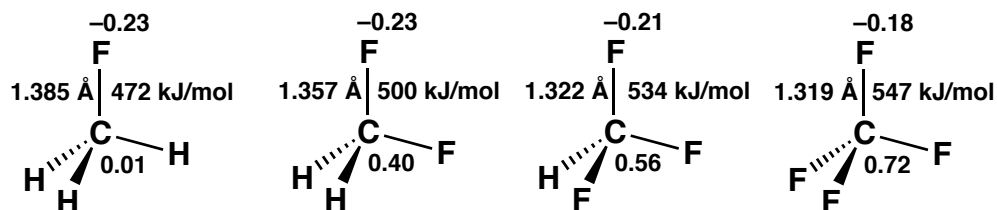


Chart 1.4 – Bond lengths, bond strengths and partial charges as fluorine substitution increases.

Fluorine substitution in organic molecules also has a pronounced effect on the geometry of a molecule, leading to variations in bond angles that are opposite to what is expected from steric arguments. A series of papers published by Henry Bent explains how the high electronegativity of fluorine gives rise to these variations in molecular geometries, stating, “*the atomic p character tends to concentrate in orbitals that are directed toward electronegative groups.*”⁸⁹ To put this in context, the ideal interatomic bond angles about an sp^3 -hybridized atom is 109.5° , and as the s -character increases from sp^3 to sp , the bond angle increases to 180° , conversely, as the p -character increases, the interatomic bond angle decreases. If the atomic p -character is concentrated towards electronegative groups, we can expect a decrease in the bond angles involving the electronegative substituent, and an increase in bond angles involving more electropositive substituents. For example, difluoromethane has a F–C–F bond angle (108.4°) slightly less than the ideal tetrahedral angle, indicative of increased p -character, while the H–C–H angle (113.8°) is noticeably larger than 109.5° ,⁹⁰ indicating that the latter bonds contain slightly more carbon s -character. Furthermore, these bond angles are the opposite of what is expected based on steric arguments, for which slightly larger fluorines which also are subject to lone pair – lone pair repulsions, should repel one another, resulting in a greater F–C–F angle at the expense of the H–C–H angle. The difference in bond polarities between C–H and C–F bonds also influence these distorted bond angles, with the more polarized C–F bond having less electron density near carbon, therefore allowing the orbitals to arrange more acutely compared to C–H bonds, which are less polarized, and therefore have more electron density proximal to the carbon atom, creating repulsion, leading to an increase in the inter-orbital angle.

A second feature of fluorine's propensity to attract atomic p -character is its thermodynamic preference for carbon centres that contain higher p -character ($sp^3 > sp^2 > sp$), and the corresponding increase in carbons ability to donate electron density to fluorine.⁸⁹ This is exemplified by the stability of hexafluoroethane, a nonflammable gas, while tetrafluoroethylene readily polymerizes in the absence of an inhibitor and difluoroacetylene polymerizes even more readily and has never been isolated as a monomer.⁷⁷

These electronic factors make the activation of C–F bonds difficult from a kinetic and thermodynamic standpoint. One method for overcoming the thermodynamic stability of C–F bonds involves using an external reagent that will undergo ‘*metathesis*’ with a C–F bond, creating products that contain even stronger atom-fluorine bonds. Common reagents that achieve this include protic acids (H^+), for which the driving force is the formation of a strong H–F bond (BDE_{H-F} = 570 kJ/mol), and silylium cations (R_3Si^+), which behave in a similar manner to protic acids with the formation of strong Si–F bonds (BDE_{Si-F} = 565 kJ/mol) being the thermodynamic driving force.

Transition-metal complexes have a long (if not too extensive) history in facilitating the cleavage of C–F bonds, and numerous reviews have been published over the past few decades outlining the various ways in which transition-metal complexes can aid in C–F bond activation.¹¹⁻¹⁷ One review in particular, by Braun and Perutz,¹⁵ has divided C–F activation by transition metal complexes into two different classes, (I) intermolecular activation and (II) intramolecular activation, and within each class all reported transition metal-mediated C–F bond activations are described in terms of a series of six reaction types.

1.3.2 Intermolecular Activation. The first class described, that of intermolecular activation, is further divided into 6 categories:¹⁵ (i) oxidative addition; (ii) metal-carbon bond formation with hydrogen-fluorine bond elimination; (iii) metal-carbon bond formation with fluorosilane elimination; (iv) hydrodefluorination with metal-fluorine bond formation; (v) nucleophilic attack by a transition metal complex; and (vi) defluorination. These are summarized in Table 1.4.

Table 1.4 – Intermolecular C–F activation processes

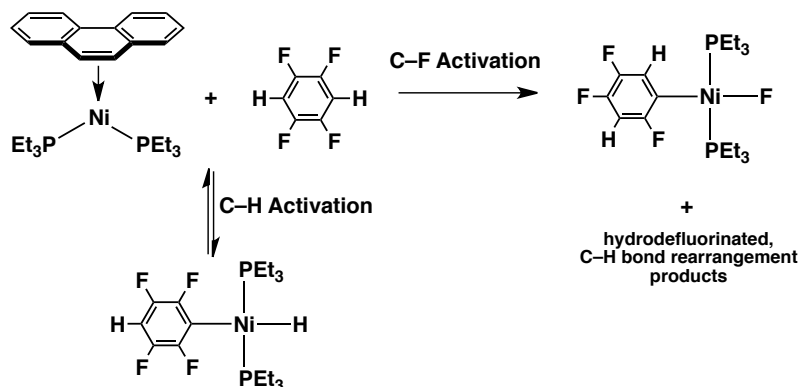
| Reaction | Example |
|--|--|
| (i) Oxidative addition | $[M] + R^F-F \longrightarrow R^F-[M]-F$ |
| (ii) M-C bond formation, HF elimination | $[M]-H + R^F-F \longrightarrow R^F-[M] + H-F$ |
| (iii) M-C bond formation, SiF elimination | $[M]-SiR_3 + R^F-F \longrightarrow R^F-[M] + R_3Si-F$ |
| (iv) Hydrodefluorination, M-F bond formation | $[M]-H + R^F-F \longrightarrow F-[M] + R^F-H$ |
| (v) Nucleophilic attack | $[M]^- + R^F-F \longrightarrow R^F-[M] + F^-$ |
| (vi) Defluorination | $2[M] + (R^F)_2FC-CF(R^F)_2 \longrightarrow 2 F-[M] + (R^F)_2C=C(R^F)_2$ |

Not all fluorinated substrates react by all six reactions described above. Fluoroaromatics are the most versatile, with reports of C–F activation for all of the above routes except defluorination. Fluoroalkenes can react with transition metal complexes by routes (ii) – (v); however, no examples are known involving oxidative addition or defluorination. Fluoroalkyls can react by methods (iv) – (vi); although, nucleophilic attack by a metal complex on fluoroalkyls is rare.¹⁵

Although the concerted oxidative addition of C–H bonds with transition metal complexes is a common method for cleaving C–H bonds, the concerted oxidative addition of C–F bonds is relatively rare, and has only been shown to occur with fluoroaromatics, and for the most part with nickel complexes.⁹¹⁻¹⁰¹ The first report of oxidative addition of C–F bonds was reported in 1977,⁹¹ when Fahey and Mahan observed a reaction between perfluorobenzene and $[Ni(PEt_3)_4]$, producing *trans*- $[Ni(C_6F_5)(F)(PEt_3)_2]$ in 7% yield. At the time, the product was characterized by infrared spectroscopy and elemental analysis and it was not until 1997 that Perutz and coworkers were able to obtain the full spectroscopic and crystallographic characterization.⁹²

DFT calculations by Perutz and coworkers have shown that oxidative addition of arene C–F bonds follows a similar pathway to that of arene C–H oxidative addition, whereby an η^2 -interaction between the metal and C–C π -system facilitates overlap of the metal with the C–X (X = H or F) bond. However, C–F bond activation is thermodynamically preferred over C–H bond activation in these systems, in large part due to the strength of the Ni–F bond compared to the Ni–H bond.⁹⁵ Interestingly, palladium and platinum are not as successful at oxidative addition of C–F bonds due to a significant increase in energy of the transition state for the C–F oxidative addition, while the transition state for C–H oxidative addition remains the same. This is attributed to the greater $5d\pi$ - $p\pi$ repulsion between platinum and the lone pairs on fluorine, decreasing the stability of the Pt–F interaction, whereas this repulsion is absent between platinum and hydrogen.⁹⁵

Studies by Johnson and coworkers have shown that $[\text{Ni}(\text{PEt}_3)_2(\eta^2\text{-C}_{14}\text{H}_{10})]$ (a convenient source of $\text{Ni}(\text{PEt}_3)_2$) reacts with 1,2,4,5-tetrafluorobenzene (and also with pentafluorobenzene) to initially give detectable amounts of the reversible C–H activation product, $[\text{Ni}(\text{H})(\text{C}_6\text{F}_4\text{H})(\text{PEt}_3)_2]$, as shown in Scheme 1.11, while longer reaction times result in the formation of the thermodynamically favoured C–F activated product, $[\text{Ni}(\text{F})(\text{C}_6\text{F}_3\text{H}_2)(\text{PEt}_3)_2]$, along with other hydrodefluorination and C–H bond rearrangement products.⁹⁶



Scheme 1.11 – C–H and C–F bond activation of 1,2,4,5-tetrafluorobenzene.⁹⁶

1.3.3 Intramolecular Activation. The second class of C–F bond activation reactions involves intramolecular activations, in which the fluorocarbyl fragment is pre-coordinated to the transition metal complex. Again this class was subdivided by Braun and Perutz¹⁵ into six different reaction types, although the generalization of these reactions are much more difficult compared to the intermolecular reactions. They include: (i) [1,2]-fluoride shift (α -elimination); (ii) [1,3]-fluoride shift (β -elimination); (iii) F[−] abstraction induced by Lewis or Brønsted acids; (iv) F[−] abstraction with [1,2]-shift of H or CH₃ induced by Lewis or Brønsted acids; (v) acid-induced HF elimination; and (vi) defluorination,¹⁵ as outlined in Table 1.5.

Table 1.5 – Intramolecular C–F activation processes.

| Reaction | Example |
|---|---------|
| (i) [1,2]-F shift | |
| (ii) [1,3]-F shift | |
| (iii) F [−] abstraction induced by acid | |
| (iv) F [−] abstraction and [1,2]-shift of H or CH ₃ induced by acid | |
| (v) Acid-induced HF elimination | |
| (vi) Defluorination | |

Of these six reactions for intramolecular activation, four involve activation of the carbon-fluorine bond in the α -position to the metal. The increased lability of these α -C–F bonds can be rationalized on the basis of π back donation from the metal into the σ^* -orbitals of the carbon-fluorine bond, which in turn weakens this bond, making it susceptible to removal by strong electrophiles (refer to Chart 1.5).¹⁰²⁻¹⁰⁶ An analogous effect in organic chemistry is referred to as negative hyperconjugation, in which a C–R bond is responsible for the back donation into the σ^* -orbital rather than a metal.^{107,108}

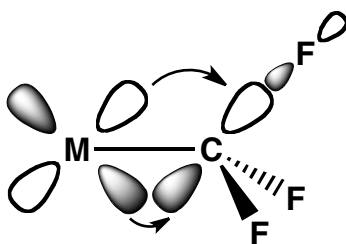


Chart 1.5 – π -Back donation from the metal d-orbital into the carbon-fluorine σ^* -orbital.

Hughes has reported numerous examples of α -C–F activation of fluoroalkyl groups and their subsequent conversion to carbon-hydrogen, carbon-carbon, carbon-oxygen and carbon-sulfur bonds.^{13,109-114} His work has made significant progress towards understanding both the role that the metal plays in the intramolecular activation of α -C–F bonds, as well as the importance of fluorine substitution in stabilizing the carbocation intermediate upon fluoride loss. He reports that the reactivity of α -C–F bonds towards electrophiles (intramolecular reactions iii, iv, and v) increases as fluorine substitution at the α -carbon increases, ie. $M-CF_3 > M-CF_2R_F > M-CF(R_F)_2$.¹³ This is predominately due to the stability of the carbocation intermediate resulting from fluoride ion loss, with the π -donation from the transition metal centre and the β -substituents to carbon being greatest for $M-CF_2^+$, followed by $M-C(F)R_F^+$, and finally $M-C(R_F)_2^+$.

Caulton has also reported examples of α -C–F activation involving the isomerization of the trifluoromethyl ligand to its difluoromethylene/fluoride

tautomer in late transition-metal systems.^{115,116} Using Me_3SiCF_3 as a formal source of nucleophilic CF_3 , he found that CF_3 adds to $[\text{MHF}(\text{CO})\text{L}_2]$ ($\text{M} = \text{Ru}$ or Os ; $\text{L} = \text{P}^t\text{Bu}_2\text{Me}$) to produce exclusively the difluoromethylene/fluoride isomer, namely $[\text{M}(\text{H})(\text{F})(\text{CF}_2)(\text{CO})(\text{P}^t\text{Bu}_2\text{Me})_2]$ and Me_3SiF , however, the addition of CO induced fluoride migration to the difluoromethylene moiety, reforming the trifluoromethyl ligand. He proposed the initial formation of a trifluoromethyl intermediate, which undergoes a [1,2]-fluoride shift through a α -fluoride agostic transition state to produce the difluoromethylene/fluoride tautomer.

1.3.4 C–F Activation of Fluoroolefins. Although the majority of C–F activation reactions reported involve fluoroaromatics, numerous examples of fluoroolefin activation appear in the literature. As described below, the majority of examples involving C–F activation of fluoroolefins involve tetrafluoroethylene, although examples involving vinylfluoride, 1,1-difluoroethylene, *cis*-difluoroethylene, *trans*-difluoroethylene, trifluoroethylene, and larger fluoroolefins are known.

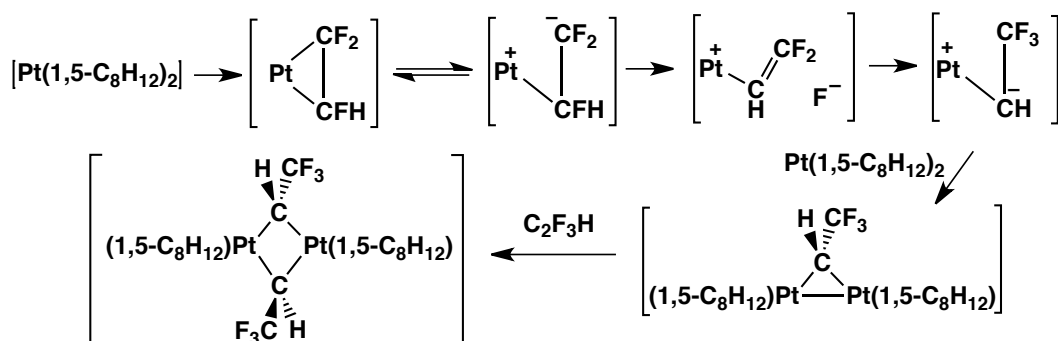
Vinylfluoride has shown limited reactivity with transition-metal complexes, with the only documented reaction type being hydrodefluorination.¹¹⁷⁻¹²⁰ Caulton and coworkers were the first to report C–F activation of vinyl fluoride, in which the $\text{Os}(\text{IV})$ complex, $[\text{Os}(\text{H})_3\text{Cl}(\text{P}^i\text{Pr}_3)_2]$, catalytically converts vinylfluoride to ethylene in the presence of hydrogen, while in the absence of hydrogen gas, the carbyne complex, $[\text{OsHFCl}(\text{CCH}_3)(\text{P}^i\text{Pr}_3)_2]$, is produced.¹¹⁷ Another report describes similar reactivity with an analogous osmium hydride complex, $[\text{Os}(\text{H})(\text{Ph})(\text{CO})(\text{P}^t\text{Bu}_2\text{Me})]$, which in the presence of primary, secondary or tertiary silanes catalytically converts vinylfluoride to ethylene.¹¹⁸ Similar reactivity has also been reported with Wilkinson's catalyst, $[\text{RhCl}(\text{PPh}_3)_3]$, which was found to catalytically convert vinylfluoride to ethylene in the presence of triethylsilane.^{119,120}

Before the work originating from our group,^{121,122} C–F bond activation of 1,1-difluoroethylene had only been reported with the early transition metal system, $[\text{Cp}^*_2\text{ZrH}_2]$, in which complete hydrodefluorination yielded a 2:1 mixture of $[\text{Cp}^*_2\text{ZrHF}]$ and $[\text{Cp}^*_2\text{ZrH}(\text{Et})]$,¹²³ respectively, with the latter being the result

of the hydrodefluorinated product, ethylene, inserting into the Zr–H bond of the zirconium dihydride starting material.

Under particularly harsh conditions, a mixture of both *cis*- and *trans*-difluoroethylene can be defluorinated to produce acetylene by a gas-phase reaction with $[\text{Mn}(\text{CO})_3]^-$ in the presence of SO_2 .¹²⁴ The reaction is proposed to proceed by concomitant loss of carbon monoxide and coordination of difluoroethylene, producing $[\text{Mn}(\text{C}_2\text{F}_2\text{H}_2)]^-$, followed by the formation of $[(\text{O}_2\text{S})\text{MnF}_2]^-$ and C_2H_2 , as evidenced by mass spectrometry. Similar reactivity is observed with trifluoroethylene and tetrafluoroethylene, resulting in the transformation to fluoroacetylene and difluoroacetylene, respectively, although the assignment these products is solely based upon mass balance and were not directly detected.¹²⁴

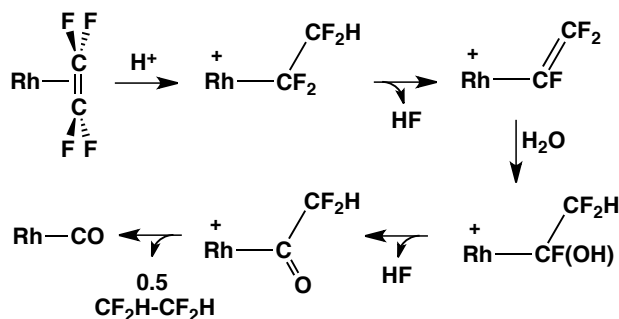
An interesting transformation of trifluoroethylene was reported by Stone and coworkers in 1977, in which the monometallic complex, $[\text{Pt}(\text{COD})_2]$ (COD = 1,5-cyclooctadiene), coordinates one equivalent of trifluoroethylene, followed by a [1,2]-fluoride shift along with coordination to a second equivalent of $[\text{Pt}(\text{COD})_2]$ to give a bridging 2,2,2-trifluoroethylidene functionality, as shown in Scheme 1.12.¹²⁵ In the presence of excess trifluoroethylene, a second equivalent coordinates and undergoes the same [1,2]-shift.¹²⁵ The authors proposed that this fluoride shift occurs via loss of F^- to the outer-sphere, followed by nucleophilic attack on the β -carbon.



Scheme 1.12 – Proposed mechanism for [1,2]-fluoride shift of trifluoroethylene.

As noted earlier, tetrafluoroethylene is the most studied fluoroolefin with regards to C–F activation, for which only three reaction types have been reported, all of which are intramolecular C–F activations ([1,2]–fluoride shift,^{126,127} fluoride abstraction induced by acid¹²⁸ and defluorination^{129,130}). Haszeldine and coworkers first reported a [1,2]-fluoride shift of tetrafluoroethylene with the binuclear compound $[\text{Co}_2(\text{CO})_8]$, initially producing the tetrafluoroethylene-bridged product, $[(\text{CO})_4\text{Co}(\mu\text{-C}_2\text{F}_4)\text{Co}(\text{CO})_4]$, which upon loss of CO yields the final product, $[(\text{CO})_3\text{Co}(\mu\text{-C}(\text{F})\text{CF}_3)(\mu\text{-CO})\text{Co}(\text{CO})_3]$.¹²⁶ Similarly, Ibers, Poilblanc and coworkers reported an analogous [1,2]-fluoride shift with the tetrafluoroethylene group of the diiridium complex, $[(\mu\text{-SCH}_3)_2(\mu\text{-C}_2\text{F}_4)\text{Fe}_2(\text{CO})_6]$, producing $[(\mu\text{-SCH}_3)_2(\mu\text{-C}(\text{F})\text{CF}_3)\text{Fe}_2(\text{CO})_6]$.¹²⁷ This reaction proceeds in a similar manner to Haszeldine's example, with prior coordination of tetrafluoroethylene in the bridging position between the two iron centres, followed by a [1,2]-fluoride shift to give a 1,2,2,2-tetrafluoroethylidene moiety. Interestingly, the addition of BF_3 to this rearranged product results in F^- -abstraction, producing a terminal trifluoromethylcarbyne moiety.¹²⁷

One of the more fascinating reactions with tetrafluoroethylene involves fluoride ion abstraction in the presence of water, converting the fluoroolefin into carbon monoxide with concomitant elimination of HF, as shown in Scheme 1.13.¹²⁸ This has been reported for a variety of mono- and bimetallic rhodium(I) complexes, including $[\text{RhCl}(\text{PPh}_3)_3]$ and $[\text{Rh}_2\text{Cl}_2\text{L}_4]$ ($\text{L} = \text{PPh}_3, \text{P}(\text{C}_6\text{F}_5)_3, \text{P}(\text{C}_6\text{F}_5)_2\text{Ph}, \text{and } \text{P}(\text{C}_6\text{F}_5)\text{Ph}_2$), in which coordination of tetrafluoroethylene is followed by a series of acid induced fluoride abstractions to give the coordinated carbonyl. Hughes has also reported this reactivity with other α -fluoroalkyl complexes of iridium and rhodium.¹³



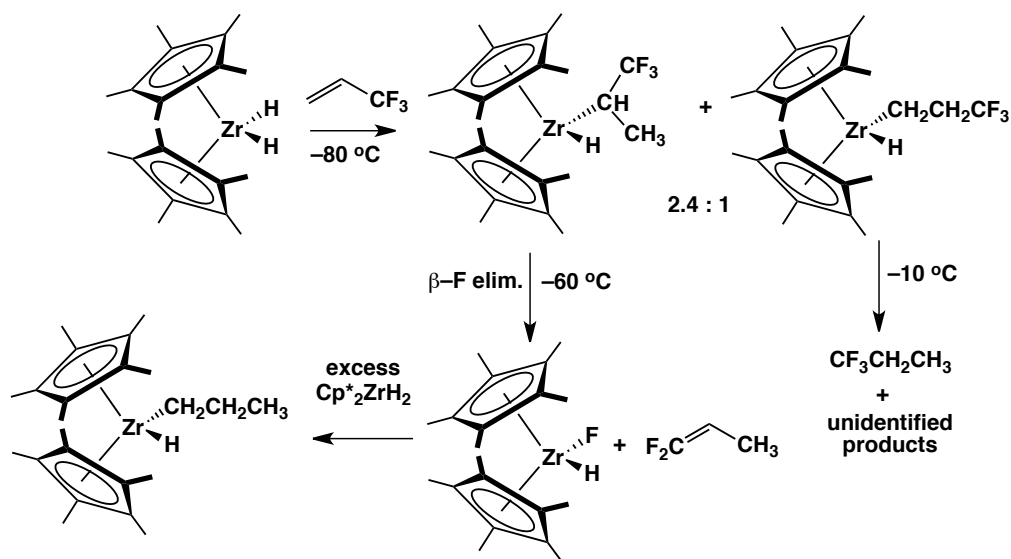
Scheme 1.13 – Hydrolysis of tetrafluoroethylene to carbon monoxide.

Defluorination of tetrafluoroethylene has been accomplished in both $[\text{Pt}(\text{C}_2\text{F}_4)(\text{PPh}_3)_2]$ ¹²⁹ and $[\text{Pd}(\text{C}_2\text{F}_4)(\text{PPh}_3)_2]$,¹³⁰ with each complex containing fluorines on α -carbons, facilitating fluoride ion abstraction by lithium iodide, producing a trifluorovinyl ligand and lithium fluoride. In the more recent palladium example, the trifluorovinyl moiety couples to arylzinc reagents, giving the first example of palladium-catalyzed coupling of tetrafluoroethylene to substituted arenes, yielding α,β,β -trifluorostyrene derivatives.¹³⁰

The activation of larger fluoroolefins, such as perfluoropropene,^{125,131-135} 3,3,3-trifluoropropene^{123,136-138} and perfluorobutadiene^{112,139} have also attracted interest in recent years, with hydrodefluorination being the most reported type of C–F activation regarding these fluoroolefins. The groups of Jones^{123,136,137} and Braun^{131,132,135} have extensively studied early and late transition-metal complexes, respectively, and their studies represent over half the reports concerning hydrodefluorination of larger fluoroolefins.

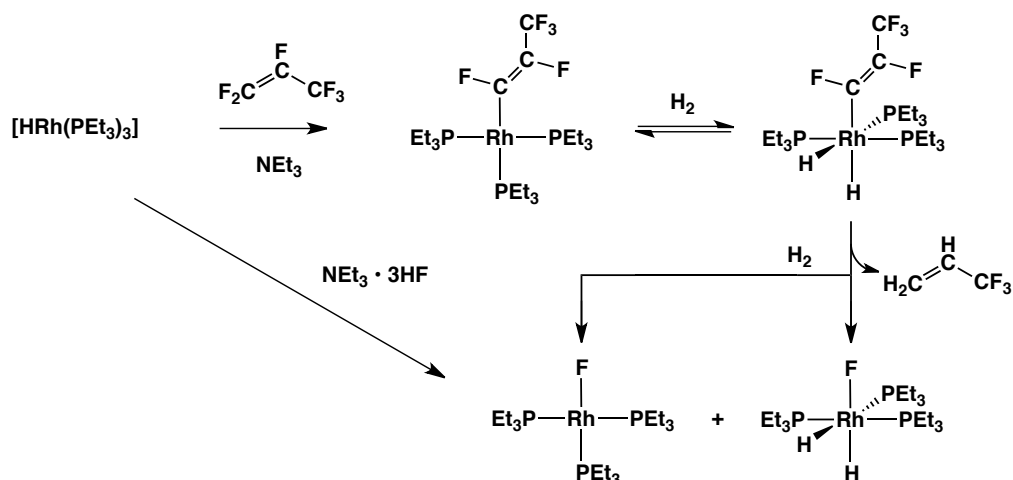
Jones and coworkers have found that the zirconocene derivatives, $[\text{Cp}^*_2\text{ZrHF}]$ and $[\text{Cp}^*_2\text{ZrH}_2]$, are useful catalysts for the hydrodefluorination of 3,3,3-trifluoropropene. Although 3,3,3-trifluoropropene only contains sp^3 -hybridized C–F bonds, the mechanism, proposed by Jones, suggests that intermediate fluoroolefins, containing fluorines bonded to sp^2 -hybridized carbons, are also being activated, as shown in Scheme 1.14. The proposed mechanism involves insertion of the fluoroolefins into the Zr–H bond, followed by β -F elimination, eventually removing all fluorines; the final product, propene, was not

isolated due to its propensity to insert into the zirconium-hydride bond of the starting material.



Scheme 1.14 – Proposed mechanism for the hydrodefluorination of 1,1,1-trifluoropropene.¹³⁶

Braun and coworkers have reported the ability of $[\text{Rh}(\text{H})(\text{PEt}_3)_3]$ to readily hydrodefluorinate perfluoropropene in the presence of hydrogen gas to produce 3,3,3-trifluoropropene (outlined in Scheme 1.15).¹³¹ This represents a rare example showing selective hydrodefluorination of *olefinic* C–F bonds, while the *fluoroalkyl* C–F bonds remain untouched. In this case, the rhodium complex is responsible for activating the C–F bonds while dihydrogen is used for the reduction of perfluoropropene to 3,3,3-trifluoropropene, whereas in the study reported by Jones,¹³⁶ $[\text{Cp}^*_2\text{ZrH}_2]$ functioned as the hydrogen source in the C–F bond activation.



Scheme 1.15 – Mechanism for the selective hydrodefluorination of 1,1,1-trifluoropropene.¹³¹

With a limited number of examples reported, involving the C–F activation of fluoroolefins, the second goal of this thesis was to continue the preliminary studies of Dr. D. Jason Anderson in our group, involving C–F activation of fluoroolefins using the transition metal complex $[\text{Ir}_2(\text{CH}_3)(\text{CO})_2(\text{dppm})_2][\text{OTf}]$.⁷⁶ Our group had previously reported that fluoroolefins containing a geminal pair of fluorines can coordinate in the bridging position, resulting in rehybridization from sp^2 to sp^3 , producing a bridging dimetallofluoroalkane moiety, which is analogous to two metal fluoroalkyl groups, as shown in Chart 1.6.⁷²

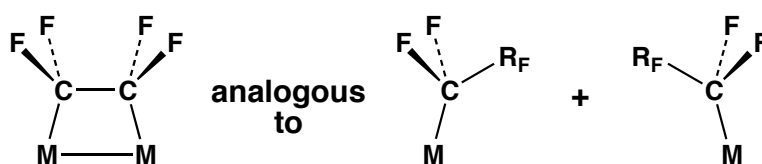


Chart 1.6 – The analogy between a bridging fluoroolefin and two metal fluoroalkyl groups.

As previously mentioned, α -C–F bonds in transition metal fluoroalkyl complexes are susceptible to fluoride ion abstraction upon the addition of relatively strong electrophiles.¹³ Preliminary studies by Jason found that the addition of trimethylsilyltriflate (Me_3SiOTf) successfully abstracts a fluoride-ion, producing a series of metal complexes that were proposed to contain bridging $\kappa^1:\eta^2$ -fluorovinyl groups, although some of the NMR data reported were

inconsistent with the proposed structures.^{76,121} He also reported double fluoride-ion abstraction in the presence of excess Me₃SiOTf, resulting in vinylidene complexes. Finally, functionalization studies were investigated, whereby hydrogen was found to functionalize the trifluorovinyl and difluorovinyl moieties, effectively converting tetrafluoroethylene to trifluoroethylene, and trifluoroethylene to *cis*-difluoroethylene. Jason also reported that carbon monoxide could also be used to functionalize the activated fluoroolefins by inducing the reductive elimination of the fluorovinyl fragment with the precoordinated methyl ligand. This led to the conversion of trifluoroethylene to *cis*-difluoropropene and 1,1-difluoroethylene to 2-fluoropropene. Although significant progress had been made by Jason, many of the details were missing (owing to his unexpectedly premature departure to take up an Instructor's position at Red Deer College) and a number of pieces of conflicting data needed to be clarified.

In Chapters 2 and 3, this chemistry will be explored in detail by first repeating the initial experiments to confirm the compounds identified and to sort out the apparent discrepancies observed, followed by investigating other methods for C–F bond activation, including weaker electrophilic sources such as water. Finally, I wished to explore a larger scope for functionalization of the activated fluorocarbyl fragments. Although the addition of hydrogen (to replace the activated C–F bond with a C–H bond) and carbon monoxide (to promote the reductive elimination of the fluorocarbyl fragment with the precoordinated methyl ligand) have already been briefly explored with a few compounds, these experiments needed to be investigated with *all* activated complexes.

Finally, in Chapter 5, I will describe initial studies regarding the C–F activation of fluoroolefins by the depm complex, [Ir₂(CO)₃(μ–H)(dep_m)₂][BAR^F₄]. Earlier in this chapter the potential advantages of the depm ligand over dp_{pm} were discussed in the context of C–H activation. It seemed that these advantages could also be put to use in the activation of C–F bonds, both in allowing better substrate access to the metals and in stabilizing the cationic species generated upon fluoride ion removal. The logic behind the use of a hydride ligand instead

of a methyl group, as previously used in the dppm chemistry, rests in its potential to behave as an internal hydrogen source for the functionalization of the C–F activated fragments, and furthermore, the presence of either hydrogen or silanes could potentially regenerate the hydride starting material, thus completing the catalytic cycle.

1.4 References

- (1) Arndtsen, B. A.; Bergman, R. G.; Mobley, T. A.; Peterson, T. H. *Acc. Chem. Res.* **1995**, *28*, 154.
- (2) Bergman, R. G. *Nature* **2007**, *446*, 391.
- (3) Jia, C. G.; Kitamura, T.; Fujiwara, Y. *Acc. Chem. Res.* **2001**, *34*, 633.
- (4) Labinger, J. A.; Bercaw, J. E. *Nature* **2002**, *417*, 507.
- (5) Ryabov, A. D. *Chem. Rev.* **1990**, *90*, 403.
- (6) Shilov, A. E.; Shul'pin, G. B. *Chem. Rev.* **1997**, *97*, 2879.
- (7) Grushin, V. V.; Alper, H. In *Activation of Unreactive Bonds and Organic Synthesis*; Murai, S., Ed.; Springer: 1999, p 193.
- (8) Luh, T. Y.; Leung, M. K.; Wong, K. T. *Chem. Rev.* **2000**, *100*, 3187.
- (9) Lin, Y.-S.; Yamamoto, A. In *Activation of Unreactive Bonds and Organic Synthesis*; Murai, S., Ed.; Springer: 1999, p 161.
- (10) Yamamoto, A. In *Advances in Organometallic Chemistry*; Stone, F. G. A., Robert, W., Eds.; Academic Press: 1992; Vol. 34, p 111.
- (11) Amii, H.; Uneyama, K. *Chem. Rev.* **2009**, *109*, 2119.
- (12) Burdeniuc, J.; Jedlicka, B.; Crabtree, R. H. *Chem. Ber. Recl.* **1997**, *130*, 145.
- (13) Hughes, R. P. *Eur. J. Inorg. Chem.* **2009**, *2009*, 4591.
- (14) Kiplinger, J. L.; Richmond, T. G.; Osterberg, C. E. *Chem. Rev.* **1994**, *94*, 373.
- (15) Perutz, R. N.; Braun, T. In *Comprehensive Organometallic Chemistry III* 2007; Vol. 1, p 725.
- (16) Richmond, T. In *Activation of Unreactive Bonds and Organic Synthesis*; Murai, S., Alper, H., Gossage, R., Grushin, V., Hidai, M., Ito, Y., Jones, W., Kakiuchi, F., van Koten, G., Lin, Y. S., Mizobe, Y., Murai, S., Murakami, M., Richmond, T., Sen, A., Suginome, M., Yamamoto, A., Eds.; Springer Berlin / Heidelberg: 1999; Vol. 3, p 243.
- (17) Torrens, H. *Coord. Chem. Rev.* **2005**, *249*, 1957.
- (18) Crabtree, R. H. *Chem. Rev.* **1985**, *85*, 245.
- (19) Jun, C.-H. *Chem. Soc. Rev.* **2004**, *33*.

- (20) Murakami, M.; Ito, Y. In *Activation of Unreactive Bonds and Organic Synthesis*; Murai, S., Ed.; Springer: 1999, p 97.
- (21) Oro, L. A.; Carmona, D.; Fraile, J. M. In *Metal-Catalysis in Industrial Organic Processes*; Chiusoli, G. P., Maitlis, P. M., Eds.; The Royal Society of Chemistry: Cambridge, 2006, p 79.
- (22) Maitlis, P. M.; Haynes, A. In *Metal-Catalysis in Industrial Organic Processes*; Chiusoli, G. P., Maitlis, P. M., Eds.; The Royal Society of Chemistry: Cambridge, UK, 2006, p 114.
- (23) Crabtree, R. H. *The Organometallic Chemistry of the Transition Metals*; John Wiley & Sons, Inc.: Hoboken, New Jersey, 2005; Vol. Fourth Edition.
- (24) Ellis, D. A.; Mabury, S. A.; Martin, J. W.; Muir, D. C. G. *Nature* **2001**, *412*, 321.
- (25) Wallington, T. J.; Schneider, W. F.; Worsnop, D. R.; Nielsen, O. J.; Sehested, J.; Debruyne, W. J.; Shorter, J. A. *Environ. Sci. Technol.* **1994**, *28*, A320.
- (26) Jones, W. D.; Kraft, B. M.; Lachicotte, R. J. *J. Am. Chem. Soc.* **2001**, *123*, 10973.
- (27) Key, B. D.; Howell, R. D.; Criddle, C. S. *Environ. Sci. Technol.* **1997**, *31*, 2445.
- (28) Trnka, T. M.; Grubbs, R. H. *Acc. Chem. Res.* **2001**, *34*, 18.
- (29) Huheey, J. E. *Inorganic Chemistry - Principles of Structure and Reactivity*; Harper & ROW, Publishers: New York, 1983.
- (30) Allred, A. L.; Rochow, E. G. *J. Inorg. Nucl. Chem.* **1958**, *5*, 264.
- (31) Silberberg, M. S. In *Chemistry – The Molecular Nature of Matter and Change*; Peterson, K. A., Ed.; McGraw-Hill: New York, 2006, p 328.
- (32) Elschenbroich, C. *Organometallics: Third, Completely Revised and Extended Edition*; Wiley-VCH: Weinheim, Germany, 2006.
- (33) McMurray, J. *Organic Chemistry*; Thomson Learning: Belmont, CA, 2004.
- (34) Godula, K.; Sames, D. *Science* **2006**, *312*, 67.

- (35) Jazzar, R.; Hitce, J.; Renaudat, A.; Sofack-Kreutzer, J.; Baudoin, O. *Chem. Eur. J.* **2010**, *16*, 2654.
- (36) Stahl, S. S.; Labinger, J. A.; Bercaw, J. E. *Angew. Chem. Int. Ed.* **1998**, *37*, 2181.
- (37) Hartwig, J. F. *Organotransition Metal Chemistry: From Bonding to Catalysis*; University Science Books: Sausalito, California, 2010.
- (38) Nolan, S. P.; Hoff, C. D.; Stoutland, P. O.; Newman, L. J.; Buchanan, J. M.; Bergman, R. G.; Yang, G. K.; Peters, K. S. *J. Am. Chem. Soc.* **1987**, *109*, 3143.
- (39) Chatt, J.; Davidson, J. M. *J. Chem. Soc.* **1965**, 843
- (40) Janowicz, A. H.; Bergman, R. G. *J. Am. Chem. Soc.* **1982**, *104*, 352.
- (41) Hoyano, J. K.; Graham, W. A. G. *J. Am. Chem. Soc.* **1982**, *104*, 3723
- (42) Stoutland, P. O.; Bergman, R. G. *J. Am. Chem. Soc.* **1985**, *107*, 4581.
- (43) Haddleton, D. M.; Perutz, R. N. *J. Chem. Soc., Chem. Commun.* **1986**, 1734.
- (44) Silvestre, J.; Calhorda, M. J.; Hoffmann, R.; Stoutland, P. O.; Bergman, R. G. *Organometallics* **1986**, *5*, 1841.
- (45) Wenzel, T. T.; Bergman, R. G. *J. Am. Chem. Soc.* **1986**, *108*, 4856.
- (46) Stoutland, P. O.; Bergman, R. G. *J. Am. Chem. Soc.* **1988**, *110*, 5732.
- (47) Bell, T. W.; Brough, S. A.; Partridge, M. G.; Perutz, R. N.; Rooney, A. D. *Organometallics* **1993**, *12*, 2933.
- (48) Tanke, R. S.; Crabtree, R. H. *Inorg. Chem.* **1989**, *28*, 3444.
- (49) Boutry, O.; Gutierrez, E.; Monge, A.; Nicasio, M. C.; Perez, P. J.; Carmona, E. *J. Am. Chem. Soc.* **1992**, *114*, 7288.
- (50) Canty, A. J.; Domingos, A. J. P.; Johnson, B. F. G.; Lewis, J. J. *J. Chem. Soc., Dalton Trans.* **1973**, 2056.
- (51) Canty, A. J.; Johnson, B. F. G.; Lewis, J. J. *Organomet. Chem.* **1972**, *43*, C35.
- (52) Domingos, A. J. P.; Johnson, B. F. G.; Lewis, J. J. *Organomet. Chem.* **1972**, *36*, C43.

- (53) Wadepohl, H.; Borchert, T.; Pritzkow, H. *J. Chem. Soc., Chem. Commun.* **1995**, 1447.
- (54) Wadepohl, H.; Borchert, T.; Pritzkow, H. *Chem. Ber. Recl.* **1997**, *130*, 593.
- (55) Bell, T. W.; Haddleton, D. M.; McCamley, A.; Partridge, M. G.; Perutz, R. N.; Willner, H. *J. Am. Chem. Soc.* **1990**, *112*, 9212.
- (56) Boncella, J. M.; Green, M. L. H. *J. Organomet. Chem.* **1987**, *325*, 217.
- (57) Boncella, J. M.; Green, M. L. H.; O'Hare, D. *J. Chem. Soc., Chem. Commun.* **1986**, 618.
- (58) Deeming, A. J.; Hasso, S.; Underhill, M.; Canty, A. J.; Johnson, B. F. G.; Jackson, W. G.; Lewis, J.; Matheson, T. W. *J. Chem. Soc., Chem. Commun.* **1974**, 807.
- (59) Deeming, A. J.; Underhill, M. *J. Organomet. Chem.* **1972**, *42*, C60.
- (60) Deeming, A. J.; Underhill, M. *J. Chem. Soc., Chem. Commun.* **1973**, 277.
- (61) Deeming, A. J.; Underhill, M. *J. Chem. Soc., Dalton Trans.* **1974**, 1415.
- (62) Ristic-Petrovic, D.; Torkelson, J. R.; Hilts, R. W.; McDonald, R.; Cowie, M. *Organometallics* **2000**, *19*, 4432.
- (63) Suzuki, H.; Omori, H.; Lee, D. H.; Yoshida, Y.; Fukushima, M.; Tanaka, M.; Moro-oka, Y. *Organometallics* **1994**, *13*, 1129.
- (64) Ghosh, C. K.; Hoyano, J. K.; Krentz, R.; Graham, W. A. G. *J. Am. Chem. Soc.* **1989**, *111*, 5480.
- (65) Ghosh, C. K.; Graham, W. A. G. *J. Am. Chem. Soc.* **1989**, *111*, 375.
- (66) Jones, W. D.; Feher, F. J. *J. Am. Chem. Soc.* **1982**, *104*, 4240.
- (67) Jones, W. D.; Feher, F. J. *J. Am. Chem. Soc.* **1984**, *106*, 1650.
- (68) Alper, H.; Gossage, R. A.; Grushin, V.; Hidai, M.; Ito, Y.; Jones, W. D.; Kakiuchi, F.; van Koten, G.; Lin, Y.-S.; Mizobe, Y.; Murai, S.; Murakami, M.; Richmond, T. G.; Sen, A.; Suginome, M.; Yamamoto, A. *Activation of Unreactive Bonds in Organic Synthesis*; Springer: Berlin, 1999.
- (69) Bruce, M. I. *Chem. Rev.* **1991**, *91*, 197.
- (70) Werner, H. *Angewandte Chemie-International Edition in English* **1990**, *29*, 1077.

- (71) Fryzuk, M. D.; Jones, T.; Einstein, F. W. B. *Organometallics* **1984**, *3*, 185.
- (72) Ristic-Petrovic, D.; Anderson, D. J.; Torkelson, J. R.; McDonald, R.; Cowie, M. *Organometallics* **2003**, *22*, 4647.
- (73) Reinking, M. K.; Fanwick, P. E.; Kubiak, C. P. *Angew. Chem. Int. Ed.* **1989**, *28*, 1377.
- (74) Reinking, M. K.; Ni, J. F.; Fanwick, P. E.; Kubiak, C. P. *J. Am. Chem. Soc.* **1989**, *111*, 6459.
- (75) Ristic-Petrovic, D., Ph.D. Thesis, University of Alberta, 2002.
- (76) Anderson, D. J., Ph.D. Thesis, University of Alberta, 2007.
- (77) Lemal, D. M. *J. Org. Chem.* **2004**, *69*, 1.
- (78) Isanbor, C.; O'Hagan, D. *J. Fluorine Chem.* **2006**, *127*, 303.
- (79) Ismail, F. M. D. *J. Fluorine Chem.* **2002**, *118*, 27.
- (80) Kirk, K. L. *J. Fluorine Chem.* **2006**, *127*, 1013.
- (81) O'Hagan, D. *J. Fluorine Chem.* **2010**, *131*, 1071.
- (82) Park, B. K.; Kitteringham, N. R.; O'Neill, P. M. *Annu. Rev. Pharmacol. Toxicol.* **2001**, *41*, 443.
- (83) Metz, B.; Kuijpers, L.; Solomon, S.; Andersen, S. O.; Davidson, O.; Pons, J.; de Jager, D.; Kestin, T.; Manning, M.; Meyer, L. *Safeguarding the Ozone Layer and the Global Climate System: Issues Related to Hydrofluorocarbons and Perfluorocarbons*, 2005.
- (84) Giesy, J. P.; Kannan, K. *Environ. Sci. Technol.* **2002**, *36*, 146A.
- (85) Kennedy, G. L.; Butenhoff, J. L.; Olsen, G. W.; O'Connor, J. C.; Seacat, A. M.; Perkins, R. G.; Biegel, L. B.; Murphy, S. R.; Farrar, D. G. *Crit. Rev. Toxicol.* **2004**, *34*, 351.
- (86) Sweetman, A. J.; Paul, A. G.; Jones, K. C. *Environ. Sci. Technol.* **2009**, *43*, 386.
- (87) Narita, T. *Polym. J.* **2011**, *43*, 497.
- (88) Shi, J.; He, J. A.; Wang, H. J. *J. Phys. Org. Chem.* **2011**, *24*, 65.
- (89) Bent, H. A. *Chem. Rev.* **1961**, *61*, 275.
- (90) O'Hagan, D. *Chem. Soc. Rev.* **2008**, *37*, 308.
- (91) Fahey, D. R.; Mahan, J. E. *J. Am. Chem. Soc.* **1977**, *99*, 2501.

- (92) Cronin, L.; Higgitt, C. L.; Karch, R.; Perutz, R. N. *Organometallics* **1997**, *16*, 4920.
- (93) Bosque, R.; Clot, E.; Fantacci, S.; Maseras, F.; Eisenstein, O.; Perutz, R. N.; Renkema, K. B.; Caulton, K. G. *J. Am. Chem. Soc.* **1998**, *120*, 12634.
- (94) Archibald, S. J.; Braun, T.; Gaunt, J. A.; Hobson, J. E.; Perutz, R. N. *J. Chem. Soc., Dalton Trans.* **2000**, 2013.
- (95) Reinhold, M.; McGrady, J. E.; Perutz, R. N. *J. Am. Chem. Soc.* **2004**, *126*, 5268.
- (96) Johnson, S. A.; Huff, C. W.; Mustafa, F.; Saliba, M. *J. Am. Chem. Soc.* **2008**, *130*, 17278.
- (97) Doster, M. E.; Johnson, S. A. *Angew. Chem. Int. Ed.* **2009**, *48*, 2185.
- (98) Johnson, S. A.; Taylor, E. T.; Cruise, S. J. *Organometallics* **2009**, *28*, 3842.
- (99) Hatnean, J. A.; Beck, R.; Borrelli, J. D.; Johnson, S. A. *Organometallics* **2010**, *29*, 6077.
- (100) Clot, E.; Eisenstein, O.; Jasim, N.; Macgregor, S. A.; McGrady, J. E.; Perutz, T. *Acc. Chem. Res.* **2011**, *44*, 333.
- (101) Johnson, S. A.; Mroz, N. M.; Valdizon, R.; Murray, S. *Organometallics* **2011**, *30*, 441.
- (102) Cotton, F. A.; McCleverty, J. A. *J. Organomet. Chem.* **1965**, *4*, 490.
- (103) Cotton, F. A.; Wing, R. M. *J. Organomet. Chem.* **1967**, *9*, 511.
- (104) Graham, W. A. G. *Inorg. Chem.* **1968**, *7*, 315.
- (105) Lichenberger, D. L.; Fenske, R. F. *Inorg. Chem.* **1974**, *13*, 486.
- (106) Hall, M. B.; Fenske, R. F. *Inorg. Chem.* **1972**, *11*, 768.
- (107) Dixon, D. A.; Fukunaga, T.; Smart, B. E. *J. Am. Chem. Soc.* **1986**, *108*, 4027.
- (108) Farnham, W. B.; Dixon, D. A.; Calabrese, J. C. *J. Am. Chem. Soc.* **1988**, *110*, 2607.
- (109) Hughes, R. P.; Laritchev, R. B.; Zakharov, L. N.; Rheingold, A. L. *J. Am. Chem. Soc.* **2004**, *126*, 2308.

- (110) Hughes, R. P.; Lindner, D. C.; Rheingold, A. L.; LiableSands, L. M. *J. Am. Chem. Soc.* **1997**, *119*, 11544.
- (111) Hughes, R. P.; Lindner, D. C.; Smith, J. M.; Zhang, D. H.; Incarvito, C. D.; Lam, K. C.; Liable-Sands, L. M.; Sommer, R. D.; Rheingold, A. L. *Dalton Trans.* **2001**, 2270.
- (112) Hughes, R. P.; Rose, P. R.; Rheingold, A. L. *Organometallics* **1993**, *12*, 3109.
- (113) Hughes, R. P.; Smith, J. M. *J. Am. Chem. Soc.* **1999**, *121*, 6084.
- (114) Hughes, R. P.; Zhang, D. H.; Zakharov, L. N.; Rheingold, A. L. *Organometallics* **2002**, *21*, 4902.
- (115) Caulton, K. G. *J. Organomet. Chem.* **2001**, *617*, 56.
- (116) Huang, D. J.; Koren, P. R.; Folting, K.; Davidson, E. R.; Caulton, K. G. *J. Am. Chem. Soc.* **2000**, *122*, 8916.
- (117) Ferrando-Miguel, G.; Gerard, H.; Eisenstein, O.; Caulton, K. G. *Inorg. Chem.* **2002**, *41*, 6440.
- (118) Renkema, A.; Werner-Zwanziger, U.; Pagel, M. D.; Caulton, K. G. *J. Mol. Catal. A: Chem.* **2004**, *224*, 125.
- (119) Peterson, A. A.; McNeill, K. *Organometallics* **2006**, *25*, 4938.
- (120) Peterson, A. A.; Thoreson, K. A.; McNeill, K. *Organometallics* **2009**, *28*, 5982.
- (121) Anderson, D. J.; McDonald, R.; Cowie, M. *Angew. Chem. Int. Ed.* **2007**, *46*, 3741.
- (122) Slaney, M. E.; Anderson, D. J.; Ristic-Petrovic, D.; McDonald, R.; Cowie, M. *Accepted by Chem. Eur. J.*, Nov. 8, 2011.
- (123) Kraft, B. M.; Jones, W. D. *J. Am. Chem. Soc.* **2002**, *124*, 8681.
- (124) Jones, M. T.; McDonald, R. N. *Organometallics* **1988**, *7*, 1221.
- (125) Green, M.; Laguna, A.; Spencer, J. L.; Stone, F. G. A. *J. Chem. Soc., Dalton Trans.* **1977**, 1010.
- (126) Booth, B. L.; Haszeldine, R. N.; Mitchell, P. R.; Cox, J. J. *Chem. Comm.* **1967**, 529.

- (127) Bonnet, J. J.; Mathieu, R.; Poilblanc, R.; Ibers, J. A. *J. Am. Chem. Soc.* **1979**, *101*, 7487.
- (128) Kemmitt, R. D. W.; Nichols, D. I. *J. Chem. Soc. A* **1969**, 1577.
- (129) Hacker, M. J.; Littlecott, G. W.; Kemmitt, R. D. W. *J. Organomet. Chem.* **1973**, *47*, 189.
- (130) Ohashi, M.; Kambara, T.; Hatanaka, T.; Saijo, H.; Doi, R.; Ogoshi, S. *J. Am. Chem. Soc.* **2011**, *133*, 3256.
- (131) Braun, T.; Noveski, D.; Neumann, B.; Stammler, H. G. *Angew. Chem. Int. Ed.* **2002**, *41*, 2745.
- (132) Braun, T.; Salomon, M. A.; Altenhoner, K.; Teltewskoi, M.; Hinze, S. *Angew. Chem. Int. Ed.* **2009**, *48*, 1818.
- (133) Kirkham, M. S.; Mahon, M. F.; Whittlesey, M. K. *Chem. Comm.* **2001**, 813.
- (134) Maples, P. K.; Green, M.; Stone, F. G. A. *J. Chem. Soc., Dalton Trans.* **1973**, 2069.
- (135) Noveski, D.; Braun, T.; Schulte, M.; Neumann, B.; Stammler, H. G. *Dalton Trans.* **2003**, 4075.
- (136) Jones, W. D. *Dalton Trans.* **2003**, 3991.
- (137) Kraft, B. M.; Lachicotte, R. J.; Jones, W. D. *J. Am. Chem. Soc.* **2000**, *122*, 8559.
- (138) Kuhnel, M. F.; Lentz, D. *Angew. Chem. Int. Ed.* **2010**, *49*, 2933.
- (139) Roundhill, D. M.; Lawson, D. N.; Wilkinson, G. *J. Chem. Soc. A* **1968**, 845.

Chapter 2 – The Bridged Binding Mode as a New, Versatile Template for the Selective Activation of Carbon-Fluorine Bonds in Fluoroolefins: Activation of Trifluoroethylene[†]

2.1 Introduction

The selective activation of otherwise inert chemical bonds using metal complexes has been one of the pivotal achievements in chemistry over the past few decades,¹ presaging the use of plentiful, yet unreactive substrates, such as alkanes and dinitrogen, as feedstocks for the chemical industry. Although most attention has been directed at the substantial challenges associated with the selective activation of carbon-hydrogen bonds,²⁻¹⁰ particularly in unreactive alkanes, a challenge that until recently had been considered one of the “Holy Grails” of synthetic chemistry,¹¹ there has been significant recent interest in the activation of other inert bonds such as carbon-carbon,^{9,12,13} carbon-oxygen,^{14,15} carbon-chlorine,^{16,17} and nitrogen-nitrogen,^{18,19} as new more efficient synthetic methodologies are sought for the generation of important molecules, and for the destruction of persistent pollutants.

As is the case for studies in the activation of other carbon-heteroatom bonds, the field of carbon-fluorine bond activation is relatively new, with most concerted efforts having been expended over the past 15 years or so.²⁰⁻²⁵ Studies in C–F bond activation are being driven in part by the important applications of fluorocarbons in areas such as pharmaceuticals, pesticides, polymers and refrigerants and the consequent need to develop new synthetic routes to the required fluorocarbon products.^{26,27} Recent studies also indicate that chlorofluorocarbons (CFC's) and hydrochlorofluorocarbons (HCFC's) are significant contributors to the degradation of the earth's ozone layer and major

[†] The work presented in this chapter has previously been reported. See Slaney, M.E.; Anderson, D.J.; McDonald, R.; Ferguson, M. J.; Cowie, M. *J. Am. Chem. Soc.* **2010**, *132*, 16544

contributors as greenhouse gases, thereby necessitating investigations into methods of degrading these otherwise persistent molecules.²⁸⁻³⁰

Complexes involving a range of metals from across the periodic table have shown a propensity to activate carbon-fluorine bonds,²⁰⁻²⁴ and although significant successes have been achieved in the activation of fluorinated aryl systems,³¹⁻³⁷ including catalytic hydrodefluorination of perfluorobenzene,³⁸ surprisingly little has been reported on metal-promoted activation of fluorine-containing olefins.³⁹⁻⁴⁹ The main focus involving fluoroolefin activation has involved hydrodefluorination, a process in which a C–F bond is replaced by a C–H bond.⁵⁰⁻⁵⁶ However, the main objective of this reaction has been to replace as many C–F bonds as possible with C–H bonds, and as such, selectivity has not been the main focus. In fact, only a few examples of selective C–F bond activation of fluoroolefins have been reported,^{40,52,57-61} and of those, the selectivity observed has mainly differentiated between C–F bonds involving sp^2 and sp^3 -hybridized carbons.^{40,57,61} Braun and coworkers have shown that $[\text{HRh}(\text{PEt}_3)_3]$ can exclusively activate the sp^2 -hybridized bonds of hexafluoropropene, leaving all sp^3 -hybridized C–F bonds untouched, which in the presence of hydrogen gas yields 1,1,1-trifluoropropane.⁵⁷ Another study by Jones and coworkers has shown Cp^*ZrH_2 to be an effective reagent for the C–F bond activation of hexafluoropropene, in which the byproduct is Cp^*ZrHF ; as a result, 6 equivalents of the dihydride are necessary to activate all C–F bonds.⁵² The addition of only 1 equivalent results in the selectively hydrodefluorinated product 1,2,3,3,3-pentafluoropropene. This study has recently been expanded to perfluorocyclobutene and perfluorocyclopentene, in which selective sp^2 -hybridized C–F activation has been demonstrated with perfluorocyclobutene and a preference for sp^2 -hybridized over sp^3 -hybridized C–F activation in the case of perfluorocyclopentene.⁶¹

Another selective transformation observed in fluoroolefin C–F bond activation is the [1,2]-fluoride shift, which has been shown to occur in a few multimetallic systems, involving trifluoroethylene,⁵⁹ tetrafluoroethylene^{62,63} and hexafluoropropene.⁵⁹ Although selectivity is not an issue in the [1,2]-fluoride shift

in which a 1,2,2,2-tetrafluoroethylidene-bridged species is generated from tetrafluoroethylene, owing to its symmetry, selectivity has been observed in the case of trifluoroethylene, in which the lone vicinal fluorine is exclusively transferred, resulting in a 2,2,2-trifluoroethylidene-bridged product, and also with hexafluoropropene, in which the fluorine geminal to the trifluoromethyl group is exclusively transferred, giving a hexafluoroisopropylidene group. In all cases, the proposed mechanism involves fluoride-ion abstraction, to give a fluorovinyl group, followed by nucleophilic attack at the β -carbon of the fluorovinyl group by fluoride ion, giving the final [1,2]-fluoride-shift product,^{59,62,63} although it is not clear what species is responsible for the fluoride-abstraction step.

Our strategy for effecting the facile and selective activation of C–F bonds in fluoroolefins has been to use adjacent metals that can interact with the fluoroolefins in a cooperative manner. In a bridging arrangement, the fluoroolefin can be viewed as a 1,2-dimetallated fluoroalkane, in which complete rehybridization of the olefin carbons to sp^3 has occurred, as shown for the trifluoroethylene ligand in Chart 2.1. In such an arrangement each end of the bridging fluoroolefin can be viewed as a fluoroalkyl group and as such should be susceptible to fluoride ion abstraction from the α -carbons, as is well documented in fluoroalkyl complexes of late transition metal complexes.^{21,50,64-67}

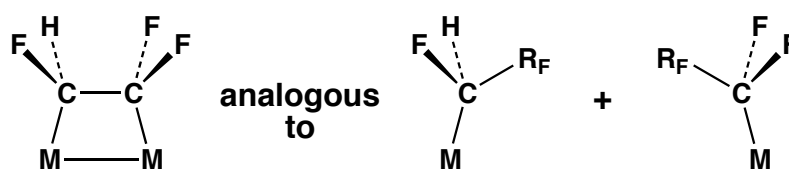


Chart 2.1 – How a bridging fluoroolefin unit is analogous to two substituted fluoroalkyl ligands.

We have previously reported that the binuclear complex $[\text{Ir}_2(\text{CH}_3)(\text{CO})_2(\text{dppm})_2][\text{OTf}]$ (**1**) binds a number of fluoroolefins ($\text{C}_2\text{H}_x\text{F}_{(4-x)}$, $x = 0 - 4$) either in the traditional η^2 -coordination mode at a single metal (ethylene, vinylfluoride, *cis*-difluoroethylene and 1,1-difluoroethylene) or in a bridging mode between the pair of metals (1,1-difluoroethylene, trifluoroethylene and

tetrafluoroethylene). For 1,1-difluoroethylene, which can bond in both the terminal and bridging modes, we reported facile C–F bond activation at –40 °C, in the bridging mode, while even at ambient temperature the terminally bound olefin was unreactive.^{39,68,69} In this chapter, parts of which have been previously communicated,³⁸ we describe a series of C–F bond activation processes involving trifluoroethylene and outline the selective functionalization of this fluoroolefin under mild conditions yielding a number of fluorocarbon products.

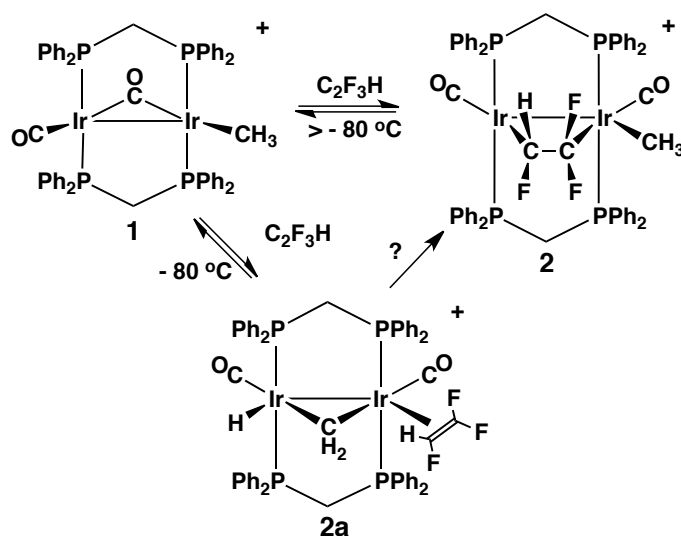
2.2 Results

2.2.1 Trifluoroethylene Coordination

The diiridium complex, $[\text{Ir}_2(\text{CH}_3)(\text{CO})_2(\text{dppm})_2][\text{CF}_3\text{SO}_3]$ (**1**) reacts with trifluoroethylene at –80 °C to form the highly labile adduct $[\text{Ir}_2(\text{H})(\eta^2\text{-CF}_2=\text{CFH})(\text{CO})_2(\mu\text{-CH}_2)(\text{dppm})_2][\text{CF}_3\text{SO}_3]$ (**2a**) in approximately 10% yield together with starting material. Binding of the olefin in an η^2 -fashion at one metal is accompanied by C–H activation of the methyl group at the adjacent metal yielding bridging methylene and terminal hydride fragments, as outlined in Scheme 2.1. Owing to the low abundance of **2a** some of the spectral parameters could not be observed. Nevertheless, substrate attack at one metal in **1** accompanied by methyl C–H activation at the adjacent metal, as proposed for **2a**, is well precedented reactivity, having been observed with a number of olefins⁶⁹ and monodentate ligands (CO, PR_3).⁷⁰ Furthermore, the spectral parameters for these previously characterized products match well with those of **2a**, allowing us to confidently assign the structure shown.

The $^{31}\text{P}\{^1\text{H}\}$ NMR spectrum of **2a** appears as two complex, unresolved multiplets at δ –4.9 and –5.7. Although a two-resonance pattern is suggestive of an AA'BB' spin system, the binding of the prochiral trifluoroethylene ligand, as shown, should give rise to a more complex pattern, characteristic of an ABCD spin system, by virtue of “left/right” and “top/bottom” asymmetry in **2a**, (as viewed in Scheme 2.1). However, the complex nature of the $^{31}\text{P}\{^1\text{H}\}$ patterns suggest coincidental overlap of two sets of the four expected resonances of the

ABCD spin pattern. In the ^1H NMR spectrum only two resonances appear for the dppm methylene resonances, again presumably due to coincidental overlap involving pairs of the four expected signals, while the signals for the metal-bridged methylene group and the olefin hydrogen could not be resolved from the signals of starting materials. The hydride ligand is observed as a broad unresolved signal at $\delta -12.70$ that appears unaffected by ^{31}P decoupling experiments. In the $^{13}\text{C}\{^1\text{H}\}$ NMR spectrum of a ^{13}CO -enriched sample the carbonyl resonances appear as broad signals at $\delta 187.6$ and 195.2 , close to the values previously noted for analogous species,^{39,69,70} while in a sample derived from $^{13}\text{CH}_3$ -enriched **1**, the methylene carbon appears at $\delta 44.2$, typical of a bridging CH_2 group in related diiridium systems.⁷⁰ In addition to free trifluoroethylene and triflate ion, the ^{19}F NMR spectrum shows three distinct signals for the coordinated olefin. Two doublets appear at $\delta -94.4$ and -97.3 for the pair of geminal fluorines, and their mutual coupling of 156.8 Hz, compared to 83 Hz geminal coupling in the free olefin, suggests significant olefin rehybridization towards sp^3 .⁷¹ The third fluoroolefin resonance appears as an unresolved multiplet at $\delta -220.1$. In a previous study of fluoroolefin binding to **1** this low-temperature $\eta^2\text{-C}_2\text{F}_3\text{H}$ adduct was not observed,⁶⁹ although analogous adducts have been observed with ethylene,⁶⁹ allenes⁷² and 1,1-difluoroethylene.^{39,69}



Scheme 2.1 – Coordination of trifluoroethylene to compound **1**.

Warming this sample above $-80\text{ }^{\circ}\text{C}$ brings about the disappearance of **2a** and the accompanying appearance of $[\text{Ir}_2(\text{CH}_3)(\text{CO})_2(\mu\text{-C}_2\text{F}_3\text{H})(\text{dppm})_2][\text{CF}_3\text{SO}_3]$ (**2**), such that at $-60\text{ }^{\circ}\text{C}$ none of **2a** remains, with only **2** appearing as a product together with unreacted **1**. The formation of **2** is slow at lower temperatures, and even at $-20\text{ }^{\circ}\text{C}$ quantitative formation of **2** requires approximately 1h. This product is less stable than its tetrafluoroethylene analogue,^{39,69} reverting to starting materials at ambient temperature over a period of 2 h. In Scheme 2.1 we have indicated the possibility of direct transformation of **2a** to **2**. However, owing to the low concentration of **2a** we cannot differentiate between this path and the path occurring via $\text{C}_2\text{F}_3\text{H}$ dissociation and recoordination, proceeding through the precursor (**1**).

Compound **2** has been previously reported;^{39,69} however, our inability to obtain some of the spectroscopic data at the time led us to incorrectly assign the orientation of the fluoroolefin ligand, which we now, with better NMR data, can confidently assign as that shown in Scheme 2.1. The full spectroscopic characterization of **2**, carried out at $0\text{ }^{\circ}\text{C}$, is now reported.

The $^{31}\text{P}\{^1\text{H}\}$ NMR resonances of compound **2** appear as multiplets at δ 17.2 (1P), 14.4 (1P) and 5.1 (2P), in which two resonances are coincidentally overlapped. The lack of symmetry is consistent with the structure shown, in which there is left/right asymmetry by virtue of the differing metal environments, while the top/bottom asymmetry results from coordination of the prochiral olefin to give a chiral centre at the CHF end of this unit. The ^1H NMR spectrum confirms the unsymmetrical nature of **2**, with the resonances for the dppm methylene protons appearing as broad multiplets at δ 3.97 (1H), 3.92 (2H), and 3.56 (1H), with coincidental overlap of the middle two resonances. The iridium-bound methyl group appears as a triplet, integrating for three protons, at δ 0.34, coupling equally to the pair of adjacent phosphorus nuclei (see 2.5 Experimental for coupling information). Selective phosphorus decoupling experiments have shown that this moiety is coupled to the ^{31}P nuclei giving rise to the overlapping resonances at δ 5.1 in the ^{31}P NMR spectrum. It is not surprising

that the overlapping ^{31}P signals correspond to the side of the molecule in the more symmetrical environment adjacent to the CF_2 end of the olefin. The unique olefinic hydrogen appears as a broad doublet of doublets of doublets at δ 6.90, at -60°C in the ^1H NMR spectrum, showing distinct coupling to all three associated fluorines. In the original report of this compound, this resonance was not identified.⁶⁹ The $^{13}\text{C}\{^1\text{H}\}$ NMR spectrum of a ^{13}CO -enriched sample of **2** shows two inequivalent terminal carbonyl resonances as broad multiplets at δ 185.6 and 197.2 and selective ^{31}P decoupling experiments establish that each carbonyl is bound to a different metal. In the ^{19}F NMR spectrum three broad signals are observed at δ -53.4 , -82.2 and -194.4 , all of which are shifted to low field from the free ligand, the corresponding resonances of which appear at δ -100 , -126 and -205 , respectively. This shift to lower-field, with the geminal pair having moved the farthest, is consistent with rehybridization of the associated carbons toward sp^3 , and is consistent with the addition of this group across the pair of metals. A similar, yet not nearly as pronounced an effect is also observed in the η^2 -adduct (**2a**); however, rehybridization is more pronounced in the bridging complex, and the large mutual coupling of 253.3 Hz between the two lower-field resonances is also indicative of an sp^3 hybridized $-\text{CF}_2$ group.⁷³ The significant decrease in the $^3J_{\text{FF}}$ *trans*-coupling to 24.8 Hz, from the value of 115 Hz in the free ligand further supports the bridging arrangement, in which substantial rehybridization has occurred. ^{19}F NMR experiments with selective ^{31}P -decoupling have also shown that the high-field resonance at δ -194.4 , assignable to the vicinal fluorine, is coupled to the ^{31}P resonances at δ 14.4 and 17.2, while the two low-field resonances at δ -53.4 and -82.2 , assignable to the two geminal fluorines, are coupled to the ^{31}P resonance at δ 5.1. This suggests that the more-fluorinated end of the fluoroolefin, is bound to the metal associated with the methyl group.

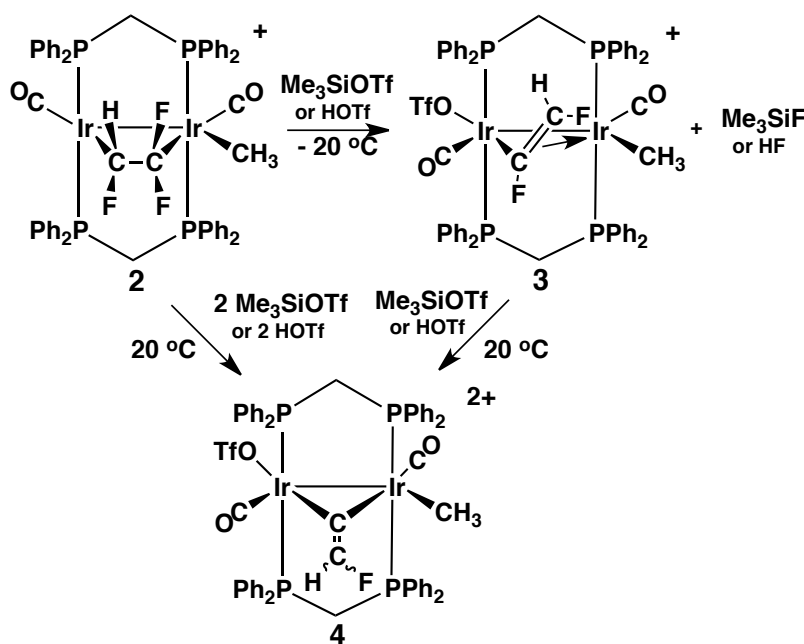
Such an orientation of the olefin is not that predicted on the basis of steric arguments, having the slightly more encumbered disubstituted end of the olefin bound to the more crowded metal centre. However, the orientation now proposed is the electronically favoured arrangement, in which the more electron-withdrawing olefin substituents are adjacent to the more electron-rich metal,

having the donor methyl group attached and assuming the positive charge of the complex is localized on the other metal giving two mutually bonded Ir(II) centres.

As noted above, we had anticipated that the bridged arrangement of fluoroolefin ligands and the resulting rehybridization could lead to labilization of the fluoride substituents, making carbon-fluorine bond activation feasible, so we set out to investigate the different ways in which such activation could be initiated. In what follows, we discuss the different C–F bond activation steps, followed by functionalization of the generated fluorocarbyl units to generate transformed fluorocarbons.

2.2.2 C–F Bond Activation

2.2.2.1 Activation by Strong Lewis Acids. The reaction of **2** with either triflic acid (HOSO₂CF₃) or trimethylsilyl triflate (Me₃SiOSO₂CF₃) at –20 °C quantitatively yields the *cis*-difluorovinyl-bridged product, [Ir₂(CH₃)(OTf)(CO)₂(μ - κ^1, η^2 -CF=CFH)(dppm)₂][CF₃SO₃] (**3**), as outlined in Scheme 2.2. This product is stable at ambient temperature allowing for its isolation and complete characterization.



Scheme 2.2 – C–F bond activation of the bridging trifluoroethylene moiety by Me₃SiOTf and/or HOTf.

The $^{31}\text{P}\{^1\text{H}\}$ NMR spectrum of **3** again reveals a pattern that is characteristic of an ABCD spin system having four inequivalent phosphorus nuclei, as shown in Figure 2.1, which is consistent with the structure shown in Scheme 2.2. Mutual coupling of $^2J_{\text{PP}} = 336.5$ Hz is observed for the resonances at $\delta -2.0$ and -19.3 while the resonances at $\delta 9.5$ and -3.3 display mutual coupling of 331.1 Hz; the magnitude of these $^2J_{\text{PP}}$ values establishes that the diphosphine units have remained *trans* at both metal centres.

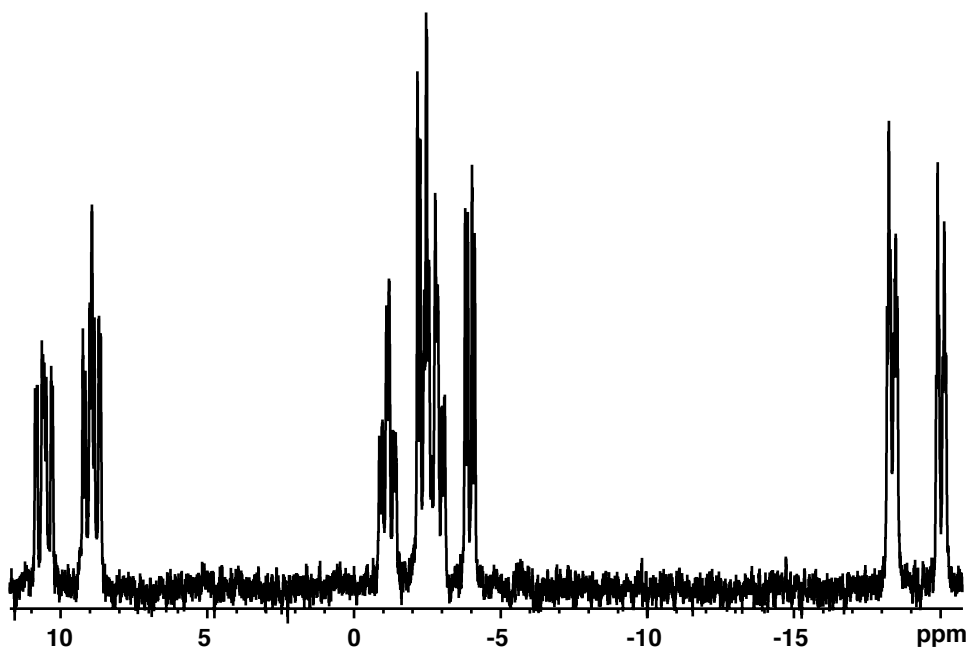


Figure 2.1 – $^{31}\text{P}\{^1\text{H}\}$ NMR spectrum (202 MHz) of compound **3**, displaying the large *trans*-phosphine couplings of an ABCD spin-system.

In the ^1H NMR spectrum the dppm methylene protons appear as four multiplets at $\delta 6.14$ (1H), 5.69 (1H), 5.57 (1H) and 4.70 (1H), consistent with the absence of top/bottom and front/back symmetry in the product, as shown in Figure 2.2. The iridium-bound methyl group appears as a triplet at $\delta 1.44$, displaying equal coupling to the adjacent two phosphorus nuclei at $\delta -2.0$ and -19.3 , while the vinylic proton is identified by its distinct splitting pattern, appearing as a multiplet (dddd) at $\delta 6.00$. The most prominent coupling is the diagnostic geminal hydrogen-fluorine coupling ($^2J_{\text{HF}}$) of 65.6 Hz consistent with an approximate sp^2 hybridized $-\text{C}(\text{H})\text{F}$ group.⁷¹ The smaller coupling ($^3J_{\text{HF}} =$

10.3 Hz) is suggestive of a *trans*-arrangement of H and the second fluorine across the olefinic bond. These couplings are consistent with those seen in the ^{19}F NMR spectrum. Selective $^1\text{H}\{^{31}\text{P}\}$ decoupling experiments establish that two of the additional couplings are due to the neighboring phosphorus atoms. The smaller coupling ($^3J_{\text{HP}} = 5.4$ Hz) arises through the η^2 -interaction of the fluorovinyl framework and involves the phosphorus atom in a pseudo-*cis* arrangement, whereas the larger coupling ($^3J_{\text{HP}} = 16.6$ Hz) is assigned to the pseudo-*trans* phosphorus again through the η^2 -interaction. No coupling is observed between the vinylic proton and the two phosphorus atoms adjacent to the metal-vinyl σ -bond.

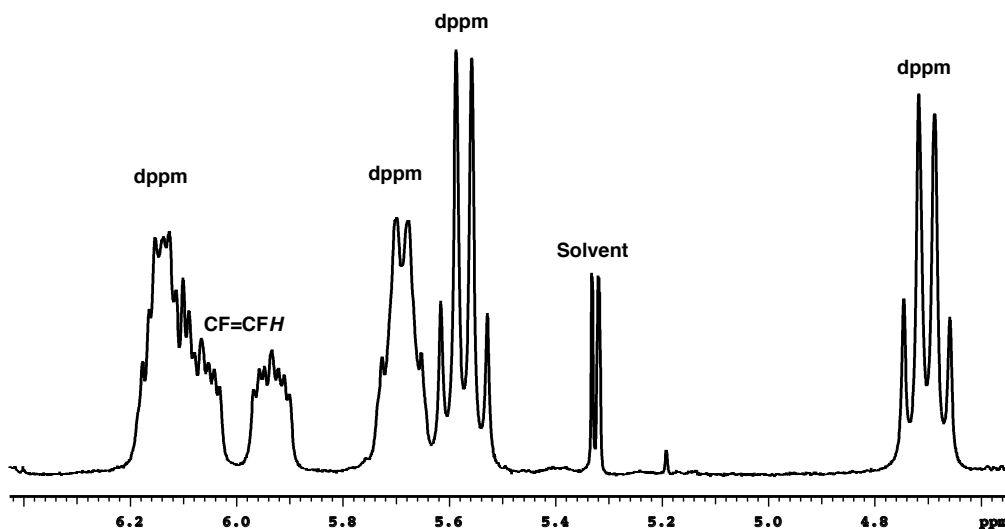


Figure 2.2 – ^1H NMR spectrum (498 MHz) of compound **3**, displaying four unique methylene proton resonances, confirming the loss of 'front/back' and 'top/bottom' symmetry.

The $^{13}\text{C}\{^1\text{H}\}$ NMR spectrum of a ^{13}CO -enriched sample of **3** shows two multiplets at δ 165.9 and 172.1, consistent with a terminal arrangement of both, and selective ^{31}P decoupling establishes that each carbonyl is bound to a different metal. Furthermore, the stretches at 2053 and 2007 cm^{-1} in the IR spectrum support the terminal binding of both.

In the ^{19}F NMR spectrum the free and the coordinated triflate ions appear at δ -79.5 and -77.7, respectively, together with two complex multiplets at δ -

24.2 and -172.7 for the difluorovinyl group displaying fluorine-phosphorus, fluorine-proton, and fluorine-fluorine coupling. The fluorine-proton coupling is consistent with that described above, with the higher field signal corresponding to the geminal partner to the proton. This signal also shows coupling of 33.2 Hz to the *cis* fluorine. Selective $^{19}\text{F}\{^{31}\text{P}\}$ decoupling experiments have established that both fluorine atoms couple to ^{31}P nuclei on different ends of the framework; however, only peak sharpening was observable as the actual coupling was unresolved.

An X-ray crystallographic study of **3** confirms the geometry proposed above, as shown for one of the two independent cations in Figure 2.3, clearly showing the unique κ^1, η^2 -bridging coordination mode of the vinyl unit and the mutually *cis* arrangement of fluorine atoms. Although $\mu\text{-}\kappa^1, \eta^2$ -vinyl ligands are quite common,⁷⁴⁻⁸² we are unaware of any other examples in which this binding mode is adopted by fluorovinyl groups. The orientation shown for the bridging fluorovinyl unit clearly demonstrates why all four phosphorus, as well as all four dppm methylene protons, are rendered chemically inequivalent, as observed in the NMR experiments. The arrangement of the ancillary ligands in the complex, as proposed from the spectroscopy, is also confirmed in this X-ray study. All metrical parameters within the complex are essentially as expected. The Ir(1) – C(3) σ -vinyl linkage, at 1.95(1) and 1.93(1) Å (for the independent molecules) is typical while the distances of the vinyl carbons to the adjacent metal (Ir(2) – C(3) = 2.24(1) and 2.26(1) Å; Ir(2) – C(4) = 2.15(1) and 2.22(1)) are somewhat longer for this π interaction. The vinylic C(3) – C(4) bond (1.37(2) and 1.39(2)) is somewhat elongated from that (*ca.* 1.34 Å) in an uncomplexed vinyl group.

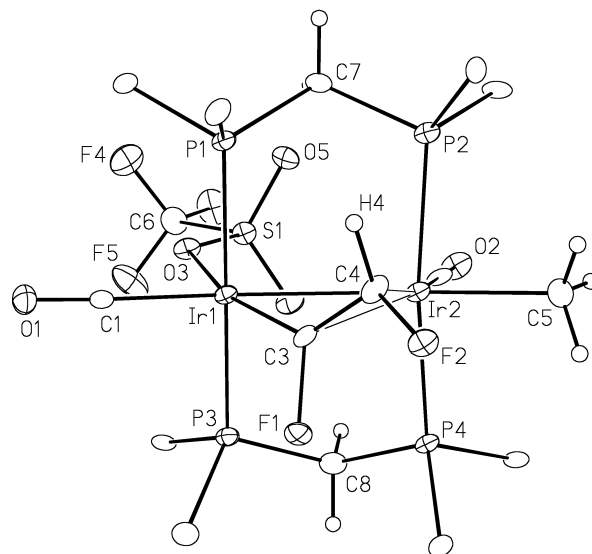


Figure 2.3 – Perspective view of one of the two crystallographically-independent $[\text{Ir}_2(\text{CH}_3)(\text{OSO}_2\text{CF}_3)(\text{CO})_2(\mu\text{-}\kappa^1, \eta^2\text{-CF=CHF})(\text{dppm})_2]^+$ (**3**) complex ions (molecule A) showing the atom labelling scheme. Non-hydrogen atoms are represented by Gaussian ellipsoids at the 20% probability level. Hydrogen atoms are shown with arbitrarily small thermal parameters. For the phenyl groups only the ipso carbons are shown. Relevant bond distances (Å) and angles ($^\circ$) for the pair of independent molecules: Ir(1)-Ir(2) = 2.8778(7), 2.8767(7); Ir(1)-C(3) = 1.95(1), 1.93(1); Ir(2)-C(3) = 2.24(1), 2.26(1); Ir(2)-C(4) = 2.15(1), 2.22(1); C(3)-C(4) = 1.37(2), 1.39(2); F(1)-C(3) = 1.41(1), F(2)-C(4) = 1.42(1), 1.38(1); Ir(1)-C(3)-F(1) = 116.1(8), 119.5(8); F(1)-C(3)-C(4) = 112.7(10), 108.3(10); F(2)-C(4)-C(3) = 116.2(11), 122.0(10).

2.2.2.2 Removal of a Second Fluoride Ion. Reaction of compound **3** with an additional equivalent of Me_3SiOTf at ambient temperature, overnight, results in C-F activation and fluoride ion removal from the α -position of the difluorovinylidene group to yield the monofluorovinylidene-bridged product, $[\text{Ir}_2(\text{CH}_3)(\text{OTf})(\text{CO})_2(\mu\text{-C}_2\text{FH})(\text{dppm})_2][\text{CF}_3\text{SO}_3]_2$ (**4**), as shown in Scheme 2.2. Compound **4** can be prepared directly from **2** by reaction with two or more equivalents of Me_3SiOTf at ambient temperature.

The $^{31}\text{P}\{^1\text{H}\}$ spectrum of **4** shows two resonances owing to the inequivalence of the two metals. In this case, the fluorovinylidene group lies in the equatorial plane of the CO, CH_3 and OTf ligands resulting in mirror symmetry relating the two bridging dppm ligands. The ^1H NMR spectrum shows the iridium-bound methyl group as a triplet, integrating for three protons, at the relatively down-field chemical shift of δ 2.15 and selective ^{31}P -decoupling

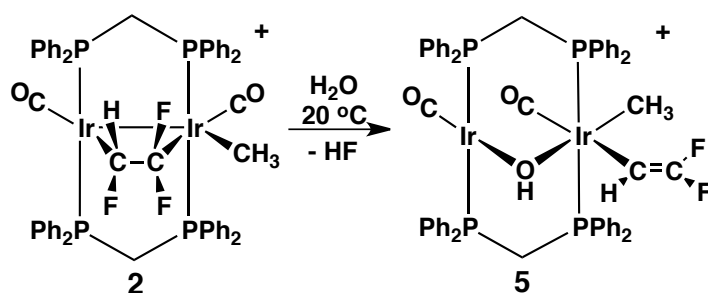
experiments indicate that these protons couple to the pair of phosphorus nuclei at $\delta -5.0$. The chemical shift of the fluorovinylidene proton appears as a broad doublet at $\delta 8.60$, showing 85.2 Hz coupling to fluorine. In a ^{13}C -enriched sample of **4**, the $^{13}\text{C}\{^1\text{H}\}$ NMR spectrum shows two broad multiplet carbonyl resonances at $\delta 153.4$ and 176.8. Whereas the high-field carbonyl shows coupling only to the pair of phosphorus nuclei on the non-methylated metal ($\delta -21.0$) of 11.5 Hz, and is therefore presumably terminally bound to this metal, the lower-field carbonyl shows coupling to both sets of diphosphine resonances, the larger 16.6 Hz coupling to the pair of phosphorus nuclei resonating at $\delta -5.0$, and small, unresolvable coupling to the phosphorus nuclei at $\delta -21.0$, suggesting small $^3J_{\text{C-P}}$ coupling through the metal-metal bond. The ^{13}C -enriched methyl group displays a broad, relatively low-field singlet at $\delta 40.5$, presumably shifted downfield due to the higher positive charge on the complex. In the ^{19}F NMR spectrum the monofluorovinylidene group appears as a doublet at $\delta -107.4$, having a $^2J_{\text{HF}}$ coupling of 86.0 Hz, comparable to the values seen in related fluorovinyl complexes that display geminal H–F coupling ($^2J_{\text{HF}}$).⁸³

In all reactions involving fluoride-ion abstraction by trimethylsilyl triflate, the resulting trimethylsilyl fluoride is obvious in the ^{19}F NMR spectrum, displaying a distinctive resonance at $\delta -159.2$ with coupling to the methyl protons along with the corresponding doublet in the ^1H NMR at $\delta 0.25$ ($^3J_{\text{HF}} = 7.5$ Hz),^{84,85} while in these small-scale reactions involving triflic acid, the HF produced is never directly detected, although etching of the NMR tubes occurs.

2.2.2.3 Activation by Water. Remarkably, compound **2** even reacts with water, leading to facile and selective C-F activation over 30 min at ambient temperature to give $[\text{Ir}_2(\text{CH}_3)(\kappa^1\text{-C(H)=CF}_2)(\text{CO})_2(\mu\text{-OH})(\text{dppm})_2][\text{OTf}]$ (**5**) as outlined in Scheme 2.3. This reaction differs from those involving triflic acid and trimethylsilyl triflate in several ways. Replacement of the coordinated triflate in **3** by hydroxide ion leads to an hydroxide-bridged product, owing to the greater tendency of this anion to bridge, and results in the fluorovinyl group being displaced from a bridging position, as in **3**, to a terminal position in **5**. More

significantly, however, activation by water has occurred with a different regiochemistry, by abstraction of the lone fluoride adjacent to hydrogen to give the 2,2-difluorovinyl product, instead of a *cis*-difluorovinyl product as observed in 3.

The $^{31}\text{P}\{^1\text{H}\}$ NMR spectrum of $[\text{Ir}_2(\text{CH}_3)(\kappa^1\text{-C(H)=CF}_2)(\text{CO})_2(\mu\text{-OH})(\text{dppm})_2][\text{OTf}]$ again appears as two resonances; while the resonance at δ 13.3 is a well resolved multiplet, the other at δ -15.3 is a broad, unresolvable multiplet due to additional coupling to one fluorine of the fluorovinyl unit.



Scheme 2.3 – C–F bond activation of the bridging trifluoroethylene moiety by water.

The ^1H NMR signals are as expected, with the exception of the methyl peak which appears at δ 0.39 as a *doublet* of triplets; in addition to the anticipated coupling of this group to the pair of adjacent ^{31}P nuclei, coupling of 2.5 Hz to a vinylic fluorine is also observed, as evidenced by collapse of the methyl signal to a doublet in the $^1\text{H}\{^{31}\text{P}\}$ experiment. The bridging hydroxide proton appears as a broad singlet at δ 1.73, the two sets of dppm methylene protons appear as multiplets at δ 3.39 and 4.44, while the vinylic proton appears at δ 4.17 as a doublet of doublets, displaying fluorine couplings of 45.4 and 13.8 Hz, assigned to *trans* and *cis* coupling, respectively. No resolvable coupling of the broad hydroxyl proton to phosphorus is observed although the signal sharpens significantly upon broadband phosphorus decoupling.

Carbon-13 labelling of the carbonyls and the methyl group leads to three distinct resonances in the $^{13}\text{C}\{^1\text{H}\}$ NMR spectrum. The two carbonyl resonances at δ 174.4 (doublet of triplets) and 170.8 (triplet) indicate terminally bound

groups. Each displays coupling to the pair of adjacent ^{31}P nuclei on different metals, while the former signal displays additional coupling to one of the vinylic fluorines ($^4J_{\text{CF}} = 12.0$ Hz). The methyl carbon signal also displays coupling to the pair of adjacent phosphorus nuclei together with coupling to one fluorine nucleus ($^2J_{\text{CP}} = 4.8$ Hz, $^2J_{\text{CF}} = 4.8$ Hz).

The ^{19}F NMR spectrum shows, in addition to the triflate anion, two signals appearing at $\delta -65.9$ and -86.1 for the pair of vinylic fluorines. The downfield signal appears as a doublet of doublets, with coupling of $^2J_{\text{FF}} = 55.9$ Hz and $^3J_{\text{FH}} = 13.2$ Hz, while the upfield signal appears as a broad, unresolved resonance.

An X-ray structure determination confirms the structural assignment, and is shown, for the complex cation, in Figure 2.4. This structure has an octahedral geometry at Ir(1), consistent with an Ir(III) oxidation state, while the adjacent metal, which shares the bridging hydroxide ligand, has a square-planar geometry, characteristic of Ir(I). The difluorovinyl unit confirms the geminal arrangement of the two fluorines, with the C(4) – F(1) bond slightly shorter at 1.311(5) Å compared to the C(4) – F(2) distance of 1.347(4). We attach no chemical significance to this difference, owing to the elongated thermal ellipsoids for these atoms which may disguise a slight disorder. The C(4) – C(5) bond length of 1.278(4) is shorter than expected for a C-C double bond; however, this may also be a consequence of the apparent vibrational motion. We assume that the spin-spin coupling noted above between the methyl group and one fluorine nucleus results from a through-space interaction between the adjacent methyl and difluorovinyl groups, with the closest approach between F(1) and the methyl protons being 2.22 Å. The iridium – iridium separation, at 3.246(2) Å, is beyond bonding distance. The hydroxyl proton is involved in a hydrogen bond with both the triflate counter anion (H(30) – O(4) = 0.84 Å).

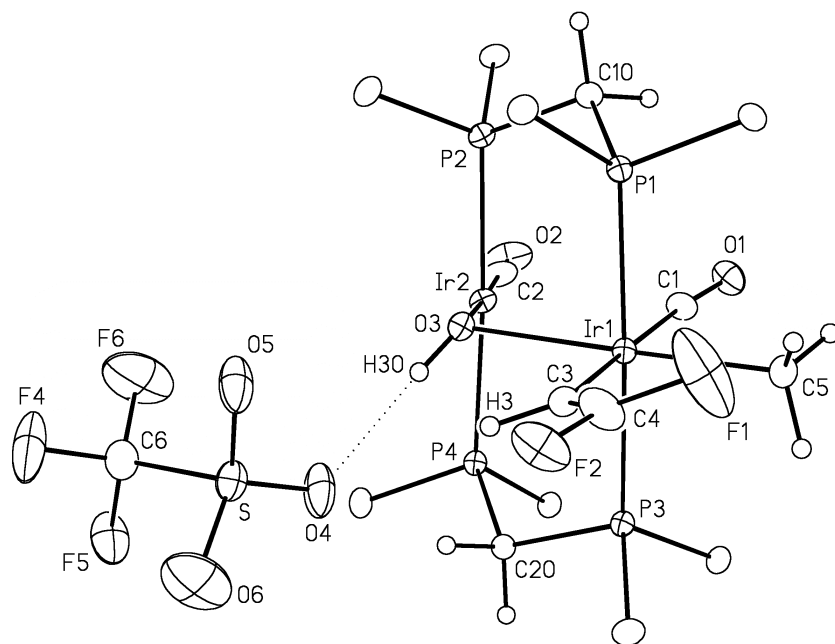
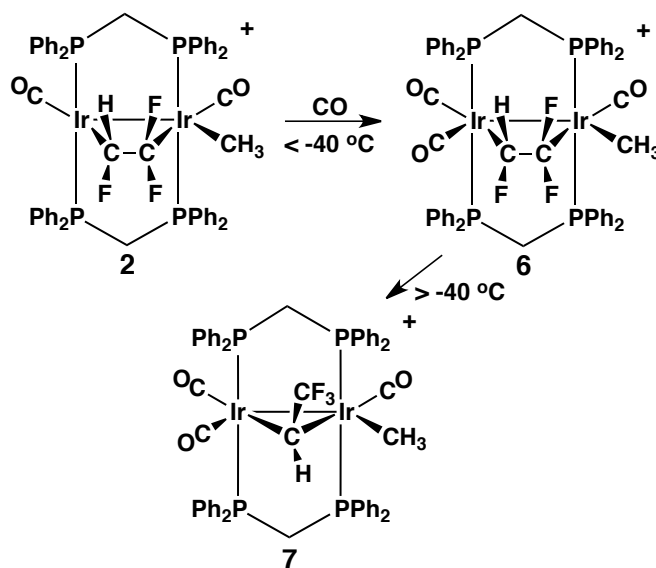


Figure 2.4 – Perspective view of $[\text{Ir}_2(\text{CH}_3)(\kappa^1\text{-C(H)=CF}_2)(\text{CO})_2(\mu\text{-OH})(\text{dppm})_2][\text{OTf}]$ (**5**) showing the atom labelling scheme. Only the ipso carbons of the dppm phenyl rings are shown, while the thermal parameters for the other atoms are as described in Figure 2.3. Relevant bond distances (Å) and angles (°): $\text{Ir}(1)\text{-C}(3) = 2.093(3)$, $\text{C}(3)\text{-C}(4) = 1.278(4)$, $\text{F}(1)\text{-C}(4) = 1.311(5)$, $\text{F}(2)\text{-C}(4) = 1.347(4)$, $\text{Ir}(1)\text{-C}(3)\text{-C}(4) = 135.7(3)$, $\text{F}(1)\text{-C}(4)\text{-C}(3) = 128.6(4)$, $\text{F}(2)\text{-C}(4)\text{-C}(3) = 126.4(4)$, $\text{F}(1)\text{-C}(4)\text{-F}(2) = 104.7(3)$.

2.2.2.4 [1,2]-Fluoride Shift. Reaction of **2** with CO at -80 °C yields the expected carbonyl adduct $[\text{Ir}_2(\text{CH}_3)(\text{CO})_3(\mu\text{-C}_2\text{F}_3\text{H})(\text{dppm})_2][\text{CF}_3\text{SO}_3]$ (**6**), which like **2** displays four resonances in the $^{31}\text{P}\{^1\text{H}\}$ NMR spectrum; again the large couplings between pairs of ^{31}P nuclei confirm that the phosphines have remained *trans* at the two metals.

In the ^1H NMR spectrum the four methylene protons are also unique, while the methyl signal appears as a broad singlet at δ 0.72, and the unique olefinic proton appears as a doublet of doublet of doublets at δ 5.94. In this last resonance the largest coupling of 49.7 Hz is comparable to the geminal H–F coupling observed in **2** ($^2J_{\text{HF}} = 34.9$ Hz). The $^{13}\text{C}\{^1\text{H}\}$ NMR spectrum of a ^{13}C O-enriched sample shows three carbonyl resonances: two overlapping multiplets at δ 179.0 and a doublet of triplets at δ 156.3. The latter signal displays coupling to one side of the diphosphine framework (11.5 Hz) and $^3J_{\text{CC}}$ of 11.5 Hz to the ^{13}C -labelled

methyl group. The ^{19}F NMR spectrum shows three broad signals at δ -67.8 , -81.9 , -169.8 , however no coupling could be resolved owing to their breadth.



Scheme 2.4 – The addition of carbon monoxide to compound 2, producing a bridging 2,2,2-trifluoroethylidene ligand (7).

Upon warming to -20°C , compound 6 converts irreversibly to 7 over 30 min via a 1,2-fluoride shift yielding the 2,2,2-trifluoroethylidene-bridged product shown. The $^{31}\text{P}\{^1\text{H}\}$ NMR spectrum of 7 again reveals four signals, indicating that all ^{31}P nuclei remain chemically inequivalent, and again the large coupling between pairs of ^{31}P nuclei indicate a *trans* dppm arrangement at both metals.

The ^1H NMR spectrum shows the lone proton of the bridging trifluoroethylidene group as a multiplet at δ 5.82, with coupling to the three neighboring fluorine atoms together with coupling to all four phosphorus nuclei. Upon broadband phosphorus decoupling, this signal collapses to a quartet with 17.6 Hz coupling to the three fluorines. Four unique methylene protons from the bridging diphosphines appear as multiplets at δ 5.44 (1H), 4.08 (1H), 3.88 (1H) and 3.85 (1H), in which the upfield signal is comprised of two overlapping resonances. Finally, the iridium-bound methyl group appears as a pseudo triplet at δ 0.71 (3H), showing equal coupling to the two phosphorus nuclei on the same metal.

A $^{13}\text{C}\{^1\text{H}\}$ NMR spectrum on a non-enriched sample of **7** was obtained, showing three different signals at δ 179.7, 177.6, and 162.8, consistent with three terminal carbonyls. The terminal methyl group was also observed at δ -25.2, typical of an iridium-bound methyl group.

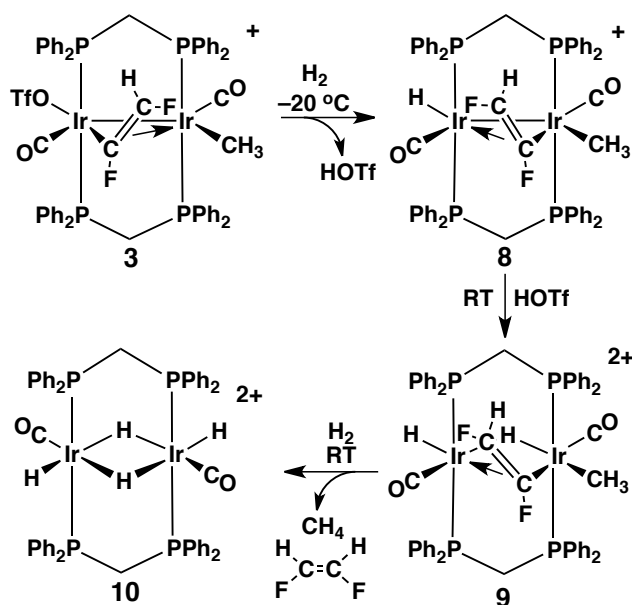
In the ^{19}F NMR spectrum, the free triflate counterion appears together with a doublet at δ -42.4 having a coupling constant of $^3J_{\text{HF}} = 17.7$ Hz, corresponding to the newly formed $-\text{CF}_3$ group of the trifluoroethylidene unit.

2.2.3 Fluorocarbyl Group Functionalization

2.2.3.1 Hydrogenolysis. The addition of H_2 to compound **3** at -20 °C gives an immediate reaction as demonstrated by the replacement of the $^{31}\text{P}\{^1\text{H}\}$ NMR resonances of **3** by a new set of signals, due to the monohydride species, $[\text{Ir}_2(\text{CH}_3)(\text{H})(\text{CO})_2(\mu-\kappa^1:\eta^2\text{-CF}=\text{CFH})(\text{dppm})_2]^+$ (**8**). The appearance of **8** is accompanied by the appearance of a broad single peak at δ 12.00 in the ^1H NMR spectrum, consistent with a methylene chloride solution of triflic acid at comparable concentrations (See Scheme 2.5).

Compound **8** retains the four-resonance $^{31}\text{P}\{^1\text{H}\}$ NMR spectrum characteristic of chemically inequivalent environments for all phosphorus atoms, with large *trans* coupling between pairs of resonances. No evidence was observed for an initial H_2 adduct down to -80 °C; instead, facile heterolytic cleavage of H_2 results in the formation of triflic acid and the mono-hydride complex **8**. The new hydride resonance appears in the ^1H NMR spectrum at δ -6.92 as a pseudo doublet of triplets, showing 14.0 Hz coupling each to the two adjacent phosphorus nuclei (δ -2.0 and 18.2) and 6.0 Hz coupling to the β -fluorine of the bridging difluorovinyl group. The ^1H NMR spectrum also shows four separate signals for the dppm methylene protons, while the methyl group appears as a pseudo-triplet at δ 1.01 ($^3J_{\text{HP}} = 5.0$ Hz). Selective decoupling upon irradiation of the two ^{31}P resonances corresponding to one side of the diphosphine framework (δ -6.0 and 9.0) each results in a collapse of this signal to a doublet. The vinylic proton appears as a multiplet at δ 4.94, displaying two major resolvable couplings, the larger of which ($^2J_{\text{HF}} = 63.2$ Hz) is consistent with the

geminal coupling of an sp^2 hybridized C(H)F group, and the smaller of which ($^3J_{\text{HF}} = 14.7$ Hz) is consistent with a *trans*-arrangement to the other fluorine. Selective decoupling $^1\text{H}\{^{31}\text{P}\}$ experiments also indicate that the vinylic proton is coupled to the same two phosphorus nuclei as is the hydride, displaying 4.4 Hz coupling to the phosphorus nucleus at δ 18.2 and 18.6 Hz coupling to the phosphorus at δ -2.0. This coupling suggests that the difluorovinyl unit is η^2 -bound to the non-methyl-containing iridium, indicating that it has migrated from one metal to the other in the transformation from **3**. The $^{13}\text{C}\{^1\text{H}\}$ NMR spectrum of a ^{13}CO - and $^{13}\text{CH}_3$ -enriched sample shows two terminal carbonyl resonances at δ 179.2 and 175.5, while the methyl carbon is a broad singlet at δ -21.7.



Scheme 2.5 – Functionalization of the *cis*-difluorovinyl ligand with H₂, resulting in the elimination of *cis*-difluoroethylene.

In the ^{19}F NMR spectrum, two signals appear at δ -60.2 and -172.9, however both are broad (*ca.* 132 and 118 Hz at half-height respectively). $^{19}\text{F}\{^{31}\text{P}\}$ experiments result in peak sharpening of the β -fluorine when the ^{31}P resonances on the adjacent metal are decoupled suggesting that the weak coupling observed occurs through the π -bonding interaction. No coupling is observed between the α -fluorine and the two phosphorus nuclei via the σ -bond. A similar

coupling pattern was also evident in compound **3** and is suggestive of a bridging orientation of the fluorovinyl moiety.

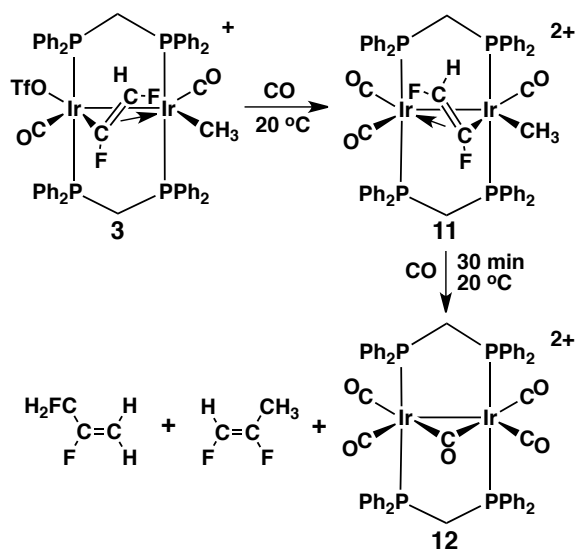
As the temperature is raised to ambient the resonances due to **8** are replaced by a new set of four multiplets in the $^{31}\text{P}\{^1\text{H}\}$ spectrum due to **9**. Concomitant with the appearance of this new species is the disappearance of triflic acid in the ^1H NMR spectrum and the appearance of two new hydride signals, a triplet at $\delta -11.00$ ($^2J_{\text{PH}} = 12.0$ Hz), and a broad unresolved signal at $\delta -14.40$. The methyl resonance now appears as a triplet at $\delta 0.80$. Selective ^{31}P decoupling demonstrates that the hydride at $\delta -11.00$ and the methyl group are coupled to different ends of the diphosphines, so are presumably bound to different metals, while the slight sharpening of the unresolved hydride resonance at $\delta -14.40$ upon selective and broad-band ^{31}P decoupling suggests a bridging arrangement for this group. Unfortunately, the vinylic proton was not identified in the ^1H NMR spectrum, presumably being obscured by the dppm phenyl resonances. In a $^{13}\text{CH}_3$ -enriched sample the methyl carbon appears as a broad singlet at $\delta -17.9$ in the $^{13}\text{C}\{^1\text{H}\}$ NMR spectrum, while a ^{13}CO -enriched sample shows two broad resonances at $\delta 168.2$ and 160.4 , suggesting terminal arrangements for these groups.

In the ^{19}F NMR spectrum the two fluorines appear as a broad multiplet at $\delta -87.9$ and a doublet of doublets at $\delta -144.1$. The couplings involving the latter ($^2J_{\text{FH}} = 60.9$, $^3J_{\text{FF}} = 26.6$ Hz) are again consistent with the *cis*-arrangement of the fluorines.

Left at ambient temperature under an atmosphere of H_2 , complete conversion of **9** to the previously characterized tetrahydride product, $[\text{Ir}_2(\text{H})_2(\text{CO})_2(\mu\text{-H})_2(\text{dppm})_2][\text{CF}_3\text{SO}_3]_2$ ⁸⁶ is observed over a 30 min period, resulting from hydrogenolysis and subsequent elimination of methane and *cis*-difluoroethylene, as confirmed for the latter by comparison of the ^1H and ^{19}F NMR spectra with that of an authentic sample.⁷³

Addition of H_2 to compounds **4**, **5**, and **7** was also investigated, but no reaction was observed in these cases.

2.2.3.2 Reductive Elimination of Difluoropropenes. Addition of carbon monoxide to compound **3** at ambient temperature results in an immediate reaction, as demonstrated by the disappearance of its $^{31}\text{P}\{^1\text{H}\}$ NMR resonances and the corresponding appearance of a new set of signals due to the tricarbonyl compound $[\text{Ir}_2(\text{CH}_3)(\text{CO})_3(\mu\text{-}\kappa^1\text{:}\eta^2\text{-CF=CFH})(\text{dppm})_2][\text{CF}_3\text{SO}_3]_2$ (**11**), in which the triflate ion has been replaced by a carbonyl group, as shown in Scheme 2.6. The $^{31}\text{P}\{^1\text{H}\}$ NMR spectrum of compound **11** again reveals four complex multiplets, indicative of four inequivalent phosphorus environments, like that of the precursor.



Scheme 2.6 – Functionalization of the cis-difluoroethylene unit with CO, resulting in the reductive elimination of two difluoropropene isomers.

The ^1H NMR spectrum of **11** shows the expected four resonances for the dppm methylene protons, the methyl ligand appears as a broad triplet at δ 1.13 and the vinylic proton at δ 6.66 is identifiable by its characteristic multiplet splitting pattern, with two of the resolvable couplings being diagnostic of hydrogen-fluorine coupling. The most prominent coupling involving the fluorovinyl proton is $^2J_{\text{HF}}$, with a value of 65.2 Hz, consistent with the geminal coupling of an sp^2 hybridized-C(H)F group, while the smaller coupling ($^3J_{\text{HF}} = 15.3$ Hz) confirms that the H and other F atom are in a *trans*-arrangement across the vinylic centre. Selective ^{31}P -decoupling experiments demonstrate that the

vinyllic proton is coupling through the π -bond to two phosphorus nuclei at δ 4.0 and -18.2 , suggesting that the vinyl group has again migrated to the other iridium centre, as was observed in the reaction with H_2 . The $^{13}C\{^1H\}$ NMR spectrum of a ^{13}CO -enriched sample shows three carbonyl resonances at δ 173.8, 167.8 and 159.0, while a $^{13}CH_3$ -enriched sample shows a singlet for this group at δ -13.4 . The arrangement of these ligands at both metals has been established by ^{31}P -decoupling experiments. In the ^{19}F NMR spectrum two characteristic signals displaying fluorine-proton and fluorine-fluorine coupling are observed, the values of which again suggest a bridging orientation of the fluorovinyl moiety. The first is a broad unresolved signal at δ -53.4 , whereas the other is a higher field signal at δ -157.8 displaying fluorine-proton coupling ($^2J_{HF} = 65.2$ Hz), consistent with it being geminal to the vinyllic proton. This signal also shows coupling of 30.9 Hz to the other fluorine, indicative of a *cis*-arrangement of these atoms across the vinyllic centre. The absence of a ^{19}F resonance for coordinated triflate ion and the appearance of only free triflate ion confirms substitution of this group by CO.

Left under an atmosphere of CO at ambient temperature, compound **11** completely converts, within 30 min, to the previously characterized $[Ir_2(CO)_5(dppm)_2][CF_3SO_3]_2$ ⁸⁷ by reductive elimination of the mutually adjacent methyl and difluorovinyl groups to give *cis*-difluoropropene and its isomer 2,3-difluoropropene (see Scheme 2.6) in an approximate 1:2 ratio.

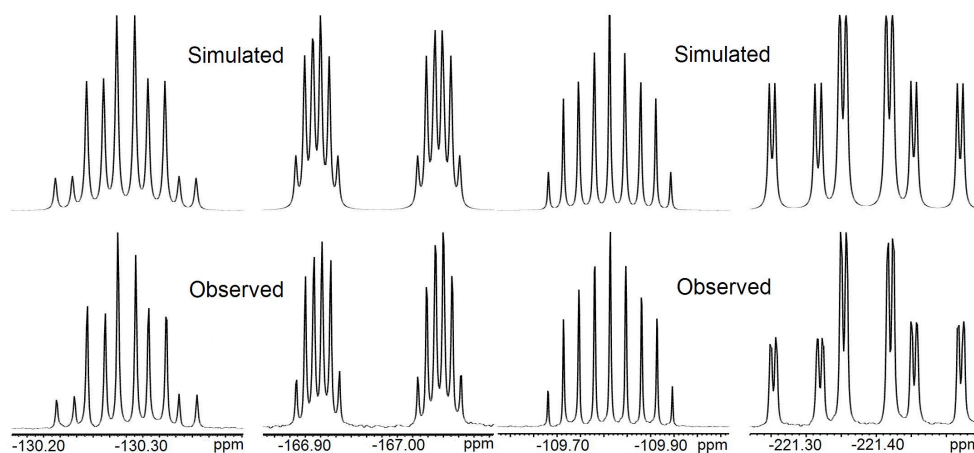


Figure 2.5 – Observed and simulated ^{19}F NMR spectra (376 MHz) of *cis*-difluoropropene (left two spectra) and 2,3-difluoropropene (right two spectra).

No spectral data were found in the literature for either *cis*-difluoropropene or 2,3-difluoropropene, thus the identities of these fluoroolefins were established by simulation of the ^{19}F NMR spectra for these species together with their ^1H and ^{13}C (of a $^{13}\text{CH}_3$ -enriched sample) NMR spectra. The ^{19}F NMR spectrum of both isomers are shown in Figure 2.5 and the derived coupling constants are given in Table 2.1. In the case of *cis*-difluoropropene (^{19}F NMR: δ -130.3 and -166.9), the H-F geminal coupling (74.5 Hz) and the *cis* F-F coupling (9.8 Hz) are observed, establishing this arrangement. In the case in which $^{13}\text{CH}_3$ -enriched precursor **3** was used, the $^1J_{\text{CH}}$ value (129.2 Hz) is typical for a methyl group and the geminal carbon-fluorine coupling constant (24.6 Hz) is as expected.⁸⁸ This is the anticipated product of reductive elimination of the *cis*-difluorovinyl and the methyl groups.

In contrast, the appearance of 2,3-difluoropropene (^{19}F NMR: δ -109.8 and 221.4) was not anticipated and has resulted from a 1,3-hydrogen shift from the methyl group to the other end of the olefinic unit. This antarafacial transformation is presumably metal mediated. In 2,3-difluoropropene, one fluorine is now bonded to an sp^3 -hybridized carbon centre and displays coupling to two methyl protons ($^2J_{\text{HF}} = 47.5$ Hz) as well as coupling to the olefinic fluorine ($^3J_{\text{FF}} = 30.9$ Hz), both of which are comparable to literature values for 1,2,3,3-tetrafluoropropene (*E*) ($^2J_{\text{HF}} = 51.29$ Hz and $^3J_{\text{FF}} = 18.36$ Hz).⁸⁹ The olefinic fluorine shows *cis*- and *trans*-proton coupling of $^3J_{\text{HFcis}} = 15.5$ Hz and $^3J_{\text{HFtrans}} = 46.0$ Hz respectively, correlating with observed coupling constants for *cis*-difluoroethylene ($^3J_{\text{HFtrans}} = 41.8$ Hz) and *trans*-difluoroethylene ($^3J_{\text{HFcis}} = 19.9$ Hz).⁹⁰ Finally, $^1J_{\text{CH}}$ values of 162.8 and 160.8 Hz were observed in the sample prepared from $^{13}\text{CH}_3$ -labelled **3**, and are typical values for sp^2 hybridized centres.⁹¹ The complete list of derived coupling constants is given in Table 2.1.

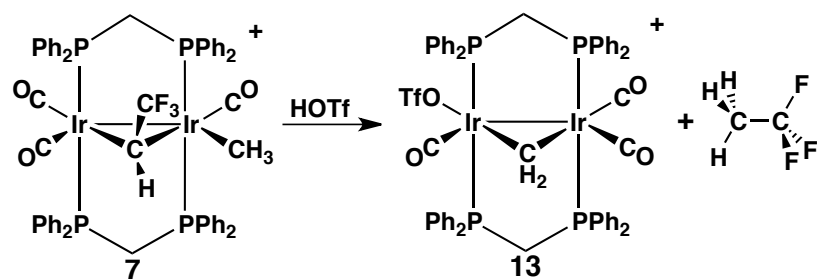
No reaction was observed upon the addition of CO to compounds **4**, **5**, or **7**.

Table 2.1 – Derived coupling constants for *cis*-difluoropropene and 2,3-difluoropropene.

| Nuclei | <i>J</i> (Hz) |
|---------------------------------|---------------|---------------------------------|---------------|---------------------------------|---------------|---------------------------------|---------------|
| H _a – H _b | 1.5 | H _b – F _y | 74.5 | H _a – F _y | 47.5 | F _x – F _y | 30.9 |
| H _a – F _x | 17.5 | F _x – F _y | 9.8 | H _a – F _x | 15.0 | H _a – C _m | 3.0 |
| H _a – F _y | 5.3 | H _a – C _m | 129.2 | H _b – H _c | 4.0 | H _b – C _m | 162.8 |
| H _b – F _x | 17.5 | F _x – C _m | 24.6 | H _b – F _y | 4.0 | H _c – C _m | 160.8 |
| | | | | H _b – F _x | 46.0 | F _y – C _m | 7.2 |
| | | | | H _c – F _x | 15.5 | F _x – C _m | 16.2 |

2.2.3.3. Protonation. The reaction of **7** with triflic acid proceeds instantly at ambient temperature to yield the methylene-bridged compound, [Ir₂(OTf)(CO)₃(μ-CH₂)(dppm)₂][OTf] (**13**), and 1,1,1-trifluoroethane, as shown in Scheme 2.7.

In the ¹H NMR spectrum, only three signals are observed (excluding the dppm phenyl protons), associated with the metal-containing product, all of which correspond to methylene groups. The first, at δ 6.57, represents that bridging the two metals, and appears as a pseudo quintet, with coupling to all four ³¹P nuclei. Selective decoupling of each set of phosphorus signals results in collapse of this signal to a triplet, and broadband ³¹P decoupling results in complete collapse to a singlet. Both sets of dppm methylene protons appear as multiplets at δ 5.93 and 5.48, which upon broadband ³¹P decoupling yields an AB quartet. Confirmation of this structure was obtained through X-ray crystallography, and a representation of the cation is shown in Figure 2.6.



Scheme 2.7 – Functionalization of the bridging 2,2,2-trifluoroethylidene moiety by triflic acid.

The structure of **13** is as expected; each Ir centre has a distorted octahedral environment, sharing the metal-metal bond and the bridging methylene unit, which is slightly unsymmetrical (Ir(1) – C(4) = 2.037(8) Å; Ir(2) – C(4) = 2.119(8) Å) owing to the different groups (OTf, CO) in *trans* positions at the two metals. The most significant difference in the geometries at each metal results from the triflate anion coordinated on Ir(1) in place of a carbonyl at Ir(2).

In the ^{19}F NMR spectrum of the reaction mixture the resonance for 1,1,1-trifluoroethane was observed as a quartet at $\delta -61.4$ with $^3J_{\text{HF}} = 13.1$ Hz. Upon adding deuterated triflic acid ($^2\text{HOSO}_2\text{CF}_3$), the resulting product is 1,1,1-trifluoro-2-deuteroethane, for which the ^{19}F NMR spectrum now appears as a 1:2:1 triplet, with additional 1.9 Hz coupling to ^2H , as shown in Figure 2.7, in which both isotopomers (from reaction with a mixture of HOTf and $^2\text{HOTf}$) appear, establishing that the one hydrogen required in the conversion of the $\mu\text{-CHCF}_3$ group to trifluoroethane comes from the acid and the other from the conversion of the Ir-bound methyl to a methylene group.

Attempts to protonate compounds **4** and **5** resulted in no reaction, while addition of triflic acid to compound **3** leads to a second C–F activation to produce **4**, as discussed above.

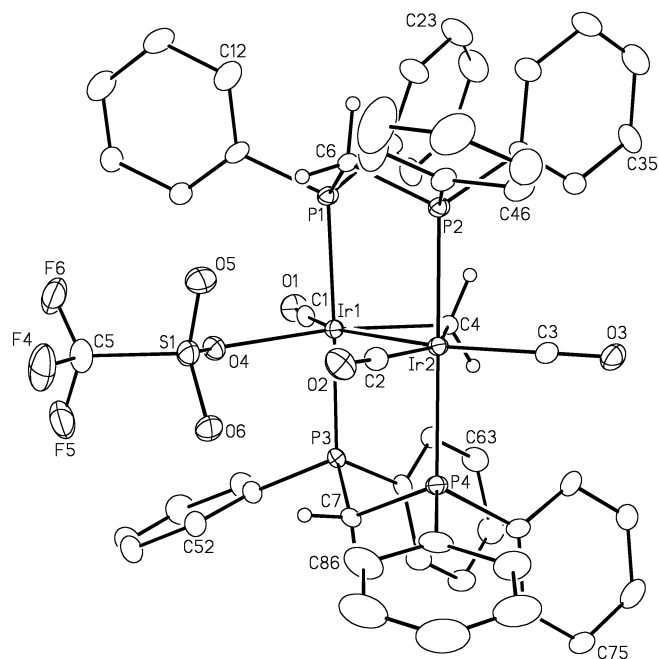


Figure 2.6 – Perspective view of one of two crystallographically independent $[\text{Ir}_2(\text{O}_3\text{SCF}_3)(\text{CO})_3(\mu\text{-CH}_2)(\text{dppm})_2]^+$ (**13**) cations showing the atom labelling scheme. Thermal parameters are as described in Figure 2.3. Relevant bond distances (Å) and angles (°): $\text{Ir}(1)\text{-Ir}(2) = 2.8059(4), 2.7952(5)$; $\text{Ir}(1)\text{-C}(4) = 2.037(8), 2.051(8)$; $\text{Ir}(2)\text{-C}(4) = 2.119(8), 2.090(9)$; $\text{Ir}(1)\text{-C}(4)\text{-Ir}(2) = 84.9(3), 84.9(4)$.

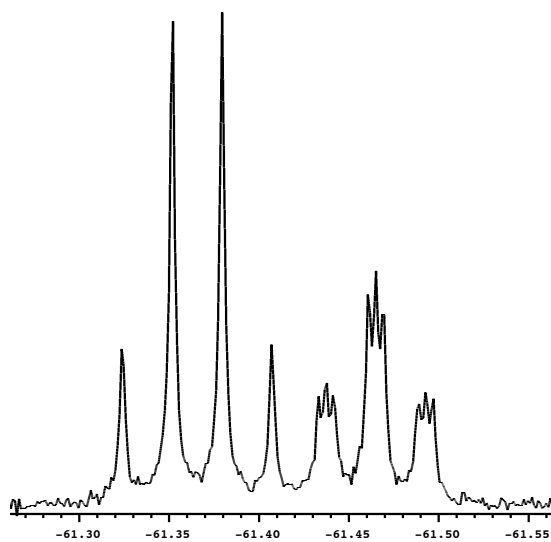


Figure 2.7 – ^{19}F NMR spectrum (469 MHz) of 1,1,1-trifluoroethane (left) and 1,1,1-trifluoro-2-deuteroethane.

2.3 Discussion

2.3.1 Olefin Binding

The reaction of trifluoroethylene with $[\text{Ir}_2(\text{CH}_3)(\text{CO})_2(\text{dppm})_2][\text{CF}_3\text{SO}_3]$ (**1**) yields two products. The kinetic product, observed in only minor amounts at $-80\text{ }^\circ\text{C}$ has the olefin weakly bound in an η^2 -manner to one metal. Upon warming slightly, this species immediately disappears, being replaced by a product in which the olefin bridges the pair of metals (see Scheme 2.1), and this product persists until approximately $0\text{ }^\circ\text{C}$, at which temperature slow reversion to starting materials occurs. Although olefin coordination to **1** in an η^2 -mode is the common kinetic product for a variety of fluoroolefins,^{39,68,69} the thermodynamically favoured product, in which the fluoroolefin bridges the metals, is only observed for fluoroolefins having at least one pair of geminal fluorine substituents.⁶⁹ In the bridging position the olefin can be considered as a 1,2-dimetallated alkane, in which rehybridization of the olefinic carbons from sp^2 to sp^3 has occurred, as observed in the structures of several tetrafluoroethylene-bridged species.^{62,68,69} It appears that the reorganization energy^{92,93} required for pyramidalization of the planar olefin is only compensated for when at least one of the olefinic carbons has two attached fluorines. This effect, in which binding of an element to fluorine is more favourable the greater the p-character of the hybrid orbitals involved,⁹⁴ is one consequence of the “gem-difluoro effect”.⁹⁵⁻¹⁰⁰ Another consequence of this effect in this study is the orientation of the bridging fluoroolefin ligand in $[\text{Ir}_2(\text{CH}_3)(\text{CO})_2(\mu\text{-C}_2\text{F}_3\text{H})(\text{dppm})_2][\text{CF}_3\text{SO}_3]$ (**2**), in which the difluoro-substituted end is bound to the more electron-rich metal, maximizing electron donation to this end of the olefin and its resulting pyramidalization.

2.3.2 C–F Activation

Our premise in this study was that in the bridging coordination mode, the fluoroolefin, having attained sp^3 hybridization, should behave very much like a fluoroalkyl group, and as such the α -fluorine substituents should be susceptible to fluoride ion abstraction, as is well documented in fluoroalkyl complexes.²¹ Based on this reasoning it was anticipated that fluoride ion abstraction from

trifluoroethylene, in a bridging orientation, should occur readily. This has been shown to be the case and three variations of this reactivity are observed, each of which is highly selective. The rationalization noted above also suggests that the pair of geminal fluorines, attached to the carbon that is more sp^3 -like, should be more labile. Although this has been shown to be the case in the addition of the strong fluorophiles, H^+ and Me_3Si^+ , this is not the case in two other modes of C–F activation, as will be discussed.

Removal of a fluoride ion from the coordinated trifluoroethylene ligand in **2**, as either HF or Me_3SiF , by reaction with either triflic acid or trimethylsilyl triflate respectively, occurs readily at subambient temperatures yielding the *cis*-difluorovinyl product (**3**) (see Scheme 2.2). In no case was another isomer observed. The stereoselectivity of this transformation is consistent with our ideas above that one of the geminal fluorines would be removed, and the absence of a *trans*-difluorovinyl product is in keeping with the *cis*-effect⁹⁵⁻¹⁰⁰ in which the *cis*-difluorovinyl arrangement is thermodynamically favoured over the *trans* arrangement, and has been rationalized on the basis of hyperconjugation.^{97,100} We propose that removal of either of the geminal fluorines yields the same transient fluorocarbene species, shown in Chart 2.2, (similar to fluoride abstraction from a CF_3 ligand)^{64,101} in which the metal-carbene plane bisects the HCF angle at the adjacent carbon. Rapid rearrangement of this species yields the more favourable η^2 -vinyl product and migration of this fluorovinyl unit from one metal to the other gives the structure observed for **3** (see Chart 2.3).

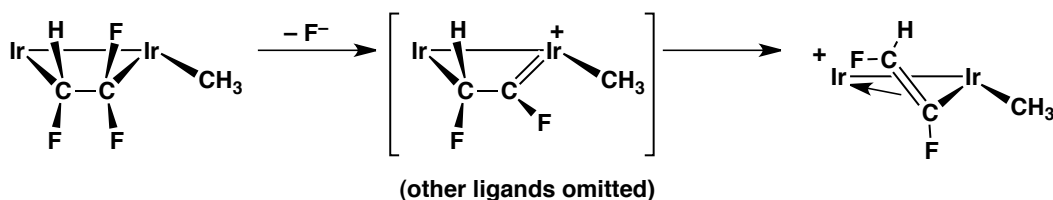


Chart 2.2 – Proposed mechanism for fluoride-ion abstraction to produce a *cis*-difluorovinyl unit.

Removal of a second fluoride ion, from the bridging *cis*-difluorovinyl ligand in **3** is also possible, yielding a monofluorovinylidene-bridged product (**4**).

In this case it is the fluorine on the α -carbon that is removed. Removal of this fluoride is more difficult than was removal of the first from the bridging trifluoroethylene ligand, described above, presumably because the η^2 -coordination of this group results in only partial rehybridization towards sp^3 , unlike the complete rehybridization in the olefin-bridged adduct (**2**). Consistent with the need for metal involvement in the activation step, fluoride removal from the β -carbon of the terminally bound 2,2-difluorovinyl group in compound **5** was not observed. Only one product is observed for the fluorovinylidene-bridged species (**4**), however, we were unable to determine whether the fluorine substituent in this product is *cis* or *trans* to the methyl-bound metal.

Surprisingly, even water can be used to effect facile C–F activation of the bridging trifluoroethylene ligand, although in this case the selectivity is different from that noted above, instead yielding the *gem*-difluorovinyl product through activation of the lone vicinal C–F bond (see Chart 2.3). We propose that the regioselectivity of this transformation is dictated by the position of the vacant coordination site in **2** which lies adjacent to the “CHF” end of the fluoroolefin. Water coordination at a cationic metal centre will lead to increased acidity of this group, and this has been shown to facilitate fluoride-ion abstraction in fluorocarbyl ligands.^{102,103} Water coordination, as shown in Chart 2.3, is then proposed to result in fluoride abstraction from the adjacent “CHF” group, yielding the final product **5** by movement of the resulting OH[−] group to the bridging site and accompanied by a “merry-go-round” migration of the other ligands around the Ir₂ core.

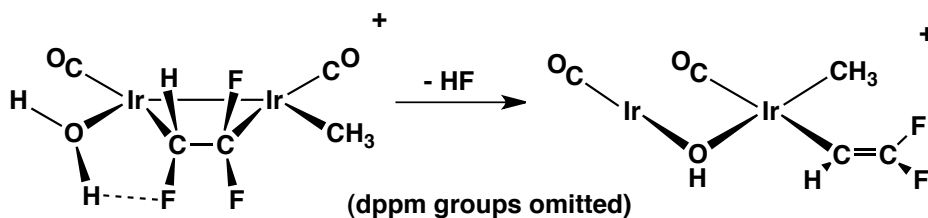


Chart 2.3 – Proposed mechanism for the activation of **2** by water.

The bridging trifluoroethylene arrangement in **2** is subject to a third form of C–F activation in which fluoride migration from the “CHF” end of the

fluoroolefin to the “CF₂” moiety yields a 2,2,2-trifluoroethylidene bridging unit, as diagrammed earlier in Scheme 2.4. This migration, which occurs instantly at ambient temperature, is initiated by carbonyl coordination at the vacant site, and is presumably driven by the increase in C–F bond strengths that occurs upon increasing the fluorine substitution at carbon.⁹⁴ The transformation of a trifluoroethylene-bridged species to a trifluoroethylidene-bridged product has been proposed in a Pt₂ system, as shown in Scheme 1.12,⁵⁹ although in this case the transformation was not selective and a number of other unidentified products also resulted. A very closely related isomerization of a bridging tetrafluoroethylene to a bridging perfluoroethylidene group has also been reported.^{62,63} The mechanism of this 1,2-fluoride migration is not known, however a second example of a 1,2-fluoride shift of trifluoroethylene, in which the reaction is promoted by the presence of water, is described in Chapter 5.

2.3.3 Fluoroolefin Functionalization

Having effected the regio- and/or stereoselective activation of olefinic C–F bonds in a number of ways, as described above, we next investigated routes for the conversion of the activated products into transformed fluorocarbons.

The first route addressed was that of hydrogenolysis, producing fluoroolefins in which one or two of the fluorines in the original trifluoroethylene have been replaced by hydrogens. This has proven to be successful in the case of the *cis*-difluorovinyl compound (**3**) which under an atmosphere of hydrogen cleanly generates *cis*-difluoroethylene, together with methane, which results from accompanying hydrogenolysis of the metal-methyl bond in **3** (see Scheme 2.5). As a result, the stoichiometric and selective transformation of trifluoroethylene to *cis*-difluoroethylene has been achieved.

Unfortunately, under the conditions used (1 atm. of H₂, ambient temperature) the 2,2-difluorovinyl species (**5**), obtained in the activation of **2** by water, and the fluorovinylidene-bridged species (**4**), obtained from double C–F activation of **2**, were unreactive and no hydrogenolysis products were observed. Other ways of converting these species to the hydrogen-containing fluoroolefins will be investigated, since if this conversion were successful, the selective

conversion of trifluoroethylene into either *cis*-difluoroethylene, 1,1-difluoroethylene, or vinyl fluoride under the appropriate conditions could be effected.

Similarly, the 2,2,2-trifluoroethylidene-bridged product (**7**), which has resulted from a 1,2-fluoride shift in the trifluoroethylene-bridged (**2**), was unreactive towards H₂. This lack of reactivity is not surprising since compound **7** is coordinatively saturated. However, protonation of **7** results in facile, stoichiometric formation of 1,1,1-trifluoroethane, in which one of the hydrogens (H⁺) has originated from the acid while the other (H⁻) has come from the methyl ligand in **7**. Attempts to protonate the vinyl-containing products, (**3**) and (**5**), did not succeed.

We also considered the possibility of reductive elimination of the methyl and difluorovinyl ligands in compounds **3** and **5** to generate the respective *cis*-difluoropropene and 1,1-difluoropropene. In both cases warming of these complexes under refluxing conditions did not result in the targeted elimination products. However, we reasoned that replacement of the anionic triflate ligand in **3** by a neutral group would increase the tendency for reductive elimination by increasing the positive charge on the species. Furthermore, in the case in which the neutral replacement ligand was a strong π acceptor, such as CO, which should further reduce the electron density at Ir, the tendency for reductive elimination should be further increased. In line with these ideas, triflate-ion replacement by CO results in quantitative reductive elimination at ambient temperature. Although the anticipated product of reductive elimination, *cis*-difluoropropene, was obtained, it was the minor product (in a 1:2 ratio) with the major product being 2,3-difluoropropene, the result of a 1,3-hydrogen shift from the methyl ligand to the remote olefinic carbon. This conversion is favoured since a fluorine that was bound to an sp^2 carbon now resides on an sp^3 carbon (rationalized by Bent's rule).⁹⁴ This antarafacial conversion is presumably metal-mediated.

2.4 Conclusions

Binding of trifluoroethylene in a bridging position between two metals activates it to fluoride-ion abstraction under very mild conditions. This together with previous^{39,69} and ongoing work with tetrafluoroethylene and 1,1-difluoroethylene suggests that the bridged binding mode of fluoroolefins is a general route to C–F activation. With trifluoroethylene, strong fluorophiles remove a geminal fluoride to give the *cis*-difluorovinyl product, and under marginally harsher conditions the second of the formerly geminal fluorides can be similarly removed to yield a fluorovinylidene-bridged product. Water can also effect fluoride-ion abstraction, but with a different regiochemistry, yielding a *gem* difluorovinyl group. A third activation process is also possible upon CO addition to the trifluoroethylene adduct (**2**), in which a 1,2-fluoride shift in the bridging trifluoroethylene ligand yields a 2,2,2-trifluoroethylidene-bridged product. Although some of these products are unreactive under the conditions investigated, others have been transformed under mild conditions such that the original trifluoroethylene substrate has been selectively converted into *cis*-difluoroethylene, 1,1,1-trifluoroethane and a 1:2 mix of difluoropropenes – the latter by reductive elimination of the *cis*-difluorovinyl and methyl ligands in the complex.

This use of pairs of adjacent metals for the selective activation and subsequent conversion of fluoroolefins into a number of products represents a new strategy in carbon-fluoride bond activation.

2.5 Experimental

2.5.1 General Comments

All solvents were dried (using appropriate drying agents), distilled before use and stored under dinitrogen. Deuterated solvents used for NMR experiments were freeze-pump-thaw degassed (three cycles) and stored under nitrogen or argon over molecular sieves. Reactions were carried out under argon using standard Schlenk techniques, and compounds that were obtained as solids were purified by

recrystallization. Prepurified argon and nitrogen were purchased from Praxair, carbon-13 enriched CO (99%) was supplied by Isotec Inc, and trifluoroethylene was supplied by SynQuest Fluorochemicals. All purchased gases were used as received. All other reagents were obtained from Aldrich and were used as received (unless otherwise stated). The compound $[\text{Ir}_2(\text{CH}_3)(\text{CO})(\mu\text{-CO})(\text{dppm})_2][\text{CF}_3\text{SO}_3]$ (**1**) was prepared as previously reported.⁷⁰ Proton NMR spectra were recorded on Varian Unity 400 or 500 spectrometers, or on a Bruker AM400 spectrometer. Carbon-13 NMR spectra were recorded on Varian Unity 400 or 500 or Bruker AM300 spectrometers. Phosphorus-31 and fluorine-19 NMR spectra were recorded on Varian Unity 400 or 500 or Bruker AM400 spectrometers. Two-dimensional NMR experiments (COSY, NOESY and ^1H - ^{13}C HMQC) were obtained on Varian Unity 400 or 500 spectrometers.

2.5.2 Preparation of Compounds

(a) $[\text{Ir}_2(\text{CH}_3)(\text{CO})_2(\mu\text{-C}_2\text{F}_3\text{H})(\text{dppm})_2][\text{CF}_3\text{SO}_3]$ (**2**). Into a brick-red solution of compound (**1**) (50 mg, 0.037 mmol) in 0.7 mL of CD_2Cl_2 in an NMR tube that was cooled to $-20\text{ }^\circ\text{C}$ in a freezer was transferred 2 mL of trifluoroethylene gas onto the solution via a gas-tight syringe, and the subsequent reaction was investigated via multinuclear NMR spectroscopy. Upon holding the sample at $-20\text{ }^\circ\text{C}$ for 1½ h, NMR spectroscopy showed quantitative conversion of **1** to compound **2**, which could be further reacted at this stage. This product was only characterized in solution, via NMR spectroscopy, since at higher temperatures loss of substrate and subsequent regeneration of starting materials occurred. ^1H NMR (400 MHz, CD_2Cl_2 , $-20\text{ }^\circ\text{C}$): δ 6.90 (m, 1H, $\text{F}_2\text{C-CFH}$), 3.97 (m, 1H, $\text{Ph}_2\text{P-CH}_2\text{-PPh}_2$), 3.92 (m, 2H, $\text{Ph}_2\text{P-CH}_2\text{-PPh}_2$), 3.56 (m, 1H, $\text{Ph}_2\text{P-CH}_2\text{-PPh}_2$), 0.34 (t, 3H, $^3J_{\text{HP}} = 6.0$ Hz, CH_3). $^{13}\text{C}\{^1\text{H}\}$ NMR (101 MHz, CD_2Cl_2 , $-20\text{ }^\circ\text{C}$): δ 197.2 (b, 1C, CO), 185.6 (b, 1C, CO), -8.9 (s, 1C, CH_3). ^{19}F NMR (376 MHz, CD_2Cl_2 , $-20\text{ }^\circ\text{C}$): δ -53.4 (m, 1F, $^2J_{\text{FF}} = 253.3$ Hz), -78.9 (s, 3F, OTF), -82.2 (m, 1F, $^2J_{\text{FF}} = 253.3$ Hz, $^3J_{\text{FF}} = 24.8$ Hz), -194.4 (m, 1F, $^3J_{\text{FF}} = 24.8$ Hz). $^{31}\text{P}\{^1\text{H}\}$ NMR

(162 MHz, CD₂Cl₂, -20 °C): δ 17.2 (dm, 1P, $^2J_{PP} = 299.4$ Hz), 14.4 (dm, 1P, $^2J_{PP} = 299.4$ Hz), 5.1 (m, 2P).

(b) **[Ir₂(H)(CO)₂(η^2 -C₂F₃H)(μ -CH₂)(dppm)₂][CF₃SO₃] (2a).** To a brick-red solution of compound **1** (50 mg, 0.037 mmol), dissolved in 0.7 mL of CD₂Cl₂ in an NMR tube, cooled in a Dry ice-acetone bath, was transferred 2 mL of trifluoroethylene gas onto the solution via a gas-tight syringe, and the subsequent reaction was investigated via multinuclear NMR spectroscopy. At -80 °C, the $^{31}\text{P}\{^1\text{H}\}$ spectrum showed the presence of small amounts of **2a** (approximately 10%) along with the resonances for the starting material (**1**). ^1H NMR (400 MHz, CD₂Cl₂, -80 °C): δ 5.23 (m, 2H, Ph₂P-CH₂-PPh₂), 5.02 (m, 2H, Ph₂P-CH₂-PPh₂), -12.70 (b, 1H, Ir-H). $^{13}\text{C}\{^1\text{H}\}$ NMR (101 MHz, CD₂Cl₂, -80 °C): δ 195.2 (b, 1C, CO), 187.6 (b, 1C, CO), 44.2 (bs, 1C, -CH₂-). ^{19}F NMR (376 MHz, CD₂Cl₂, -80 °C): δ -79.1 (s, 3F, OTF), -94.4 (d, 1F, $^2J_{FF} = 156.8$ Hz), -97.3 (d, 1F, $^2J_{FF} = 156.8$ Hz), -220.1 (m, 1F). $^{31}\text{P}\{^1\text{H}\}$ NMR (162 MHz, CD₂Cl₂, -80 °C): δ -4.9 (m, 2P), -5.7 (m, 2P).

(c) **[Ir₂(CH₃)(OTf)(CO)₂(μ - κ^1 : η^2 -C(F)=CFH)(dppm)₂][CF₃SO₃] (3).**
Method (A): 10 μL of Me₃SiOTf was added dropwise to a 10 mL dichloromethane solution of compound **2** (50 mg, 0.034 mmol) that had been cooled to -20 °C. This mixture was subsequently mixed and warmed to room temperature for 1/2 h. The resulting yellow-orange solution was reduced *in vacuo* to ca. 5 mL, and Et₂O was added to precipitate a pale yellow microcrystalline compound **3**. The product was washed twice with 10 mL of Et₂O, the supernatant decanted, and then the solid was dried briefly under a stream of argon and then *in vacuo*. **Method (B):** 7 μL of HOTf was added to a solution of compound **2** (100 mg, 0.068 mmol) that had been cooled to -20 °C in CD₂Cl₂. The solution was mixed and slowly brought to ambient temperature. 10 mL of Et₂O was added to induce precipitation of a yellow microcrystalline solid, which was filtered and washed with 2 x 10 mL of Et₂O and dried under a stream of argon followed by vacuum. Crystals of

compound **3** were grown via slow diffusion of pentane into a CH₂Cl₂ solution of the compound. All crystallographic parameters are given in Supporting Information. (65% yield) ¹H NMR (498 MHz, CD₂Cl₂): δ 6.14 (m, 1H, Ph₂P-CH₂-PPh₂), 6.00 (dddd, 1H, ²J_{HF} = 65.6 Hz, ³J_{HF} = 10.3 Hz, ³J_{HP} = 16.6 Hz, ³J_{HP} = 5.4 Hz, -C(F)=C(F)(H)), 5.69 (m, 1H, Ph₂P-CH₂-PPh₂), 5.57 (m, 1H, Ph₂P-CH₂-PPh₂), 4.70 (m, 1H, Ph₂P-CH₂-PPh₂), 1.44 (t, 3H, ³J_{HP} = 6.0 Hz, CH₃). ¹³C{¹H} NMR (125 MHz, CD₂Cl₂): δ 172.1 (b, 1C, CO), 165.9 (b, 1C, CO), -23.5 (s, 1C, CH₃). ¹⁹F NMR (469 MHz, D₂Cl₂): δ -24.2 (m, 1F, ²J_{FF} = 33.2 Hz), -77.7 (s, 3F, Ir-OTf), -79.5 (s, 3F, OTf), -172.7 (dd, 1F, ²J_{FH} = 66.4 Hz, ³J_{FF} = 33.2 Hz). ³¹P{¹H} NMR (202 MHz, CD₂Cl₂): δ 9.5 (dm, 1P, ²J_{PP} = 331.1 Hz), -2.0 (dm, 1P, ²J_{PP} = 336.5 Hz), -3.3 (dm, 1P, ²J_{PP} = 331.1 Hz), -19.3 (dm, 1P, ²J_{PP} = 336.5 Hz); IR (KBr): ν bar = 2053, 2007 cm⁻¹ (C=O); HRMS *m/z* calc. for [¹⁹³Ir]₂P₄O₅C₅₆H₄₈F₅S [M*]⁺: 1437.1346, found 1437.1367. Anal. Calcd. for Ir₂S₂P₄F₈O₈C₅₇H₄₈•0.5CH₂Cl₂: C, 42.42; H, 3.03. Found: C, 42.37; H, 3.27%.

(d) [Ir₂(CH₃)(OTf)(CO)₂(μ-C=CFH)(dppm)₂][CF₃SO₃]₂ (**4**). **Method (A)**: Compound **3**, [Ir₂(CH₃)(OTf)(CO)₂(μ-κ¹:η²-CF=CFH)(dppm)₂][CF₃SO₃] (50 mg, 0.032 mmol), was dissolved in 7 mL of CH₂Cl₂, to which was added dropwise 30 μL of Me₃SiOTf, and the mixture stirred at ambient temperature overnight. **Method (B)**: To a sample of **3** dissolved in 0.7 mL of CH₂Cl₂ was added 15 μL of HOTf. The reaction mixture was stirred at ambient temperature overnight. In both methods, attempts to isolate the compound resulted in decomposition, therefore (**4**) has only been characterized in solution. (61% yield) ¹H NMR (498 MHz, CD₂Cl₂): δ 8.60 (d, 1H, ²J_{HF} = 85.2 Hz, -C=C(H)(F)), 4.30 (m, 2H, Ph₂P-CH₂-PPh₂), 2.80 (m, 2H, Ph₂P-CH₂-PPh₂), 2.15 (t, 3H, ³J_{HP} = 9.0 Hz, CH₃). ¹³C{¹H} NMR (125 MHz, CD₂Cl₂): δ 176.8 (bm, 1C, ²J_{CP} = 16.6 Hz, CO), 153.4 (b, 1C, ²J_{CP} = 11.5 Hz, CO), 40.5 (s, 1C, CH₃). ¹⁹F NMR (469 MHz, CD₂Cl₂): δ -76.4 (s, 3F, Ir-OTf), -79.5 (s, 3F, OTf), -107.4 (d, 1F, ²J_{FH} = 86.0 Hz). ³¹P{¹H} NMR (202

MHz, CD₂Cl₂): δ -5.0 (pseudo triplet, 2P, $^2J_{PP} = 23.0$ Hz), -21.0 (pseudo triplet, 2P, $^2J_{PP} = 23.0$ Hz).

(e) **[Ir₂(κ^1 -C(H)=CF₂)(CH₃)(CO)₂(μ -OH)(dppm)₂][CF₃SO₃] (5).** 10 μ L of freshly distilled H₂O was added to a NMR sample of compound **2** (50 mg, 0.034 mmol) in CD₂Cl₂ that had been cooled to 0 °C. The solution was slowly warmed to ambient temperature and left for 30 min. The resulting yellow orange solution was stripped to dryness *in vacuo* and the product was redissolved in 1 mL of THF. To the resulting solution was added pentane (10 mL) to precipitate a bright yellow microcrystalline compound **5**. The product was washed twice with 10 mL of pentane, the supernatant decanted, and then the solid was dried briefly under a stream of argon and then *in vacuo*. Crystals of compound **5** were grown via slow diffusion of diethylether into a CH₂Cl₂ solution of the compound. All crystallographic parameters are given in Supporting Information. (73% yield) ¹H NMR (498 MHz, CD₂Cl₂): δ 4.44 (m, 2H, Ph₂P-CH₂-PPh₂), 4.17 (ddt, 1H, $^3J_{HF} = 13.8$ Hz, $^3J_{HF} = 45.4$ Hz, $^3J_{HP} = 4.1$ Hz -C(H)=CF₂), 3.39 (m, 2H, Ph₂P-CH₂-PPh₂), 1.73 (bs, 1H, -OH), 0.39 (dt, 3H, $^3J_{HP} = 6.0$ Hz, $^1J_{HF} = 2.5$ Hz, CH₃). ¹³C{¹H} NMR (125 MHz, CD₂Cl₂): δ 174.4 (dt, 1C, $^2J_{CP} = 8.3$ Hz, $^4J_{CF} = 12.0$ Hz, CO), 170.8 (t, 1C, $^2J_{CP} = 10.7$ Hz, CO), -28.7 (dt, 1C, $^2J_{CP} = 4.8$ Hz, $^2J_{CF} = 4.8$ Hz, CH₃). ¹⁹F NMR (469 MHz, CD₂Cl₂): δ -65.9 (dd, 1F, $^2J_{FF} = 55.9$ Hz, $^3J_{FH} = 13.2$ Hz), -79.5 (s, 3F, OTf), -86.1 (bs, 1F). ³¹P{¹H} NMR (202 MHz, CD₂Cl₂): δ 13.3 (pseudo triplet, 2P, $^2J_{PP} = 9.5$ Hz), -15.3 (bm, 2P). IR (KBr): ν bar= 1989, 1971 cm⁻¹ (C=O); HRMS *m/z* calc. for [¹⁹³Ir]₂P₄O₃C₅₅H₄₉F₂ [M*]⁺: 1305.1853, found 1305.1883. Anal. Calcd. for Ir₂SP₄F₅O₆C₅₆H₄₉•CH₂Cl₂•0.5C₄H₁₀O : C, 44.98; H, 3.58. Found: C, 44.59; H, 3.79%.

(f) **Reaction of 2 with CO.** An NMR tube containing **2** was cooled to -80°C and 4 mL of CO was added via gas tight syringe. The reaction was monitored by NMR spectroscopy at -60°C, at which temperature the formation of

[Ir₂(CH₃)(CO)₃(μ-C₂F₃H)(dppm)₂][CF₃SO₃] (6) was observed. Upon warming the solution above -20°C, the formation of a new compound, **[Ir₂(CH₃)(CO)₃(μ-C(H)(CF₃))(dppm)₂][CF₃SO₃] (7)**, was observed. The conversion took approximately 30 min to proceed at -20°C and was instantaneous at ambient temperature. To the final product, 10 mL of ether was added to precipitate a yellow powder. (96% yield) Compound 6: ¹H NMR (400 MHz, CD₂Cl₂, -60 °C): δ 5.94 (m, 1H, ²J_{HF} = 49.7 Hz, -C(H)(F)-CH₂-), 5.02 (m, 1H, Ph₂P-CH₂-PPh₂), 4.76 (m, 1H, Ph₂P-CH₂-PPh₂), 4.49 (m, 1H, Ph₂P-CH₂-PPh₂), 4.13 (m, 1H, Ph₂P-CH₂-PPh₂), 0.72 (bs, 3H, CH₃). ¹³C{¹H} NMR (101 MHz, CD₂Cl₂, -60 °C): δ 179.0 (m, 2C, CO), 156.3 (dt, 1C, ²J_{CP} = 11.5 Hz, ³J_{CC} = 11.5 Hz, CO), -14.8 (bs, 1C, CH₃). ¹⁹F NMR (376 MHz, CD₂Cl₂, -60 °C): δ -67.8 (bs, 1F), -79.5 (s, 3F, OTf), -81.9 (bs, 1F), -169.8 (bs, 1F). ³¹P{¹H} NMR (162 MHz, CD₂Cl₂, -60 °C): δ -3.7 (dm, 1P, ²J_{PP} = 352.1 Hz), -7.3 (dm, 1P, ²J_{PP} = 352.1 Hz), -16.6 (dm, 1P, ²J_{PP} = 301.8 Hz), -20.8 (dm, 1P, ²J_{PP} = 301.8 Hz). Compound 7: ¹H NMR (498 MHz, CD₂Cl₂): δ 5.82 (m, 1H, ³J_{HF} = 17.6 Hz, Ir-C(H)(CF₃)-Ir), 5.44 (m, 1H, Ph₂P-CH₂-PPh₂), 4.08 (m, 1H, Ph₂P-CH₂-PPh₂), 3.88 (m, 1H, Ph₂P-CH₂-PPh₂), 3.85 (m, 1H, Ph₂P-CH₂-PPh₂), 0.71 (t, 3H, ³J_{HP} = 5.7 Hz, CH₃). ¹³C{¹H} NMR (125 MHz, CD₂Cl₂): δ 179.7 (m, 1C, CO), 177.6 (m, 1C, CO), 162.8 (m, 1C, CO), -25.2 (1C, CH₃). ¹⁹F NMR (469 MHz, CD₂Cl₂): δ -42.4 (d, 3F, ³J_{FH} = 17.7 Hz), -79.5 (s, 3F, OTf). ³¹P{¹H} NMR (202 MHz, CD₂Cl₂): δ -9.9 (dm, ²J_{PP} = 392.4 Hz, 1P), -12.6 (dm, ²J_{PP} = 392.4 Hz, 1P), -15.5 (dm, ²J_{PP} = 316.5 Hz, 1P), -17.2 (dm, ²J_{PP} = 316.5 Hz, 1P). Anal. Calcd. for Ir₂S₂P₄F₆O₆¹³CC₅₅H₄₉: C, 46.16; H, 3.33. Found: C, 45.94; H, 3.39%.

- (g) **Reaction of 3 with H₂.** Compound 3 (50 mg, 0.033 mmol) was dissolved in 0.7 mL of CD₂Cl₂ cooled to -78 °C, and 3 mL of hydrogen gas was added by a gas tight syringe. No reaction was observed at this temperature, however warming to -20 °C gave rise to a new set of peaks corresponding to **[Ir₂(CH₃)(H)(CO)₂(μ-κ¹:η²-CF=CFH)(dppm)₂][CF₃SO₃] (8)**. Further

warming to ambient temperature led to the formation of $[\text{Ir}_2(\text{CH}_3)(\text{H})(\text{CO})_2(\mu\text{-H})(\mu\text{-}\kappa^1:\eta^2\text{-CF=CFH})(\text{dppm})_2][\text{CF}_3\text{SO}_3]_2$ (**9**), and after 30 min led to the previously characterized product $[\text{Ir}_2(\mu\text{-H})_2(\text{H})_2(\text{CO})_2(\text{dppm})_2][\text{CF}_3\text{SO}_3]$ (**10**).⁸⁶ Compound **8**: ^1H NMR (400 MHz, CD_2Cl_2 , $-20\text{ }^\circ\text{C}$): δ 6.38 (m, 1H, $\text{Ph}_2\text{P-CH}_2\text{-PPh}_2$), 4.94 (dddd, 1H, $^2J_{\text{HF}} = 63.2\text{ Hz}$, $^3J_{\text{HF}} = 14.7\text{ Hz}$, $^3J_{\text{HP}} = 18.6\text{ Hz}$, $^3J_{\text{HP}} = 4.4\text{ Hz}$, $-\text{C}(\text{F})=\text{C}(\text{H})(\text{F})$), 4.26 (m, 1H, $\text{Ph}_2\text{P-CH}_2\text{-PPh}_2$), 3.62 (m, 1H, $\text{Ph}_2\text{P-CH}_2\text{-PPh}_2$), 3.23 (m, 1H, $\text{Ph}_2\text{P-CH}_2\text{-PPh}_2$), 1.01 (t, 3H, $^3J_{\text{HP}} = 5.0\text{ Hz}$, CH_3), -6.92 (dt, 1H, $^2J_{\text{HP}} = 14.0\text{ Hz}$, $^3J_{\text{HF}} = 6.0\text{ Hz}$). $^{13}\text{C}\{^1\text{H}\}$ NMR (101 MHz, CD_2Cl_2 , $-20\text{ }^\circ\text{C}$): δ 179.2 (b, 1C, CO), 175.5 (b, 1C, CO), -21.7 (m, 1C, CH_3). ^{19}F NMR (376 MHz, CD_2Cl_2 , $-20\text{ }^\circ\text{C}$): δ -60.2 (m, 1F), -79.5 (s, 3F, OTf), -172.9 (m, 1F). $^{31}\text{P}\{^1\text{H}\}$ NMR (162 MHz, CD_2Cl_2 , $-20\text{ }^\circ\text{C}$): δ 18.2 (m, 1P), 9.0 (m, 1P), -2.0 (m, 1P), -6.0 (m, 2P). Compound **9**: ^1H NMR (400 MHz, CD_2Cl_2): δ 6.05 (m, 1H, $\text{Ph}_2\text{P-CH}_2\text{-PPh}_2$), 5.71 (m, 1H, $\text{Ph}_2\text{P-CH}_2\text{-PPh}_2$), 5.18 (m, 1H, $\text{Ph}_2\text{P-CH}_2\text{-PPh}_2$), 4.07 (m, 1H, $\text{Ph}_2\text{P-CH}_2\text{-PPh}_2$), 0.80 (t, 3H, $^3J_{\text{HP}} = 5.5\text{ Hz}$, CH_3), -11.00 (t, 1H, $^2J_{\text{HP}} = 12.0\text{ Hz}$), -14.40 (bs, 1H). $^{13}\text{C}\{^1\text{H}\}$ NMR (101 MHz, CD_2Cl_2): δ 168.2 (b, 1C, CO), 160.4 (b, 1C, CO), -17.9 (bs, 1C, $-\text{CH}_3$). ^{19}F NMR (376 MHz, CD_2Cl_2): δ -79.5 (s, 3F, OTf), -87.9 (m, 1F), -144.1 (dd, 1F, $^2J_{\text{FH}} = 60.9\text{ Hz}$, $^3J_{\text{FF}} = 26.6\text{ Hz}$). $^{31}\text{P}\{^1\text{H}\}$ NMR (162 MHz, CD_2Cl_2): δ 16.2 (m, 1P), 1.7 (m, 1P), -1.7 (m, 1P), -13.5 (m, 2P).

- (h) **Attempted reactions of 4, 5 and 7 with H_2 .** To a solution of either compound **4**, **5**, or **7** dissolved in 0.7 mL of CH_2Cl_2 , 3 mL of H_2 was added via a gas tight syringe. No reaction was observed in any case.
- (i) **Reaction of 3 with CO.** 50 mg of compound **3** (0.032 mmol) was dissolved in 0.7 mL of CD_2Cl_2 in a J-Young tube and 3 mL of CO gas was added by a gas-tight syringe. The reaction was then monitored by NMR spectroscopy. Compound **3** instantly reacted with excess CO gas, initially resulting in the formation of $[\text{Ir}_2(\text{CH}_3)(\text{CO})_3(\mu\text{-}\kappa^1:\eta^2\text{-C}_2\text{F}_2\text{H})(\text{dppm})_2][\text{CF}_3\text{SO}_3]_2$ (**11**) at –

20 °C. Upon warming to ambient temperature, the liberation of both *cis*-difluoropropene and 2,3-difluoropropene was observed, leaving behind the previously characterized compound $[\text{Ir}_2(\text{CO})_5(\text{dppm})_2][\text{CF}_3\text{SO}_3]_2$ (**12**).⁸⁷ Characterization of *cis*-difluoropropene and 2,3-difluoropropene are presented in the results section. Compound **11**: ^1H NMR (400 MHz, CD_2Cl_2 , -20 °C): δ 6.66 (m, 1H, $^2J_{\text{HF}} = 65.2$ Hz, $^3J_{\text{HF}} = 15.3$ Hz, $-\text{C}(\text{F})=\text{C}(\text{H})(\text{F})$), 6.44 (m, 1H, $\text{Ph}_2\text{P}-\text{CH}_2-\text{PPh}_2$), 5.10 (m, 1H, $\text{Ph}_2\text{P}-\text{CH}_2-\text{PPh}_2$), 4.38 (m, 1H, $\text{Ph}_2\text{P}-\text{CH}_2-\text{PPh}_2$), 3.71 (m, 1H, $\text{Ph}_2\text{P}-\text{CH}_2-\text{PPh}_2$), 1.13 (t, 3H, $^3J_{\text{HP}} = 4.8$ Hz, CH_3). $^{13}\text{C}\{^1\text{H}\}$ NMR (101 MHz, CD_2Cl_2 , -20 °C): δ 173.8 (b, 1C, CO), 167.8 (b, 1C, CO), 159.0 (b, 1C, CO), -13.4 (s, 1C, CH_3). ^{19}F NMR (376 MHz, CD_2Cl_2 , -20 °C): δ -53.4 (bm, 1F), -79.5 (s, 3F, OTf), -157.8 (dd, 1F, $^2J_{\text{FH}} = 65.2$ Hz, $^3J_{\text{FF}} = 30.9$ Hz). $^{31}\text{P}\{^1\text{H}\}$ NMR (162 MHz, CD_2Cl_2 , -20 °C): δ 7.4 (m, 1P), 4.0 (m, 1P), -9.4 (m, 1P), -18.2 (m, 2P).

- (j) **Attempted reactions of 4, 5, or 7 with CO.** To a solution of either compound **4**, **5**, or **7** dissolved in 0.7 mL of CH_2Cl_2 , 3 mL of CO was added via a gas tight syringe. No reaction was observed in any case.
- (k) **Reaction of 7 with HOTf.** A sample of **7** was dissolved in 0.7 mL CD_2Cl_2 in an NMR tube and 5 μL of HOTf was added, resulting in a change in color from light orange to light yellow resulting in the formation of $[\text{Ir}_2(\text{OTf})(\text{CO})_3(\mu\text{-CH}_2)(\text{dppm})_2][\text{CF}_3\text{SO}_3]$ (**13**). The solution was transferred to a 100 mL round bottom flask and 20 mL of ether was added to induce precipitation. The resulting yellow powder was further washed with ether and dried under vacuum. Spectral parameters for 1,1,1-trifluoroethane are presented in results section. Crystals of compound **13** were grown via slow diffusion of diethylether into a CH_2Cl_2 solution of the compound. All crystallographic parameters are given in Supporting Information. (63% yield) ^1H NMR (500 MHz, CD_2Cl_2): δ 6.57 (m, 2H, $\text{Ir}-\text{CH}_2-\text{Ir}$), 5.93 (m, 2H, $\text{Ph}_2\text{P}-\text{CH}_2-\text{PPh}_2$), 5.48 (m, 2H, $\text{Ph}_2\text{P}-\text{CH}_2-\text{PPh}_2$). $^{13}\text{C}\{^1\text{H}\}$ NMR (125 MHz, CD_2Cl_2): δ 178.3 (m, 1C, CO), 167.5 (t, 1C, $^2J_{\text{CP}} = 12.5$ Hz, CO), 163.1 (t,

1C, $^2J_{CP} = 11.3$ Hz, CO), 51.4 (quin., 1C, $^2J_{CP} = 5.0$ Hz, Ir-CH₂-Ir). ^{19}F NMR (469 MHz, CD₂Cl₂): δ -77.4 (s, 3F, Ir-OTf), -79.2 (s, 3F, OTf). $^{31}\text{P}\{^1\text{H}\}$ NMR (202 MHz, CD₂Cl₂): δ -2.3 (pseudo triplet, 2P, $^2J_{PP} = 37.7$ Hz), -19.7 (pseudo triplet, 2P, $^2J_{PP} = 37.7$ Hz). HRMS m/z calc. for [^{193}Ir]₂P₄O₆C₅₄¹³CH₄₆F₃S [M*]⁺: 1402.1204, found 1402.1215.

- (l) **Attempted reactions of 4 and 5 with HOTf.** A sample of either 4 or 5 was dissolved in 0.7 mL of CH₂Cl₂. In both cases, an approximately 1.2-fold excess of HOTf was added via a micro-syringe, resulting in no observable difference. NMR spectroscopy confirmed that no reaction had taken place in either case.

2.5.3 X-ray Structure Determinations

2.5.3.1 General. Crystals were grown via slow diffusion of pentane into a CH₂Cl₂ solution of the compound (**3**), or diffusion of ether into a CH₂Cl₂ solution of the compound (**5**, **13**). Data were collected using a Bruker APEX-II CCD detector/D8 diffractometer¹⁰⁴ with the crystals cooled to -100 °C; all data were collected using Mo K α radiation ($\lambda = 0.71073$ Å). The data were corrected for absorption through use of a multi-scan model (*TWINABS*¹⁰⁴) (**3**) or through Gaussian integration from indexing of the crystal faces (**5**, **13**). Structures were solved using Patterson search/structure expansion (*DIRDIF-2008*¹⁰⁵) (**3**), direct methods/structure expansion (*SIR97*¹⁰⁶) (**5**), or direct methods (*SHELXS-97*¹⁰⁷) (**13**). Refinements were completed using the program *SHELXL-97*.¹⁰⁷ Hydrogen atoms were assigned positions based on the sp^2 or sp^3 hybridization geometries of their attached carbon or oxygen atoms, and were given thermal parameters 20% greater than those of their parent atoms. See Supporting Information for a listing of crystallographic experimental data.

2.5.3.2 Special Refinement Conditions. (i) **3**: The crystal used for data collection was found to display non-merohedral twinning. Both components of the twin were indexed with the program *CELL_NOW*¹⁰⁴ (ver. 2008-2). The second twin component can be related to the first component by 180° rotation

about the $[1\ 1/8\ -1/2]$ axis in real space and about the $[1\ 0\ 1]$ axis in reciprocal space. Integrated intensities for the reflections from the two components were written into a *SHELXL-97* HKLF 5 reflection file with the data integration program *SAINTE*¹⁰⁴ (ver. 7.53A), using all reflection data (exactly overlapped, partially overlapped and non-overlapped). The refined value of the twin fraction (*SHELXL-97* BASF parameter) was 0.3377(6). Distance restraints were applied to some of the solvent CH₂Cl₂ and *n*-pentane molecules: $d(\text{Cl}(7\text{S})\text{--C}(4\text{S})) = d(\text{Cl}(8\text{S})\text{--C}(4\text{S})) = 1.80(1)\ \text{\AA}$; $d(\text{Cl}(7\text{S})\cdots\text{Cl}(8\text{S})) = 2.95(1)\ \text{\AA}$; $d(\text{C}(11\text{S})\text{--C}(12\text{S})) = d(\text{C}(12\text{S})\text{--C}(13\text{S})) = d(\text{C}(13\text{S})\text{--C}(14\text{S})) = d(\text{C}(14\text{S})\text{--C}(15\text{S})) = d(\text{C}(21\text{S})\text{--C}(22\text{S})) = d(\text{C}(22\text{S})\text{--C}(23\text{S})) = d(\text{C}(23\text{S})\text{--C}(24\text{S})) = d(\text{C}(24\text{S})\text{--C}(25\text{S})) = 1.54(1)\ \text{\AA}$; $d(\text{C}(11\text{S})\cdots\text{C}(13\text{S})) = d(\text{C}(12\text{S})\cdots\text{C}(14\text{S})) = d(\text{C}(13\text{S})\cdots\text{C}(15\text{S})) = d(\text{C}(21\text{S})\cdots\text{C}(23\text{S})) = d(\text{C}(22\text{S})\cdots\text{C}(24\text{S})) = d(\text{C}(23\text{S})\cdots\text{C}(25\text{S})) = 2.52(1)\ \text{\AA}$. (ii) **5**: The disordered/partially occupied solvent molecules had the following distance restraints applied: for dichloromethane, C–Cl, 1.800(2) Å, Cl⋯Cl, 2.870(2) Å; for diethylether, C–C 1.530(2) Å, C–O, 1.430(2) Å, C⋯O, 2.420(2) Å, C⋯C, 2.340(2) Å. (iii) **13**: Attempts to refine peaks of residual electron density as disordered or partial-occupancy solvent dichloromethane carbon or chlorine atoms were unsuccessful. The data were corrected for disordered electron density through use of the SQUEEZE procedure¹⁰⁸ as implemented in *PLATON*.¹⁰⁹⁻¹¹¹ A total solvent-accessible void volume of 4905 Å³ with a total electron count of 982 (consistent with 24 molecules of solvent dichloromethane, or 1.5 molecules per formula unit of the [Ir₂(CO)₃(CH₂)(O₃SCF₃)(dppm)₂][CF₃SO₃] molecule) was found in the unit cell.

2.6 Acknowledgements

We thank the Natural Sciences and Engineering Research Council of Canada (NSERC) and the University of Alberta for financial support for this research and NSERC for funding the Bruker PLATFORM/SMART 1000 CCD diffractometer, the Bruker D8/APEX II CCD diffractometer and the Nicolet Avator IR spectrometer. We thank the Department's Mass Spectrometry Facility and the

NMR Spectroscopy and Analytical and Instrumentation Laboratories. We also thank Dr. Russell Hughes for discussions. Finally, we thank NSERC and Alberta Innovates – Technology Futures (formerly Alberta Ingenuity Fund) for funding support for M.E.S.

2.7 References

- (1) Gossage, R. A.; van Koten, G. *Top. Organomet. Chem.* **1999**, *3*, 1.
- (2) Bergman, R. G. *Nature* **2007**, *446*, 391.
- (3) Godula, K.; Sames, D. *Science* **2006**, *312*, 67.
- (4) Jia, C. G.; Kitamura, T.; Fujiwara, Y. *Acc. Chem. Res.* **2001**, *34*, 633.
- (5) Labinger, J. A.; Bercaw, J. E. *Nature* **2002**, *417*, 507.
- (6) Shilov, A. E.; Shul'pin, G. B. *Chem. Rev.* **1997**, *97*, 2879.
- (7) Stahl, S. S.; Labinger, J. A.; Bercaw, J. E. *Angew. Chem. Int. Ed.* **1998**, *37*, 2181.
- (8) Jazzar, R.; Hitce, J.; Renaudat, A.; Sofack-Kreutzer, J.; Baudoin, O. *Chem. Eur. J.* **2010**, *16*, 2654.
- (9) Crabtree, R. H. *Chem. Rev.* **1985**, *85*, 245.
- (10) Ryabov, A. D. *Chem. Rev.* **1990**, *90*, 403.
- (11) Arndtsen, B. A.; Bergman, R. G.; Mobley, T. A.; Peterson, T. H. *Acc. Chem. Res.* **1995**, *28*, 154.
- (12) Jun, C.-H. *Chem. Soc. Rev.* **2004**, *33*.
- (13) Murakami, M.; Ito, Y. In *Activation of Unreactive Bonds and Organic Synthesis*; Murai, S., Ed.; Springer: 1999, p 97.
- (14) Lin, Y.-S.; Yamamoto, A. In *Activation of Unreactive Bonds and Organic Synthesis*; Murai, S., Ed.; Springer: 1999, p 161.
- (15) Yamamoto, A. In *Advances in Organometallic Chemistry*; Stone, F. G. A., Robert, W., Eds.; Academic Press: 1992; Vol. 34, p 111.
- (16) Luh, T. Y.; Leung, M. K.; Wong, K. T. *Chem. Rev.* **2000**, *100*, 3187.
- (17) Grushin, V. V.; Alper, H. In *Activation of Unreactive Bonds and Organic Synthesis*; Murai, S., Ed.; Springer: 1999, p 193.
- (18) Chirik, P. J. *Organometallics* **2010**, *29*, 1500.
- (19) MacLachlan, E. A.; Fryzuk, M. D. *Organometallics* **2006**, *25*, 1530.
- (20) Burdeniuc, J.; Jedlicka, B.; Crabtree, R. H. *Chem. Ber. Recl.* **1997**, *130*, 145.
- (21) Hughes, R. P. *Eur. J. Inorg. Chem.* **2009**, *2009*, 4591.

- (22) Kiplinger, J. L.; Richmond, T. G.; Osterberg, C. E. *Chem. Rev.* **1994**, *94*, 373.
- (23) Perutz, R. N.; Braun, T. In *Comprehensive Organometallic Chemistry III* 2007; Vol. 1, p 725.
- (24) Torrens, H. *Coord. Chem. Rev.* **2005**, *249*, 1957.
- (25) Amii, H.; Uneyama, K. *Chem. Rev.* **2009**, *109*, 2119.
- (26) *Organofluorine Chemistry: Principles and Commercial Applications*; Plenum: New York, 1994.
- (27) Hiyama, T. *Organofluorine Compounds*; Springer: Berlin, 2000.
- (28) Amii, H.; Kobayashi, T.; Uneyama, K. *Abstr. Paper. Am. Chem. Soc. Natl. Meet.* **2003**, *226*, U520.
- (29) Wallington, T. J.; Schneider, W. F.; Worsnop, D. R.; Nielsen, O. J.; Sehested, J.; Debruyne, W. J.; Shorter, J. A. *Environ. Sci. Technol.* **1994**, *28*, A320.
- (30) Metz, B.; Kuijpers, L.; Solomon, S.; Andersen, S. O.; Davidson, O.; Pons, J.; Jager, D. d.; Kestin, T.; Manning, M.; Meyer, L. *Safeguarding the Ozone Layer and the Global Climate System: Issues Related to Hydrofluorocarbons and Perfluorocarbons*, 2005.
- (31) Buckley, H. L.; Wang, T. E.; Tran, O.; Love, J. A. *Organometallics* **2009**, *28*, 2356.
- (32) Wang, T. G.; Love, J. A. *Organometallics* **2008**, *27*, 3290.
- (33) Kraft, B. M.; Jones, W. D. *J. Organomet. Chem.* **2002**, *658*, 132.
- (34) Schaub, T.; Backes, M.; Radius, U. *J. Am. Chem. Soc.* **2006**, *128*, 15964.
- (35) Schaub, T.; Fischer, P.; Steffen, A.; Braun, T.; Radius, U.; Mix, A. *J. Am. Chem. Soc.* **2008**, *130*, 9304.
- (36) Reade, S. P.; Mahon, M. F.; Whittlesey, M. K. *J. Am. Chem. Soc.* **2009**, *131*, 1847.
- (37) Nova, A.; Reinhold, M.; Perutz, R. N.; Macgregor, S. A.; McGrady, J. E. *Organometallics* **2010**, *29*, 1824.
- (38) Aizenberg, M.; Milstein, D. *Science* **1994**, *265*, 359.

- (39) Anderson, D. J.; McDonald, R.; Cowie, M. *Angew. Chem. Int. Ed.* **2007**, *46*, 3741.
- (40) Braun, T.; Salomon, M. A.; Altenhoner, K.; Teltewskoi, M.; Hinze, S. *Angew. Chem. Int. Ed.* **2009**, *48*, 1818.
- (41) Hacker, M. J.; Littlecott, G. W.; Kemmitt, R. D. W. *J. Organomet. Chem.* **1973**, *47*, 189.
- (42) Hughes, R. P.; Rose, P. R.; Rheingold, A. L. *Organometallics* **1993**, *12*, 3109.
- (43) Jones, M. T.; McDonald, R. N. *Organometallics* **1988**, *7*, 1221.
- (44) Kemmitt, R. D. W.; Nichols, D. I. *J. Chem. Soc. A* **1969**, 1577.
- (45) Kirkham, M. S.; Mahon, M. F.; Whittlesey, M. K. *Chem. Comm.* **2001**, 813.
- (46) Maples, P. K.; Green, M.; Stone, F. G. A. *J. Chem. Soc., Dalton Trans.* **1973**, 2069.
- (47) Ristic-Petrovic, D.; Wang, M.; McDonald, R.; Cowie, M. *Organometallics* **2002**, *21*, 5172.
- (48) Roundhill, D. M.; Lawson, D. N.; Wilkinson, G. *J. Chem. Soc. A* **1968**, 845.
- (49) Roundhill, D. M.; Wilkinson, G. *J. Chem. Soc. A* **1968**, 506.
- (50) Ferrando-Miguel, G.; Gerard, H.; Eisenstein, O.; Caulton, K. G. *Inorg. Chem.* **2002**, *41*, 6440.
- (51) Jones, W. D. *Dalton Trans.* **2003**, 3991.
- (52) Kraft, B. M.; Lachicotte, R. J.; Jones, W. D. *J. Am. Chem. Soc.* **2000**, *122*, 8559.
- (53) Noveski, D.; Braun, T.; Schulte, M.; Neumann, B.; Stammler, H. G. *Dalton Trans.* **2003**, 4075.
- (54) Peterson, A. A.; McNeill, K. *Organometallics* **2006**, *25*, 4938.
- (55) Peterson, A. A.; Thoreson, K. A.; McNeill, K. *Organometallics* **2009**, *28*, 5982.
- (56) Kuhnel, M. F.; Lentz, D. *Angew. Chem. Int. Ed.* **2010**, *49*, 2933.

- (57) Braun, T.; Noveski, D.; Neumann, B.; Stammeler, H. G. *Angew. Chem. Int. Ed.* **2002**, *41*, 2745.
- (58) Kraft, B. M.; Jones, W. D. *J. Am. Chem. Soc.* **2002**, *124*, 8681.
- (59) Green, M.; Laguna, A.; Spencer, J. L.; Stone, F. G. A. *J. Chem. Soc., Dalton Trans.* **1977**, 1010.
- (60) Hughes, R. P.; Laritchev, R. B.; Zakharov, L. N.; Rheingold, A. L. *J. Am. Chem. Soc.* **2004**, *126*, 2308.
- (61) Kraft, B. M.; Clot, E.; Eisenstein, O.; Brennessel, W. W.; Jones, W. D. *J. Fluorine Chem.* **2010**, *131*, 1122.
- (62) Bonnet, J. J.; Mathieu, R.; Poilblanc, R.; Ibers, J. A. *J. Am. Chem. Soc.* **1979**, *101*, 7487.
- (63) Booth, B. L.; Haszeldin, R. N.; Mitchell, P. R.; Cox, J. J. *Chem. Comm.* **1967**, 529.
- (64) Huang, D. J.; Koren, P. R.; Folting, K.; Davidson, E. R.; Caulton, K. G. *J. Am. Chem. Soc.* **2000**, *122*, 8916.
- (65) Brothers, P. J.; Burrell, A. K.; Clark, G. R.; Rickard, C. E. F.; Roper, W. R. *J. Organomet. Chem.* **1990**, *394*, 615.
- (66) Burrell, A. K.; Clark, G. R.; Jeffrey, J. G.; Rickard, C. E. F.; Roper, W. R. *J. Organomet. Chem.* **1990**, *388*, 391.
- (67) Burrell, A. K.; Clark, G. R.; Rickard, C. E. F.; Roper, W. R. *J. Organomet. Chem.* **1994**, *482*, 261.
- (68) Anderson, D. J., *Ph.D. Thesis*, University of Alberta, 2007.
- (69) Ristic-Petrovic, D.; Anderson, D. J.; Torkelson, J. R.; McDonald, R.; Cowie, M. *Organometallics* **2003**, *22*, 4647.
- (70) Torkelson, J. R.; Antwi-Nsiah, F. H.; McDonald, R.; Cowie, M.; Pruis, J. G.; Jalkanen, K. J.; DeKock, R. L. *J. Am. Chem. Soc.* **1999**, *121*, 3666.
- (71) Foris, A. *Magnetic Resonance in Chemistry* **2004**, *42*, 534.
- (72) Ristic-Petrovic, D.; Anderson, D. J.; Torkelson, J. R.; Ferguson, M. J.; McDonald, R.; Cowie, M. *Organometallics* **2005**, *24*, 3711.
- (73) Dungan, C. H.; Wazer, J. R. V. *Compilation of reported ¹⁹F NMR chemical shifts, 1951 to mid-1967*, Wiley-Interscience, New York, **1970**.

- (74) Alvarez, M. A.; Garcia, M. E.; Ramos, A.; Ruiz, M. A. *J. Organomet. Chem.* **2009**, *694*, 3864.
- (75) Alvarez, M. A.; Garcia, M. E.; Ramos, A.; Ruiz, M. A.; Lanfranchi, M.; Tiripicchio, A. *Organometallics* **2007**, *26*, 5454.
- (76) Busetto, L.; Maitlis, P. M.; Zanotti, V. *Coord. Chem. Rev.* **2010**, *254*, 470.
- (77) Frohnapfel, D. S.; Templeton, J. L. *Coord. Chem. Rev.* **2000**, *206*, 199.
- (78) Gao, Y.; Jennings, M. C.; Puddephatt, R. J. *Dalton Trans.* **2003**, 261.
- (79) Jackson, A. B.; Khosla, C.; White, P. S.; Templeton, J. L. *Inorg. Chem.* **2008**, *47*, 8776.
- (80) Le Goff, A.; Le Roy, C.; Petillon, F. Y.; Schollhammer, P.; Talarmin, J. *New J. Chem.* **2007**, *31*, 265.
- (81) Li, X. W.; Vogel, T.; Incarvito, C. D.; Crabtree, R. H. *Organometallics* **2005**, *24*, 62.
- (82) Stone, K. C.; Jamison, G. M.; White, P. S.; Templeton, J. L. *Organometallics* **2003**, *22*, 3083.
- (83) Dewolf, M. Y.; Baldeschwieler, J. D. *J. Mol. Spec.* **1964**, *13*, 344.
- (84) Danyluk, S. S. *J. Am. Chem. Soc.* **1964**, *86*, 4504.
- (85) Johannesen, R. B.; Brinckman, F. E.; Coyle, T. D. *J. Phys. Chem.* **1967**, *72*, 660
- (86) McDonald, R.; Sutherland, B. R.; Cowie, M. *Inorg. Chem.* **1987**, *26*, 3333.
- (87) Sutherland, B. R.; Cowie, M. *Organometallics* **1985**, *4*, 1637.
- (88) Pettinari, C.; Rafaiiani, G. In *Encyclopedia of Spectroscopy and Spectrometry*; John, C. L., Ed.; Elsevier: Oxford, 1999, p 489.
- (89) Foris, A. *Magn. Reson. Chem.* **2004**, *42*, 534.
- (90) Beaudet, R. A.; Baldeschwieler, J. D. *J. Mol. Spec.* **1962**, *9*, 30.
- (91) Lynden-Bell, R. M.; Sheppard, N. *Proc. R. Soc. London, Ser. A* **1962**, *269*, 385.
- (92) Cedeño, D. L.; Weitz, E. *J. Am. Chem. Soc.* **2001**, *123*, 12857.
- (93) Cedeño, D. L.; Weitz, E.; Berces, A. *J. Phys. Chem. A* **2001**, *105*, 8077.
- (94) Bent, H. A. *Chem. Rev.* **1961**, *61*, 275.
- (95) Bingham, R. C. *J. Am. Chem. Soc.* **1976**, *98*, 535.

- (96) Craig, N. C.; Piper, L. G.; Wheeler, V. L. *J. Phys. Chem.* **1971**, *75*, 1453.
- (97) Goodman, L.; Gu, H. B.; Pophristic, V. *J. Phys. Chem. A* **2005**, *109*, 1223.
- (98) Waldron, J. T.; Snyder, W. H. *J. Am. Chem. Soc.* **1973**, *95*, 5491.
- (99) Lemal, D. M. *J. Org. Chem.* **2004**, *69*, 1.
- (100) O'Hagan, D. *Chem. Soc. Rev.* **2008**, *37*, 308.
- (101) Yuan, J.; Hughes, R. P.; Golen, J. A.; Rheingold, A. L. *Organometallics* **2010**, *29*, 1942.
- (102) Hughes, R. P.; Lindner, D. C.; Rheingold, A. L.; LiableSands, L. M. *J. Am. Chem. Soc.* **1997**, *119*, 11544.
- (103) Hughes, R. P.; Lindner, D. C.; Smith, J. M.; Zhang, D. H.; Incarvito, C. D.; Lam, K. C.; Liable-Sands, L. M.; Sommer, R. D.; Rheingold, A. L. *Dalton Trans.* **2001**, 2270.
- (104) Programs for diffractometer operation, unit cell indexing, data collection, data reduction and absorption correction were those supplied by Bruker.
- (105) The DIRDIF-2008 program system. Crystallography Laboratory, Radboud University Nijmegen, The Netherlands
- (106) Altomare, A.; Burla, M. C.; Camalli, M.; Cascarano, G. L.; Giacovazzo, C.; Guagliardi, A.; Moliterni, A. G. G.; Polidori, G.; Spagna, R. *J. Appl. Cryst.* **1999**, *32*, 115.
- (107) Sheldrick, G. M. *Acta Crystallogr.* **2008**, *A64*, 112.
- (108) van der Sluis, P.; Spek, A. L. *Acta Crystallogr.* **1990**, *A46*, 194.
- (109) Spek, A. L. *Acta Crystallogr.* **1990**, *A46*, C34.
- (110) Spek, A. L. *J. Appl. Cryst.* **2003**, *36*, 7.
- (111) *PLATON* - a multipurpose crystallographic tool. Utrecht University, Utrecht, The Netherlands.

Chapter 3 – Facile Carbon-Fluorine Bond Activation and Subsequent Functionalization of 1,1-Difluoroethylene and Tetrafluoroethylene Promoted by Adjacent Metal Centres[†]

3.1 Introduction

Fluorocarbons are currently widely used in a variety of applications, as surfactants, refrigerants, polymers, pharmaceuticals and agrochemicals,¹⁻⁴ in which the physical and chemical properties giving rise to these applications result, in large part, from the high polarity and inertness of the very strong C–F bond,⁵ combined with the small size of fluorine which results in minimal changes in steric properties upon substitution of hydrogen by fluorine. The rapidly expanding use of fluorocarbons requires the development of new, more efficient synthetic routes to these species and demands a better understanding of the chemistry associated with C–F bonds in order to develop catalytic routes for the replacement of fluorine substituents by other groups.⁶⁻¹¹ However, the inert nature of C–F bonds that is so important in many of the useful characteristics of fluorocarbons can also be a detriment leading to the persistence of global-warming and ozone-depleting fluorocarbons in the atmosphere.^{12,13} Addressing the problems posed by these persistent pollutants requires more effective routes for their degradation into environmentally more benign derivatives, again necessitating a better understanding of the reactivity of C–F bonds.

Much of the work to date on carbon–fluorine bond activation has focused on the cleavage of aryl C–F bonds using a variety of transition metal complexes.¹⁴⁻²⁷ Although numerous examples now exist describing the activation of olefinic carbon–fluorine bonds,²⁸⁻³⁵ the majority involve hydrodefluorination,³⁶⁻⁴² with little emphasis on the selective activation of olefinic C–F bonds.

[†] The work presented in this chapter has been accepted for publication. Slaney, M.E.; Anderson, D.J.; Ristic-Petrovic, D.; McDonald, R.; Cowie, M. Accepted, *Chem. Eur. J.*, Nov 8, 2011. Manuscript #: chem.201101835

Tetrafluoroethylene, one of the most studied fluoroolefins, has been shown to undergo C–F activation by a number of routes, including [1,2]-fluoride shifts,^{43,44} and F[−]-ion abstraction induced by either Lewis or Bronsted acids,⁴⁴⁻⁴⁹ in which coordination of the fluoroolefin to the metal results in labilization of the C–F bonds, possibly a result of back donation into the C–F σ^* -orbitals, rendering the coordinated olefin susceptible to fluoride abstraction by strong electrophiles.^{5,50-54}

Perfluoropropene has also been well studied in C–F activation, displaying similar reactivity to that shown by tetrafluoroethylene, including [1,2]-fluoride shifts to give bridging perfluoroisopropylidene groups,⁵⁵ acid-induced HF elimination,⁵⁶ and F[−] abstraction by SnCl₄ giving a range of chlorine-substituted products.⁵⁷ The most common method for activating perfluoropropene involves hydrodefluorination.^{39,58,59} Braun and coworkers have shown that [RhH(PEt₃)₃] readily activates sp²-hybridized C–F bonds of perfluoropropene, resulting in the formation of 1,1,1-trifluoropropane, in the presence of hydrogen.^{39,58} Recently, these workers also reported that the addition of the Lewis acid, HBpin (HBpin = 4,4,5,5-tetramethyl-1,3,2-dioxaborolane, pinacolborane) to [RhH(PEt₃)₃] renders it catalytically active towards hydrodefluorination of perfluoropropene, resulting in a variety of borylalkanes; in all cases the sp³-hybridized C–F bonds remain intact.⁵⁹

In contrast, 1,1-difluoroethylene has received much less attention, and to our knowledge, only two examples exist apart from our own preliminary report.⁴⁸ The first example demonstrates that [RhCl(PPh₃)₃] and other related Rh(I) complexes react with 1,1-difluoroethylene under hydrolysis conditions to form the carbonyl complex, [RhCl(CO)(PPh₃)₂], in which the carbonyl carbon originates from the difluoroethylene ligand,⁴⁵ and more recently, Jones and coworkers have accomplished hydrodefluorination of 1,1-difluoroethylene by Cp^{*}₂ZrH₂, producing two equivalents of Cp^{*}₂ZrHF along with the formation of Cp^{*}₂Zr(Et)H, the result of the hydrodefluorinated product ethylene being trapped by Cp^{*}₂ZrH₂.^{38,60}

Our emphasis in activating fluoroolefins is directed towards the use of pairs of adjacent metals to perform the activation.^{48,61} We have shown that fluoroolefins containing a pair of *geminal* fluorines can coordinate to binuclear systems in a bridging mode, in which they are highly susceptible to C–F activation.^{48,61} In addition, when the environments of the two metals differ, olefin activation can be both stereo- and regioselective. In Chapter 2, trifluoroethylene was shown to undergo a series of stereo- and regioselective C–F bond activations while bridging two iridium centres, the selectivity of which could be varied by changing the conditions.⁶¹ Recall the trifluoroethylene-bridged precursor, $[\text{Ir}_2(\text{CH}_3)(\text{CO})_2(\mu\text{-C}_2\text{F}_3\text{H})(\text{dppm})_2]^+$ (**2**) reacts with one or two equivalents of either HOTf or $(\text{CH}_3)_3\text{SiOTf}$, yielded the corresponding *cis*-difluorovinyl- or fluorovinylidene-bridged products, respectively, the former of which yielded two isomers of difluoropropene under CO or *cis*-difluoroethylene under H_2 . C–F bond activation of **2** could also be accomplished by water, yielding a 2,2-difluorovinyl product, and was even possible under CO, resulting in isomerization of the trifluoroethylene to a 2,2,2-trifluoroethylidene moiety, which on protonation yielded 1,1,1-trifluoroethane.⁶¹

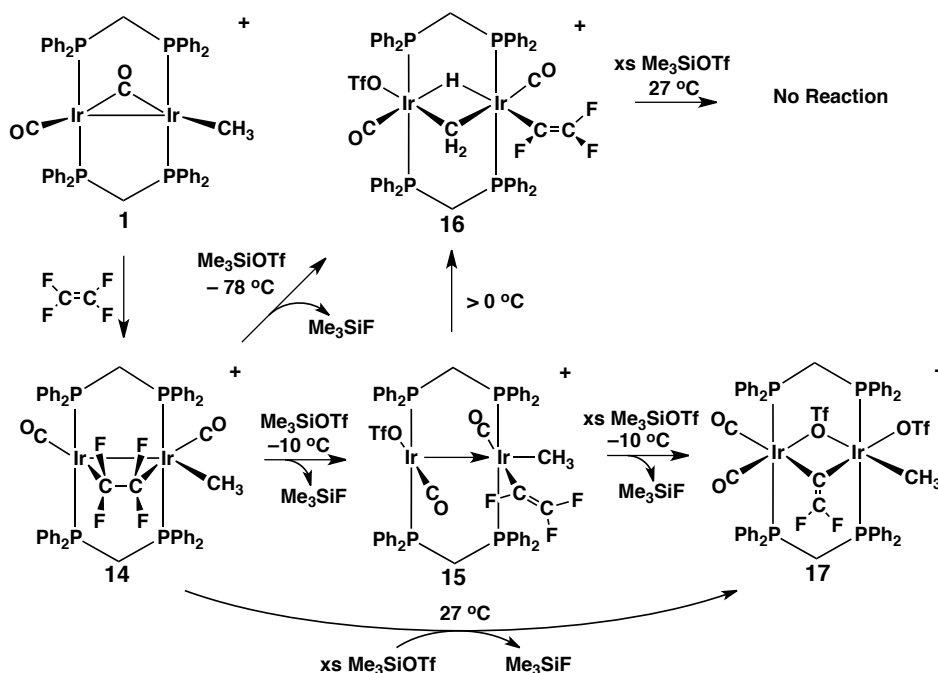
In this Chapter, we report facile C–F bond activation in tetrafluoroethylene and 1,1-difluoroethylene by a number of routes, along with methods for functionalizing the resulting fluorocarbyl fragments and compare this chemistry to that of trifluoroethylene.⁶¹ Although a preliminary report of some of this work has appeared,⁴⁸ subsequent studies, reported herein, have allowed us to detect important differences in the reactivity of these three fluoroolefins, permitting a better understanding of the factors influencing the cooperative C–F activation of fluoroolefins by adjacent metal centres.

3.2 Results

3.2.1 C–F Bond Activation by Lewis Acids.

3.2.1.1 Tetrafluoroethylene. At ambient temperature $[\text{Ir}_2(\text{CH}_3)(\text{CO})_2(\text{dppm})_2][\text{OTf}]$ (**1**) reacts with tetrafluoroethylene (5 equiv over 1 h) to yield the tetrafluoroethylene-bridged product $[\text{Ir}_2(\text{CH}_3)(\text{CO})_2(\mu\text{-C}_2\text{F}_4)(\text{dppm})_2][\text{OTf}]$ (**14**),

diagrammed in Scheme 3.1. The spectroscopic characterization of **14** has been described previously⁶² and its structure is now confirmed by the X-ray determination shown (for the complex cation of one independent molecule) in the ORTEP view in Figure 3.1.



Scheme 3.1 – Coordination of tetrafluoroethylene to $[\text{Ir}_2(\text{CH}_3)(\text{CO})_2(\text{dppm})_2][\text{OTf}]$ (**1**) and subsequent C–F bond activations.

This figure clearly demonstrates the bridging tetrafluoroethylene coordination mode, accompanied by rehybridization of the olefinic carbons from sp^2 to sp^3 , as seen by the C(4)–C(5) bond length (average, 1.560(9) Å for the six independent molecules), typical of a carbon-carbon single bond (1.54 Å), while the geometries at C(4) and C(5) are close to tetrahedral. The F(1)–C(4)–F(2) and F(3)–C(5)–F(4) angles (average, 101.7(5)° and 101.2(4)°, respectively), which are less than the tetrahedral value, are in keeping with Bent's rule.⁶³ In such a geometry, rehybridization of the olefinic carbons to sp^3 suggests that the fluoroolefin can be viewed as a 1,2-dimetallated fluoroalkane or alternatively, from the perspective of each metal, as a fluoroalkyl ligand. On this basis we had previously proposed that the olefinic C–F bonds, which are adjacent to each

metal, should be susceptible to fluoride-ion abstraction as is commonly observed in other fluoroalkyls.¹¹

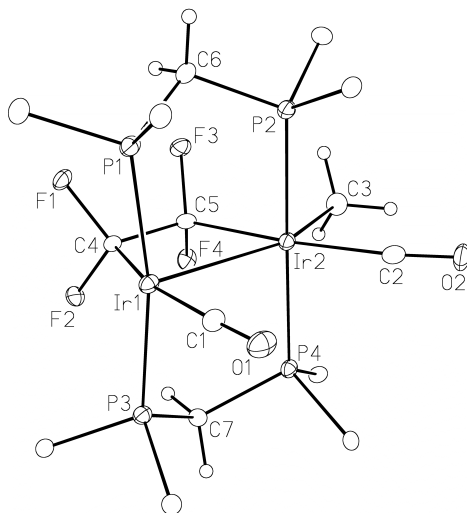


Figure 3.1 – Perspective view of one of the six crystallographically-independent $[\text{Ir}_2(\text{CH}_3)(\text{CO})_2(\mu\text{-C}_2\text{F}_4)(\text{dppm})_2]^+$ cations of compound **14** showing the atom labelling scheme. Non-hydrogen atoms are represented by Gaussian ellipsoids at the 20% probability level. Hydrogen atoms attached to C(3), C(6), and C(7) are shown with arbitrarily small thermal parameters, while only the ipso carbons of the dppm phenyls groups are shown. Relevant average bond distances (Å) and angles (°) for the complex cations: Ir(1) – Ir(2) = 2.8840(4); Ir(1) – C(4) = 2.113(6); Ir(2) – C(5) = 2.093(6); C(4) – C(5) = 1.560(9); Ir(1) – Ir(2) – C(5) = 70.6(1); Ir(2) – Ir(1) – C(4) = 72.6(2); F(1) – C(4) – F(2) = 101.7(5); F(3) – C(5) – F(4) = 101.2(5). Estimated standard deviation values are those of an individual determination.

In keeping with this proposal, compound **14** reacts with trimethylsilyltriflate at $-10\text{ }^\circ\text{C}$ over 2 h to yield the trifluorovinyl species, $[\text{Ir}_2(\kappa^1\text{-C}_2\text{F}_3)(\text{CH}_3)(\text{OTf})(\text{CO})_2(\text{dppm})_2][\text{OTf}]$ (**15**), accompanied by the formation of trimethylsilyl fluoride. In the original report on this product,⁴⁸ a bridging $\kappa^1:\eta^2$ -coordination mode was proposed for the trifluorovinyl group, as has been established for the *cis*-difluorovinyl group in $[\text{Ir}_2(\text{CH}_3)(\text{OTf})(\text{CO})_2(\mu\text{-}\kappa^1:\eta^2\text{-CF=CFH})(\text{dppm})_2][\text{OTf}]$.⁶¹ However, further NMR studies suggest that in **15** the trifluorovinyl group is terminally bound to one metal as shown in Scheme 3.1. Owing to the instability of **15** at temperatures above $0\text{ }^\circ\text{C}$ its characterization is limited to NMR spectroscopy at low temperature.

The $^{31}\text{P}\{^1\text{H}\}$ NMR spectrum of **15** at $-10\text{ }^\circ\text{C}$ appears as two resonances (characteristic of an AA'BB' spin system) at δ 13.0 and -7.8 , showing mutual

coupling ($J_{PP} = 24.7$ Hz). This pattern is indicative of two chemical environments for the pairs of ^{31}P nuclei, and effectively rules out a bridged $\kappa^1:\eta^2$ -binding mode for the fluorovinyl unit, which should give rise to four ^{31}P resonances, by virtue of both “top/bottom” and “left/right” asymmetry that would arise with this bridging arrangement (for example, see Chapter 2). The two ^1H resonances observed for the dppm methylene groups (at δ 4.51 and 3.54) again argue against a bridging C_2F_3 group, which would be expected to give rise to four chemically inequivalent methylene protons. The methyl protons appear as a doublet of triplets ($J_{\text{HF}} = 5.3$ Hz, $^3J_{\text{HP}} = 4.9$ Hz) displaying coupling to one fluorine and to the pair of adjacent ^{31}P nuclei. As described in what follows, the H–F spin-spin coupling results from a through-space interaction involving the fluorine that is *cis* to the Ir–vinyl bond, suggesting that both groups are adjacent, probably on the same metal.

The ^{19}F NMR spectrum displays three fluorovinyl signals at δ –81.0, –120.8 and –131.8, all appearing as doublets of doublets, resulting from fluorine-fluorine coupling; the downfield signal shows 26.6 Hz *cis* coupling and 73.9 Hz *geminal* coupling, the signal at δ –120.8 shows *geminal* and *trans* couplings of 73.9 and 101.4 Hz, respectively, and the upfield signal shows *cis* and *trans* couplings of 26.6 and 101.4 Hz, respectively. Although the breadth of the signals do not allow direct observation of coupling to the methyl protons, signal enhancement shows additional non-resolvable coupling within the signal at δ –120.8, which is absent in the other ^{19}F signals, suggesting coupling to the methyl protons. Two ^{19}F signals also appear at δ –77.1 and –79.4, corresponding to coordinated and free triflate ions, respectively.

The structure proposed for **15** in Scheme 3.1 is equivocal, since the breadth of the NMR signals do not allow the spin-spin coupling, that could help identify the geometry at each metal, to be determined. The structural assignment is made on the assumption that activation of a C–F bond adjacent to the methyl ligand is favoured. The “Ir(CH₃)” end of the complex should be more electron rich than the other end, carrying the positive charge, suggesting that back donation into the C–F σ^* orbitals should be more prominent at this end. Although steric arguments might favour C–F bond activation adjacent to the vacant

coordination site on the other iridium, our previous report⁶¹ shows that activation of coordinated trifluoroethylene by triflic acid or trimethylsilyl triflate occurs exclusively at the C–F bond adjacent to the methyl ligand and not at the sterically less crowded site.

Above 0 °C, compound **15** transforms irreversibly over 2 h into the methylene/hydride isomer, $[\text{Ir}_2(\kappa^1\text{-C}_2\text{F}_3)(\text{OTf})(\text{CO})_2(\mu\text{-H})(\mu\text{-CH}_2)(\text{dppm})_2][\text{OTf}]$ (**16**) resulting from C–H activation of the methyl group. Conversely, compound **16** can also be prepared by refluxing the tetrafluoroethylene-bridged species (**14**) in benzene for 30 min in the presence of Me_3SiOTf . Again, the $^{31}\text{P}\{^1\text{H}\}$ NMR spectrum indicates the presence of two chemical environments for these nuclei, while three resonances (2:2:2 ratio) appear in the ^1H NMR spectrum for the dppm and metal-bridged methylene groups, with the two dppm methylene signals being overlapped. The presence of an upfield shift ($\delta -12.23$) due to the hydride ligand is also diagnostic. The unusual process whereby the methyl group is converted into hydride and methylene groups on *opposite* faces of the complex will be rationalized later.

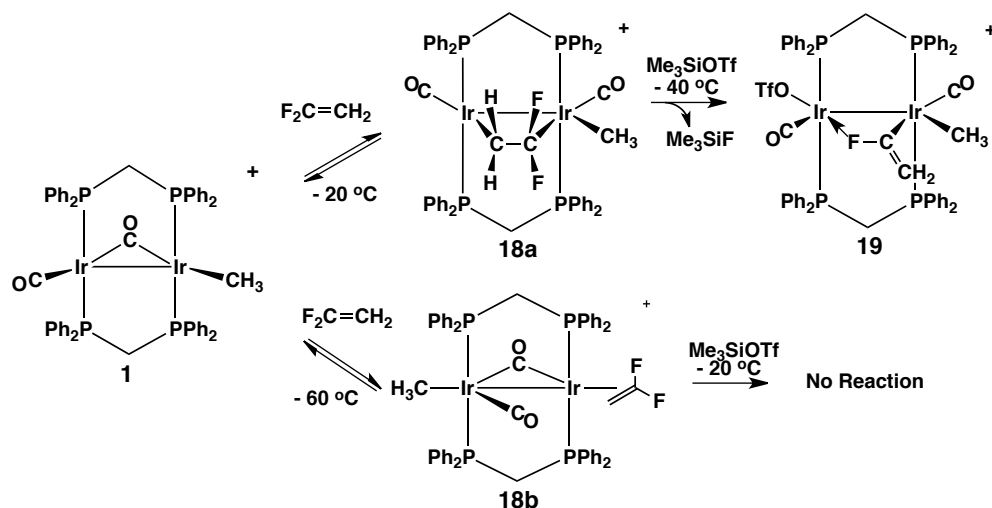
Although the preliminary communication on compound **16** reported its X-ray structure determination,⁴⁸ this structure was disordered, having cocrystallized with $[\text{Ir}_2(\text{OTf})(\text{CO})_3(\mu\text{-CH}_2)(\text{dppm})_2][\text{OTf}]$, an apparent result of trifluoroethylene elimination from and CO addition to **16** (presumably from decomposition during recrystallization). We have subsequently been able to crystallize **16** without this impurity and its X-ray structure is now reported. Figure 3.2 confirms the proposed structure of compound **16**, showing the bridging methylene and hydride groups on opposite faces of the complex, having the trifluorovinyl group terminally bound opposite the $\mu\text{-H}$ ligand. Although pure, the structure of **16** displays a minor disorder, in this case over two orientations of the trifluorovinyl group (in a 3:1 ratio) by an approximate 180° rotation around the Ir(1) – C(4) bond. This disorder also gives rise to minor differences in phenyl group orientations between the two disordered forms, the major occupancy one of which is shown in Figure 3.2. The C(4)–C(5) distances within the two disordered orientations of the trifluorovinyl group (1.28(1) and 1.36(2) Å) are consistent with

driving force for the conversion of **15** and **16** is assumed to be the attainment of the stable Ir(III)/Ir(III) state in which both metals have a favoured octahedral geometry.

A bridging triflate ion is assumed for **17** in order to give both Ir(III) centres their favoured 18-electron configuration; as such, this species should display four ^{31}P resonances for the chemically inequivalent ^{31}P nuclei (a result of the inequivalence of both metals together with top-bottom asymmetry from the bridging triflate). However only two signals are seen, presumably since the slight “top/bottom” differentiation, resulting from the $\mu\text{-OTf}$ group, is small enough to result in the accidental equivalences of the corresponding resonances (not unlike that displayed later for compound **21**). In the ^{19}F NMR spectra three unique signals appear for the bridging ($\delta -76.3$), terminal ($\delta -78.0$) and free ($\delta -78.9$) triflate ions, along with two doublets ($\delta -69.3, -84.6$) corresponding to the inequivalent fluorines of the difluorovinylidene group, displaying mutual *geminal* coupling of 97.0 Hz. The $^{13}\text{C}\{^1\text{H}\}$ NMR spectrum shows two carbonyl resonances and selective ^{31}P decoupling experiments establish that both carbonyls are bound to the same metal, having the methyl group on the adjacent metal which is presumably also the site of the terminally coordinated triflate group. Although not as common as terminally bound groups, bridging triflate groups are not uncommon, especially with late transition metals.⁶⁴⁻⁷²

3.2.1.2 1,1-Difluoroethylene. As reported previously,⁶² 1,1-difluoroethylene reacts with **1** to yield three isomers of $[\text{Ir}_2(\text{CH}_3)(\text{CO})_2(\text{C}_2\text{F}_2\text{H}_2)(\text{dppm})_2][\text{OTf}]$ (**18**), depending on the reaction conditions. The kinetic isomer, (not shown) is stable only at temperatures below $-60\text{ }^\circ\text{C}$ while isomers **18a** and **18b**, diagrammed in Scheme 3.2, coexist at approximately $-20\text{ }^\circ\text{C}$, as **18b** slowly transforms into **18a** at this temperature. Cooling to $-40\text{ }^\circ\text{C}$ slows this conversion to a rate at which it cannot be detected over a several hour period, allowing us the opportunity to compare the reactivity of η^2 - and μ -bound fluoroolefins, and in particular to test our hypothesis^{48,61} that coordination in the bridging site results in more facile fluoride-ion abstraction than from an η^2 -fluoroolefin bound to a single metal. Addition of 1.2 equiv of Me_3SiOTf to a 1:1 mixture of **18a** and **18b** at -40

$^{\circ}\text{C}$ results in the conversion of **18a** to $[\text{Ir}_2(\text{CH}_3)(\text{OTf})(\text{CO})_2(\mu-\kappa^1:\kappa^1\text{-C,F-C(F)=CH}_2)(\text{dppm})_2][\text{OTf}]$ (**19**) in which a unique $\mu-\kappa^1:\kappa^1$ -bridging mode is proposed (Scheme 3.2). Under these conditions **18b** remains unreacted, and even warming to 0°C , at which conversion of **18b** to **18a** is still slow, compound **18b** persists in the presence of Me_3SiOTf . This experiment clearly demonstrates significantly more facile C–F activation of the fluoroolefin in the bridging site, than when bound in an η^2 -manner to one metal.



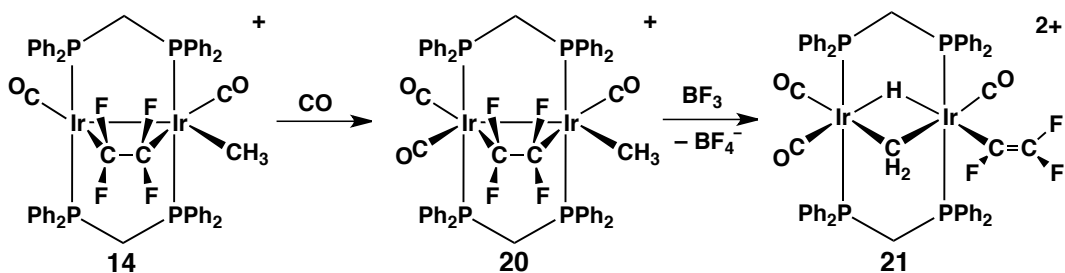
Scheme 3.2 – Two isomers of $[\text{Ir}_2(\text{CH}_3)(\text{CO})_2(\text{C}_2\text{F}_2\text{H}_2)(\text{dppm})_2][\text{OTf}]$ (**18**) and fluoride abstraction from **18a**.

Compound **19** is unstable above -20°C , so its characterization is based on NMR spectroscopy at this temperature. In our earlier communication,⁴⁸ compound **19** was proposed to have a $\kappa^1:\eta^2$ -binding mode for the fluorovinyl group as demonstrated for the *cis*-difluorovinyl analogue.⁶¹ However, subsequent studies have shown that this is not the case, and instead an unprecedented binding mode is now proposed, demonstrating an interesting contrast in the structures of the otherwise closely related trifluorovinyl, *cis*-difluorovinyl¹⁶ and monofluorovinyl products. The $^{31}\text{P}\{^1\text{H}\}$ NMR spectrum of **19** displays two signals, a doublet of multiplets at δ 1.2 and a multiplet at δ -5.5, again consistent with "top/bottom" symmetry in the compound. The additional splitting in the downfield signal is a result of coupling ($^2J_{\text{PF}} = 47.0$ Hz) to the fluorine of the bridging fluorovinyl ligand, and corresponds closely to literature values for *cis*-

$^2J_{\text{PF}}$ couplings;⁷³⁻⁷⁷ this coupling is also observed in the ^{19}F spectrum, with a triplet appearing upfield at $\delta -211.2$, well within the typical range for iridium fluoride compounds.⁷⁶⁻⁷⁸ In the ^1H NMR spectrum, the pair of dppm methylene resonances again suggest "top/bottom" symmetry and the two vinylic protons appear as broad multiplets at $\delta 6.09$ and 5.41 . Signal enhancement indicates that the downfield signal displays 6.3 Hz coupling to fluorine while the upfield signal shows 14.2 Hz fluorine coupling; these values are typical of *cis*- and *trans* H–F coupling and indicate that the fluorovinyl group has remained intact. GCOSY experiments along with signal enhancement of the ^1H NMR spectrum confirm that the two *geminal* vinylic protons are mutually coupled, although this coupling is too small to be resolved in the non-enhanced ^1H NMR spectrum. The carbonyl resonances appear at $\delta 171.7$ and 163.6 , with fluorine coupling of 61.0 Hz present in the latter, indicating that this carbonyl is bound *trans* to the coordinated fluoride. To our knowledge, only one other report discusses *trans*-C–F coupling between a fluoride and a carbonyl, in which $^2J_{\text{CF}} = 61$ Hz was observed for $[\text{Ir}(\text{F})(\text{C}(\text{O})\text{F})(\text{CO})_2(\text{PEt}_3)_2]^+$.⁷⁶ To our knowledge, this binding mode has not been observed for any substituted or unsubstituted vinyl ligand.

3.2.2 C–F Activation Promoted by CO Addition.

3.2.2.1 Tetrafluoroethylene. A number of reports have appeared in which the addition of CO to fluoroolefin-bridged compounds gives rise to a 1,2-fluoride ion migration to yield the corresponding fluoroethylidene-bridged units.^{43,44,55,61} Such a transformation has been reported for tetrafluoroethylene-bridged $[\text{Fe}_2(\text{CO})_6(\mu\text{-SCH}_3)_2(\mu\text{-C}_2\text{F}_4)]$,⁴⁴ upon heating, to give the perfluoroethylidene-bridged product, and we have recently reported the conversion of the trifluoroethylene-bridged analogue of compounds **14** and **18a**,⁶¹ into a 2,2,2-trifluoroethylidene-bridged product under CO. Attempts to duplicate this reactivity in **14** by CO addition merely yields the carbonyl adduct, $[\text{Ir}_2(\text{CH}_3)(\text{CO})_3(\mu\text{-C}_2\text{F}_4)(\text{dppm})_2][\text{OTf}]$ (**20**) by CO coordination at the vacant site in **14**, as shown in Scheme 3.3. Heating to 80 °C, as required for the diiron compound,⁴⁴ also does not give rise to C–F bond cleavage but leaves **20** intact. Compound **20** has been previously reported⁶² so its characterization is not discussed here.



Scheme 3.3 – Sequential reaction of compound **14** with CO and BF₃ in attempts to induce a 1,2-fluoride shift.

Conversion of the tetrafluoroethylene-bridged diiron compound, noted above, to a perfluoroethylidene-bridged product was also achieved in the presence of BF₃,⁴⁴ in which BF₃ abstracts a fluoride ion with the resulting BF₄⁻ then delivering F⁻ to the β-carbon of the resulting trifluorovinyl group. Although reaction of either **14** or **20** with BF₃ yields the respective trifluorovinyl products [Ir₂(κ^l-C₂F₃)(OTf)(CO)₂(μ-H)(μ-CH₂)(dppm)₂][BF₄] (**16-BF₄**) or [Ir₂(κ^l-C₂F₃)(CO)₃(μ-H)(μ-CH₂)(dppm)₂][OTf][BF₄] (**21-OTf-BF₄**), fluoride-ion transfer back to the fluorovinyl units, to yield the targeted perfluoroethylidene products, was not observed in either case. On the assumption that BF₄⁻ might not be nucleophilic enough to give rise to fluoride transfer to the trifluorovinyl group, we added Bu₄NF to **15** assuming that this source of F⁻ might yield the perfluoroethylidene product; however no reaction was observed. Fluoride ion dissociation from tetrafluoroethylene⁴⁴ or perfluoropropene⁵⁵ species followed by fluoride-ion attack at the resulting fluorovinyl species, yielding the perfluoroethylidene- and perfluoroisopropylidene-bridged products, has been reported.

The spectral parameters for the ditriflate salt (see Experimental Section) of compound **21** are as expected with the exception of the ³¹P{¹H} NMR spectrum, which displays only a singlet at δ -20.3. Although two ³¹P resonances are expected, owing to the chemical inequivalence of both metals, the appearance of only one signal, even when cooled to -80 °C, suggests coincidental overlap of the two signals. Slow diffusion of diethyl ether into a concentrated dichloromethane

solution of **21** provided crystals suitable for X-ray diffraction and the structure of the complex cation, shown in Figure 3.3, clearly confirms the structure proposed and the chemical inequivalence of the two metals (in contradiction to ^{31}P NMR data). The geometry of **21** is closely related to that of **21** (without disorder of the trifluorovinyl ligand), in which the triflate ion has been replaced by CO. All parameters are as expected, and in particular, the C(4)–C(5) bond, at 1.37(1) Å, is as expected for a vinyl group.

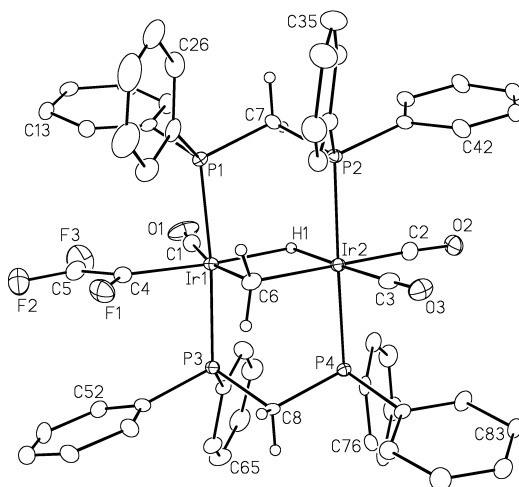
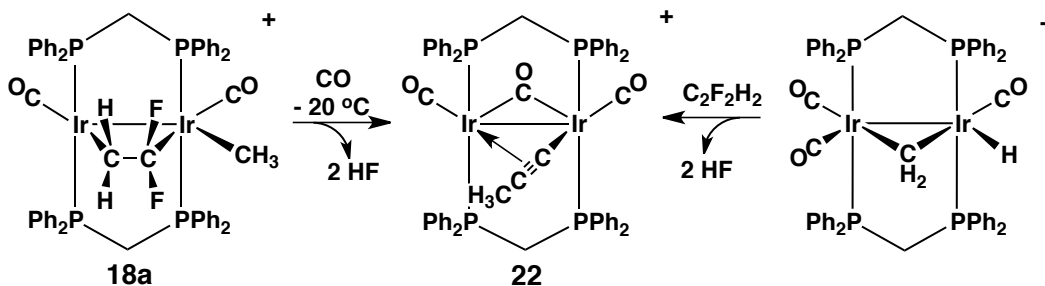


Figure 3.3 – Perspective view of the complex cation of $[\text{Ir}_2(\kappa^1\text{-C}_2\text{F}_3)(\text{CO})_3(\mu\text{-CH}_2)(\mu\text{-H})(\text{dppm})_2][\text{OTf}]_2$ (**21**) showing the atom labelling scheme. Thermal parameters are as described in Figure 3.1. Relevant bond distances (Å) and angles ($^\circ$) for the complex cation: Ir(1) – Ir(2) = 2.9068(4); Ir(1) – C(4) = 2.00(1); C(4) – C(5) = 1.37(1); C(4) – F(1) = 1.35(1); C(5) – F(2) = 1.31(2); C(5) – F(3) = 1.30(2); Ir(1) – C(4) – C(5) = 129(1); C(5) – C(4) – F(1) = 110(1); F(2) – C(5) – F(3) = 111(1).

3.2.2.2 1,1-Difluoroethylene. Unlike **14**, the 1,1-difluoroethylene-bridged product **18a** does undergo C–F bond activation in the presence of carbon monoxide, through the unexpected and unprecedented loss of 2 equivalents of HF and migration of the methyl ligand to the resulting “acetylide” moiety yielding the propynyl-bridged product, $[\text{Ir}_2(\text{CO})_3(\mu\text{-}\kappa^1\text{:}\eta^2\text{-C}\equiv\text{CCH}_3)(\text{dppm})_2][\text{OTf}]$ (**22**) after 1 h, as shown in Scheme 3.4. Compound **22** also results from the addition of an excess of 1,1-difluoroethylene (5 equiv) to the previously reported $[\text{Ir}_2(\text{H})(\text{CO})_3(\mu\text{-CH}_2)(\text{dppm})_2][\text{OTf}]$.⁷⁹ In this case, the reaction proceeds much

slower, requiring 24 h, but the final product is much cleaner – a result, in the former reaction, of compound **18a** always being contaminated with **18b**, and owing to the lability of the 1,1-difluoroethylene ligand, as discussed earlier.



Scheme 3.4 – Unprecedented loss of 2 equivalents of HF from 1,1-difluoroethylene.

The $^{31}\text{P}\{^1\text{H}\}$ NMR spectrum of **22**, which appears as a singlet, suggesting the chemical equivalence of all four ^{31}P nuclei, is inconsistent with the static structure shown in Scheme 3.4, for which two ^{31}P resonances would be expected, owing to the chemical inequivalence of the metals. However, we propose that the compound is fluxional, even at -80°C , in which the propynyl unit moves from metal-to-metal in a “windshield-wiper” motion, as has previously been observed in other alkynyl-bridged species.⁸⁰⁻⁸⁴ In the ^1H NMR spectrum the methyl group appears as a singlet at δ 1.30 and its lack of ^{31}P coupling is consistent with its migration to the “C₂” unit. Labelling studies involving the CD₃ analogue of **18a** and the reaction of $[\text{Ir}_2(\text{D})(\text{CO})_3(\mu\text{-CD}_2)(\text{dppm})_2][\text{OTf}]$ with 1,1-difluoroethylene demonstrates that HF loss occurs exclusively from the difluoroethylene unit in both cases with no hydrogen incorporation into the perdeuterated propynyl group of **22**. In order to test whether adventitious water played a role in this highly unusual removal of 2 equivalents of HF, the reaction of **18a** and CO was repeated in the presence of 15 equivalents of water, but showed no rate enhancement compared to that described above. Although, as will be described below, **18a** reacts readily with H₂O, this does not occur in the presence of CO.

The X-ray structure determination of compound **22**, as diagrammed in Figure 3.4, confirms the propynyl-bridged structure proposed above. The iridium–iridium separation of 2.8889(4) Å is indicative of a metal–metal bond,

while the C(4) – C(5) distance of 1.23(1) Å is consistent with a somewhat elongated triple bond (a typical C≡C bond is *ca.* 1.18 Å),⁸⁵ resulting from the η^2 -interaction with Ir(2) (Ir(2) – C(4) = 2.323(7) Å; Ir(2) – C(5) = 2.351(7) Å). Otherwise the structural parameters for **22** are as expected.

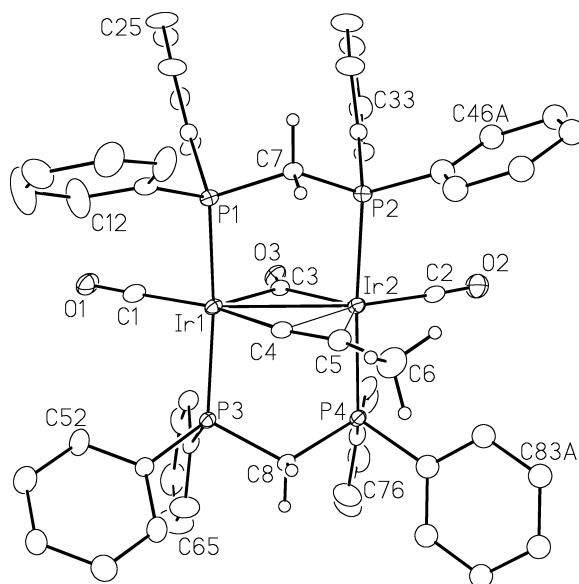
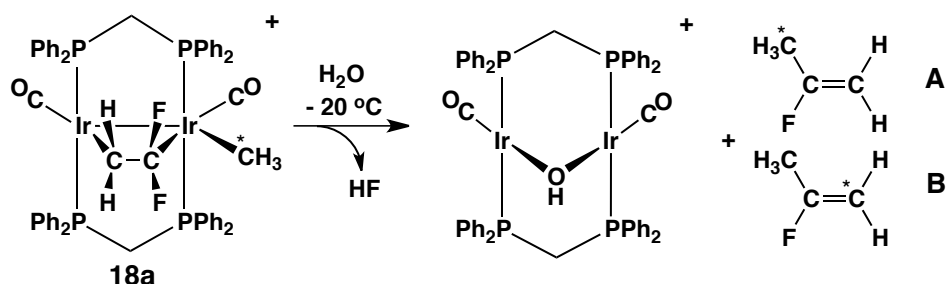


Figure 3.4 – Perspective view of the complex cation of $[\text{Ir}_2(\text{CO})_3(\mu\text{-}\kappa^1:\eta^2\text{-C}\equiv\text{CCH}_3)(\text{dppm})_2][\text{OTf}]$ (**22**) showing the atom labelling scheme. Thermal parameters as described in Figure 3.1. Relevant bond lengths (Å) and angles ($^\circ$): Ir(1) – Ir(2) = 2.8889(4); Ir(2) – C(3) = 2.082(6); Ir(2) – C(4) = 2.323(7); Ir(2) – C(5) = 2.351(7); C(4) – C(5) = 1.23(1); C(5) – C(6) = 1.48(1); Ir(1) – C(4) – C(5) = 158.4(6); C(4) – C(5) – C(6) = 155.9(8).

3.2.3 C–F Activation Promoted by H₂O Addition.

In Chapter 2, we had demonstrated that the trifluoroethylene-bridged species, analogous to **14** and **18a**, undergoes facile fluoride-ion loss in the reaction with water, yielding $[\text{Ir}_2(\text{CH}_3)(\kappa^1\text{-CH}=\text{CF}_2)(\text{CO})_2(\mu\text{-OH})(\text{dppm})_2][\text{OTf}]$. Carbon-fluorine bond activation by water is well documented,^{11,31,45,86,87} and Hughes and coworkers have shown that coordination of water can increase its acidity sufficiently to allow it to protonate an α -fluorine,^{11,31,86,87} leading to its loss as HF. We therefore sought to determine whether water-promoted C–F activation could also occur with the C₂F₄- and 1,1-C₂F₂H₂-bridged groups (**14**, **18a** or **20**).

Compounds **14** and **20** show no reactivity with water up to temperatures of 70 °C; however compound **18a** undergoes facile C–F activation in the presence of water at –20 °C, resulting in the elimination of 1 equivalent of HF and the formation of the previously reported compound, $[\text{Ir}_2(\text{CO})_2(\mu\text{-OH})(\text{dppm})_2][\text{OTf}]$,⁸⁸ together with 2-fluoropropene – the result of reductive elimination of the fluorovinyl fragment and the methyl ligand, as shown in Scheme 3.5. The presence of 2-fluoropropene was confirmed by comparison of its ¹H and ¹⁹F NMR spectra with those reported.⁸⁹ The chemical shifts and observable coupling constants are outlined in Figure 3.5.



Scheme 3.5 – C–F activation of compound **18a** with water, yielding $[\text{Ir}_2(\text{CO})_2(\mu\text{-OH})(\text{dppm})_2][\text{OTf}]$ and 2-fluoropropene. Carbon-13 enrichment of the methyl ligand yields the two isotopomers (**A** and **B**) shown.

When ¹³CH₃-labeled **18a** is used, the two isotopologues shown in Scheme 3.5 are obtained, in which the ¹³C-label appears in equal proportions at either the 1- or 3-position of 2-fluoropropene. Isotopologue **A** is that expected on the basis of reductive elimination of the fluorovinyl group and the ¹³CH₃ ligand, while **B** could result either from a subsequent metal-promoted 1,3-hydrogen shift in fluoropropene or by the involvement of a “ $\text{Ir}_2(\mu\text{-H})(\mu\text{-CH}_2)$ ” complex prior to coupling with the fluorovinyl unit; facile conversion of a methyl complex to its methylene/hydride tautomer has been reported here and elsewhere.^{62,79,90} We have no data to distinguish between these possible mechanisms since CD₃-labeled **18a** would yield CDH₂C(F)=CD₂ by either route.

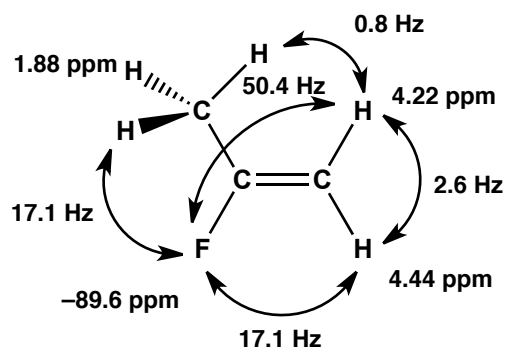


Figure 3.5 – NMR chemical shifts and coupling constants for 2-fluoropropene.

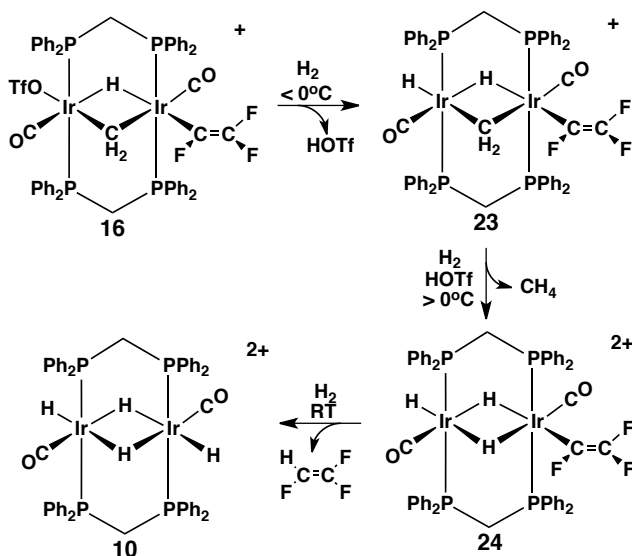
In the case of trifluoroethylene activation by H₂O,⁶¹ we had proposed that coordination of water at the vacant coordination site adjacent to the “CHF” end of the olefin had resulted in the selective abstraction of this fluorine as HF. In this geometry, not only is proton migration from water to the adjacent fluoride facilitated, but coordination of H₂O at this metal should increase back donation to the C–F σ^* orbital labilizing this adjacent fluorine. Although compound **18a** also has a vacant site, as shown in Scheme 3.5, this site is *not* adjacent to the CF₂ moiety, suggesting a different mechanism for F[–] abstraction. Furthermore, if the intermediate in the reaction of **18a** and water had a structure similar to that of the difluorovinyl species, [Ir₂(CH₃)(κ^1 -CH=CF₂)(CO)₂(μ -OH)(dppm)₂]⁺, resulting from water-promoted C–F activation of trifluoroethylene,⁶¹ it is not clear why this product would be stable, while the monofluorovinyl intermediate in the hydrolysis of **18a** undergoes facile reductive elimination of 2-fluoropropene. In fact, one would expect the opposite, since fluorine substitution at the α -position should strengthen the metal-vinyl bond, while fluorines at the β -position should have little effect.

3.2.4 Fluorovinyl Group Functionalization.

Two routes were explored for the functionalization of the fluorovinyl moiety in compounds **14** and **18a**. The first involves reaction with H₂ in order to promote hydrogenolysis of the fluorovinyl group, and the second involves reductive elimination of the fluorovinyl and methyl groups, much as reported

above in the activation of **18a** by water, and as we have previously shown in a *cis*-difluorovinyl-bridged methyl compound.⁶¹

3.2.4.1 Reactions with H₂. The addition of hydrogen to compound **15** at temperatures below 0 °C gives no observable reaction and warming above 0 °C results in the slow conversion of **15** to **16**, as described earlier. However, compound **16** does react with hydrogen, as outlined in Scheme 3.6. Upon cooling to –20 °C, the reaction of **16** with H₂ readily occurs, resulting in H₂ heterolysis, as seen by a broad ¹H resonance at δ 12.0, characteristic of an acid proton and the formation of [Ir₂(κ¹-C₂F₃)(H)(CO)₂(μ-H)(μ-CH₂)(dppm)₂][OTf] (**23**).



Scheme 3.6 – H₂ addition to compound **16** at –20 °C and subsequent hydrogenolysis upon warming.

The formation of triflic acid (possibly hydrogen bonded to the other triflate ion or to adventitious water) occurs at temperatures as low as –80 °C without any evidence for formation of a dihydrogen adduct. Heterolytic H₂ cleavage and the resulting replacement of OTf[–] by H[–] instead of H₂ oxidative addition presumably reflects the reluctance of Ir(III) to be oxidized further. The NMR spectroscopy of compound **23** is as expected, displaying two resonances in the ³¹P{¹H} spectrum, corresponding to the ends of the diphosphines bound to the inequivalent metals. The ¹H NMR spectrum has two different methylene signals

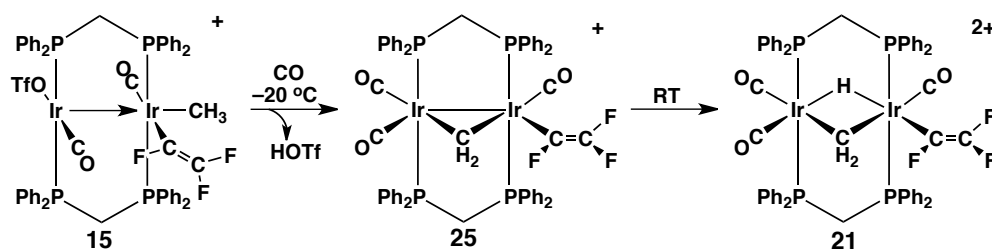
from the dppm backbones, together with a third set of methylene protons (a triplet of triplets at δ 3.72) corresponding to the group bridging the two iridium centres. Most importantly, the presence of two different hydride signals, one terminal (δ – 12.31) and one bridging (δ –15.03), along with the presence of the broad downfield acid signal, confirms the heterolytic cleavage of hydrogen. The reaction of compound **16** with D₂ results in deuterium labelling of the terminal hydride, along with the formation of "DOTf", as evidenced by loss of these two signals in the ¹H NMR spectrum.

Warming compound **23** to temperatures above 0 °C results in the irreversible conversion to compound **24**, accompanied by methane loss. The presence of methane is confirmed in both the ¹H and ¹³C{¹H} NMR spectra, along with labelling studies showing carbon-13 labeled methane is eliminated when the original methylene group in **24** is carbon-13 labeled. The NMR spectroscopy of compound **24** is similar to that of compound **23**, with the exception of loss of the downfield acid peak and the methylene resonance, accompanied by the appearance of three upfield hydride peaks. The bridging hydrides (δ –16.90, – 21.58) again appear at significantly higher field than the terminal hydride (δ – 9.93). Warming the deuterio product (**23-D**) described above, gives rise to D/H scrambling through the hydride positions in **24** and in the methane produced.

Under a headspace of hydrogen gas at ambient temperature, **24** slowly transforms to the known species, [Ir₂(H)₂(CO)₂(μ -H)₂(dppm)₂][OTf]⁹¹ and trifluoroethylene, the latter of which was confirmed by comparing the ¹⁹F NMR spectrum to the spectrum of an authentic sample of the gas.

Neither the difluorovinylidene-bridged **17** nor the fluorovinyl-bridged **19** reacts with H₂. In the case of the latter, no reaction is observed at temperatures below 0 °C, while at this temperature and higher thermal decomposition occurs as noted earlier. In the case of **17**, the failure to undergo H₂ oxidative addition to a saturated Ir(III)/Ir(III) species is not surprising. However, we had considered that triflate-assisted heterolytic cleavage of H₂, as described above for **16**, might result to give a monohydride species.

3.2.4.2 Reactions with CO. Compound **15** reacts readily with carbon monoxide at $-20\text{ }^{\circ}\text{C}$ yielding $[\text{Ir}_2(\kappa^1\text{-C}_2\text{F}_3)(\text{CO})_3(\mu\text{-CH}_2)(\text{dppm})_2][\text{OTf}]$ (**25**) together with triflic acid (Scheme 3.7), as seen by the broad resonance at δ 12.0 in the ^1H NMR spectrum. The spectroscopy of **25** is as expected, with the $\mu\text{-CH}_2$ group appearing as a multiplet at δ 3.76, and the absence of a hydride signal in the ^1H NMR spectrum. The formation of compound **25** from **15** gives some insight into how the rearrangement from a terminal methyl group in **15** can occur to give the methylene/hydride isomer (**16**) (Scheme 3.1) in which the bridging methylene and bridging hydride groups are found on *opposite* faces of the Ir_2P_4 plane. Clearly, triflate anion is playing a role in the deprotonation/reprotonation sequence, facilitating proton migration.



Scheme 3.7 – Addition of carbon monoxide to compound **15**.

Warming the reaction mixture to ambient temperature results in the formation of compound **21** by protonation of the Ir–Ir bond opposite the bridging methylene group, accompanied by the disappearance of the broad downfield proton resonance. Recall that compound **21** (as the OTf⁻/BF₄⁻ salt) can also be prepared by reacting compound **20** with BF₃, as discussed earlier, and is more directly obtained by triflate ion substitution by CO in compound **16**. Leaving compound **21** under a headspace of carbon monoxide does not result in any further reactivity.

Surprisingly, the difluorovinylidene-bridged **17** is unreactive toward CO, demonstrating the lack of lability of the coordinated triflate ions, which may also explain its failure to react with H₂, via heterolytic cleavage, as noted earlier.

The monofluorovinyl-bridged compound (**19**) does not react with carbon monoxide at temperatures below $-10\text{ }^{\circ}\text{C}$, which is again surprising considering the lability of coordinated triflate ions in these complexes, usually being readily replaced by carbon monoxide. However, at $0\text{ }^{\circ}\text{C}$, compound **19** readily reacts with CO to give the known compound, $[\text{Ir}_2(\text{CO})_5(\text{dppm})_2][\text{OTf}]_2$,⁸⁸ with liberation of 2-fluoropropene, again resulting from reductive elimination of the fluorovinyl and methyl groups. We assume that elimination of 2-fluoropropene is preceded by triflate ion replacement by CO. In the resulting *dicationic* species, in which a donor triflate ion has also been replaced by a predominately acceptor carbonyl ligand, both factors would favour reductive elimination by destabilizing the higher oxidation state.

3.3 Conclusions

This study confirms our earlier hypothesis^{48,61} in which fluoroolefins that are bridging two metal centres are more susceptible to fluoride-ion abstraction compared to their η^2 -bound analogues. This appears to be a result of greater rehybridization of the fluoroolefins in the bridging position, facilitating donation into the σ^* -C–F orbital, thereby weakening the carbon-fluorine bond. This has been clearly demonstrated in this chapter by the competitive experiment between the terminally bound difluoroethylene adduct and the bridging difluoroethylene moiety, in which the former is resistant to fluoride-ion loss at temperatures up to $0\text{ }^{\circ}\text{C}$, whereas the latter is susceptible to fluoride-ion loss at $-40\text{ }^{\circ}\text{C}$. For both the tetrafluoroethylene- and 1,1-difluoroethylene-bridged species, $[\text{Ir}_2(\text{CH}_3)(\text{CO})_2(\mu\text{-olefin})(\text{dppm})_2]^+$ (olefin = C_2F_4 (**14**), $\text{C}_2\text{F}_2\text{H}_2$ (**18a**)), abstraction of a fluoride ion is readily achieved upon the reaction with Me_3SiOTf . Although a fluoride ion could also be removed from **14** using BF_3 , this olefin adduct is much less reactive than the 1,1-difluoroethylene analogue (**18a**) which is also readily activated by water yielding 2-fluoropropene and $[\text{Ir}_2(\text{CO})_2(\mu\text{-OH})(\text{dppm})_2]^+$, through reductive elimination of the resulting 1-fluorovinyl group and the methyl ligand. Amazingly, **18a** can even undergo C–F activation at $-20\text{ }^{\circ}\text{C}$ in the presence of CO, in which *both* equivalents of HF in the olefin are expelled, accompanied by

methyl migration to the remaining “C₂” fragment, yielding the propynyl-bridged species, $[\text{Ir}_2(\text{CO})_3(\mu-\kappa^1:\eta^2-\text{C}\equiv\text{CCH}_3)(\text{dppm})_2]^+$. This activation mode is unprecedented and again demonstrates the unusual reactivity that can be imparted by a pair of activating metals.

In the case of the tetrafluoroethylene-bridged species (**14**), a pair of geminal fluorines can be removed upon reaction with two equivalents of Me₃SiOTf to give the difluorovinylidene-bridged product, $[\text{Ir}_2(\text{CH}_3)(\text{OTf})(\text{CO})_2(\mu-\text{C}=\text{CF}_2)(\mu-\text{OTf})(\text{dppm})_2]^+$. Unfortunately this difluorovinylidene unit is unreactive and attempts to functionalize it have been unsuccessful.

It is curious that while the trifluorovinyl group that results from fluoride-ion removal from **14** is terminally bound in the conventional κ^1 -geometry, the 1-fluorovinyl group in **19** adopts a novel bridging mode in which the fluoride substituent forms a dative bond to the adjacent metal. The failure of the trifluorovinyl group to adopt this binding mode may be a consequence of its slightly larger size and the resulting destabilizing interactions that would result with the dppm phenyl groups; however, it is also likely that the additional electronegative fluorine substituents in this group lower the ability of the α -fluorine to function as an effective donor.

Activation of one C–F bond in either tetrafluoroethylene or 1,1-difluoroethylene can also lead to olefin functionalization in two ways. Under hydrogen, hydrogenolysis of the trifluorovinyl complex, resulting from F[–] abstraction from the tetrafluoroethylene adduct, yields trifluoroethylene. Unfortunately, hydrogenolysis of the monofluorovinyl complex derived from 1,1-difluoroethylene did not occur owing to the instability of this species, and led instead to decomposition. However, the quantitative conversion of 1,1-difluoroethylene into 2-fluoropropene could be effected by hydrolysis of the 1,1-difluoroethylene-bridged adduct (**18a**) by reductive elimination of the resulting fluorovinyl group and the methyl ligand. The reductive elimination of a fluorovinyl and a methyl group was confirmed by the reaction of the unusual fluorovinyl/methyl species (**19**) with CO. The analogous reductive elimination of

the trifluorovinyl and methyl ligands in **15** did not occur; presumably the presence of the additional electronegative fluorine substituents in the trifluorovinyl group results in too strong an Ir–C₂F₃ bond.

The reactivity displayed herein by the tetrafluoroethylene and 1,1-difluoroethylene adducts complements that from Chapter 2 for the analogous trifluoroethylene adduct.⁶¹ The tetrafluoroethylene and derived species are the least reactive, presumably a result of the additional fluorine substitution strengthening the interactions of the fluorocarbyl ligands with the metals, while the 1,1-difluoroethylene and derived products, having the fewest fluorines, are the most labile. Unfortunately, this lability led to decomposition in a number of cases, limiting somewhat the scope of reactivity observed. However, as noted, the extrusion of both equivalents of HF from this coordinated olefin under extremely mild conditions is one remarkable result of its activation.

3.4 Experimental

3.4.1 General Comments

All solvents were dried (using appropriate drying agents), distilled before use and stored under dinitrogen. Deuterated solvents used for NMR experiments were freeze-pump-thaw degassed (three cycles) and stored under nitrogen or argon over molecular sieves. Reactions were carried out under argon using standard Schlenk techniques, and compounds that were obtained as solids were purified by recrystallization. Prepurified argon and nitrogen were purchased from Praxair, carbon-13 enriched CO (99%) was supplied by Isotec Inc, tetrafluoroethylene was supplied by SynQuest Fluorochemicals and 1,1-difluoroethylene was supplied by Aldrich. All purchased gases were used as received. All other reagents were obtained from Aldrich and were used as received (unless otherwise stated). The compounds [Ir₂(H)(CO)₃(μ-CH₂)(dppm)₂][CF₃SO₃] and [Ir₂(CH₃)(CO)₂(dppm)₂][CF₃SO₃] (**1**), along with their ¹³CH₃ and/or CD₃ analogues were prepared as previously reported.⁷⁹

Proton NMR spectra were recorded on Varian Unity 400 or 500 spectrometers, or on a Bruker AM400 spectrometer. Carbon-13 NMR spectra were recorded on Varian Unity 400 or 500 or Bruker AM300 spectrometers. Phosphorus-31 and fluorine-19 NMR spectra were recorded on Varian Unity 400 or 500 or Bruker AM400 spectrometers. Two-dimensional NMR experiments (COSY, NOESY and ^1H - ^{13}C HMQC) were obtained on Varian Unity 400 or 500 spectrometers.

3.4.2 Preparation of Compounds

(a) $[\text{Ir}_2(\text{CH}_3)(\text{CO})_2(\mu\text{-C}_2\text{F}_4)(\text{dppm})_2][\text{OTf}]$ (14**).** In an NMR tube, $[\text{Ir}_2(\text{CH}_3)(\text{CO})_2(\text{dppm})_2][\text{OTf}]$ (**1**) (48 mg, 0.034 mmol) was dissolved in 0.8 mL of CD_2Cl_2 . To the orange solution was added 4 mL of tetrafluoroethylene (*ca.* 4 equiv) via gas tight syringe. The sample was mixed and left for 2 h, after which time the solution had turned to a dark red/purple. Quantitative conversion to compound **1** was observed via NMR. The sample was transferred to a Schlenk tube and 10 mL of diethyl ether was added to induce precipitation of an orange solid. The product was washed with 2 x 10 mL of diethyl ether and dried under vacuum. (Yield: 96%) ^1H NMR (498 MHz, CD_2Cl_2): δ = 3.91 (m, 2H, dppm), 3.90 (m, 2H, dppm), 0.43 (t, 3H, $^3J_{\text{HP}} = 4.5$ Hz, Ir-CH₃); $^{31}\text{P}\{^1\text{H}\}$ NMR (202 MHz, CD_2Cl_2): δ = 16.8 (m, 2P), 5.2 (m, 2P); $^{13}\text{C}\{^1\text{H}\}$ NMR (125 MHz, CD_2Cl_2): δ = 192.0 (m, 1C, Ir-CO), 181.7 (m, 1C, Ir-CO), -7.7 (t, 1C, Ir-CH₃); ^{19}F NMR (469 MHz, CD_2Cl_2): δ = -79.2 (s, 3F, OTf⁻), -79.8 (bm, 2F), -86.4 (bm, 2F); elemental analysis calcd (%) for $\text{Ir}_2\text{SP}_4\text{F}_7\text{O}_5\text{C}_{56}\text{H}_{47}$ (1473.4): C 45.65, H 3.22; found: C 45.38, H, 3.02.

(b) $[\text{Ir}_2(\kappa^1\text{-C}_2\text{F}_3)(\text{CH}_3)(\text{OTf})(\text{CO})_2(\text{dppm})_2][\text{OTf}]$ (15**).** In an NMR tube, $[\text{Ir}_2(\text{CH}_3)(\text{CO})_2(\mu\text{-C}_2\text{F}_4)(\text{dppm})_2][\text{OTf}]$ (**14**) (44 mg, 0.030 mmol) was dissolved in 0.8 mL of CD_2Cl_2 . The clear red/orange solution was cooled to -78 °C in a dry ice/acetone bath and 1.2 equiv of trimethylsilyl trifluoromethanesulfonate (Me_3SiOTf) (6.5 μL , 0.036 mmol) was added. The

sample was warmed to $-10\text{ }^{\circ}\text{C}$ for 2 h, after which complete conversion to compound **15** was observed by low temperature NMR. ^1H NMR (400 MHz, CD_2Cl_2 , $-10\text{ }^{\circ}\text{C}$): $\delta = 4.51$ (m, 2H, dppm), 3.54 (m, 2H, dppm), 1.44 (dt, 3H, $^4J_{\text{HF}} = 5.3$ Hz, $^3J_{\text{HP}} = 4.9$ Hz, Ir- CH_3); $^{31}\text{P}\{^1\text{H}\}$ NMR (162 MHz, CD_2Cl_2 , $-10\text{ }^{\circ}\text{C}$): $\delta = 13.0$ (t, 2P, $^2J_{\text{PP}} = 24.7$ Hz), -7.8 (t, 2P, $^2J_{\text{PP}} = 24.7$ Hz); $^{13}\text{C}\{^1\text{H}\}$ NMR (101 MHz, CD_2Cl_2 , $-10\text{ }^{\circ}\text{C}$): $\delta = 178.0$ (bm, 1C, Ir-CO), 161.3 (bm, 1C, Ir-CO), -18.5 (dt, 1C, $^3J_{\text{CF}} = 13.6$ Hz, $^2J_{\text{CP}} = 3.0$ Hz, Ir- CH_3); ^{19}F NMR (376 MHz, CD_2Cl_2 , $-10\text{ }^{\circ}\text{C}$): $\delta = -76.3$ (s, 3F, Ir-OTf), -78.5 (s, 3F, OTf $^-$), -80.2 (dd, 1F, $^3J_{\text{FF}} = 26.6$ Hz, $^2J_{\text{FF}} = 73.9$ Hz), -119.9 (dd, 1F, $^2J_{\text{FF}} = 73.9$ Hz, $^3J_{\text{FF}} = 101.4$ Hz), -131.0 (dd, 1F, $^3J_{\text{FF}} = 26.6$ Hz, $^3J_{\text{FF}} = 101.4$ Hz).

(c) $[\text{Ir}_2(\kappa^1\text{-C}_2\text{F}_3)(\text{OTf})(\text{CO})_2(\mu\text{-H})(\mu\text{-CH}_2)(\text{dppm})_2][\text{OTf}]$ (16**). Method (i)** In an NMR tube, compound **14** (39 mg, 0.026 mmol) was dissolved in 0.8 mL of CD_2Cl_2 . To the clear red/orange solution was added 1.2 equiv of Me_3SiOTf (5.7 μL , 0.032 mmol). The sample was warmed to ambient temperature for 2 h, after which complete conversion to a clear yellow solution was observed. The solution was transferred to a round-bottom flask, and 20 mL of ether was added to induce precipitation of a yellow solid. The supernatant was removed via cannula and the solid was further washed with 3x10 mL of ether and dried under vacuum. **Method (ii)** To a three-necked round-bottom flask fitted with a gas inlet, condenser and septum was added compound **14** (97 mg, 0.066 mmol) and 10 mL of benzene, giving an orange slurry. To the slurry was added 1.2 equiv of Me_3SiOTf (14.2 μL , 0.0790 mmol), resulting in a slight lightening in color. The mixture was refluxed for 1 h, resulting in lightening to a clear yellow solution. Once cooled, the benzene was removed under vacuum and the product was redissolved in 5 mL of CH_2Cl_2 , followed by the addition of 20 mL of ether to induce precipitation of a yellow solid. The supernatant was removed via cannula and the solid was further washed with 3x10 mL of ether and dried under vacuum. (Yield: 74%) ^1H NMR (498 MHz, CD_2Cl_2): $\delta = 6.43$ (quin, 2H, $^3J_{\text{HP}} = 8.0$ Hz, Ir- CH_2 -Ir), 5.06 (bm, 4H, dppm), -12.23 (bs, 1H, Ir-H-Ir); $^{31}\text{P}\{^1\text{H}\}$ NMR (202 MHz, CD_2Cl_2): $\delta = -0.6$ (t, 2P,

$^2J_{\text{PP}} = 26.5$ Hz), -28.4 (t, 2P, $^2J_{\text{PP}} = 26.5$ Hz); $^{13}\text{C}\{^1\text{H}\}$ NMR (125 MHz, CD_2Cl_2): $\delta = 165.5$ (t, 1C, $^2J_{\text{CP}} = 11.5$ Hz, Ir–CO), 163.8 (dt, 1C, $^3J_{\text{CF}} = 21.6$ Hz, $^2J_{\text{CP}} = 8.8$ Hz, Ir–CO), 37.9 (bm, 1C, Ir–CH₂–Ir); ^{19}F NMR (469 MHz, CD_2Cl_2): $\delta = -77.5$ (s, 3F, Ir–OTf), -79.1 (s, 3F, OTf[−]), -93.1 (dd, 1F, $^3J_{\text{FF}} = 37.4$ Hz, $^2J_{\text{FF}} = 83.6$ Hz), -121.2 (dd, 1F, $^2J_{\text{FF}} = 83.6$ Hz, $^3J_{\text{FF}} = 115.2$ Hz), -123.7 (dd, 1F, $^3J_{\text{FF}} = 37.4$ Hz, $^3J_{\text{FF}} = 115.2$ Hz); elemental analysis calcd (%) for $\text{Ir}_2\text{S}_2\text{P}_4\text{F}_9\text{O}_8\text{C}_{57}\text{H}_{47}$ (1603.4): C 42.70, H 2.95; found: C 42.94, H, 3.12.

(d) $[\text{Ir}_2(\text{CH}_3)(\text{OTf})(\text{CO})_2(\mu\text{-C}=\text{CF}_2)(\mu\text{-OTf})(\text{dppm})_2][\text{OTf}]$ (17). In an NMR tube, compound **14** (53 mg, 0.036 mmol) was dissolved in 0.8 mL of CD_2Cl_2 . The clear red/orange solution was cooled to -78 °C in a dry ice/acetone bath and 10 equiv of Me_3SiOTf (65.0 μL , 0.359 mmol) was added. The sample was removed from the bath and warmed to ambient temperature, upon which conversion to compound **17** was observed after 1 h. The reaction mixture was transferred to a Schlenk flask and 15 mL of ether was added to induce precipitation. The yellow solid was further washed with 3x10 mL of ether and dried under vacuum, giving a yellow solid. (Yield: 65%) ^1H NMR (498 MHz, CD_2Cl_2): $\delta = 4.08$ (bm, 2H, dppm), 2.95 (bm, 2H, dppm), 1.95 (t, 3H, $^3J_{\text{HP}} = 9.0$ Hz, Ir–CH₃); $^{31}\text{P}\{^1\text{H}\}$ NMR (202 MHz, CD_2Cl_2): $\delta = -6.3$ (t, 2P, $^2J_{\text{PP}} = 21.0$ Hz), -20.5 (t, 2P, $^2J_{\text{PP}} = 21.0$ Hz); $^{13}\text{C}\{^1\text{H}\}$ NMR (125 MHz, CD_2Cl_2): $\delta = 174.2$ (dm, 1C, $^2J_{\text{CC}} = 24.3$ Hz, Ir–CO), 150.9 (dm, 1C, $^2J_{\text{CC}} = 24.3$ Hz, Ir–CO), 38.1 (m, 1C, Ir–CH₃); ^{19}F NMR (469 MHz, CD_2Cl_2): $\delta = -69.3$ (d, 1F, $^2J_{\text{FF}} = 97.0$ Hz), -76.3 (s, 3F, Ir–OTf–Ir), -78.0 (s, 3F, Ir–OTf), -78.9 (s, 3F, OTf[−]), -85.0 (d, 1F, $^2J_{\text{FF}} = 97.0$ Hz); elemental analysis calcd (%) for $\text{Ir}_2\text{S}_3\text{P}_4\text{F}_{11}\text{O}_{11}\text{C}_{58}\text{H}_{47}$ (1733.5): C 40.19, H 2.72; found: C 40.40, H, 3.15.

(e) $[\text{Ir}_2(\text{CH}_3)(\text{CO})_2(\mu\text{-C}_2\text{F}_2\text{H}_2)(\text{dppm})_2][\text{OTf}]$ (18a). In an NMR tube, compound **1** (46 mg, 0.033 mmol) was dissolved in 0.8 mL of CD_2Cl_2 . The orange solution was cooled to -80 °C in a dry ice/acetone bath and 4 mL of 1,1-difluoroethylene (*ca.* 4 equiv) was added via gas tight syringe. The sample was mixed and left for 24 h in a freezer at -20 °C, during which time the solution slowly turned to dark red/purple. The sample was placed into the

NMR probe cooled to $-20\text{ }^{\circ}\text{C}$ and the reaction was monitored by multinuclear NMR. A typical experiment gave a 4:1 ratio of $[\text{Ir}_2(\text{CH}_3)(\text{CO})_2(\mu\text{-C}_2\text{F}_2\text{H}_2)(\text{dppm})_2][\text{OTf}]$ (**18a**) to $[\text{Ir}_2(\text{CH}_3)(\text{CO})_2(\eta^2\text{-C}_2\text{F}_2\text{H}_2)(\text{dppm})_2][\text{OTf}]$ (**18b**). Warming the solution above $-20\text{ }^{\circ}\text{C}$ resulted in the conversion back to starting material after 30 min. ^1H NMR (400 MHz, CD_2Cl_2 , $-20\text{ }^{\circ}\text{C}$): $\delta = 4.47$ (m, 2H, dppm), 3.36 (m, 2H, dppm), 2.48 (m, 2H, $\mu\text{-C}_2\text{F}_2\text{H}_2$), 0.12 (t, 3H, $^3J_{\text{HP}} = 5.3$ Hz, Ir- CH_3); $^{31}\text{P}\{^1\text{H}\}$ NMR (162 MHz, CD_2Cl_2 , $-20\text{ }^{\circ}\text{C}$): $\delta = 15.6$ (m, 2P), 5.6 (bm, 2P); $^{13}\text{C}\{^1\text{H}\}$ NMR (101 MHz, CD_2Cl_2 , $-20\text{ }^{\circ}\text{C}$): $\delta = 195.3$ (bs, 1C, Ir-CO), 184.1 (bm, 1C, Ir-CO), -9.7 (bs, 1C, Ir- CH_3); ^{19}F NMR (376 MHz, CD_2Cl_2 , $-20\text{ }^{\circ}\text{C}$): $\delta = -45.8$ (m, 2F, $\mu\text{-C}_2\text{F}_2\text{H}_2$), -79.4 (s, 3F, OTf $^-$).

(f) $[\text{Ir}_2(\text{CH}_3)(\text{OTf})(\text{CO})_2(\mu\text{-}\kappa^1:\kappa^1\text{-C,F-C(F)=CH}_2)(\text{dppm})_2][\text{OTf}]$ (**19**). In an NMR tube, a mixture of compounds **18a/18b** (50 mg, 0.035 mmol) was dissolved in 0.8 mL of CD_2Cl_2 , cooled to $-20\text{ }^{\circ}\text{C}$ in a freezer and 1.2 equiv of Me_3SiOTf (7.5 μL , 0.042 mmol) was added. The reaction was monitored via variable temperature NMR. Holding the sample at $-20\text{ }^{\circ}\text{C}$ for 2.5 hours resulted in the conversion of compound **18a** to **19**, while no reaction occurred with **18b**. Warming the sample above $0\text{ }^{\circ}\text{C}$ resulted in decomposition to numerous unidentified products. ^1H NMR (400 MHz, CD_2Cl_2 , $-20\text{ }^{\circ}\text{C}$): $\delta = 6.09$ (bm, 1H, C(F)=CHH), 5.41 (bm, 1H, C(F)=CHH), 4.29 (m, 2H, dppm), 3.02 (m, 2H, dppm), 0.20 (t, 3H, $^3J_{\text{HP}} = 6.4$ Hz, Ir- CH_3); $^{31}\text{P}\{^1\text{H}\}$ NMR (162 MHz, CD_2Cl_2 , $-20\text{ }^{\circ}\text{C}$): $\delta = 1.2$ (dt, 2P, $^2J_{\text{PF}} = 47.0$ Hz, $^2J_{\text{PP}} = 17.8$ Hz), -5.5 (t, 2P, $^2J_{\text{PP}} = 17.8$ Hz); $^{13}\text{C}\{^1\text{H}\}$ NMR (101 MHz, CD_2Cl_2 , $-20\text{ }^{\circ}\text{C}$): $\delta = 171.7$ (t, 1C, $^2J_{\text{CP}} = 10.2$ Hz, Ir-CO), 163.6 (d, 1C, $^2J_{\text{CF}} = 61.0$ Hz, Ir-CO), 4.6 (s, 1C, Ir- CH_3); ^{19}F NMR (376 MHz, CD_2Cl_2 , $-20\text{ }^{\circ}\text{C}$): $\delta = -78.5$ (s, 3F, Ir-OTf), -78.9 (s, 3F, OTf $^-$), -211.2 (t, 1F, $^2J_{\text{PF}} = 47.0$ Hz).

(g) **Reaction of 2 with CO.** In an NMR tube, compound **14** (45 mg, 0.031 mmol) was dissolved in 0.8 mL of CD_2Cl_2 . To the clear, red solution was added 3 mL of CO via a gas tight syringe. The solution was mixed, instantly

resulting in a color change from red to yellow owing to the formation of **[Ir₂(CH₃)(OTf)(CO)₃(μ-C₂F₄)(dppm)₂][OTf] (20)**. The solution was transferred to a Schlenk tube and 15 mL of ether was added to induce precipitation. The precipitate was washed with 2 x 10 mL of ether and dried under reduced pressure to give a yellow powder. (Yield: 96%) ¹H NMR (498 MHz, CD₂Cl₂): δ = 4.65 (bm, 4H, dppm), 0.80 (t, 3H, ³J_{HP} = 6.2 Hz, Ir-CH₃); ³¹P{¹H} NMR (202 MHz, CD₂Cl₂): δ = -7.7 (m, 2P), -15.2 (m, 2P); ¹³C{¹H} NMR (125 MHz, CD₂Cl₂): δ = 179.1 (m, 1C, Ir-CO), 178.0 (m, 1C, Ir-CO), 156.7 (m, 1C, Ir-CO), -13.4 (bs, 1C, Ir-CH₃); ¹⁹F NMR (469 MHz, CD₂Cl₂): δ = -73.5 (t, 2F, ³J_{FP} = 18.9 Hz), -79.2 (s, 3F, OTf⁻), -84.6 (bm, 2F).

(h) [Ir₂(κ¹-C₂F₃)(CO)₃(μ-H)(μ-CH₂)(dppm)₂][OTf]₂ (21). **Method (i)** In an NMR tube, compound **20** (36 mg, 0.024 mmol) was dissolved in 0.8 mL of CD₂Cl₂. At ambient temperature, 1.1 equiv of Me₃SiOTf (4.8 μL, 0.026 mmol) was added, resulting in a slight lightening of the yellow solution. The solution was transferred to a Schlenk flask and 10 mL of ether was added to induce precipitation of a yellow solid. The solid was washed with a further 2 x 10 mL of ether and dried under vacuum to give compound **18**. **Method (ii)** In an NMR tube containing compound **15** (34 mg, 0.021 mmol) in CD₂Cl₂ at -10 °C, 2 mL of CO was added via a gas-tight syringe. The solution was allowed to warm to room temperature, resulting in the immediate change from a dark orange/red to light yellow. The solution was transferred to a Schlenk flask and isolated as described in Method i. **Method (iii)** A sample of compound **16** (65 mg, 0.041 mmol) was dissolved in 10 ml of CH₂Cl₂. To the yellow solution was added 5 mL of CO via a gas-tight syringe. The solution was left to stir for 1 h, during which time the solvent was removed under vacuum. The yellow resin was redissolved in 2 mL of CH₂Cl₂, and the product was isolated as described in Method (i). **Method (iv)** A sample of compound **20** (0.38 mg, 0.024 mmol) was dissolved in 0.8 mL CD₂Cl₂. To the solution was added (C₂H₅)₂O•BF₃ (5 μL, 0.047), resulting in a change to yellow. The solution was transferred to a Schlenk flask and 20 mL ether was

added to induce precipitation of a yellow solid. The solid was washed with a further 2 x 10 mL ether and dried under vacuum. (Yield: 89%) ^1H NMR (498 MHz, CD_2Cl_2): $\delta = 5.88$ (quin., 2H, $^3J_{\text{HP}} = 8.7$ Hz, Ir- CH_2 -Ir), 4.93 (bm, 2H, dppm), 4.49 (bm, 2H, dppm), -14.60 (bs, 1H, Ir- H -Ir); $^{31}\text{P}\{^1\text{H}\}$ NMR (202 MHz, CD_2Cl_2): $\delta = -20.3$ (s, 4P); $^{13}\text{C}\{^1\text{H}\}$ NMR (125 MHz, CD_2Cl_2): $\delta = 165.3$ (m, 1C, Ir-CO), 157.3 (m, 1C, Ir-CO), 156.2 (m, 1C, Ir-CO), 42.7 (bm, 1C, Ir- CH_2 -Ir); ^{19}F NMR (469 MHz, CD_2Cl_2): $\delta = -78.4$ (s, 3F, OTf^-), -95.1 (bm, 1F), -118.7 (bm, 2F); elemental analysis calcd (%) for $\text{Ir}_2\text{S}_2\text{P}_4\text{F}_9\text{O}_9\text{C}_{58}\text{H}_{47}$ (1631.4): C 42.65, H 2.90; found: C 42.95, H, 3.16.

- (i) **$[\text{Ir}_2(\text{CO})_3(\kappa^1\text{-}\eta^2\text{-C}\equiv\text{CCH}_3)(\text{dppm})_2][\text{OTf}]$ (22) Method (A)** In an NMR tube, compounds **18a/18b** (36 mg, 0.025 mmol) were dissolved in 0.8 mL of CD_2Cl_2 and cooled to -20 °C in a freezer. To the cooled solution was added 4 mL of CO via a gas tight syringe. The mixture was mixed vigorously and allowed to warm to ambient temperature. The solution was transferred to a Schlenk tube and compound **22** was isolated via precipitation upon the addition of ether. The product was further washed with 2 x 10 mL of ether and dried under vacuum. **Method B)** A sample of $[\text{Ir}_2(\text{H})(\text{CO})_3(\mu\text{-CH}_2)(\text{dppm})_2][\text{OTf}]^{79}$ (63 mg, 0.045 mmol) was dissolved in 5 mL of CH_2Cl_2 in a Schlenk flask, to which 5 mL of 1,1-difluoroethylene was added (~ 5 equiv) via a gas tight syringe. The mixture was allowed to stir for 30 min, at which point 30 mL of ether was added to induce precipitation. The solid was washed with 2 x 10 mL of ether and dried under vacuum. (Yield: 64%) ^1H NMR (498 MHz, CD_2Cl_2): $\delta = 3.60$ (m, 2H, dppm), 3.38 (m, 2H, dppm), 1.30 (s, 3H, Ir-C \equiv C- CH_3); $^{31}\text{P}\{^1\text{H}\}$ NMR (202 MHz, CD_2Cl_2): $\delta = -4.1$ (s, 4P); $^{13}\text{C}\{^1\text{H}\}$ NMR (125 MHz, CD_2Cl_2): $\delta = 185.6$ (m, 1C, Ir-CO-Ir), 172.9 (m, 2C, Ir-CO), 9.8 (s, 1C, Ir-C \equiv C- CH_3); ^{19}F NMR (469 MHz, CD_2Cl_2): $\delta = -79.1$ (s, 3F, OTf^-).

- (j) **Reaction of 18a with H_2O .** In an NMR tube, compounds **18a/18b** (57 mg, 0.040 mmol) were dissolved in 0.8 mL of CD_2Cl_2 , cooled to -20 °C in a

freezer and 1.2 equiv of H₂O (0.9 μL, 0.05 mmol) was added. The reaction was monitored via low temperature NMR spectroscopy. Holding the mixture at 0 °C for 30 min results in the conversion of compound **18a** to the previously reported [Ir₂(CO)₂(μ-OH)(dppm)₂][OTf]⁸⁸ was observed along with the liberation of 2-fluoropropene.

(k) Attempted reaction of 15 with H₂. In an NMR tube, compound **15** (56 mg, 0.035 mmol) was dissolved in 0.8 mL of CD₂Cl₂. The mixture was cooled to –80 °C in a dry ice/acetone bath, during which time 5 mL of H₂ was injected into the tube via a gas tight syringe. The reaction was warmed to –10 °C in the NMR spectrometer while monitoring by ³¹P{¹H} NMR. No observable reaction between **15** and H₂ occurred.

(l) Reaction of 16 with H₂. In an NMR tube, compound **16** (61 mg, 0.038 mmol) was dissolved in 0.8 mL of CD₂Cl₂ and cooled in a CO_{2(s)}/acetone bath to –78 °C. To the solution was added 4 mL of H₂ via a gas tight syringe. The solution was warmed to 0 °C in the NMR spectrometer during which time the reaction was monitored. Complete conversion to [Ir₂(κ¹-C₂F₃)(H)(CO)₂(μ-H)(μ-CH₂)(dppm)₂][OTf] (**23**), along with the presence of triflic acid, was observed after 15 min. Warming the solution to ambient temperature resulted in the slow conversion (2 hours) of compound **23** to [Ir₂(κ¹-C₂F₃)(H)(CO)₂(μ-H)₂(dppm)₂][OTf]₂ (**24**), along with the disappearance of triflic acid and the appearance of methane. Leaving the solution at ambient temperature for 24 h resulted in the complete conversion to the previously characterized [Ir₂(H)₂(CO)₂(μ-H)₂(dppm)₂][OTf]₂⁹¹ along with the liberation of trifluoroethylene. Compound **23**: ¹H NMR (400 MHz, CD₂Cl₂, 0 °C): δ = 4.32 (m, 2H, dppm), 3.72 (m, 2H, Ir-CH₂-Ir), 3.57 (m, 2H, dppm), –12.31 (bs, 1H, Ir-H), –15.03 (bs, 1H, Ir-H-Ir); ³¹P{¹H} NMR (162 MHz, CD₂Cl₂, 0 °C): δ = –5.5 (t, 2P, ²J_{PP} = 26.2 Hz), –7.8 (bm, 2P); ¹³C{¹H} NMR (101 MHz, CD₂Cl₂, 0 °C): δ = 169.6 (dt, 1C, ³J_{CF} = 17.7 Hz, ²J_{CP} = 5.5 Hz, Ir-CO), 166.6

(bm, 1C, Ir–CO), 33.1 (bm, 1C, Ir–CH₂–Ir); ¹⁹F NMR (376 MHz, CD₂Cl₂, 0 °C): δ = –79.0 (s, 3F, OTf[–]), –97.8 (b, 1F), –122.9 (b, 1F), –132.7 (s, 1F). Compound **24**: ¹H NMR (400 MHz, CD₂Cl₂, 10 °C): δ = 5.76 (m, 2H, dppm), 5.28 (m, 2H, dppm), –9.93 (bm, 1H, Ir–H), –16.90 (bm, 1H, Ir–H–Ir), –21.58 (bm, 1H, Ir–H–Ir); ³¹P {¹H} NMR (162 MHz, CD₂Cl₂, 10 °C): δ = –0.3 (t, 2P, ²J_{PP} = 21.8 Hz), –10.0 (t, 2P, ²J_{PP} = 21.8 Hz); ¹³C {¹H} NMR (101 MHz, CD₂Cl₂, 10 °C): δ = 166.2 (bm, 1C, Ir–CO), 162.1 (t, 1C, ²J_{CP} = 10.5 Hz, Ir–CO); ¹⁹F NMR (376 MHz, CD₂Cl₂, 10 °C): δ = –79.3 (s, 3F, OTf[–]), –97.2 (dd, 1F, ³J_{FF} = 40.6 Hz, ²J_{FF} = 89.1 Hz), –122.7 (dd, 1F, ²J_{FF} = 89.1 Hz, ³J_{FF} = 108.2 Hz), –125.0 (bd, 1F, ³J_{FF} = 108.2 Hz).

(m) Attempted reaction of 19 with H₂. To an NMR sample containing compound **19** (38 mg, 0.024 mmol) dissolved in 0.8 mL of CD₂Cl₂ cooled to –20 °C was added 5 mL of H₂ via a gas-tight syringe. The reaction was monitored by NMR spectroscopy while warming the mixture. No reaction with H₂ was observed below 0 °C and warmer temperatures led to decomposition of **19**.

(n) Attempted reaction of 22 with H₂. To an NMR tube containing compound **22** (59 mg, 0.041 mmol) in 0.8 mL of CD₂Cl₂ was added 5 mL of H₂ via gas-tight syringe at 27 °C. Monitoring by NMR spectroscopy confirmed that no reaction occurred.

(o) Reaction of 15 with CO. In an NMR tube, compound **15** (34 mg, 0.021 mmol) was dissolved in 0.8 mL of CD₂Cl₂ and was cooled to –80 °C via a CO_(s)/acetone bath. While at –80 °C, 2 mL of CO gas was via a gas tight syringe. The reaction was monitored via variable temperature NMR. At –20 °C, quantitative conversion of **15** to [Ir₂(κ¹-C₂F₃)(CO)₃(μ-CH₂)(dppm)₂][OTf]₂ (**25**) was observed along with free triflic acid. Warming to ambient temperature resulted in the conversion of **25** to [Ir₂(κ¹-C₂F₃)(CO)₃(μ-H)(μ-CH₂)(dppm)₂][OTf]₂ (**21**). Compound **25**: ¹H NMR

(400 MHz, CD₂Cl₂, -20 °C): δ = 4.14 (m, 2H, dppm), 3.76 (m, 2H, Ir-CH₂-Ir), 3.40 (m, 2H, dppm); ³¹P{¹H} NMR (162 MHz, CD₂Cl₂, -20 °C): δ = -13.4 (bm, 2P), -14.2 (bm, 2P); ¹³C{¹H} NMR (101 MHz, CD₂Cl₂, -20 °C): δ = 184.2 (bm, 1C, Ir-CO), 161.9 (bm, 1C, Ir-CO), 157.6 (bm, 1C, Ir-CO), 50.3 (s, 1C, Ir-CH₂-Ir); ¹⁹F NMR (376 MHz, CD₂Cl₂, -20 °C): δ = -78.9 (s, 3F, OTf⁻), -95.1 (bm, 1F), -122.2 (bm, 1F), -125.3 (bm, 1F).

(p) Reaction of 19 with CO. To a NMR tube containing compound **19** (40 mg, 0.026 mmol) in 0.8 mL of CD₂Cl₂, cooled to -80 °C via a CO₂(s)/acetone(l) bath, was added 2 mL of CO gas via a gas tight syringe. The reaction was monitored via variable temperature NMR spectroscopy. No reaction was observed until -10 °C, upon which multiple phosphorus-containing decomposition products were observed, the major being the previously characterized [Ir₂(CO)₅(dppm)₂][OTf]₂,⁸⁸ along with 2-fluoropropene (*ca.* 35 – 40%).

3.4.3 X-ray Structure Determinations

3.4.3.1 General. Crystals were grown via slow diffusion of diethyl ether into a CH₂Cl₂ solution of the compound (**14**, **21**), diffusion of pentane into a CH₂Cl₂ solution of the compound (**16**), or slow evaporation of a CH₂Cl₂ solution of the compound (**22**). Data were collected using a Bruker APEX II CCD detector/D8 diffractometer⁹² with the crystals cooled to -100 °C (**14**, **21**) or a Bruker SMART 1000 CCD detector/PLATFORM diffractometer⁹² with the crystals cooled to -80 °C (**16**, **22**); all data were collected using Mo K α radiation (λ = 0.71073 Å). The data were corrected for absorption through Gaussian integration from indexing of the crystal faces. Structures were solved using direct methods (*SHELXS-97*⁹³ for **14** and **16**) or Patterson search/structure expansion (*DIRDIF-2008*⁹⁴ for **21**, *DIRDIF-96*⁹⁵ for **22**). Refinements were completed using the program *SHELXL-97*.⁹³ Non-hydridic hydrogen atoms were assigned positions based on the *sp*² or *sp*³ hybridization geometries of their attached carbon or oxygen atoms, and were given isotropic displacement parameters 20 % greater than those of their parent

atoms. The bridging hydrido ligands of **16** and **21** were located from difference Fourier map; these were given fixed isotropic displacement parameters and their atomic coordinates were allowed to freely refine. See Supporting Information for a listing of crystallographic experimental data.

3.4.3.2 Special refinement conditions. (i) **14**: Distance restraints applied within the disordered triflate ion: $d(\text{S}(6\text{A})\text{--O}(601)) = d(\text{S}(6\text{A})\text{--O}(602)) = d(\text{S}(6\text{A})\text{--O}(603)) = d(\text{S}(6\text{B})\text{--O}(604)) = d(\text{S}(6\text{B})\text{--O}(605)) = d(\text{S}(6\text{B})\text{--O}(606)) = 1.45(1) \text{ \AA}$; $d(\text{S}(6\text{A})\text{--C}(601)) = d(\text{S}(6\text{B})\text{--C}(602)) = 1.80(1) \text{ \AA}$; $d(\text{F}(601)\text{--C}(601)) = d(\text{F}(601)\text{--C}(601)) = d(\text{F}(601)\text{--C}(601)) = d(\text{F}(601)\text{--C}(601)) = d(\text{F}(601)\text{--C}(601)) = 1.35(1) \text{ \AA}$; $d(\text{S}(6\text{B})\cdots\text{F}(604)) = d(\text{S}(6\text{B})\cdots\text{F}(605)) = d(\text{S}(6\text{B})\cdots\text{F}(606)) = 2.56(1) \text{ \AA}$; $d(\text{F}(604)\cdots\text{F}(605)) = d(\text{F}(604)\cdots\text{F}(606)) = d(\text{F}(605)\cdots\text{F}(606)) = 2.15(1) \text{ \AA}$. Distance restraints applied within the solvent dichloromethane molecules: $d(\text{Cl}(11)\text{--C}(6\text{S})) = d(\text{Cl}(12)\text{--C}(6\text{S})) = d(\text{Cl}(13)\text{--C}(7\text{S})) = d(\text{Cl}(14)\text{--C}(7\text{S})) = d(\text{Cl}(15)\text{--C}(8\text{S})) = d(\text{Cl}(16)\text{--C}(8\text{S})) = d(\text{Cl}(17)\text{--C}(9\text{S})) = d(\text{Cl}(18)\text{--C}(9\text{S})) = 1.75(1) \text{ \AA}$; $d(\text{Cl}(11)\cdots\text{Cl}(12)) = d(\text{Cl}(13)\cdots\text{Cl}(14)) = d(\text{Cl}(15)\cdots\text{Cl}(16)) = d(\text{Cl}(17)\cdots\text{Cl}(18)) = 2.85(1) \text{ \AA}$. Distance restraints applied within the solvent diethyl ether molecules: $d(\text{O}(30\text{S})\text{--C}(31\text{S})) = d(\text{O}(30\text{S})\text{--C}(33\text{S})) = 1.46(1) \text{ \AA}$; $d(\text{C}(31\text{S})\text{--C}(32\text{S})) = d(\text{C}(33\text{S})\text{--C}(34\text{S})) = 1.52(1) \text{ \AA}$; $d(\text{O}(30\text{S})\cdots\text{C}(32\text{S})) = d(\text{O}(30\text{S})\cdots\text{C}(34\text{S})) = 2.43(1) \text{ \AA}$; $d(\text{C}(31\text{S})\cdots\text{C}(33\text{S})) = 2.38(1) \text{ \AA}$. Attempts to refine peaks of residual electron density as disordered or partial-occupancy solvent dichloromethane chlorine or carbon atoms were unsuccessful. The data were corrected for disordered electron density through use of the SQUEEZE procedure⁹⁶ as implemented in *PLATON*.⁹⁷⁻
⁹⁹ A total solvent-accessible void volume of 662.4 \AA^3 with a total electron count of 94 (consistent with two molecules of solvent dichloromethane, or 1/6 molecule of CH_2Cl_2 per formula unit of the diiridium complex ion) was found in the unit cell. (ii) **16**: The Ir(1)–C(4A) and Ir(1)–C(4B) distances (involving the disordered trifluorovinyl group in which the two molecules differ by an approximately 180° rotation about the Ir(1)–C(4) bond, as shown in Figure 3.6) were constrained to be equal (within 0.03 \AA) during refinement. The F–C distances within the minor

conformer of the disordered trifluorovinyl group were restrained during refinement: $d(\text{F}(1\text{B})-\text{C}(4\text{B})) = d(\text{F}(2\text{B})-\text{C}(5\text{B})) = d(\text{F}(3\text{B})-\text{C}(5\text{B})) = 1.35(1) \text{ \AA}$. The trifluorovinyl group disorder was accompanied by slight differences in orientations of the dppm phenyl groups, which is not shown.

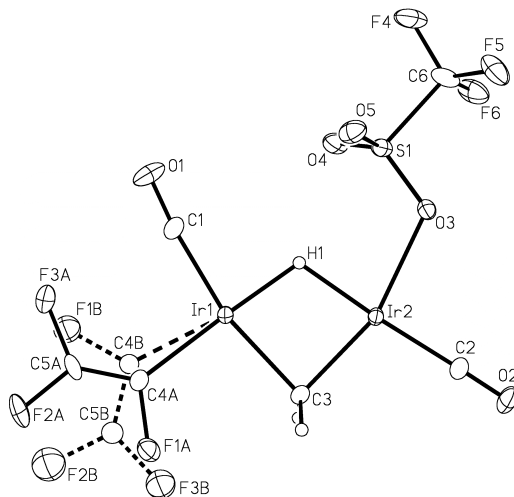


Figure 3.6 – Perspective view of the complex cation of $[\text{Ir}_2(\text{CO})_2(\text{C}_2\text{F}_3)(\text{OTf})(\mu\text{-CH}_2)(\mu\text{-H})(\text{dppm})_2][\text{CF}_3\text{SO}_3]$ (**16**), showing the disorder of the trifluorovinyl group (dppm groups above and below the plane of the drawing are omitted for clarity). The solid lines represent the major disordered form while the dashed lines represent the minor disordered form.

Restraints were applied during refinement to distances within the disordered noncoordinated triflate ion: $d(\text{S}(2\text{A})-\text{O}(91\text{A})) = d(\text{S}(2\text{A})-\text{O}(92\text{A})) = d(\text{S}(2\text{A})-\text{O}(93\text{A})) = d(\text{S}(2\text{B})-\text{O}(91\text{B})) = d(\text{S}(2\text{B})-\text{O}(92\text{B})) = d(\text{S}(2\text{B})-\text{O}(93\text{B})) = 1.45(1) \text{ \AA}$; $d(\text{S}(2\text{A})-\text{C}(91\text{A})) = d(\text{S}(2\text{B})-\text{C}(91\text{B})) = 1.80(1) \text{ \AA}$; $d(\text{F}(91\text{A})-\text{C}(91\text{A})) = d(\text{F}(92\text{A})-\text{C}(91\text{A})) = d(\text{F}(93\text{A})-\text{C}(91\text{A})) = d(\text{F}(91\text{B})-\text{C}(91\text{B})) = d(\text{F}(92\text{B})-\text{C}(91\text{B})) = d(\text{F}(93\text{B})-\text{C}(91\text{B})) = 1.35(1) \text{ \AA}$. Attempts to refine peaks of residual electron density as disordered or partial-occupancy solvent dichloromethane chlorine or carbon atoms were unsuccessful. The data were corrected for disordered electron density as for compound **14** (*PLATON/SQUEEZE*⁹⁶⁻⁹⁹). A total solvent-accessible void volume of 1320.7 \AA^3 with a total electron count of 544 (consistent with 12 molecules of solvent dichloromethane, or 3 molecules per formula unit of the diiridium complex cation) was found in the unit cell. (iii) **21**: The value of the Flack absolute structure parameter¹⁰⁰⁻¹⁰² indicated the structure to be racemic twinned. This was accommodated during the refinement using the

*SHELXL-97*⁹³ TWIN instruction. (iv) **22**: An idealized geometry was imposed upon the disordered triflate anion through use of the following distance restraints: $d(\text{S}-\text{C}(91\text{A})) = d(\text{S}-\text{C}(91\text{B})) = 1.80 \text{ \AA}$; $d(\text{S}-\text{O}(91\text{A})) = d(\text{S}-\text{O}(92\text{A})) = d(\text{S}-\text{O}(93\text{A})) = d(\text{S}-\text{O}(91\text{B})) = d(\text{S}-\text{O}(92\text{B})) = d(\text{S}-\text{O}(93\text{B})) = 1.45 \text{ \AA}$; $d(\text{F}(91\text{A})-\text{C}(91\text{A})) = d(\text{F}(92\text{A})-\text{C}(91\text{A})) = d(\text{F}(93\text{A})-\text{C}(91\text{A})) = d(\text{F}(91\text{B})-\text{C}(91\text{B})) = d(\text{F}(92\text{B})-\text{C}(91\text{B})) = d(\text{F}(93\text{B})-\text{C}(91\text{B})) = 1.35 \text{ \AA}$; $d(\text{F}(91\text{A})\cdots\text{F}(92\text{A})) = d(\text{F}(91\text{A})\cdots\text{F}(93\text{A})) = d(\text{F}(91\text{B})\cdots\text{F}(92\text{B})) = d(\text{F}(91\text{B})\cdots\text{F}(93\text{B})) = d(\text{F}(92\text{B})\cdots\text{F}(93\text{B})) = 2.20 \text{ \AA}$; $d(\text{O}(91\text{A})\cdots\text{O}(92\text{A})) = d(\text{O}(91\text{A})\cdots\text{O}(93\text{A})) = d(\text{O}(91\text{B})\cdots\text{O}(92\text{B})) = d(\text{O}(91\text{B})\cdots\text{O}(93\text{B})) = d(\text{O}(92\text{B})\cdots\text{O}(93\text{B})) = 2.37 \text{ \AA}$; $d(\text{F}(91\text{A})\cdots\text{O}(92\text{A})) = d(\text{F}(91\text{A})\cdots\text{O}(93\text{A})) = d(\text{F}(92\text{A})\cdots\text{O}(91\text{A})) = d(\text{F}(92\text{A})\cdots\text{O}(93\text{A})) = d(\text{F}(93\text{A})\cdots\text{O}(91\text{A})) = d(\text{F}(93\text{A})\cdots\text{O}(92\text{A})) = d(\text{F}(91\text{B})\cdots\text{O}(92\text{B})) = d(\text{F}(91\text{B})\cdots\text{O}(93\text{B})) = d(\text{F}(92\text{B})\cdots\text{O}(91\text{B})) = d(\text{F}(92\text{B})\cdots\text{O}(93\text{B})) = d(\text{F}(93\text{B})\cdots\text{O}(91\text{B})) = d(\text{F}(93\text{B})\cdots\text{O}(92\text{B})) = 3.04 \text{ \AA}$.

3.5 Acknowledgements

We thank the Natural Sciences and Engineering Research Council of Canada (NSERC) and the University of Alberta for financial support for this research and NSERC for funding the Bruker D8/APEX II CCD diffractometer. We thank the Department's NMR Spectroscopy and Analytical and Instrumentation Laboratories. Finally, we thank NSERC and Alberta Innovates–Technology (formerly Alberta Ingenuity Fund) for scholarships to M.E.S.

3.6 References

- (1) Imae, T. *Curr. Opin. Colloid Interface Sci.* **2003**, *8*, 307.
- (2) Theodoridis, G. In *Advances in Fluorine Science*; Alain, T., Ed.; Elsevier: 2006; Vol. 2, p 121.
- (3) Isanbor, C.; O'Hagan, D. *J. Fluorine Chem.* **2006**, *127*, 303.
- (4) Fromel, T.; Knepper, T. P. *Chemosphere* **2010**, *80*, 1387.
- (5) O'Hagan, D. *Chem. Soc. Rev.* **2008**, *37*, 308.
- (6) Kiplinger, J. L.; Richmond, T. G.; Osterberg, C. E. *Chem. Rev.* **1994**, *94*, 373.
- (7) Burdeniuc, J.; Jedlicka, B.; Crabtree, R. H. *Chem. Ber. Recl.* **1997**, *130*, 145.
- (8) Richmond, T. In *Activation of Unreactive Bonds and Organic Synthesis*; Murai, S., Alper, H., Gossage, R., Grushin, V., Hidai, M., Ito, Y., Jones, W., Kakiuchi, F., van Koten, G., Lin, Y. S., Mizobe, Y., Murai, S., Murakami, M., Richmond, T., Sen, A., Suginome, M., Yamamoto, A., Eds.; Springer Berlin / Heidelberg: 1999; Vol. 3, p 243.
- (9) Torrens, H. *Coord. Chem. Rev.* **2005**, *249*, 1957.
- (10) Perutz, R. N.; Braun, T. In *Comprehensive Organometallic Chemistry III* 2007; Vol. 1, p 725.
- (11) Hughes, R. P. *Eur. J. Inorg. Chem.* **2009**, *2009*, 4591.
- (12) Wallington, T. J.; Schneider, W. F.; Worsnop, D. R.; Nielsen, O. J.; Sehested, J.; Debruyne, W. J.; Shorter, J. A. *Environ. Sci. Technol.* **1994**, *28*, A320.
- (13) Metz, B.; Kuijpers, L.; Solomon, S.; Andersen, S. O.; Davidson, O.; Pons, J.; de Jager, D.; Kestin, T.; Manning, M.; Meyer, L. *Safeguarding the Ozone Layer and the Global Climate System: Issues Related to Hydrofluorocarbons and Perfluorocarbons*, 2005.
- (14) Aizenberg, M.; Milstein, D. *Science* **1994**, *265*, 359.
- (15) Edelbach, B. L.; Jones, W. D. *J. Am. Chem. Soc.* **1997**, *119*, 7734.
- (16) Sladek, M. I.; Braun, T.; Neumann, B.; Stammeler, H. G. *J. Chem. Soc., Dalton Trans.* **2002**, 297.

- (17) Schaub, T.; Backes, M.; Radius, U. *J. Am. Chem. Soc.* **2006**, *128*, 15964.
- (18) Wang, T.; Alfonso, B. J.; Love, J. A. *Org. Lett.* **2007**, *9*, 5629.
- (19) Camadanli, S.; Beck, R.; Florke, U.; Klein, H. F. *Dalton Trans.* **2008**, 5701.
- (20) Nova, A.; Erhardt, S.; Jasim, N. A.; Perutz, R. N.; Macgregor, S. A.; McGrady, J. E.; Whitwood, A. C. *J. Am. Chem. Soc.* **2008**, *130*, 15499.
- (21) Wang, T. G.; Love, J. A. *Organometallics* **2008**, *27*, 3290.
- (22) Buckley, H. L.; Wang, T. E.; Tran, O.; Love, J. A. *Organometallics* **2009**, *28*, 2356.
- (23) Johnson, S. A.; Taylor, E. T.; Cruise, S. J. *Organometallics* **2009**, *28*, 3842.
- (24) Reade, S. P.; Mahon, M. F.; Whittlesey, M. K. *J. Am. Chem. Soc.* **2009**, *131*, 1847.
- (25) Zheng, T. T.; Sun, H. J.; Chen, Y.; Li, X. Y.; Durr, S.; Radius, U.; Harms, K. *Organometallics* **2009**, *28*, 5771.
- (26) Buckley, H. L.; Sun, A. D.; Love, J. A. *Organometallics* **2009**, *28*, 6622.
- (27) Clot, E.; Eisenstein, O.; Jasim, N.; Macgregor, S. A.; McGrady, J. E.; Perutz, T. *Acc. Chem. Res.* **2011**, *44*, 333.
- (28) Roundhill, D. M.; Lawson, D. N.; Wilkinson, G. *J. Chem. Soc. A* **1968**, 845.
- (29) Roundhill, D. M.; Wilkinson, G. *J. Chem. Soc. A* **1968**, 506.
- (30) Hudlicky, M. *J. Fluorine Chem.* **1989**, *44*, 345.
- (31) Hughes, R. P.; Rose, P. R.; Rheingold, A. L. *Organometallics* **1993**, *12*, 3109.
- (32) Ristic-Petrovic, D.; Wang, M.; McDonald, R.; Cowie, M. *Organometallics* **2002**, *21*, 5172.
- (33) Hughes, R. P.; Laritchev, R. B.; Zakharov, L. N.; Rheingold, A. L. *J. Am. Chem. Soc.* **2004**, *126*, 2308.
- (34) Rieth, R. D.; Brennessel, W. W.; Jones, W. D. *Eur. J. Inorg. Chem.* **2007**, 2839.

- (35) Kraft, B. M.; Clot, E.; Eisenstein, O.; Brennessel, W. W.; Jones, W. D. *J. Fluorine Chem.* **2010**, *131*, 1122.
- (36) Kraft, B. M.; Lachicotte, R. J.; Jones, W. D. *J. Am. Chem. Soc.* **2000**, *122*, 8559.
- (37) Ferrando-Miguel, G.; Gerard, H.; Eisenstein, O.; Caulton, K. G. *Inorg. Chem.* **2002**, *41*, 6440.
- (38) Jones, W. D. *Dalton Trans.* **2003**, 3991.
- (39) Noveski, D.; Braun, T.; Schulte, M.; Neumann, B.; Stammer, H. G. *Dalton Trans.* **2003**, 4075.
- (40) Peterson, A. A.; McNeill, K. *Organometallics* **2006**, *25*, 4938.
- (41) Peterson, A. A.; Thoreson, K. A.; McNeill, K. *Organometallics* **2009**, *28*, 5982.
- (42) Kuhnel, M. F.; Lentz, D. *Angew. Chem. Int. Ed.* **2010**, *49*, 2933.
- (43) Booth, B. L.; Haszeldine, R. N.; Mitchell, P. R.; Cox, J. J. *Chem. Comm.* **1967**, 529.
- (44) Bonnet, J. J.; Mathieu, R.; Poilblanc, R.; Ibers, J. A. *J. Am. Chem. Soc.* **1979**, *101*, 7487.
- (45) Kemmitt, R. D. W.; Nichols, D. I. *J. Chem. Soc. A* **1969**, 1577.
- (46) Hacker, M. J.; Littlecott, G. W.; Kemmitt, R. D. W. *J. Organomet. Chem.* **1973**, *47*, 189.
- (47) Jones, M. T.; McDonald, R. N. *Organometallics* **1988**, *7*, 1221.
- (48) Anderson, D. J.; McDonald, R.; Cowie, M. *Angew. Chem. Int. Ed.* **2007**, *46*, 3741.
- (49) Ohashi, M.; Kambara, T.; Hatanaka, T.; Saijo, H.; Doi, R.; Ogoshi, S. *J. Am. Chem. Soc.* **2011**, *133*, 3256.
- (50) Craig, N. C.; Piper, L. G.; Wheeler, V. L. *J. Phys. Chem.* **1971**, *75*, 1453.
- (51) Waldron, J. T.; Snyder, W. H. *J. Am. Chem. Soc.* **1973**, *95*, 5491.
- (52) Bingham, R. C. *J. Am. Chem. Soc.* **1976**, *98*, 535.
- (53) Lemal, D. M. *J. Org. Chem.* **2004**, *69*, 1.
- (54) Goodman, L.; Gu, H. B.; Pophristic, V. *J. Phys. Chem. A* **2005**, *109*, 1223.

- (55) Green, M.; Laguna, A.; Spencer, J. L.; Stone, F. G. A. *J. Chem. Soc., Dalton Trans.* **1977**, 1010.
- (56) Kirkham, M. S.; Mahon, M. F.; Whittlesey, M. K. *Chem. Comm.* **2001**, 813.
- (57) Maples, P. K.; Green, M.; Stone, F. G. A. *J. Chem. Soc., Dalton Trans.* **1973**, 2069.
- (58) Braun, T.; Noveski, D.; Neumann, B.; Stammer, H. G. *Angew. Chem. Int. Ed.* **2002**, *41*, 2745.
- (59) Braun, T.; Salomon, M. A.; Altenhoner, K.; Teltewskoi, M.; Hinze, S. *Angew. Chem. Int. Ed.* **2009**, *48*, 1818.
- (60) Kraft, B. M.; Jones, W. D. *J. Am. Chem. Soc.* **2002**, *124*, 8681.
- (61) Slaney, M. E.; Anderson, D. J.; Ferguson, M. J.; McDonald, R.; Cowie, M. *J. Am. Chem. Soc.* **2010**, *132*, 16544.
- (62) Ristic-Petrovic, D.; Anderson, D. J.; Torkelson, J. R.; McDonald, R.; Cowie, M. *Organometallics* **2003**, *22*, 4647.
- (63) Bent, H. A. *Chem. Rev.* **1961**, *61*, 275.
- (64) Dedert, P. L.; Sorrell, T.; Marks, T. J.; Ibers, J. A. *Inorg. Chem.* **1982**, *21*, 3506.
- (65) Balch, A. L.; Olmstead, M. M.; Rowley, S. P. *Inorg. Chem.* **1988**, *27*, 2275.
- (66) Ferrara, J. D.; Tessier-Youngs, C.; Youngs, W. J. *Inorg. Chem.* **1988**, *27*, 2201.
- (67) O'Connor, J. M.; Uhrhammer, R.; Rheingold, A. L.; Staley, D. L. *J. Am. Chem. Soc.* **1989**, *111*, 7633.
- (68) Richmond, T. G.; Kelson, E. P.; Arif, A. M.; Carpenter, G. B. *J. Am. Chem. Soc.* **1988**, *110*, 2334.
- (69) Schnabel, R. C.; Roddick, D. M. *Organometallics* **1993**, *12*, 704.
- (70) Gudat, D.; Holderberg, A. W.; Kotila, S.; Nieger, M. *Chem. Ber.* **1996**, *129*, 465.
- (71) van Albada, G. A.; Smeets, W. J. J.; Spek, A. L.; Reedijk, J. *Inorg. Chim. Acta* **1997**, *260*, 151.

- (72) Baar, C. R.; Carbray, L. P.; Jennings, M. C.; Puddephatt, R. J. *Organometallics* **2000**, *19*, 2482.
- (73) Cairns, M. A.; Dixon, K. R.; Mcfarland, J. J. *J. Chem. Soc., Dalton Trans.* **1975**, 1159.
- (74) Williams, A. F.; Bhaduri, S.; Maddock, A. G. *J. Chem. Soc., Dalton Trans.* **1975**, 1958.
- (75) Cockman, R. W.; Ebsworth, E. A. V.; Holloway, J. H. *J. Am. Chem. Soc.* **1987**, *109*, 2194.
- (76) Blake, A. J.; Cockman, R. W.; Ebsworth, E. A. V.; Holloway, J. H. *J. Chem. Soc., Chem. Commun.* **1988**, 529.
- (77) Grushin, V. V.; Marshall, W. J. *J. Am. Chem. Soc.* **2004**, *126*, 3068.
- (78) Kulawiec, R. J.; Holt, E. M.; Lavin, M.; Crabtree, R. H. *Inorg. Chem.* **1987**, *26*, 2559.
- (79) Torkelson, J. R.; Antwi-Nsiah, F. H.; McDonald, R.; Cowie, M.; Pruis, J. G.; Jalkanen, K. J.; DeKock, R. L. *J. Am. Chem. Soc.* **1999**, *121*, 3666.
- (80) Cowie, M.; Loeb, S. J. *Organometallics* **1985**, *4*, 852.
- (81) Deraniyagala, S. P.; Grundy, K. R. *Organometallics* **1985**, *4*, 424.
- (82) Yam, V. W. W.; Yeung, P. K. Y.; Chan, L. P.; Kwok, W. M.; Phillips, D. L.; Yu, K. L.; Wong, R. W. K.; Yan, H.; Meng, Q. J. *Organometallics* **1998**, *17*, 2590.
- (83) Wong, K. M. C.; Hui, C. K.; Yu, K. L.; Yam, V. W. W. *Coord. Chem. Rev.* **2002**, *229*, 123.
- (84) Lam, W. H.; Yam, V. W. W. *Inorg. Chem.* **2010**, *49*, 10930.
- (85) Allen, F. H.; Kennard, O.; Watons, D. G.; Brammer, L.; Orpen, A. G.; Taylor, R. *J. Chem. Soc. Perkin Trans. II* **1987**, *12*, S1.
- (86) Hughes, R. P.; Lindner, D. C.; Rheingold, A. L.; LiableSands, L. M. *J. Am. Chem. Soc.* **1997**, *119*, 11544.
- (87) Hughes, R. P.; Lindner, D. C.; Smith, J. M.; Zhang, D. H.; Incarvito, C. D.; Lam, K. C.; Liable-Sands, L. M.; Sommer, R. D.; Rheingold, A. L. *Dalton Trans.* **2001**, 2270.
- (88) Sutherland, B. R.; Cowie, M. *Organometallics* **1985**, *4*, 1637.

- (89) Dewolf, M. Y.; Baldeschwieler, J. D. *J. Mol. Spec.* **1964**, *13*, 344.
- (90) Torkelson, J. R.; McDonald, R.; Cowie, M. *J. Am. Chem. Soc.* **1998**, *120*, 4047.
- (91) McDonald, R.; Sutherland, B. R.; Cowie, M. *Inorg. Chem.* **1987**, *26*, 3333.
- (92) Programs for diffractometer operation, unit cell indexing, data collection, data reduction and absorption correction were those supplied by Bruker.
- (93) Sheldrick, G. M. *Acta Crystallogr.* **2008**, *A64*, 112.
- (94) Beurskens, P. T.; Beurskens, G.; de Gelder, R.; Smits, J. M. M.; Garcia-Granda, S.; Gould, R. O. (2008). The DIRDIF-2008 program system. Crystallography Laboratory, Radboud University Nijmegen, The Netherlands.
- (95) Beurskens, P. T.; Beurskens, G.; Bosman, W. P.; de Gelder, R.; Garcia Granda, S.; Gould, R. O.; Israel, R.; Smits, J. M. M. (1996). The DIRDIF-96 program system. Crystallography Laboratory, Radboud University Nijmegen, The Netherlands
- (96) van der Sluis, P.; Spek, A. L. *Acta Crystallogr.* **1990**, *A46*, 194.
- (97) *PLATON* - a multipurpose crystallographic tool. Utrecht University, Utrecht, The Netherlands.
- (98) Spek, A. L. *Acta Crystallogr.* **1990**, *A46*, C34.
- (99) Spek, A. L. *J. Appl. Cryst.* **2003**, *36*, 7.
- (100) Flack, H. D. *Acta Crystallogr.* **1983**, *A39*, 876.
- (101) Flack, H. D.; Bernardinelli, G. *Acta Crystallogr.* **1999**, *A55*, 908.
- (102) Flack, H. D.; Bernardinelli, G. *J. Appl. Cryst.* **2000**, *33*, 1143.

Chapter 4 – *Bis*(diethylphosphino)methane as a Bridging Ligand in Complexes of Ir₂, Rh₂ and IrRh: Geminal C–H Activation of α -Olefins[†]

4.1 Introduction

Interest in the reactivity of binuclear complexes¹ containing either pairs of identical metals²⁻¹⁸ or two metals that differ,¹⁹⁻³³ has primarily been driven by the idea that these metals may act together in some way, either in a cooperative manner,^{18,26-36} whereby the pair of adjacent metals give rise to reactivity that differs from that observed at single-metal sites, or in tandem, whereby one metal performs one transformation, followed by a second transformation at the other metal.³⁷⁻⁴¹ A binuclear compound studied by us, namely [Ir₂(CH₃)(CO)₂(dppm)₂][X] (dppm = μ -Ph₂PCH₂PPh₂, X = anion), has demonstrated a wealth of reactivity including C–H^{42,43} and C–F^{36,44,45} bond activation, in which the pair of adjacent metals play a pivotal role. In addition to the interesting reactivity displayed by this species, its simplicity and the fact that each ligand present has one or more convenient NMR-active nuclei (³¹P, ¹³C, ¹H) has often allowed the stepwise transformations to be conveniently followed by multi-nuclear and variable-temperature NMR studies, giving us an appreciation of the roles of the adjacent metals in the chemistry.

One transformation of interest to us, that could make use of the cooperative involvement of pairs of metals, is the double activation of pairs of geminal C–H bonds in α -olefins. Although the activation of single olefinic C–H bonds is common,⁴⁶⁻⁵⁶ double, geminal C–H activation is rare with only a few examples having been reported.^{42,57-64} Of these, all but one⁶³ involve pairs of metals at some stage in the activation process.

In a previous study we observed the unusual double activation of a pair of geminal C–H bonds in 1,3-butadiene by the above diiridium complex and

[†] The work presented in this chapter has been accepted for publication. Slaney, M.E.; Anderson, D.J.; Ferguson, M.J.; McDonald, R.; Cowie, M. Accepted, *Organometallics*, *Jan. 16, 2012*. Manuscript ID: om-2011-01214z

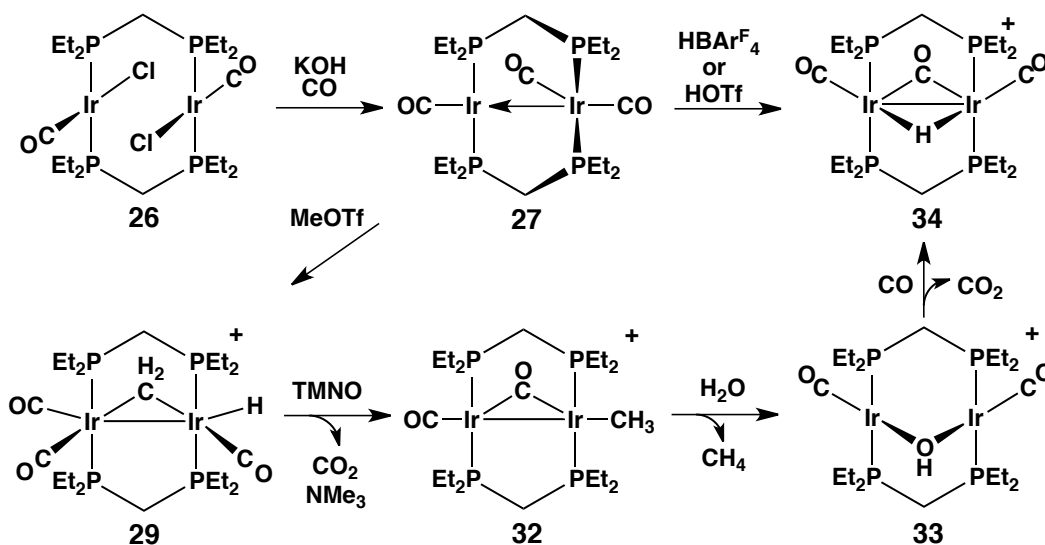
proposed the cooperative involvement of the pair of metals in this transformation.⁴² However, this reaction is extremely slow (48 hours at 22 °C) and the binding of the butadiene, in a presumed intermediate, is extremely weak and only observed at temperatures below *ca.* -50 °C. Furthermore, this reactivity was limited to butadiene substrate, with no C–H activation observed for other α -olefins investigated. Seeking to improve the scope of double, geminal C–H activation, we considered replacing the bridging dppm groups by smaller, more basic alkyl diphosphines to allow better substrate access to the metals, and to increase metal basicity, respectively. The obvious diphosphine of choice for this replacement was *bis*(dimethylphosphino)methane (dmpm) – the smallest of the alkyl-substituted diphosphines. Furthermore, the dmpm analogue of the above methyl complex, namely $[\text{Ir}_2(\text{CH}_3)(\text{CO})_2(\text{dmpm})_2]^+$ had been reported.¹¹ Unfortunately, our attempts to duplicate the reported synthesis were unsuccessful and in general we found that the dmpm chemistry deviated significantly from that of dppm in rather unpredictable ways.⁶⁵

The capricious nature of this dmpm chemistry (in our hands) led us to instead investigate the closely related depm ($\text{Et}_2\text{PCH}_2\text{PEt}_2$) ligand, the chemistry of which, we find, parallels that of dppm in a usually predictable way. In this Chapter we report the synthesis and characterization of a series of depm-bridged complexes of Ir_2 , Rh_2 and RhIr , and investigate their reactivity towards a series of α -olefins. Although the Rh/Ir and Rh_2 analogues of $[\text{Ir}_2(\text{CH}_3)(\text{CO})_2(\text{dppm})_2]^+$ were unreactive towards 1,3-butadiene, we were also interested in determining whether these Rh -containing analogues, incorporating a pair of more basic depm groups, might display reactivity towards olefin C–H activation, not previously observed with the dppm system.

4.2 Results

4.2.1 Synthesis of diiridium complexes. The addition of $[\text{IrCl}(\text{COD})]_2$ to a CH_2Cl_2 solution of *bis*(diethylphosphino)methane (dep m) followed by a slow CO purge results in the formation of *trans*- $[\text{Ir}_2\text{Cl}_2(\text{CO})_2(\text{dep}\text{m})_2]$ (**26**) in modest yields (the structure of **26** is diagrammed in Scheme 4.1). Compound **26** displays

a singlet in the $^{31}\text{P}\{^1\text{H}\}$ NMR spectrum at δ 8.3, indicating the chemical equivalence of all four ^{31}P nuclei, and the ^1H NMR spectrum also displays a single resonance at δ 2.52 for the backbone-methylene protons of depm, consistent with “front/back” symmetry in the species; this signal appears as a quintet owing to virtual coupling to all ^{31}P nuclei. The chemical equivalence of both carbonyls gives also rise to a single resonance in the $^{13}\text{C}\{^1\text{H}\}$ spectrum at δ 168.3.



Scheme 4.1 – *Synthesis of diiridium bis(diethylphosphino)methane complexes.*

A crystal suitable for X-ray diffraction was obtained, confirming the mutual trans orientation of carbonyls and chlorides on each iridium site and their transoid arrangement about the molecular centroid (Figure 4.1). The Ir–Ir’ separation (3.1274(3) Å) indicates the absence of a metal-metal interaction, and is consistent with the non-bonding distances of P(1) – P(2) (3.125(1) Å). The Cl(A) – Ir – C(1A) angle (173.3(3)°) deviates slightly from idealized 180°, presumably a result of steric repulsion between the carbonyl on one metal and the chloride on the other.

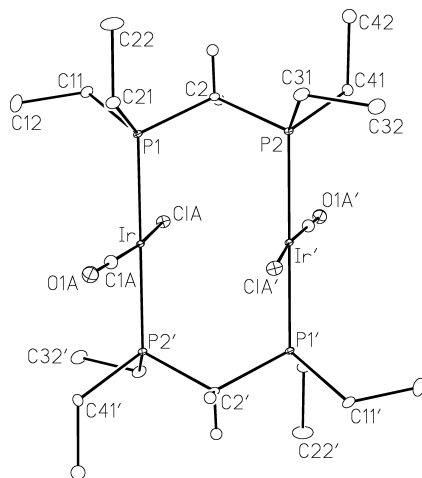
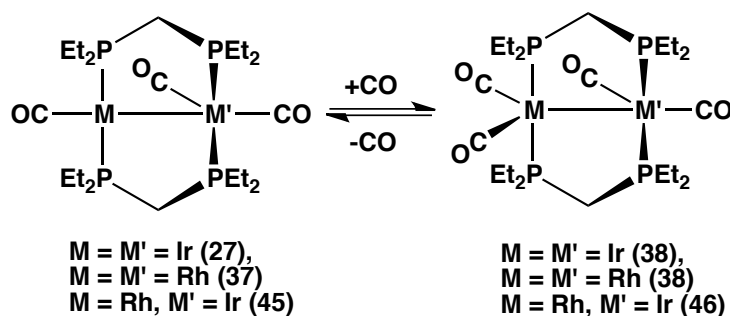


Figure 4.1 – Perspective view of the *trans*-[Ir₂Cl₂(CO)₂(depm)₂] (**26**) molecule showing the atom labelling scheme. Non-hydrogen atoms are represented by Gaussian ellipsoids at the 20% probability level. Hydrogen atoms are shown with arbitrarily small thermal parameters except for ethyl hydrogens, which are not shown. Primed atoms are related to unprimed ones via the crystallographic inversion centre (0, 0, 0). Relevant bond distances (Å) and angles (°): Ir – Ir' = 3.1274(3); P(1) – P(2) = 3.125(1); Ir – Cl(A) = 2.393(3); Ir – C(1A) = 1.79(1); Cl(A) – Ir – C(1A) = 173.3(3); P(1) – Ir – P(2') = 178.72(4).

Compound **26** is the precursor for all other Ir₂ compounds reported in this Chapter and is readily reduced under an atmosphere of CO in aqueous KOH to yield [Ir₂(CO)₃(depm)₂] (**27**). More conventional reduction methods such as the reaction with sodium borohydride or zinc powder under carbon monoxide were also investigated; however, these methods resulted in mixtures of products that were difficult to separate and consequently gave substantially lower yields of **27**, making aqueous KOH/CO the preferred method. At ambient temperature, compound **27** has spectroscopic characteristics similar to those of **26**, and its dppm congener,⁷ displaying a singlet in the ³¹P{¹H} NMR spectrum at $\delta = -11.0$, a quintet for the backbone-methylene group (Et₂PCH₂PEt₂) in the ¹H NMR spectrum at δ 2.67 and one carbonyl signal in the ¹³C{¹H} NMR spectrum at δ 185.6. However, upon cooling to -80 °C, the ³¹P{¹H} NMR spectrum displays two signals at δ 8.9 and -28.0 , consistent with the chemically inequivalent environments, and although there is no noticeable change in the ¹H NMR spectrum at this temperature, three unique CO resonances are observed in the ¹³C{¹H} NMR at δ 179.8, 189.3 and 193.8, indicating that a fluxional process is

occurring at higher temperatures. This fluxionality most likely involves a “merry-go-round” exchange of the carbonyls, accompanied by the alternating exchange of cis-to-trans phosphine arrangement at the different metals, as was also proposed in both the dppm and dmpm analogues.^{7,12} The similarities in the low-temperature NMR spectra of **27** compared to those of $[\text{Rh}_2(\text{CO})_3(\text{dppm})_2]$,⁸ $[\text{RhIr}(\text{CO})_3(\text{dppm})_2]$ ²² and $[\text{Ir}_2(\text{CO})_3(\text{dppm})_2]$ ⁷ suggest similar structures, which were established for the Rh-containing dppm species by X-ray structure determinations, in which they are shown to have a trans arrangement of diphosphines at one metal and a cis arrangement at the other.

In the presence of CO compound **27** is converted to the tetracarbonyl complex, $[\text{Ir}_2(\text{CO})_4(\text{dep}_m)_2]$ (**28**) (Scheme 4.2), while removal of the CO atmosphere causes compound **28** to revert to **27** within minutes in solution. Again at ambient temperature a singlet is observed for **28** in the $^{31}\text{P}\{^1\text{H}\}$ NMR while only a single ^{13}C resonance is observed in the $^{13}\text{C}\{^1\text{H}\}$ NMR spectrum. However, cooling a solution of **28** to $-80\text{ }^\circ\text{C}$ results in similar behavior to that of compound **27**, with two distinct $^{31}\text{P}\{^1\text{H}\}$ signals observed ($\delta -19.6$ and -41.1), along with four distinct carbonyl resonances in the $^{13}\text{C}\{^1\text{H}\}$ NMR at $\delta 181.2$, 191.8 , 194.2 and 195.2 , again indicating fluxionality, presumably analogous to that of **27**. Compound **28** is similar to the dmpm analogue, the structure of which was reported by Reinking and shown to have the unsymmetrical structure diagrammed below for our species.⁶⁶



Scheme 4.2 – Addition of carbon monoxide to compounds **27**, **37** and **45**.

In parallel with the analogous dppm-bridged diiridium species,¹⁸ reaction of **27** with methyl trifluoromethanesulfonate (MeOTf), results in the formation of $[\text{Ir}_2(\text{H})(\text{CO})_3(\mu\text{-CH}_2)(\text{dep}_m)_2][\text{OTf}]$ (**29**; Scheme 4.1), in which the methyl group has undergone C–H bond activation to produce a methylene/hydride species. The $^{31}\text{P}\{^1\text{H}\}$ NMR spectrum displays two broad resonances at δ –8.9 and –19.5, which sharpen into pseudotriplets upon cooling to –80 °C. The ^1H NMR spectrum at this temperature confirms the methylene/hydride formulation with the metal-bridged methylene protons appearing at δ 3.95, and the hydride resonance at δ –12.42. In the reaction of **27** with carbon-13 labeled MeOTf, the resulting $^{13}\text{C}\{^1\text{H}\}$ resonance appears in the methylene region at δ 44.2. Also observed in the $^{13}\text{C}\{^1\text{H}\}$ NMR spectrum for the ^{13}CO -labeled product is a single resonance at δ 177.2 for the three carbonyls, and cooling to –80 °C results in its separation into three signals (δ 166.3, 178.7 and 180.2). A spin-saturation transfer experiment on the methylene and hydride protons at ambient temperature confirms that the fluxionality at elevated temperatures involves the reversible transformation of the methylene and hydride groups to a methyl ligand, much as reported for the dppm analogue.¹⁸

An X-ray structure determination of **29** confirms the ligand orientation proposed by spectroscopy, as displayed in Figure 4.2. The Ir(1) – Ir(2) separation of 2.7887(3) Å indicates the presence of a metal-metal bond, displaying significant compression compared to the P(1) – P(2) and P(3) – P(4) distances of 3.049(2) and 3.015(2) Å, respectively, within the depm groups. The bridging methylene group is unsymmetrically bound, being slightly closer to the less crowded Ir(2) centre (Ir(2) – C(4) = 2.075(5) Å) than to Ir(1) (Ir(1) – C(4) = 2.163(5) Å). There is a 50/50 disorder of the ethyl groups on P(4), with two different orientations forcing the neighboring carbonyl (C(3) and O(3)) to also be disordered over two positions.

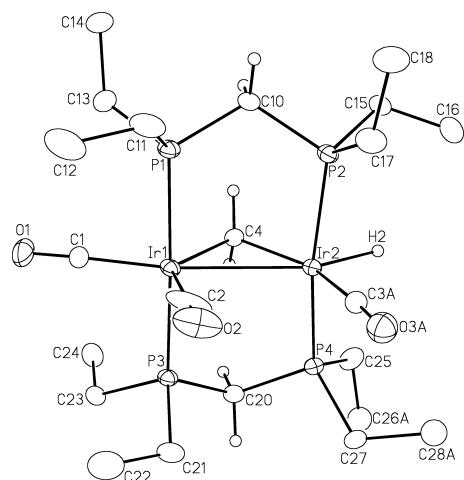
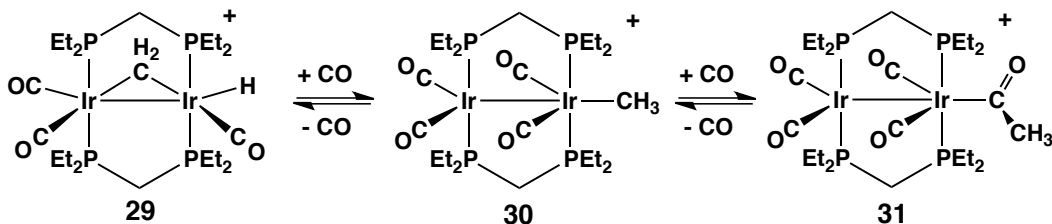


Figure 4.2 – Perspective view of the $[\text{Ir}_2(\text{H})(\text{CO})_3(\mu\text{-CH}_2)(\text{dep})_2]^+$ (**29**) cation showing the atom labelling scheme. Thermal parameters are shown at the 20% probability level. Hydrogen atoms are shown with arbitrarily small thermal parameters for the hydride, bridging methylene, and depm methylene groups. Only one pair of disordered methyl substituents of the ethyl groups on P(4), along with the disordered carbonyl on Ir(2), are shown for clarity. Relevant bond distances (Å) and angles (°): Ir(1) – Ir(2) = 2.7887(3); Ir(1) – C(4) = 2.163(5); Ir(2) – C(4) = 2.075(5); P(1) – P(2) = 3.049(2); P(3) – P(4) = 3.015(2); Ir(1) – C(4) – Ir(2) = 82.3(2).

Placing compound **29** under a CO atmosphere results in the formation of two other compounds, identified as $[\text{Ir}_2(\text{CH}_3)(\text{CO})_4(\text{dep})_2][\text{OTf}]$ (**30**) and $[\text{Ir}_2(\text{CO})_4(\text{C}(\text{O})\text{CH}_3)(\text{dep})_2][\text{OTf}]$ (**31**), the result of sequential CO uptake (Scheme 4.3). Both compounds are fluxional at ambient temperature and are susceptible to CO loss upon CO removal, resulting in reversion to **29**. In the ^1H NMR spectrum of **30**, a triplet appears at δ 0.68 ($^3J_{\text{HP}} = 5.4$ Hz) for the Ir-bound methyl group, while for **31** the methyl group appears as a singlet at δ 2.60, consistent with migration of this group to a carbonyl. In the $^{13}\text{C}\{^1\text{H}\}$ NMR spectrum two carbonyl signals (δ 187.4 and 191.1) appear for **30** in a 2:2 ratio, while for **31** three resonances appear in a 2:2:1 ratio at δ 187.8, 195.0 and 221.2; the downfield signal is typical of an Ir-bound acyl group.⁶⁷ Additional coupling of the methyl group to the acyl carbonyl ($^1J_{\text{CC}} = 28.0$ Hz) also supports the migratory insertion product. The similarities in the spectral parameters of **30** and **31** are consistent with their similar geometries.



Scheme 4.3 – Sequential carbon monoxide uptake by compound **29**.

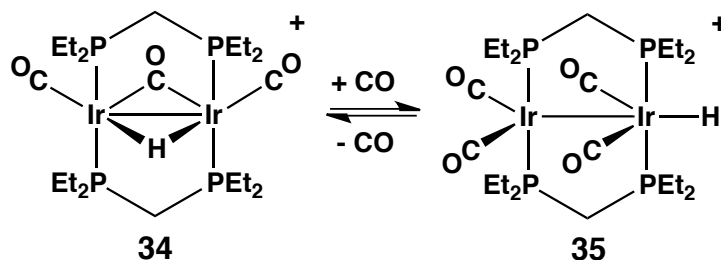
Reacting compound **29** with trimethylamine-*N*-oxide (TMNO) at ambient temperature produces the dicarbonyl product $[\text{Ir}_2(\text{CH}_3)(\text{CO})_2(\text{depm})_2][\text{OTf}]$ (**32**) as shown earlier in Scheme 4.1. Compound **32** displays a single broad resonance at ambient temperature in the $^{31}\text{P}\{^1\text{H}\}$ NMR spectrum at δ 23.2, similar to the methyl dicarbonyl analogues of dppm and dmpm.^{11,18} The ^1H NMR spectrum displays a quintet at δ 0.57 ($^3J_{\text{HP}} = 4.4$ Hz) for the methyl ligand, and the $^{13}\text{C}\{^1\text{H}\}$ NMR spectrum also displays a single carbonyl resonance at δ 174.2, suggesting a symmetric, methyl-bridged structure as reported for the dmpm analogue.¹¹ However, cooling to -80 °C gives rise to the separation of the signal into two distinct resonances at δ 26.1 and 19.8 and the appearance of two carbonyl resonances, δ 179.9 and 168.3, in the $^{13}\text{C}\{^1\text{H}\}$ NMR spectrum, suggesting an unsymmetrical structure, such as that shown in Scheme 4.1, and analogous to that observed for the dppm analogues $[\text{IrRh}(\text{CH}_3)(\text{CO})_2(\text{dppm})_2]^+$ and $[\text{Ir}_2(\text{CH}_3)(\text{CO})_2(\text{dppm})_2]^+$.^{18,25} The symmetrical structure suggested by the ambient temperature spectra is presumably the result of migration of the methyl group from metal-to-metal on one face of the Ir_2P_4 plane, in conjunction with the two CO ligands migrating across the opposite face of the metals.

Unfortunately, compound **32** is unstable in solution at ambient temperature transforming to $[\text{Ir}(\text{CO})_2(\mu\text{-OH})(\text{depm})_2][\text{OTf}]$ (**33**; Scheme 4.1) within 5 min, owing to its reaction with adventitious water that results from either the earlier aqueous KOH/CO reduction step or the use of trimethylamine-*N*-oxide, which is difficult to obtain fully dried.⁶⁸ In both cases, an azeotropic distillation in benzene or dimethylformamide, respectively, was performed in attempts to minimize residual water. However, the transformation of **32** to **33** in solution

could not be prevented by these precautions, having still occurred after 45 min. Compound **33** displays spectral parameters similar to its dppm congener,⁷ and therefore is not discussed here (refer to experimental section for NMR data).

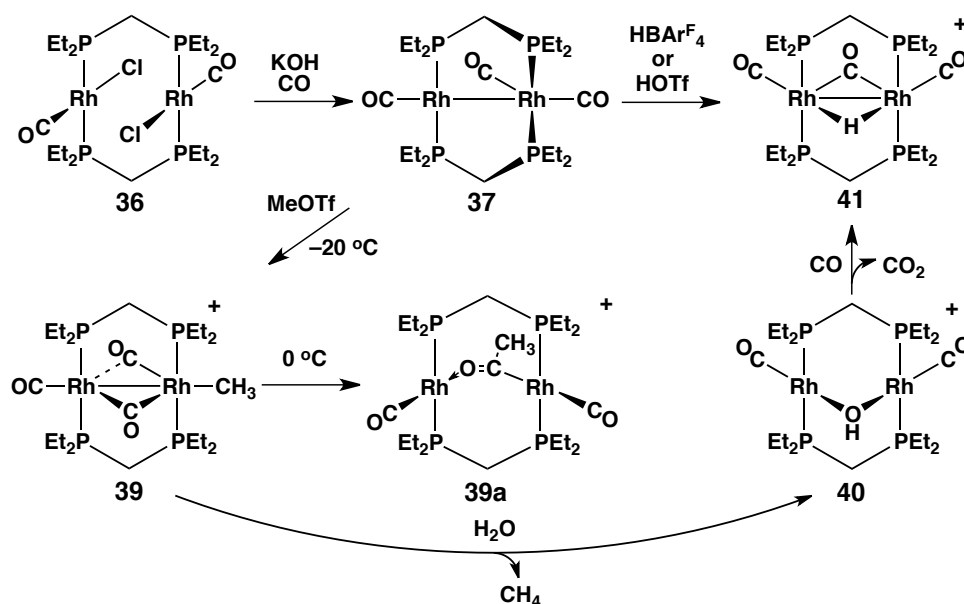
Reaction of compound **33** with CO generates the hydride-bridged species, $[\text{Ir}_2(\text{CO})_3(\mu\text{-H})(\text{depm})_2][\text{OTf}]$ (**34-OTf**), as shown in Scheme 4.1, which was obtained more directly by reaction of **27** with acid. Compound **34**, as either the triflate or $\text{BAr}_4^{\text{F}}^-$ salt, displays a singlet in the $^{31}\text{P}\{^1\text{H}\}$ NMR spectrum, while the ^1H NMR spectrum displays a single, upfield resonance at $\delta -10.40$, appearing as a quintet with equal coupling to all four phosphorus nuclei ($^2J_{\text{HP}} = 9.82$ Hz). At ambient temperature, the $^{13}\text{C}\{^1\text{H}\}$ NMR spectrum shows a single, broad resonance at $\delta 183.7$, which upon cooling to -80 °C resolves into two resonances at $\delta 185.3$ and 183.3 , in a 1:2 intensity ratio, respectively; at low temperature the $^{31}\text{P}\{^1\text{H}\}$ and ^1H NMR spectra remain unchanged, ruling out a fluxional process.

Under a CO atmosphere, compound **34** generates $[\text{Ir}_2(\text{H})(\text{CO})_4(\text{depm})_2]^+$ (**35**), in which the hydride ligand is now terminally bound to one Ir centre, as shown by the triplet in the ^1H NMR spectrum at $\delta -8.80$, displaying coupling to only one pair of ^{31}P nuclei ($^2J_{\text{HP}} = 14.4$ Hz). The appearance of only two equal intensity carbonyl resonances in the carbon-13 NMR spectrum, in conjunction with only one signal for the backbone-methylene protons, suggests that compound **35** has a similar geometry to those of compounds **30** and **31**, with front/back symmetry about the metal-phosphine plane.



Scheme 4.4 – Addition of carbon monoxide to compound **34**.

4.2.2 Synthesis of dirhodium complexes. Reacting $[\text{Rh}_2\text{Cl}_2(\text{COD})_2]$ with depm under a CO purge results in the formation of *trans*- $[\text{Rh}_2\text{Cl}_2(\text{CO})_2(\text{dep}m)_2]$ (**36**; Scheme 4.5) much as described for the Ir₂ analogue. The $^{31}\text{P}\{^1\text{H}\}$, ^1H , and $^{13}\text{C}\{^1\text{H}\}$ spectral parameters are all as expected, including rhodium-phosphorus coupling observed in the $^{31}\text{P}\{^1\text{H}\}$ NMR spectrum ($^1J_{\text{RhP}} = 117.2$ Hz) and rhodium-carbon coupling for the carbonyls in the $^{13}\text{C}\{^1\text{H}\}$ NMR spectrum ($^1J_{\text{RhC}} = 74.8$ Hz). An X-ray structure determination of compound **36** reveals a near superimposable structure to that of the diiridium analogue (**26**).



Scheme 4.5 – *Synthesis of dirhodium bis(diethylphosphino)methane complexes.*

As described earlier for the Ir₂ complex, compound **36** can also be reduced under a CO atmosphere in the presence of aqueous KOH, resulting in the formation of $[\text{Rh}_2(\text{CO})_3(\text{dep}m)_2]$ (**37**). Multinuclear NMR spectra show similarities to compound **27** at ambient temperature, with the exception of additional rhodium-phosphorus coupling ($^1J_{\text{RhP}} = 137.7$ Hz). Cooling **37** to -110 °C shows separation of the single $^{31}\text{P}\{^1\text{H}\}$ signal into two doublets of pseudo-triplets at δ 22.5 and 8.5, with rhodium-phosphorus couplings of 117.1 Hz and 152.6 Hz, respectively, along with mutual phosphorus-phosphorus coupling of 69.7 Hz. At -110 °C, the broad carbonyl resonance observed at ambient

temperature resolves at $-110\text{ }^{\circ}\text{C}$ into three signals at δ 209.1, 206.8 and 183.4 ($^1J_{\text{RhC}} = 77.0\text{ Hz}$, 71.2 Hz and 67.9 Hz , respectively). Selective $^{13}\text{C}\{^{31}\text{P}\}$ decoupling establishes that the upfield carbonyl is coupled to one end of the diphosphines (δ 22.5) while the two downfield signals are coupled to the other ends, consistent with the structure proposed in Scheme 4.5, and in agreement with the structures determined for the dppm analogues, $[\text{Rh}_2(\text{CO})_3(\text{dppm})_2]^2$ and $[\text{IrRh}(\text{CO})_3(\text{dppm})_2]$.²²

As shown earlier in Scheme 4.2, compound **37** reacts under an atmosphere of CO, producing $[\text{Rh}_2(\text{CO})_4(\text{depm})_2]$ (**38**), which is highly susceptible to CO loss. Multinuclear NMR spectroscopy displays broad resonances at ambient temperature, however cooling the sample to $-80\text{ }^{\circ}\text{C}$ produces the pattern expected for an AA'BB'XY spin system in the $^{31}\text{P}\{^1\text{H}\}$ NMR spectrum, and in conjunction with two $^{13}\text{C}\{^1\text{H}\}$ resonances at δ 214.3 and 204.1 in a 1:3 ratio, confirms the presence of a fourth carbonyl (refer to Experimental section for full spectroscopic characterization). This intensity ratio is not the 1:1:1:1 ratio expected, and appears to indicate coincidental overlap of three resonances masked by the breadth of the resulting signal.

The addition of MeOTf to compound **37** at $-20\text{ }^{\circ}\text{C}$ produces the tricarbonyl methyl species, $[\text{Rh}_2(\text{CH}_3)(\text{CO})_3(\text{depm})_2][\text{OTf}]$ (**39**), as shown in Scheme 4.5. Unlike the diiridium analogue (**29**), the methyl moiety does not undergo C–H activation to give a methylene/hydride isomer, but remains intact, as confirmed by both ^1H and $^{13}\text{C}\{^1\text{H}\}$ NMR spectroscopy at $-80\text{ }^{\circ}\text{C}$, with the methyl protons appearing as a broad multiplet at δ 0.63, and the methyl carbon appearing as a broad, unresolved resonance at δ -0.7 . The $^{13}\text{C}\{^1\text{H}\}$ NMR spectrum also displays two carbonyl resonances at δ 214.3 (2C) and 199.3 (1C), with the downfield signal suggesting two bridging carbonyls while the upfield single indicates one terminal carbonyl. The $^{13}\text{C}\{^1\text{H}, ^{31}\text{P}\}$ spectrum shows the downfield multiplet as a triplet due to coupling to rhodium (32.7 Hz), while the upfield signal resolves to a doublet from coupling to rhodium (74.9 Hz). Although the single low-field resonance for the pair of carbonyls suggests two symmetrically bridging groups, the static structure more likely resembles that

depicted in Scheme 4.5, with one bridging carbonyl and one semi-bridging carbonyl, which are rapidly exchanging with between the bridging/semi-bridging positions on the NMR timescale, as seen in a similar Rh/Os system.⁶⁹

Warming compound **39** to 0 °C results in its transformation to $[\text{Rh}_2(\text{CO})_2(\mu\text{-C}(\text{O})\text{CH}_3)(\text{depm})_2][\text{OTf}]$ (**39a**) by the migratory insertion of the CH_3 and a CO ligands, as outlined in Scheme 4.5. The ^1H NMR spectrum displays the methyl protons as a singlet with no observable coupling to phosphorus, and the $^{13}\text{C}\{^1\text{H}\}$ NMR spectrum displays a broad, downfield signal at δ 319.9, similar to its dppm counterpart,¹⁵ indicative of a bridging acetyl-moiety, as shown in Scheme 5. Unfortunately, compound **39a** readily decomposes above 0 °C, with the one product, $[\text{Rh}(\text{CO})_2(\mu\text{-OH})(\text{depm})_2][\text{OTf}]$ (**40**), resulting from reaction with adventitious H_2O . Compound **40** can be prepared in near quantitative yield by reacting **39** with water, resulting in the elimination of methane. The spectral parameters for **40** are as expected and are given in the Experimental section.

Attempts to produce the rhodium analogue of compound **32**, $[\text{Rh}_2(\text{CH}_3)(\text{CO})_2(\text{depm})_2][\text{OTf}]$, proved unsuccessful, with TMNO failing to react with compound **39** below -20 °C, while increasing the temperature to near 0 °C yields only **39a**, which is unreactive to TMNO below this temperature, while at higher temperatures the irreversible conversion to **40** and numerous unidentified decomposition products was observed. Our failure to remove a carbonyl is consistent with the lower lability of the carbonyl ligands in the presence of the smaller, more basic depm group. Also consistent with the more basic depm compared to dppm is the observation of the methyl complex **39**, the dppm analogue of which was not observed; the more basic depm groups disfavour migratory insertion owing to the resulting lower electrophilicity of the carbonyls, resulting from increased π back donation.

As observed in the Ir_2 analogue, the hydroxide-bridged Rh_2 complex (**40**) reacts with CO to produce the hydride-bridged complex, $[\text{Rh}_2(\text{CO})_3(\mu\text{-H})(\text{depm})_2][\text{OTf}]$ (**41-OTf**), which is also obtained as either the OTf^- or $\text{BAr}_4^{\text{F}-}$ salts by protonation of **37** by the appropriate acid, as shown in Scheme 4.5.

Compound **41** contains a symmetrically bridged hydride, as shown by the complex multiplet in the ^1H NMR at $\delta -10.34$ displaying couplings to both rhodium atoms ($^1J_{\text{RhH}} = 24.3$ Hz) and all four phosphorus nuclei ($^2J_{\text{HP}} = 12.2$ Hz). The $^{13}\text{C}\{^1\text{H}\}$ NMR spectrum displays three overlapped carbonyl signals at $\delta 194.3$, and upon cooling to -80 °C shows slight separation of the signal into two broad resonances in a 1:2 ratio; interestingly, the $^{13}\text{C}\{^1\text{H}\}$ chemical shifts for the bridging and terminal CO ligands do not differ significantly, much as observed earlier for the diiridium analogue.

An X-ray structure determination of **41** confirms the structure proposed, revealing a symmetrically bridged hydrido ligand with two terminal carbonyls and one bridging on the face opposite the hydride, as shown in Figure 4.3. The rhodium/rhodium separation ($\text{Rh}(1) - \text{Rh}(2) = 2.7613(3)$ Å) is significantly shorter than the non-bonding P–P distances within the diphosphine backbones ($\text{P}(1) - \text{P}(2) = 3.047(1)$, $\text{P}(3) - \text{P}(4) = 3.051(1)$ Å), indicating significant contraction along the Rh–Rh vector, consistent with a strong metal/metal interaction. Other crystallographic parameters are as expected, and are in close agreement to those reported for the dppm analogue, $[\text{Rh}_2(\text{CO})_3(\mu\text{-H})(\text{dppm})_2]^+$.²

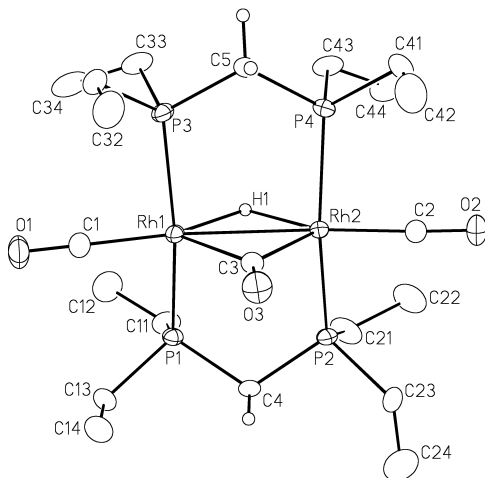
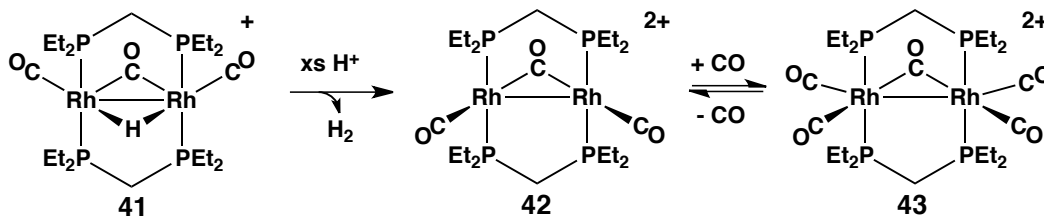


Figure 4.3 – Perspective view of the $[\text{Rh}_2(\text{CO})_2(\mu\text{-H})(\mu\text{-CO})(\text{dep})_2]^+$ (**41**) complex cation showing the atom labelling scheme. Thermal parameters are as described in Figure 1. Relevant bond distances (Å) and angles (°): $\text{Rh}(1) - \text{Rh}(2) = 2.7613(3)$; $\text{P}(1) - \text{P}(2) = 3.047(1)$; $\text{P}(3) - \text{P}(4) = 3.051(1)$; $\text{Rh}(1) - \text{C}(1) = 1.842(4)$; $\text{Rh}(1) - \text{C}(3) = 2.143(3)$; $\text{Rh}(2) - \text{C}(2) = 1.850(3)$; $\text{Rh}(2) - \text{C}(3) = 2.119(3)$; $\text{Rh}(1) - \text{C}(3) - \text{Rh}(2) = 80.8(1)$; $\text{P}(1) - \text{Rh}(1) - \text{P}(3) = 162.52(3)$; $\text{P}(2) - \text{Rh}(2) - \text{P}(4) = 163.54(3)$.

Compound **41** reacts with additional acid, producing the dicationic complex $[\text{Rh}_2(\text{CO})_3(\text{dep}m)_2]^{2+}$ (**42**), accompanied by H_2 evolution (Scheme 4.6), and this product uptakes two additional carbonyl ligands under a CO atmosphere to yield $[\text{Rh}_2(\text{CO})_5(\text{dep}m)_2]^{2+}$ (**43**), which readily reverts to **42** in the absence of CO. Both compounds **42** and **43** are fluxional at ambient temperatures, however the nature of the fluxionality was not investigated by low temperature NMR. Compound **43** is analogous to the diiridium complex, $[\text{Ir}_2(\text{CO})_4(\mu\text{-CO})(\text{dppm})_2]^{2+}$,⁷ which was shown to have fluxional behavior similar to that observed for **43** at ambient temperature.



Scheme 4.6 – Addition of excess acid to compound **41**.

The proposed structure for compound **43** has been confirmed crystallographically for the ditriflate salt, and is shown in the ORTEP representation of the cation in Figure 4.4. The structure shows a symmetrical arrangement of carbonyls with both metals having nearly identical geometries. The carbonyls oriented along the Rh–Rh bond have significantly shorter Rh–C distances (1.904(3), 1.924(3) Å) than those that are pseudo trans to the bridging carbonyl (1.992(3), 1.998(3) Å); the bridging carbonyl displays Rh–C bond lengths that are elongated relative to the terminal ligands and is unsymmetrically bound (Rh(1) – C(3) = 2.195(3) Å; Rh(2) – C(3) = 2.025(3) Å), presumably a result of non-bonding contacts involving the depm ethyl groups, which are in different orientations at each end of the depm ligands, as shown in Figure 4.4.

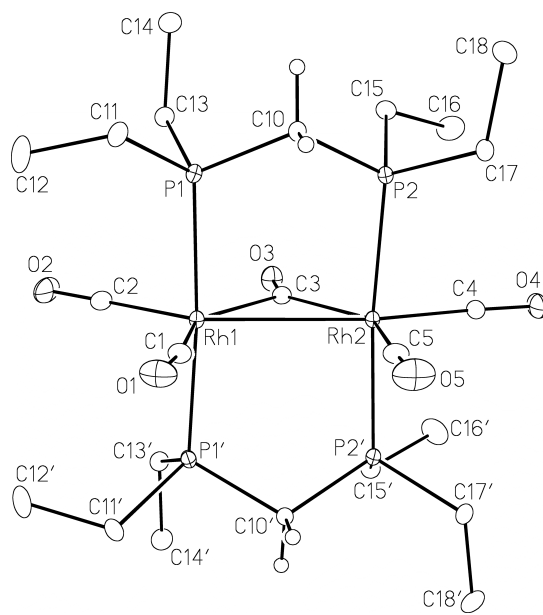
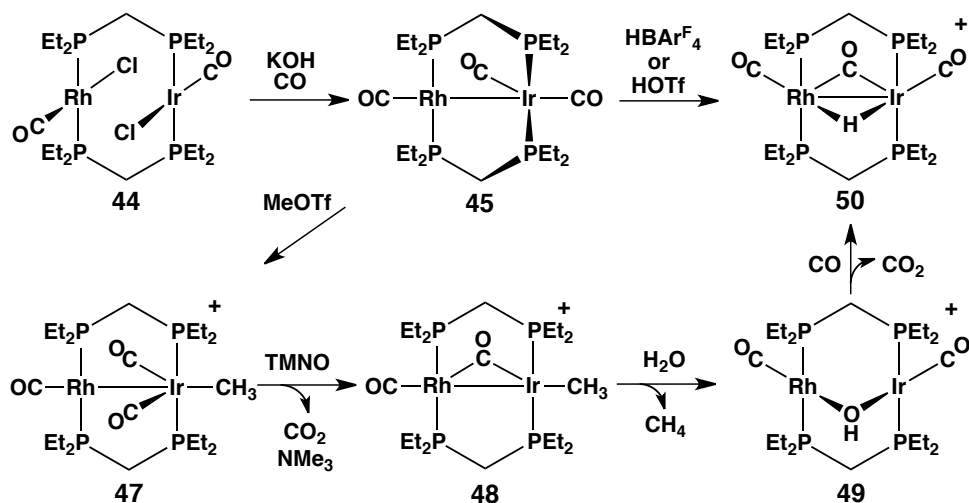


Figure 4.4 – Perspective view of the $[\text{Rh}_2(\text{CO})_4(\mu\text{-CO})(\text{dep})_2]^+$ (**43**) complex cation showing the atom labelling scheme. Thermal parameters are as described in Figure 4.1. Relevant bond distances (Å) and angles (°): $\text{Rh}(1) - \text{Rh}(2) = 2.8373(3)$; $\text{Rh}(1) - \text{C}(1) = 1.992(3)$; $\text{Rh}(1) - \text{C}(2) = 1.904(3)$; $\text{Rh}(1) - \text{C}(3) = 2.195(3)$; $\text{Rh}(2) - \text{C}(3) = 2.025(3)$; $\text{Rh}(2) - \text{C}(4) = 1.924(3)$; $\text{Rh}(2) - \text{C}(5) = 1.998(3)$; $\text{C}(1) - \text{Rh}(1) - \text{C}(2) = 117.2(1)$; $\text{C}(1) - \text{Rh}(1) - \text{C}(3) = 146.8(1)$; $\text{C}(2) - \text{Rh}(1) - \text{C}(3) = 96.0(1)$; $\text{C}(3) - \text{Rh}(2) - \text{C}(4) = 111.1(1)$; $\text{C}(3) - \text{Rh}(2) - \text{C}(5) = 141.6(1)$; $\text{C}(4) - \text{Rh}(2) - \text{C}(5) = 107.3(1)$.

4.2.3 Synthesis of iridium/rhodium complexes. The addition of depm to Vaska's complex, $[\text{IrCl}(\text{CO})(\text{PPh}_3)_2]$, followed by 0.5 equiv of $[\text{Rh}(\text{Cl})(\text{CO})_2]_2$ produces a dark orange solution of *trans*- $[\text{IrRhCl}_2(\text{CO})_2(\text{dep})_2]$ (**44**). As is the case with related dppm-bridged mixed-metal Ir/Rh systems, the $^{31}\text{P}\{^1\text{H}\}$ NMR displays two signals, corresponding to a AA'BB'X spin system, with the downfield signal displaying rhodium coupling along with the expected phosphorus coupling while the upfield signal, corresponding to the iridium-bound phosphines, shows only phosphorus coupling. All other spectral parameters for compound **44** closely match those already discussed for compounds **26** and **36**.



Scheme 4.7 – *Synthesis of mixed-metal rhodium/iridium bis(diethylphosphino)methane complexes.*

As with the homobimetallic analogues, compound **44** is readily reduced (Scheme 4.7), producing a 1:1 mixture of the neutral tricarbonyl and tetracarbonyl compounds, [IrRh(CO)₃(depm)₂] (**45**) and [IrRh(CO)₄(depm)₂] (**46**), upon the addition of aqueous KOH under a CO atmosphere. A CO purge converts **45** to **46** (Scheme 4.2), while **46** reverts to **45** in the absence of a CO atmosphere. At ambient temperature, the NMR spectra of compound **45** differs from those of its homobimetallic congeners, displaying two signals in the ³¹P{¹H} NMR spectrum, while the ¹³C{¹H} NMR spectrum shows two signals – a triplet at δ 190.2 (2C) and a doublet of triplets at δ 185.7 (1C); the additional coupling of the latter signal is due to rhodium. Interestingly, cooling to –80 °C shows separation of the downfield signal in the ¹³C{¹H} NMR spectrum into two broad singlets at δ 192.6 (1C) and 188.9 (1C), while the upfield signal remains unchanged. Although there is no evidence of exchange of the Rh- and Ir-bound carbonyls, the pair of Ir-bound carbonyls are exchanging, presumably accompanied by movement of the Ir-bound ends of the diphosphines from above the plane of the drawing in Scheme 7 to below.

At ambient temperature **46** displays broad resonances in the ³¹P{¹H}, ¹H, and ¹³C{¹H} NMR spectra, however cooling to –80 °C yields two sharp signals in the ³¹P{¹H} spectrum, and four carbonyl resonances in the ¹³C{¹H} spectrum, the

two downfield signals of which display additional coupling to rhodium ($^1J_{\text{CRh}} = 73.5 \text{ Hz}, 72.4 \text{ Hz}$). We propose a structure for **46** similar to the homobimetallic analogues, and analogous to the diiridium dmpm structure reported by Reinking.⁶⁶

Addition of MeOTf to **45** yields $[\text{IrRh}(\text{CH}_3)(\text{CO})_3(\text{depn})_2][\text{OTf}]$ (**47**), as shown in Scheme 4.7, resembling the dirhodium analogue (**39**) in which the methyl group remains intact, and in contrast to the Ir_2 analogue which undergoes intramolecular C–H activation to give the methylene/hydride compound (**29**). Unlike compound **39**, which contains two *symmetrically* bridging CO's, only one carbonyl shows coupling to rhodium, suggesting that the other two carbonyls are bound solely to iridium.

An X-ray structure confirms the proposed geometry for **47** (Figure 4.5), although the structure is disordered such that the metals are found to have 60/40 occupancy across the two sites (refer to the Experimental Section for an overlapped view of disorder). The relatively long Rh(A) – C(2A) and Rh(A) – C(3A) distances (2.695 and 2.706 Å) and the close-to-linear Ir(A) – C(2A) – O(2A) and Ir(A) – C(3A) – O(3A) angles (175(1)°, 170(4)°) indicate that any interaction with rhodium is weak, consistent with the absence of Rh coupling in the $^{13}\text{C}\{^1\text{H}\}$ NMR spectrum.

Compound **47** reacts with TMNO to give the dicarbonyl complex, $[\text{IrRh}(\text{CH}_3)(\text{CO})_2(\text{depn})_2][\text{OTf}]$ (**48**; Scheme 4.7), in which the methyl group remains terminally-bound to iridium, as demonstrated by $^1\text{H}\{^{31}\text{P}\}$ and $^{13}\text{C}\{^1\text{H}\}$ experiments; in particular, absence of rhodium coupling in the $^{13}\text{CH}_3$ resonance confirms its binding to Ir. Two equal intensity carbonyl signals are observed in the $^{13}\text{C}\{^1\text{H}\}$ NMR spectrum, with only the upfield signal displaying coupling to rhodium, suggesting two terminal carbonyls with one on each metal. Unfortunately, compound **48** is transient and within 30 min decomposes to $[\text{IrRh}(\text{CO})_2(\mu\text{-OH})(\text{depn})_2][\text{OTf}]$ (**49**), again due to adventitious water.

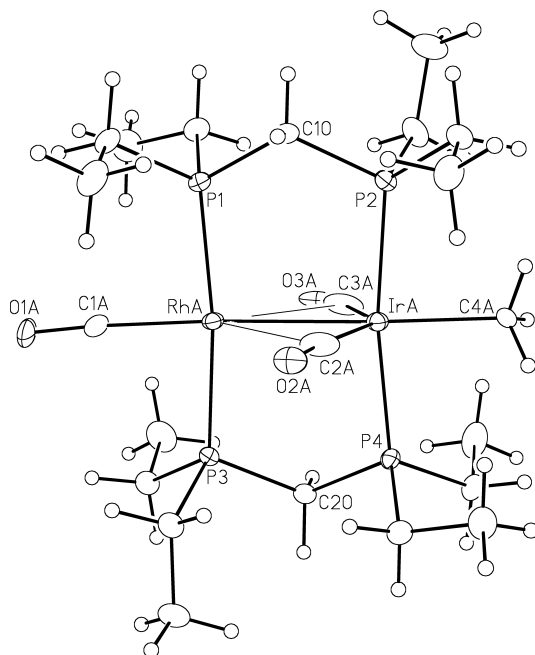
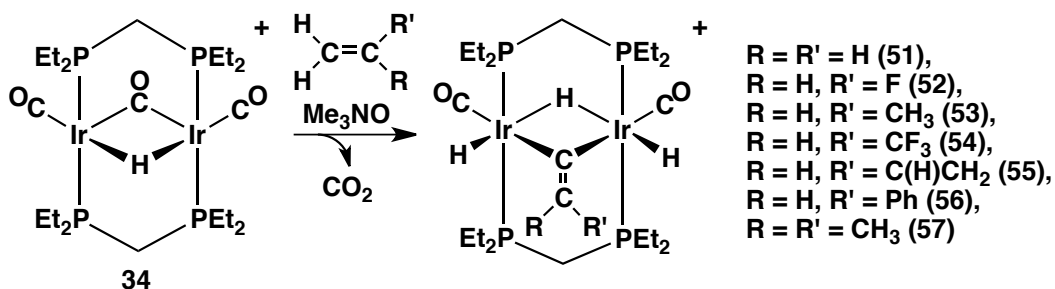


Figure 4.5 – Perspective view of the $[\text{RhIrMe}(\text{CO})_3(\text{depm})_2]^+$ cation (**47**) showing the atom labelling scheme. Only the major orientation of the disordered “ $\text{RhIr}(\text{CO})_3(\text{CH}_3)$ ” fragment (IrA , RhA , O1A , O2A , O3A , C1A , C2A , C3A , C4A) is shown. Thermal parameters are as described in Figure 4.1. Hydrogen atoms are shown with arbitrarily small thermal parameters. Relevant bond distances (\AA) and angles ($^\circ$) for the major orientation: $\text{Ir}(\text{A}) - \text{Rh}(\text{A}) = 2.7278(7)$; $\text{Ir}(\text{A}) - \text{C}(\text{4A}) = 2.10(2)$; $\text{Rh}(\text{A}) - \text{C}(\text{1A}) = 1.93(2)$; $\text{Ir}(\text{A}) - \text{C}(\text{2A}) = 1.95(1)$; $\text{Ir}(\text{A}) - \text{C}(\text{3A}) = 2.02(2)$, $\text{Rh}(\text{A}) - \text{C}(\text{2A}) = 2.695$; $\text{Rh}(\text{A}) - \text{C}(\text{3A}) = 2.706$; $\text{Ir}(\text{A}) - \text{Rh}(\text{A}) - \text{C}(\text{1A}) = 173.3(9)$; $\text{Rh}(\text{A}) - \text{Ir}(\text{A}) - \text{C}(\text{4A}) = 177.6(9)$; $\text{Ir}(\text{A}) - \text{C}(\text{2A}) - \text{O}(\text{2A}) = 175(1)$; $\text{Ir}(\text{A}) - \text{C}(\text{3A}) - \text{O}(\text{3A}) = 170(4)$.

Compound **49** is readily converted to $[\text{IrRh}(\text{CO})_3(\mu\text{-H})(\text{depm})_2][\text{OTf}]$ (**50-OTf**) upon the addition of a CO purge, or by protonation of **45** (refer to Scheme 4.7). As for the homobimetallic congeners, the hydride ligand appears to be symmetrically bridging the two metals, displaying coupling to all four phosphorus nuclei ($^2J_{\text{HP}} = 9.8$ Hz) and to rhodium ($^1J_{\text{HRh}} = 21.1$ Hz).

4.2.4 Geminal C–H activation of olefins. Compound **34** reacts with a variety of α -olefins (ethylene, vinylfluoride, propylene, 3,3,3-trifluoropropene, 1,3-butadiene, and styrene) under a variety of conditions to give the vinylidene-bridged trihydride products $[\text{Ir}_2(\text{H})_2(\text{CO})_2(\mu\text{-H})(\mu\text{-C}=\text{CRR}')(\text{depm})_2][\text{BAR}^{\text{F}}_4]$ ($\text{R} = \text{R}' = \text{H}$ (**51**); $\text{R} = \text{H}$, $\text{R}' = \text{F}$ (**52**); $\text{R} = \text{H}$, $\text{R}' = \text{CH}_3$ (**53**); $\text{R} = \text{H}$, $\text{R}' = \text{CF}_3$ (**54**); $\text{R} = \text{H}$, $\text{R}' = \text{C}(\text{H})\text{CH}_2$ (**55**); $\text{R} = \text{H}$, $\text{R}' = \text{C}_6\text{H}_5$ (**56**)), in which a pair of geminal C–H

bonds in the α -olefin have been cleaved. Although most of the above reactions take place over the course of several hours at ambient temperature, the reaction with styrene required elevated temperatures (40 °C) for several days, while the reaction with vinyl fluoride yielded **52** in only 10% yield (the major product resulting from C–F bond activation).⁷⁰ However, all products (**51** – **56**) were obtained in a fraction of the time (10 – 30 min) at ambient temperature upon the addition of TMNO to solutions of **34** and the olefin (Scheme 4.8). In addition, isobutylene, which was unreactive with **34**, yielded the dimethylvinylidene-bridged product $[\text{Ir}_2(\text{H})_2(\text{CO})_2(\mu\text{-H})(\mu\text{-C}=\text{CMe}_2)(\text{depm})_2][\text{BAR}^{\text{F}}_4]$ (**57**) in 30 min upon reaction with TMNO, and the fluorovinylidene-bridged **52** was obtained as the sole product upon inclusion of TMNO. The activation of a pair of geminal C–H bonds in α -olefins has precedent, but is not common.^{42,57-64} In attempts to obtain a difluorovinylidene analogue, **34** was exposed to 1,1-difluoroethylene in the presence of TMNO, however decomposition to numerous unidentified products was observed, with no indication of geminal C–H activation occurring.



Scheme 4.8 – Geminal C–H bond activation of α -olefins by compound **34**.

Compounds **51** and **57** each display a singlet in their $^3\text{1P}\{^1\text{H}\}$ NMR spectra due to the symmetrical nature of each bridging vinylidene unit, while compounds **52** – **56**, formed from the unsymmetrical α -olefins ($\text{R} \neq \text{R}'$), display two multiplets as a result of the unsymmetrical vinylidene group producing asymmetry at the two metals. These symmetry differences are also evident in the ^1H NMR spectra with two hydride signals, in a 2:1 ratio, for the two symmetric products (**51** and **57**), while compounds **52** – **56** each show three hydride signals

(two relatively downfield signals for the terminal hydrides and an upfield signal arising from the bridging hydride). Interestingly, no *trans* H–H coupling between the bridging and terminal hydrides is observed in any of these species; similarly, the analogous vinylvinylidene-bridged/dppm species, which was crystallographically characterized,⁴² also did not exhibit this coupling. However, the non-symmetric compounds (**52** – **56**) display long-range coupling between the two terminal hydrides, typically on the order of 9.0 Hz. Compounds **51** and **57** display a single proton resonance for the vinylidene moiety – a singlet for the vinylidene hydrogens at δ 6.57 for compound **51**, and a singlet for the methyl protons at δ 1.40 for compound **57**. The bridging fluorovinylidene unit (**52**) shows a doublet ($^2J_{\text{HF}} = 108.2$ Hz) at δ 6.61 in the ^1H NMR spectrum, with a matching doublet found at δ –72.1 in the ^{19}F NMR spectrum, while the bridging trifluoromethylvinylidene moiety shows no coupling between the proton and fluorines, each appearing as singlets in their ^1H and ^{19}F NMR spectra. The vinylvinylidene unit in **55**, formed from the double C–H activation of 1,3-butadiene, displays four proton resonances at δ 6.82, 6.28, 4.93 and 4.82, all showing mutual couplings ($^3J_{\text{HHvicinal}} = 9.9$ Hz, $^3J_{\text{HHcis}} = 9.9$ Hz, $^3J_{\text{HHtrans}} = 17.1$ Hz) that are in close agreement to the values reported for $[\text{Ir}_2(\text{CH}_3)(\text{H})(\text{CO})_2(\mu\text{-H})(\mu\text{-C}=\text{C}(\text{H})\text{C}(\text{H})=\text{CH}_2)(\text{dppm})_2]^+$ ($^3J_{\text{HHvicinal}} = 10.0$ Hz, $^3J_{\text{HHcis}} = 10.0$ Hz, $^3J_{\text{HHtrans}} = 16.5$ Hz).⁴² Finally, the $^{13}\text{C}\{^1\text{H}\}$ NMR spectra display a single carbonyl resonance for the symmetric complexes while the non-symmetric compounds each show two signals. Although we were unsuccessful in obtaining X-ray structures of these vinylidene species, their spectroscopy clearly defines the geometry of products; in particular, the spectroscopic parallels between compound **55** and the crystallographically determined dppm analogue convincingly support the proposed structure.

Labelling the bridging hydride position in the starting material (**9**) with deuterium (**34-D**) proved to be challenging due to its propensity for H/D exchange with adventitious water remaining from earlier transformations. However, the addition of D_2O to **34** gave conversion to **34-D** and **34** in a 4:1 ratio after 24 h. Repeating the experiment shown in Scheme 4.8 with **34-D** as the reactant results

in exclusive deuterium labelling in the bridging hydride position of the products, with no incorporation into the terminal hydride sites. The lone exception is the reaction of **34-D** with ethylene, which shows scrambling of deuterium across all three hydride sites along with deuterium incorporation into the bridging vinylidene ligand. This is presumably the result of ethylene insertion into the Ir–D bond of **34-D** and is confirmed by the reaction of **34** with 1,1-dideuteroethylene ($D_2C=CH_2$), which also shows deuterium scrambling across all hydride and vinylidene positions of **51**, however repeating this reaction in the presence of TMNO produces a mixture of isomers in which the original hydride ligand is found exclusively in the bridging position, indicating geminal C–H bond activation occurs at a rate much faster than insertion once a CO ligand is removed.

Attempts to bring about geminal C–H activation of the above α -olefins in reactions with $[MM'(CO)_3(\text{dep}m)_2]$ ($M = M' = \text{Ir}$ (**27**), Rh (**37**); $M = \text{Rh}$, $M' = \text{Ir}$ (**45**)) gave no reaction over a range of conditions, even in the presence of TMNO. Similarly, neither $[\text{RhIr}(CO)_3(\mu\text{-H})(\text{dep}m)_2]^+$ (**50**) nor $[\text{Rh}_2(CO)_3(\mu\text{-H})(\text{dep}m)_2]^+$ (**41**) react with these olefins, either in the presence or absence of TMNO. Furthermore, attempts to react the dppm species, $[\text{Ir}_2(CO)_3(\mu\text{-H})(\text{dpp}m)_2]^+$ with the above α -olefins under identical conditions yielded only starting materials.

4.3 Discussion

As noted in the Introduction of this Chapter, the advantages of depm over dmpm in this chemistry is that although both bridging groups contain small alkyl substituents that result in greater basicity over the more commonly used dppm ligand, and better substrate access to the metals, the depm chemistry is much better behaved than that of dmpm, allowing rational modifications to the well studied dppm system. The parallels between depm and dppm are clearly seen in the similarities between the series of Ir_2 , Rh/Ir and Rh_2 complexes involving both diphosphines, as described earlier. Nevertheless, substituting dppm by depm has had the targeted effect on the reactivity and the depm complexes are much more

reactive than the dppm analogues. One unfortunate consequence of this is the reactivity of the methyl dicarbonyl species $[\text{MM}'(\text{CH}_3)(\text{CO})_2(\text{dep}m)_2]^+$ ($\text{MM}' = \text{Ir}_2$ (**32**) and RhIr (**48**)) with adventitious water, resulting in hydrolysis of these species to hydroxide-bridged products accompanied by methane elimination. Although none of the precautions taken in this Chapter to minimize water were taken in previous studies with dppm,^{7,15,18,25} the analogous dppm complexes showed no adverse effects of water; in fact the dppm complexes were stable to the deliberate addition of water. In any future attempts to study the methyl dicarbonyl complexes, other methods for reduction of the dihalide precursors to $[\text{MM}'(\text{CO})_3(\text{dep}m)_2]$ ($\text{MM}' = \text{Ir}_2$ (**26**), Rh_2 (**36**), RhIr (**45**)) and the use of scrupulously dried TMNO or other methods for carbonyl removal will have to be employed, since subsequent water removal is problematic.

Addition of methyl triflate to the complexes $[\text{MM}'(\text{CO})_3(\text{dep}m)_2]$ ($\text{MM}' = \text{Ir}_2$ (**26**), Rh_2 (**36**), RhIr (**45**)) led to reactivity which very much paralleled that of the dppm analogues with some minor variations. As a consequence, both depm and dppm Ir_2 systems gave rise to C–H activation of the added methyl group at the pair of adjacent Ir centres, consistent with the greater tendency of the third-row metal for oxidative addition. In the Rh/Ir complexes involving either dppm or depm, the methyl group binds to Ir, having the stronger metal-carbon bond, and although we had considered the possibility of C–H activation by Rh in the depm system, as a consequence of the greater basicity of this ligand, this was not observed. Similarly in the Rh_2 systems, both depm and dppm systems yielded the acetyl product – the result of facile migratory insertion at this metal. However, here the greater basicity of depm over dppm was clearly evident in two ways. First, although the methyl tricarbonyl product was never observed in the dppm chemistry, this precursor to migratory insertion was observed with depm – presumably owing to the lower electrophilicity of the carbonyls in this more electron-rich system, which inhibits migratory insertion. In addition, although a carbonyl could be removed from the acyl-bridged dicarbonyl under reflux in the dppm system,¹⁵ we were unable to remove a carbonyl in the depm analogue, consistent with the increased π -back donation in this species (of course in the

dep_m complex its instability did not allow refluxing, and only TMNO addition was attempted).

However, the most significant consequence of replacement of dp_{pm} by dep_m is seen in the reactivity of $[\text{Ir}_2(\text{CO})_3(\mu\text{-H})(\text{dep}_m)_2]^+$ with α -olefins. Although the analogous dp_{pm} complex is inert to α -olefins under the conditions investigated, even in the presence of TMNO, this dep_m complex reacts readily with a number of α -olefins to give the corresponding vinylidene-bridged trihydride products from activation of the pair of geminal C–H bonds on the olefin. Furthermore, in the presence of TMNO these activations are extremely facile, requiring only minutes for completion at ambient temperature. Few examples of this type of reactivity are known^{42,57-64} and this system represents (by far) the most reactive system to date, reacting under very mild conditions with a number of α -olefins.

Although C–H bond activation in unsaturated substrates by mononuclear species can proceed via prior π -coordination of the substrate, Bergman *et al.* have demonstrated that this is not always necessary. In binuclear complexes a third mechanism that essentially combines these two mononuclear pathways, is also possible, whereby π -coordination at one metal positions the olefin for σ -complex formation with the adjacent metal, leading to C–H bond cleavage,⁷¹ as shown in structure **B** in Chart 4.1. Rotation of the resulting vinyl group (structure **C** \rightarrow **D**) about the metal-carbon bond can then give a vinyl orientation that allows the second metal to be involved in an agostic interaction with the second olefinic C–H bond, leading to the second activation. Although the involvement of the second metal in the second activation step seems clear, initial coordination of the olefin at one metal (structure **A**) preceding C–H activation at the adjacent metal is more speculative.

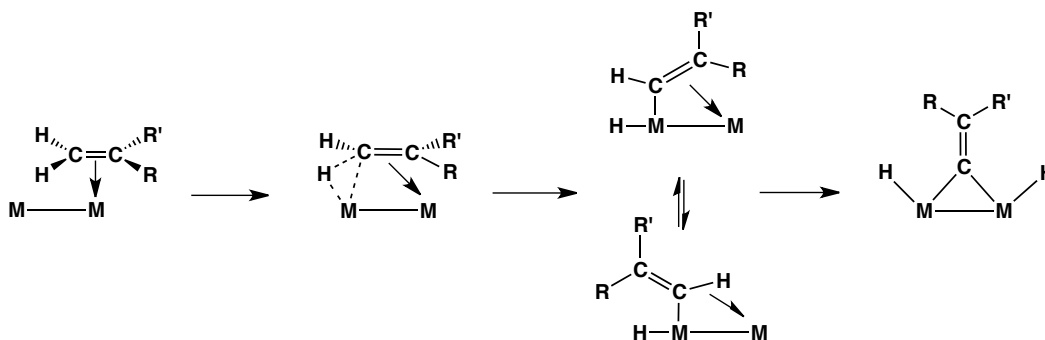


Chart 4.1 – *Proposed mechanism for geminal C–H activation of an olefin by a bimetallic complex.*

We had hoped that the increased reactivity noted above in the “Ir₂(dep_m)₂” system over that of “Ir₂(dpp_m)₂” might also be reflected in the chemistry of the Rh-containing congeners, either in allowing C–H activation at this metal or at least in allowing the Rh-containing species to model key intermediates in the double C–H activation observed for the Ir₂ system. Even in the event that the Rh centre was unreactive towards C–H activation, we anticipated that the mixed-metal species, [RhIr(CO)₃(μ-H)(dep_m)₂]⁺ (**41**; particularly in the presence of TMNO) might still result in a single C–H activation at Ir, allowing us to obtain information about the first C–H activation product. Furthermore, we anticipated that although unreactive to C–H bond cleavage, the Rh₂ systems might yield an olefin adduct, giving information about the adduct prior to C–H activation. Unfortunately, none of this is observed with the least encumbered olefin, ethylene. Although this is surprising and disappointing, it does demonstrate the cooperative nature of these activations, whereby the proximity of the unreactive Rh also deactivates the Ir centre to oxidative addition. This lack of reactivity may in fact support the “prior coordination” model whereby C–H activation at Ir requires prior coordination at Rh, which is apparently not effective enough in this role.

The steric differences between dpp_m and dep_m are evident in the range of olefins activated by the dep_m system, in which even the disubstituted isobutylene and the bulky styrene react readily in the presence of TMNO. Finally, this study reaffirms the pronounced synergistic effect that two metal centres can have in

giving rise to reactivity that is not commonly observed in single metal complexes. This example of *geminal* C–H activation of olefins represents only the fifth example of its kind,^{42,57-62,64,72,73} and appears to be the most reactive; requiring only TMNO addition to initiate facile activation, and being reactive for a range of α -olefins – even those having reasonably bulky substituents.

4.4 Experimental

4.4.1 General Comments.

All solvents were dried (using appropriate drying agents), distilled before use and stored under dinitrogen. Deuterated solvents used for NMR experiments were freeze-pump-thaw degassed (three cycles) and stored under nitrogen or argon over molecular sieves. Reactions were carried out under argon using standard Schlenk techniques, and compounds that were obtained as solids were purified by recrystallization. Prepurified argon and nitrogen were purchased from Praxair, and carbon-13 enriched CO (99%) was supplied by Isotec Inc. All purchased gases were used as received. *Bis*(diethylphosphino)methane,^{74,75} [IrCl(COD)]₂,⁷⁶ [IrCl(CO)(PPh₃)₂],⁷⁷ [RhCl(COD)]₂,⁷⁸ [RhCl(CO)₂]₂,⁷⁹ and [H(Et₂O)₂][B(3,5-(CF₃)₂C₆H₃)₄] (HBAr^F₄)⁸⁰ were all prepared as previously described. Trimethylamine-*N*-oxide dihydrate was dried by azeotropic distillation as described in literature.⁶⁸ All other reagents were obtained from Aldrich and were used as received (unless otherwise stated).

Proton NMR spectra were recorded on Varian Unity 400 or 500 spectrometers, or on a Bruker AM400 spectrometer. Carbon-13 NMR spectra were recorded on Varian Unity 400 or 500 or Bruker AM300 spectrometers. Phosphorus-31 and fluorine-19 NMR spectra were recorded on Varian Unity 400 or 500 or Bruker AM400 spectrometers. Two-dimensional NMR experiments (COSY, NOESY and ¹H–¹³C HMQC) were obtained on Varian Unity 400 or 500 spectrometers.

4.4.2 Preparation of Compounds

- (a) ***trans*-[Ir₂Cl₂(CO)₂(depm)₂] (26).** To a solution of [Ir(Cl)(COD)]₂ (200 mg, 0.30 mmol) in 25 mL of dichloromethane was quickly added, via cannula, 100 μ L (0.60 mmol) of *bis*(diethylphosphino)methane (depm) in 5 mL of dichloromethane, causing the solution to change from orange/red to yellow/orange. The solution was stirred for 15 min and then placed under a slow CO purge for 5 min. The CO was replaced by an argon purge and the solution was set to reflux for ½ h. Reducing the solution to dryness left an oily orange residue, which was redissolved into 25 mL of THF. This solution was set to reflux again for 1½ h, with a continuing argon purge, resulting in a color change to dark red/purple. The solution was reduced to ~5 mL and Et₂O (40 mL) was added to precipitate a deep red-purple solid, which was isolated, washed twice with Et₂O (2x10 mL) and dried to yield 150 mg (60 %) of **26**. HRMS *m/z* calcd for Ir₂P₄O₂C₂₀H₄₄Cl: 860.3804. Found: 860.3805. ¹H NMR (400 MHz, CD₂Cl₂, 27 °C): δ = 2.52 (quin, 4H, depm); ¹³C{¹H} NMR (101 MHz, CD₂Cl₂, 27 °C): δ = 168.3 (s, 2C, Ir-CO); ³¹P{¹H} NMR (162 MHz, CD₂Cl₂, 27 °C): δ = 8.3 (s, 4P), Elemental analysis calcd (%) for Ir₂P₄Cl₂O₂C₂₀H₄₄ (895.80): C 26.82, H 4.95; found: C 26.87, H, 5.02.
- (b) **[Ir₂(CO)₃(depm)₂] (27).** **Method i)** 100 mg (0.090 mmol) of **26** was dissolved in 10 mL of THF giving a turbid, deep scarlet-purple solution. This was placed under an atmosphere of CO resulting in a series of color changes, through red, and finally to clear orange. The addition of 2.5 mL of 1 M KOH/H₂O yielded a dark orange solution, which was stirred (closed under CO) at room temperature for ½ h. The solution was stripped to dryness, extracted with 3 x 10 mL of benzene and filtered through celite. A further 50 mL of benzene was added and the resulting solution was distilled for 2 h to remove residual water by azeotropic distillation, after which time it could be carried forward as such, or stripped again to dryness to give a dark brown-orange residue. (98 %). **Method ii)**

Compound **26** (54 mg, 0.049 mmol) was dissolved in 10 mL of acetone. Excess NaBH₄ (0.200 mmol) was added directly to the solution, which was allowed to stir for 1 h. The solvent was removed and the product redissolved in 10 mL of benzene. Filtration through celite gave a clear orange-brown solution, which was purged with CO for 5 min followed by argon for 10 min. The solvent was reduced to dryness, affording the complex as a viscous orange-brown oil. However, samples obtained via this method were always less pure, spectroscopically, and were generally obtained in poorer yields compared to the first method. **Method iii)** Compound **26** (30 mg, 0.027 mmol) was dissolved in 20 mL of acetonitrile. Excess zinc (0.500 mmol) was added directly to the solution, producing a grey slurry which was allowed to stir for 1 h under a CO purge. The mixture was filtered through celite and the clear orange solution was reduced to dryness under vacuum. The residue was redissolved in CD₂Cl₂ and the purity of the product was verified by NMR spectroscopy. This method also resulted in a product that is less pure, spectroscopically, and generally in poorer yields compared to the first method. Due to compound **27** not being isolated as a solid, an elemental analysis could not be obtained, however ³¹P{¹H} and ¹H NMR spectra showing the purity can be found in the Supporting Information. ¹H NMR (400 MHz, C₆D₆, 27 °C): δ = 2.67 (quin., 4H, depm); ¹³C{¹H} NMR (101 MHz, C₆D₆, 27 °C): δ = 185.6 (s, 3C, Ir-CO); ³¹P{¹H} NMR (162 MHz, C₆D₆, 27 °C): δ = -11.0 (s, 4P); Low Temperature Data: ¹³C{¹H} NMR (101 MHz, CD₂Cl₂, -80 °C): δ = 193.8 (bs, 1C, Ir-CO), 189.3 (bs, 1C, Ir-CO), 179.8 (bs, 1C, Ir-CO); ³¹P{¹H} NMR (162 MHz, CD₂Cl₂, -80 °C): δ = -8.9 (b, 2P), -28.0 (b, 2P).

- (c) **[Ir₂(CO)₄(dep_m)₂] (28).** Compound **27** (50 mg, 0.058 mmol) was dissolved in 10 mL of benzene and stirred under a dynamic atmosphere of CO for ½ h, causing the color to change from orange to bright yellow. The solvent was removed, giving an oily, dark yellow-orange residue

containing a mixture of **27** and **28** in variable proportions, as gauged by NMR spectroscopy, revealing the susceptibility of **28** to CO loss. The lability of this carbonyl has limited the characterization to NMR spectroscopy. ^1H NMR (400 MHz, CD_2Cl_2 , 27 °C): δ = 2.71 (quin., 4H, depm); $^{13}\text{C}\{^1\text{H}\}$ NMR (101 MHz, CD_2Cl_2 , 27 °C): δ = 189.8 (bs, 4C, Ir–CO); $^{31}\text{P}\{^1\text{H}\}$ NMR (162 MHz, CD_2Cl_2 , 27 °C): δ = –31.4 (bs, 4P); Low Temperature Data: $^{13}\text{C}\{^1\text{H}\}$ NMR (101 MHz, CD_2Cl_2 , –80 °C): δ = 195.2 (bs, 1C, Ir–CO), 194.2 (bs, 1C, Ir–CO), 191.8 (bs, 1C, Ir–CO), 181.2 (bs, 1C, Ir–CO); $^{31}\text{P}\{^1\text{H}\}$ NMR (162 MHz, CD_2Cl_2 , –80 °C): δ = –19.6 (bt, 2P, $^2J_{\text{PP}}$ = 53.7 Hz), –41.1 (bt, 2P, $^2J_{\text{PP}}$ = 53.7 Hz).

- (d) **$[\text{Ir}_2(\text{H})(\text{CO})_3(\mu\text{-CH}_2)(\text{depM})_2][\text{CF}_3\text{SO}_3]$ (**29**).** 11 μL (1.00 mmol) of neat methyl trifluoromethanesulphonate (MeOTf) was slowly added dropwise to a solution of **27** (75 mg, 0.088 mmol) in 15 mL of benzene. The resulting turbid, dark orange mixture was stirred for 1 h whereupon it was reduced to ~2 mL, followed by the dropwise addition of pentane (10 mL) to precipitate a yellow-orange solid. This solid was further washed with pentane (2 x 10 mL) and dried giving 80 mg of pale orange powder (89 % yield). HRMS m/z calcd for $\text{Ir}_2\text{P}_4\text{O}_3\text{C}_{22}\text{H}_{47}$: 867.9729. Found: 867.9732. ^1H NMR (400 MHz, CD_2Cl_2 , 27 °C): δ = 3.95 (bs, 2H, Ir– CH_2 –Ir), 2.75 (m, 4H, depm), –12.42 (t, 1H, $^2J_{\text{HP}}$ = 4.3 Hz); $^{13}\text{C}\{^1\text{H}\}$ NMR (101 MHz, CD_2Cl_2 , 27 °C): δ = 177.2 (s, 3C, Ir–CO), 44.2 (m, 1C, Ir– CH_2 –Ir); $^{31}\text{P}\{^1\text{H}\}$ NMR (162 MHz, CD_2Cl_2 , 27 °C): δ = –8.9 (bm, 2P), –19.5 (bm, 2P); Low Temperature Data: $^{13}\text{C}\{^1\text{H}\}$ NMR (101 MHz, CD_2Cl_2 , –80 °C): δ = 180.2 (bs, 1C, Ir–CO), 178.7 (bs, 1C, Ir–CO), 166.3 (bs, 1C, Ir–CO), 45.3 (m, 1C, Ir– CH_2 –Ir); $^{31}\text{P}\{^1\text{H}\}$ NMR (162 MHz, CD_2Cl_2 , –80 °C): δ = –8.9 (t, 2P, $^2J_{\text{PP}}$ = 32.4 Hz), –19.5 (t, 2P, $^2J_{\text{PP}}$ = 32.4 Hz). Elemental analysis calcd (%) for $\text{Ir}_2\text{SP}_4\text{F}_3\text{O}_6\text{C}_{23}\text{H}_{47}$ (1017.00): C 27.16, H 4.66; found: C 26.82, H, 4.55.

- (e) $[\text{Ir}_2(\text{CH}_3)(\text{CO})_4(\text{depm})_2][\text{CF}_3\text{SO}_3]$ (**30**) and $[\text{Ir}_2(\text{CO})_4(\text{C}(\text{O})\text{CH}_3)(\text{depm})_2][\text{CF}_3\text{SO}_3]$ (**31**). Excess carbon monoxide (3 mL, 0.131 mmol) was transferred via gas-tight syringe onto a solution of 50 mg (0.037 mmol) of compound **28** in 0.7 mL of CD_2Cl_2 . Under these conditions both complexes were identified and characterized through NMR spectroscopy. However, we were unable to isolate either compound due to the regeneration of **28** upon the removal of the CO atmosphere. Compound **30**: ^1H NMR (400 MHz, CD_2Cl_2 , 27 °C): $\delta = 2.75$ (quin., 4H, depm), 0.68 (t, $^3J_{\text{HP}} = 5.4$ Hz, Ir- CH_3); $^{13}\text{C}\{^1\text{H}\}$ NMR (101 MHz, CD_2Cl_2 , 27 °C): $\delta = 191.1$ (t, 2C, $^2J_{\text{CP}} = 11.2$ Hz, Ir-CO), 187.4 (t, 2C, $^2J_{\text{CP}} = 12.9$ Hz, Ir-CO), -39.9 (t, 1C, $^2J_{\text{CP}} = 5.8$ Hz, Ir- CH_3); $^{31}\text{P}\{^1\text{H}\}$ NMR (162 MHz, CD_2Cl_2 , 27 °C): $\delta = -14.9$ (m, 2P), -18.6 (m, 2P). Compound **31**: ^1H NMR (400 MHz, CD_2Cl_2 , 27 °C): $\delta = 3.35$ (quin., 4H, depm), 2.60 (s, 3H, Ir-C(O) CH_3); $^{13}\text{C}\{^1\text{H}\}$ NMR (101 MHz, CD_2Cl_2 , 27 °C): $\delta = 221.2$ (t, 1C, $^2J_{\text{CP}} = 6.3$ Hz, Ir-C(O) CH_3), 195.0 (t, 2C, $^2J_{\text{CP}} = 10.3$ Hz, Ir-CO), 187.8 (t, 2C, $^2J_{\text{CP}} = 12.9$ Hz, Ir-CO), 53.2 (m, 1C, Ir-C(O) CH_3); $^{31}\text{P}\{^1\text{H}\}$ NMR (162 MHz, CD_2Cl_2 , 27 °C): $\delta = -15.7$ (m, 2P), -20.9 (m, 2P).
- (f) $[\text{Ir}_2(\text{CH}_3)(\text{CO})_2(\text{depm})_2][\text{CF}_3\text{SO}_3]$ (**32**). To a solution of compound **28** (55 mg, 0.63 mmol) in 0.5 mL of CD_2Cl_2 was added, drop-wise, trimethylamine-*N*-oxide (TMNO) (4 mg, 0.53 mmol) in 0.3 mL of CD_2Cl_2 . The resulting solution was mixed and the reaction was monitored via NMR. The product was found to be extremely moisture-sensitive, and was susceptible to further reaction in solution, at ambient temperature, resulting in the formation compound **33** after 30 min. Therefore, compound **32** was characterized via solution spectroscopy, through comparison of its spectral parameters to those of its dppm analogue $[\text{Ir}_2(\text{CH}_3)(\text{CO})_2(\text{dppm})_2][\text{CF}_3\text{SO}_3]$.¹⁸ ^1H NMR (400 MHz, CD_2Cl_2 , 27 °C): $\delta = 2.80$ (m, 2H, depm), 2.30 (dm, 2H, depm), 0.57 (quin., 3H, $^3J_{\text{HP}} = 4.4$ Hz, Ir- CH_3); $^{13}\text{C}\{^1\text{H}\}$ NMR (101 MHz, CD_2Cl_2 , 27 °C): $\delta = 174.2$ (bs, 2C, Ir-CO), 19.5 (bs, 1C, Ir- CH_3); $^{31}\text{P}\{^1\text{H}\}$ NMR (162 MHz, CD_2Cl_2 , 27 °C):

$\delta = 23.2$ (s, 4P); Low Temperature Data: $^{13}\text{C}\{^1\text{H}\}$ NMR (101 MHz, CD_2Cl_2 , $-80\text{ }^\circ\text{C}$): $\delta = 179.9$ (bs, 1C, Ir-CO), 168.3 (bs, 1C, Ir-CO); $^{31}\text{P}\{^1\text{H}\}$ NMR (162 MHz, CD_2Cl_2 , $-80\text{ }^\circ\text{C}$): $\delta = 26.1$ (b, 2P), 19.8 (b, 2P).

(g) **$[\text{Ir}_2(\text{CO})_2(\mu\text{-OH})(\text{depm})_2][\text{CF}_3\text{SO}_3]$ (33).** To a solution of compound **32** (50 mg, 0.050 mmol), generated *in situ* at $-20\text{ }^\circ\text{C}$ in 5 mL of dichloromethane, was added 5 μL (0.277 mmol) of water and the resultant mixture stirred while warming to room temperature over the course of $\frac{1}{2}$ h. The solvent was removed and the product recrystallized from dichloromethane and pentane affording a bright yellow powder (70 % yield). ^1H NMR (400 MHz, CD_2Cl_2 , $27\text{ }^\circ\text{C}$): $\delta = 3.60$ (bs, 1H, Ir-OH-Ir), 2.85 (m, 4H, depm); $^{13}\text{C}\{^1\text{H}\}$ NMR (101 MHz, CD_2Cl_2 , $27\text{ }^\circ\text{C}$): $\delta = 184.7$ (s, 2C, Ir-CO); $^{31}\text{P}\{^1\text{H}\}$ NMR (162 MHz, CD_2Cl_2 , $27\text{ }^\circ\text{C}$): $\delta = 16.5$ (s, 4P), Elemental analysis calcd (%) for $\text{Ir}_2\text{SP}_4\text{F}_3\text{O}_6\text{C}_{21}\text{H}_{45}$ (990.97): C 25.45, H 4.58; found: C 25.65, H, 4.59.

(h) **$[\text{Ir}_2(\text{CO})_3(\mu\text{-H})(\text{depm})_2][\text{X}]$ (X = OTf (34-OTf), BAr^{F_4} (34-BAr $^{\text{F}_4}$)).**
(34-OTf): Method i) To a solution of compound **27** (100 mg, 0.118 mmol) in 25 mL of CH_2Cl_2 was slowly added neat HOTf (11 μL , 0.124 mmol) via microsyringe. The solution was stirred for 1 h, whereupon it was reduced to dryness. The solid was recrystallized from THF and pentane to afford a dark brown solid (74 % yield). **Method ii)** To a solution of **33** was added a CO purge at a rate of $1\text{ cm}^3/\text{sec}$. After 15 min, the CO purge was removed and an argon purge was added for 15 min to remove excess carbon monoxide, resulting in **34-OTf**. **(34-BAr $^{\text{F}_4}$):** To a solution of **27** (125 mg, 0.147 mmol) in 30 mL of CH_2Cl_2 was slowly added drop-wise (170 mg, 0.170 mmol) $[\text{H}(\text{Et}_2\text{O})_2][\text{B}(3,5\text{-}(\text{CF}_3)_2\text{C}_6\text{H}_3)_4]$ in 10 mL CH_2Cl_2 . The resulting mixture was stirred for 1 h whereupon it was reduced to dryness. The resulting residue was redissolved in ~ 5 mL diethylether and 10 mL pentane was added to precipitate a dark red solid which was isolated, further washed with pentane (2 x 10 mL) and dried

giving 115 mg of **34** (78 % yield). ^1H NMR (400 MHz, CD_2Cl_2 , 27 °C): δ = 2.45 (quin., 4H, depm), -10.40 (quin., 1H, $^2J_{\text{HP}}$ = 9.82 Hz, Ir-*H*-Ir); $^{13}\text{C}\{\text{H}\}$ NMR (101 MHz, CD_2Cl_2 , 27 °C): δ = 183.7 (s, 3C, Ir-CO); $^{31}\text{P}\{\text{H}\}$ NMR (162 MHz, CD_2Cl_2 , 27 °C): δ = 14.3 (s, 4P), Low Temperature Data: ^1H NMR (400 MHz, CD_2Cl_2 , -80 °C): δ = 2.45 (b, 4H, depm), -10.40 (b, 1H, Ir-*H*-Ir); $^{13}\text{C}\{\text{H}\}$ NMR (101 MHz, CD_2Cl_2 , -80 °C): δ = 185.3 (b, 1C, Ir-CO), 183.3 (b, 1C, Ir-CO); $^{31}\text{P}\{\text{H}\}$ NMR (162 MHz, CD_2Cl_2 , -80 °C): δ = 14.4 (b, 4P). Elemental analysis calcd (%) for $\text{Ir}_2\text{SP}_4\text{F}_3\text{O}_6\text{C}_{22}\text{H}_{45}$ (**34-OTf**, 1002.98): C 26.35, H 4.52; found: C 26.45, H, 4.50.

- (i) **$[\text{Ir}_2(\text{H})(\text{CO})_4(\text{depm})_2][\text{BAR}^{\text{F}}_4]$ (**35**)**. A solution of **34** dissolved in 0.7 mL of CD_2Cl_2 was placed under an atmosphere of CO resulting in the generation of **35**, as determined spectroscopically. This species was only characterized in solution, since removal of the CO atmosphere resulted in quantitative conversion to **34**. ^1H NMR (400 MHz, CD_2Cl_2 , 27 °C): δ = 3.40 (m, 4H, depm), -8.80 (t, $^2J_{\text{HP}}$ = 14.4 Hz); $^{13}\text{C}\{\text{H}\}$ NMR (101 MHz, CD_2Cl_2 , 27 °C): δ = 192.3 (t, 2C, $^2J_{\text{CP}}$ = 11.2 Hz, Ir-CO), 186.9 (t, 2C, $^2J_{\text{CP}}$ = 12.9 Hz, Ir-CO); $^{31}\text{P}\{\text{H}\}$ NMR (162 MHz, CD_2Cl_2 , 27 °C): δ = -9.5 (t, 2P, $^2J_{\text{PP}}$ = 29.8 Hz), -11.2 (t, 2P, $^2J_{\text{PP}}$ = 29.8 Hz).
- (j) ***trans*- $[\text{Rh}_2\text{Cl}_2(\text{CO})_2(\text{depm})_2]$ (**36**)**. A solution of $[\text{Rh}_2\text{Cl}_2(\text{COD})_2]$ (110 mg, 0.223 mmol) in 20 mL of acetone was placed under an atmosphere of CO and stirred for 10 min. To this solution was added dropwise, over a 5 min period, 100 μL (0.441 mmol) of depm in 10 mL of acetone, causing the color to change from yellow to orange. The solution was then refluxed for $\frac{1}{2}$ h whereupon it was cooled to room temperature and reduced to dryness. The residue was redissolved into 5 mL of THF, and Et_2O (20 mL) was added to precipitate an orange solid which was further washed with Et_2O (2 x 5 mL) and dried yielding 85 mg (53 % yield) of

spectroscopically pure **36**. HRMS m/z calcd for $\text{Rh}_2\text{P}_4\text{O}_2\text{C}_{20}\text{H}_{44}\text{Cl}$: 681.0088. Found: 681.0090. ^1H NMR (400 MHz, CD_2Cl_2 , 27 °C): δ = 2.37 (quin., 4H, depm); $^{13}\text{C}\{^1\text{H}\}$ NMR (101 MHz, CD_2Cl_2 , 27 °C): δ = 189.1 (d, 2C, $^1J_{\text{CRh}} = 74.8$ Hz, Rh–CO); $^{31}\text{P}\{^1\text{H}\}$ NMR (162 MHz, CD_2Cl_2 , 27 °C): δ = 17.9 (dm, 4P, $^1J_{\text{RHP}} = 117.2$ Hz), Elemental analysis calcd (%) for $\text{Rh}_2\text{P}_4\text{Cl}_2\text{O}_2\text{C}_{20}\text{H}_{44}$ (717.17): C 33.49, H 6.18; found: C 33.22, H, 5.85.

- (k) **[Rh₂(CO)₃(depm)₂] (37)**. Compound **36** (65 mg, 0.091 mmol) was dissolved in 20 mL of THF and stirred under a static atmosphere of CO. 2 mL of aqueous 1 M KOH was transferred dropwise, via a syringe, onto the stirred solution and the resulting mixture left to stir for 1 ½ h. The solvent was removed to give an oily brown residue, which was then extracted with benzene (3 x 10 mL). Filtration through celite gave a clear orange-brown solution, which was reduced to dryness to afforded 55 mg of the spectroscopically pure **37** as a viscous orange-brown oil (90 % yield). ^1H NMR (400 MHz, C_6D_6 , 27 °C): δ = 2.17 (quin., 4H, depm); $^{13}\text{C}\{^1\text{H}\}$ NMR (101 MHz, C_6D_6 , 27 °C): δ = 198.8 (bs, 3C, Rh–CO); $^{31}\text{P}\{^1\text{H}\}$ NMR (162 MHz, C_6D_6 , 27 °C): δ = 15.1 (d, 4P, $^1J_{\text{RHP}} = 137.7$ Hz); Low Temperature Data: $^{13}\text{C}\{^1\text{H}\}$ NMR (101 MHz, CD_2Cl_2 , –110 °C): δ = 209.1 (bd, 1C, $^1J_{\text{RhC}} = 77.0$ Hz, Rh–CO), 206.8 (bd, 1C, $^1J_{\text{RhC}} = 71.2$ Hz, Rh–CO), 183.4 (bd, 1C, $^1J_{\text{RhC}} = 67.9$ Hz, Rh–CO); $^{31}\text{P}\{^1\text{H}\}$ NMR (162 MHz, CD_2Cl_2 , –110 °C): δ = –22.5 (bd, 2P, $^1J_{\text{RHP}} = 117.1$ Hz), 8.5 (bd, 2P, $^1J_{\text{RHP}} = 152.6$ Hz).
- (l) **[Rh₂(CO)₄(depm)₂] (38)**. Compound **37** (50 mg, 0.072 mmol) was dissolved in 7 mL of CD_2Cl_2 and placed under an atmosphere of CO, causing the color of the solution to change from orange to yellow. The conversion of **37** to **38** was determined to be quantitative via NMR spectroscopy. However, removal of the CO atmosphere resulted in complete reversion back to **37**. Therefore, **38** has only been characterized

in situ via NMR spectroscopy. ^1H NMR (400 MHz, CD_2Cl_2 , 27 °C): δ = 2.60 (bm, 4H, depm); $^{13}\text{C}\{^1\text{H}\}$ NMR (101 MHz, CD_2Cl_2 , 27 °C): δ = 206.7 (bs, 4C, Rh–CO); $^{31}\text{P}\{^1\text{H}\}$ NMR (162 MHz, CD_2Cl_2 , 27 °C): δ = 12.4 (bd, $^1J_{\text{RhP}}$ = 133.2 Hz, 4P); Low Temperature Data: $^{13}\text{C}\{^1\text{H}\}$ NMR (101 MHz, CD_2Cl_2 , –80 °C): δ = 214.3 (dt, 1C, $^1J_{\text{RhP}}$ = 90.2 Hz, $^2J_{\text{CP}}$ = 29.7 Hz, Rh–CO), 204.1 (bs, 3C, Rh–CO); $^{31}\text{P}\{^1\text{H}\}$ NMR (162 MHz, CD_2Cl_2 , –80 °C): δ = 24.3 (m, 2P), –1.3 (m, 2P).

- (m) **[Rh₂(CH₃)(CO)₃(dep_m)₂][CF₃SO₃] (39) and [Rh₂(μ-κ¹:κ¹-C(O)CH₃)(CO)₂(dep_m)₂][CF₃SO₃] (39a).** To a solution of **37** (35 mg, 0.052 mmol) in 0.8 mL of CD_2Cl_2 , cooled in a dry ice/acetone ice bath to –80 °C, was slowly added, 6 μL (0.054 mmol) of neat methyl trifluoromethanesulphonate (MeOTf). The reaction was then monitored via low temperature NMR at –40 °C, showing the formation of compound **39**. Upon warming to –20 °C, **39** slowly converted to compound **39a** after 1 h. Warming to above 0 °C resulted in the decomposition of **39** to **40**, along with numerous unidentified products. Compound **39**: ^1H NMR (400 MHz, $\text{C}_3\text{D}_6\text{O}$, –80 °C): δ = 2.35 (quin., 4H, depm), 0.63 (bm, 3H, Rh–CH₃); $^{13}\text{C}\{^1\text{H}\}$ NMR (101 MHz, $\text{C}_3\text{D}_6\text{O}$, –80 °C): δ = 214.3 (bt, 2C, $^1J_{\text{CRh}}$ = 32.7 Hz, Rh–CO), 199.3 (bd, 1C, $^1J_{\text{CRh}}$ = 74.9 Hz, Rh–CO), –0.7 (bm, 1C, Rh–CH₃); $^{31}\text{P}\{^1\text{H}\}$ NMR (162 MHz, $\text{C}_3\text{D}_6\text{O}$, –80 °C): δ = 35.6 (bm, 4P). Compound **39a**: ^1H NMR (400 MHz, $\text{C}_3\text{D}_6\text{O}$, –20 °C): δ = 2.55 (quin., 4H, depm), 2.42 (s, 3H, Rh–C(O)CH₃); $^{13}\text{C}\{^1\text{H}\}$ NMR (101 MHz, $\text{C}_3\text{D}_6\text{O}$, –20 °C): δ = 319.9 (bm, 1C, Rh–C(O)CH₃), 199.8 (m, 1C, Rh–CO), 194.1 (d, 1C, $^1J_{\text{RhC}}$ = 76.3 Hz), 44.2 (s, 1C, Rh–C(O)CH₃); $^{31}\text{P}\{^1\text{H}\}$ NMR (162 MHz, $\text{C}_3\text{D}_6\text{O}$, –20 °C): δ = 22.5 (bm, 2P), 17.2 (bm, 2P).
- (n) **Addition of TMNO to 39.** To a 0.5 mL solution of **39** (32 mg, 0.038 mmol) in CD_2Cl_2 , cooled to –40 °C, was added trimethylamine-*N*-oxide (3 mg, 0.040 mmol) dissolved in 0.3 mL CD_2Cl_2 . The mixture was

monitored by variable temperature NMR. Below $-20\text{ }^{\circ}\text{C}$, no observable reaction was observed. Warming the solution to $-10\text{ }^{\circ}\text{C}$ resulted in the formation of **39a** as described above, but there was no indication of reaction with TMNO. Warming the mixture above $0\text{ }^{\circ}\text{C}$ resulted in decomposition to compound **14** along with various unidentified products.

- (o) **[Rh₂(CO)₂(μ-OH)(depm)₂][CF₃SO₃] (**40**).** To a NMR solution of **39** (34 mg, 0.041 mmol) in 0.8 mL *d*₆-acetone cooled to $-20\text{ }^{\circ}\text{C}$, was added 5 μL (0.277 mmol) of water, causing the solution to lighten in color. Maintaining this temperature for ½ h, while stirring, caused the color to become bright yellow. The solvent was subsequently removed and the residue extracted 3 times into 5 mL of ether. The extraction solvent was removed and the product was isolated as a yellow, oily material. ¹H NMR (400 MHz, CD₂Cl₂, 27 °C): δ = 2.65 (quin., 4H, depm); ¹³C{¹H} NMR (101 MHz, CD₂Cl₂, 27 °C): δ = 192.3 (dt, 2C, ¹J_{RhC} = 70.3 Hz, ²J_{CP} = 15.8 Hz, Rh-CO); ³¹P{¹H} NMR (162 MHz, CD₂Cl₂, 27 °C): δ = 21.7 (dm, 4P, ¹J_{RhP} = 120.3 Hz).
- (p) **[Rh₂(CO)₃(μ-H)(depm)₂][X] (X = OTf (**41-OTf**), BAr^F₄ (**41-BAr^F₄**)).**
(41-OTf): Method i) A solution of compound **37** (140 mg, 0.207 mmol) in 30 mL of CH₂Cl₂ was slowly added neat triflic acid (18 μL, 0.203 mmol) via microsyringe. The solution was stirred for 1 h, whereupon it was reduced to dryness. The solid was recrystallized from THF and pentane to afford a dark brown solid (81 % yield). **Method ii)** To a solution of **40** was added a CO purge at a rate of 1cm³/sec. After 15 min, the CO purge was replaced by a brief argon purge to remove excess carbon monoxide. **(41-BAr^F₄):** To a solution of **37** (100 mg, 0.148 mmol) in 30 mL of CH₂Cl₂ was slowly added drop-wise 150 mg (0.150 mmol) of [H(Et₂O)₂][B(3,5-(CF₃)₂C₆H₃)₄]. The resulting mixture was stirred for 1 h whereupon it was reduced to dryness and redissolved in ~2 mL of ether. Pentane (10 mL) was added to precipitate a dark orange-red solid that was

isolated, and further washed with pentane (2 x 10 mL), then dried, giving 155 mg of spectroscopically pure **41** (75 % yield). HRMS m/z calcd for $\text{Rh}_2\text{P}_4\text{O}_2\text{C}_{20}\text{H}_{45}$ [$\text{M}^+ - \text{CO}$]: 647.0473. Found: 647.0475. ^1H NMR (400 MHz, CD_2Cl_2 , 27 °C): $\delta = 2.23$ (quin., 4H, depm), -10.34 (m, 1H, $^1J_{\text{RhH}} = 24.3$ Hz, $^2J_{\text{HP}} = 12.2$ Hz, Rh–H–Rh); $^{13}\text{C}\{^1\text{H}\}$ NMR (101 MHz, CD_2Cl_2 , 27 °C): $\delta = 194.3$ (bm, 3C, Rh–CO); $^{31}\text{P}\{^1\text{H}\}$ NMR (162 MHz, CD_2Cl_2 , 27 °C): $\delta = 35.2$ (dm, 4P, $^1J_{\text{RHP}} = 97.4$ Hz); Low Temperature: ^1H NMR (400 MHz, CD_2Cl_2 , -80 °C): $\delta = 2.25$ (b, 4H, depm), -10.39 (b, 1H, Rh–H–Rh); $^{13}\text{C}\{^1\text{H}\}$ NMR (101 MHz, CD_2Cl_2 , -80 °C): $\delta = 195.1$ (b, 1C, Rh–CO), 194.0 (b, 2C, Rh–CO); $^{31}\text{P}\{^1\text{H}\}$ NMR (162 MHz, CD_2Cl_2 , 27 °C): $\delta = 35.2$ (b, 4P); Elemental analysis calcd (%) for $\text{Rh}_2\text{P}_4\text{F}_{24}\text{O}_3\text{C}_{53}\text{H}_{57}\text{B}$ (1538.50): C 41.38, H 3.73; found: C 41.17, H, 3.95.

- (q) **[Rh₂(CO)₃(depm)₂][CF₃SO₃]₂ (42).** To a solution of **37** (95 mg, 0.089 mmol), in 10 mL of acetone at 0 °C, was added a large excess of neat triflic acid (85 μL , 0.960 mmol) and the solution stirred for 3 h, while warming to ambient temperature. The solvent was subsequently removed, and the isolated orange solid was recrystallized from acetone and pentane, affording a yellow residue. ^1H NMR (400 MHz, $\text{C}_3\text{D}_6\text{O}$, 27 °C): $\delta = 2.70$ (quin., 4H, depm); $^{13}\text{C}\{^1\text{H}\}$ NMR (101 MHz, $\text{C}_3\text{D}_6\text{O}$, 27 °C): $\delta = 188.6$ (s, 3C, Rh–CO); $^{31}\text{P}\{^1\text{H}\}$ NMR (162 MHz, $\text{C}_3\text{D}_6\text{O}$, 27 °C): $\delta = 29.0$ (bd, 4P, $^1J_{\text{RHP}} = 93.1$ Hz).
- (r) **[Rh₂(CO)₅(depm)₂][CF₃SO₃]₂ (43).** To an NMR-scale solution (50 mg, 0.037 mmol) of **42** in 0.7 mL of d_6 -acetone was added excess CO, producing a clear yellow solution. The sample was subsequently investigated via multinuclear NMR spectroscopy. X-ray quality crystals of **43** were obtained under CO in the solid state, however removal of the CO atmosphere from a solution resulted in reversion to starting material. ^1H NMR (400 MHz, $\text{C}_3\text{D}_6\text{O}$, 27 °C): $\delta = 3.00$ (quin., 4H, depm); $^{13}\text{C}\{^1\text{H}\}$

NMR (101 MHz, C₃D₆O, 27 °C): δ = 191.7 (b, 5C, Rh–CO); ³¹P{¹H}
NMR (162 MHz, C₃D₆O, 27 °C): δ = 32.0 (bs, 4P).

(s) ***trans*-[IrRhCl₂(CO)₂(depm)₂] (44).** To a solution of Vaska's complex, [IrCl(CO)(PPh₃)₂] (250 mg, 0.320 mmol) in 15 mL of THF was added 150 μ L (0.66 mmol) of *bis*(diethylphosphino)methane (depm), which caused the solution to change from yellow to red-purple. Leaving to stir for 1 h resulted in a cloudy yellow slurry, signifying the formation of [IrCl(CO)(depm)₂]. The solvent was removed and the faint yellow solid was redissolved in 10 mL CH₂Cl₂, while in a separate flask, [RhCl(CO)₂]₂ (75 mg, 0.197 mmol) was dissolved in 7 mL of CH₂Cl₂. The [IrCl(CO)(depm)₂] solution was then added to the [RhCl(CO)₂]₂ solution, and the resulting orange mixture was stirred for 2 h. The solvent was removed and the residue redissolved in 7 mL of THF, followed by the addition of pentane (30 mL) to precipitate a dark orange solid. The solid was further washed with pentane (2 x 10 mL) and dried giving 200 mg (67 % yield). HRMS *m/z* calcd for IrRhP₄O₂C₂₀H₄₄Cl: 771.0659. Found: 771.0658. ¹H NMR (400 MHz, CD₂Cl₂, 27 °C): δ = 2.42 (quin., 4H, depm); ¹³C{¹H} NMR (101 MHz, CD₂Cl₂, 27 °C): δ = 190.0 (bs, 1C, Rh–CO), 171.8 (s, 1C, Ir–CO); ³¹P{¹H} NMR (162 MHz, CD₂Cl₂, 27 °C): δ = 18.0 (dt, 2P, ¹J_{RhP} = 118.3 Hz, ²J_{PP} = 63.9 Hz), 9.6 (t, 2P, ²J_{PP} = 63.9 Hz), Elemental analysis calcd (%) for IrRhP₄Cl₂O₂C₂₀H₄₄ (806.49): C 29.79, H 5.50; found: C 29.72, H, 5.34.

(t) **[IrRh(CO)₃(depm)₂] (45).** **Method i)** Compound **44** (275 mg, 0.341 mmol) was dissolved in 20 mL of THF and stirred under a dynamic atmosphere of CO. 8 mL of aqueous 1M KOH was transferred dropwise, via syringe, to the stirred solution and the resulting mixture was stirred for 1 ½ h. The solvent was removed under vacuum and the product extracted into 3 x 20 mL of benzene. Filtration through celite gave a clear orange-

brown solution, which was purged with CO for 5 min followed by argon for 10 min. The solvent was reduced to dryness affording the complex as a spectroscopically pure, viscous orange-brown oil. **Method ii)** Compound **44** (37 mg, 0.046 mmol) was dissolved in 10 mL of acetone. Excess NaBH₄ (0.200 mmol) was added directly to the solution, and was stirred for 1 h. The solvent was removed and the product redissolved in 10 mL of benzene or THF. Filtration through celite gave a clear orange-brown solution, which was purged with CO for 5 min followed by argon for 10 min. The solvent was reduced to dryness, affording the complex as a viscous orange-brown oil. Samples obtained via this method were always less pure, spectroscopically, and were generally obtained in poorer yields compared to the first method. (76 % yield) HRMS *m/z* calcd for IrRhP₄O₂C₂₀H₄₅ [M+H⁺-CO]: 737.1054. Found: 737.1049. ¹H NMR (400 MHz, C₆D₆, 27 °C): δ = 2.67 (quin., 4H, depm); ¹³C{¹H} NMR (101 MHz, C₆D₆, 27 °C): δ = 189.0 (bs, 2C), 185.7 (d, 1C, ¹J_{RhC} = 70.1 Hz, Rh-CO); ³¹P{¹H} NMR (162 MHz, C₆D₆, 27 °C): δ = 17.1 (dt, 2P, ¹J_{RhP} = 124.0 Hz, ²J_{PP} = 64.3 Hz), -28.8 (t, 2P, ²J_{PP} = 64.3 Hz).

- (u) **[IrRh(CO)₄(dep_m)₂] (46).** Compound **45** (275 mg, 0.341 mmol) was dissolved in 20 mL of CH₂Cl₂ and stirred under a dynamic atmosphere of CO for 1 h. NMR spectroscopy confirmed the formation of **45**, however subsequent removal of the CO atmosphere resulted in the loss of a CO, with quantitative reversion back to the starting compound. Thus, the characterization of **46** has been limited to solution ³¹P{¹H} and ¹H NMR spectroscopy. ¹H NMR (400 MHz, CD₂Cl₂, 27 °C): δ = 2.79 (bs, 4H, depm); ¹³C{¹H} NMR (101 MHz, CD₂Cl₂, 27 °C): δ = 197.5 (b, 4C); ³¹P{¹H} NMR (162 MHz, CD₂Cl₂, 27 °C): δ = -0.6 (b, 2P), -17.2 (b, 2P); ¹H NMR (400 MHz, CD₂Cl₂, -80 °C): δ = 3.15 (bs, 4H, depm); ¹³C{¹H} NMR (101 MHz, CD₂Cl₂, -80 °C): δ = 210.2 (dt, 1C, ¹J_{CRh} = 73.5 Hz, ²J_{CP} = 48.6 Hz), 200.6 (dt, 1C, ¹J_{CRh} = 72.4 Hz, ²J_{CP} = 10.5 Hz), 194.6 (m, 1C, ²J_{CC} = 20.7 Hz, ²J_{CP} = 13.7 Hz), 192.7 (m, 1C, ²J_{CC} = 10.5 Hz, ²J_{CP} = 11.1

Hz); $^{31}\text{P}\{^1\text{H}\}$ NMR (162 MHz, CD_2Cl_2 , $-80\text{ }^\circ\text{C}$): $\delta = -2.4$ (m, 2P, $^1J_{\text{PRh}} = 140.1$ Hz, $^2J_{\text{PP}} = 57.5$ Hz), -14.5 (t, 2P, $^2J_{\text{PP}} = 57.5$ Hz).

(v) **[IrRh(CH₃)(CO)₃(depm)₂][CF₃SO₃] (47)**. To a solution of **45** (75 mg, 0.098 mmol) in 10 mL of benzene was slowly added drop-wise, over a 5 min period, neat MeOTf (11 μL , 0.098 mmol). The resulting mixture was stirred for 1 h, whereupon it was reduced to dryness and redissolved in a minimum volume of THF (~2 mL). Pentane (10 mL) was added to precipitate a dark yellow-brown solid, which was isolated and further washed with pentane (2 x 10 mL) then dried under vacuum. ^1H NMR (400 MHz, CD_2Cl_2 , $27\text{ }^\circ\text{C}$): $\delta = 3.00$ (m, 4H, depm), 0.20 (t, $^3J_{\text{HP}} = 6.2$ Hz, Ir-CH₃); $^{13}\text{C}\{^1\text{H}\}$ NMR (101 MHz, CD_2Cl_2 , $27\text{ }^\circ\text{C}$): $\delta = 185.4$ (s, 2C, Ir-CO), 184.2 (dt, $^1J_{\text{RhC}} = 71.1$ Hz, $^2J_{\text{CP}} = 22.3$ Hz, Rh-CO), -34.8 (s, 1C, Ir-CH₃); $^{31}\text{P}\{^1\text{H}\}$ NMR (162 MHz, CD_2Cl_2 , $27\text{ }^\circ\text{C}$): $\delta = 33.0$ (dt, 2P, $^1J_{\text{RhP}} = 110.3$ Hz, $^2J_{\text{PP}} = 41.8$ Hz), -11.0 (t, 2P, $^2J_{\text{PP}} = 39.5$ Hz), Elemental analysis calcd (%) for IrRhSP₄F₃O₆C₂₃H₄₇ (927.69): C 29.78, H 5.11; found: C 29.64, H, 5.15.

(w) **[IrRh(CH₃)(CO)₂(depm)₂][CF₃SO₃] (48)**. To a solution of **47** (45 mg, 0.049 mmol) in 0.8 mL of CD_2Cl_2 was slowly added 100 μL of 0.5 M TMNO in CD_2Cl_2 . The reaction was monitored by NMR, which verified the formation of compound **48** after 10 min. Much like its homobinuclear congeners, this product was unstable and extremely moisture-sensitive; subsequent recrystallization attempts from various dried solvents resulted only in decomposition or hydrolysis products, thus **48** has been characterized via NMR spectroscopy. ^1H NMR (400 MHz, CD_2Cl_2 , $27\text{ }^\circ\text{C}$): $\delta = 2.70$ (m, 2H, depm), 2.40 (m, 2H, depm), 0.58 (t, 3H, $^3J_{\text{HP}} = 9.2$ Hz, Ir-CH₃); $^{13}\text{C}\{^1\text{H}\}$ NMR (101 MHz, CD_2Cl_2 , $27\text{ }^\circ\text{C}$): $\delta = 183.2$ (t, 1C, $^2J_{\text{CP}} = 7.2$ Hz, Ir-CO), 177.4 (dt, $^2J_{\text{RhC}} = 73.1$ Hz, $^2J_{\text{CP}} = 16.7$ Hz, Rh-CO), 9.9 (s, 1C, Ir-CH₃); $^{31}\text{P}\{^1\text{H}\}$ NMR (162 MHz, CD_2Cl_2 , $27\text{ }^\circ\text{C}$): $\delta = 22.5$ (dt, $^1J_{\text{RhP}} = 107.1$ Hz, $^2J_{\text{PP}} = 47.2$ Hz, 2P), 19.8 (t, $^2J_{\text{PP}} = 47.2$ Hz, 2P).

- (x) **[IrRh(CO)₂(μ-OH)(depm)₂][CF₃SO₃] (49).** To a solution of **48** (90 mg, 0.097 mmol), prepared *in situ* in 7 mL of CH₂Cl₂, was added water (5 μL, 0.277 mmol). The solution was stirred at room temperature for ½ h, during which time the color lightened to a pale orange. The solvent was removed and the product recrystallized from dichloromethane and pentane affording an orange, oily material. ¹H NMR (400 MHz, CD₂Cl₂, 27 °C): δ = 3.33 (s, 1H, Ir-OH-Rh), 2.70 (m, 2H, depm), 2.05 (m, 2H, depm); ¹³C{¹H} NMR (101 MHz, CD₂Cl₂, 27 °C): δ = 191.2 (dt, 1C, ¹J_{RhC} = 72.4 Hz, ²J_{CP} = 16.6 Hz, Rh-CO), 174.9 (t, ²J_{CP} = 11.2 Hz, Ir-CO); ³¹P{¹H} NMR (162 MHz, CD₂Cl₂, 27 °C): δ = 20.6 (dm, 2P, ¹J_{RhP} = 116.6 Hz), 17.2 (t, 2P, ²J_{PP} = 14.3 Hz).
- (y) **[IrRh(CO)₃(μ-H)(depm)₂][X] (X = OTf (50-OTf), BAr^F₄ (50-BAr^F₄)).**
(50-OTf): Method i) To a solution of compound **45** (124 mg, 0.162 mmol) in 25 mL of CH₂Cl₂ was slowly added neat triflic acid (15 μL, 0.169 mmol) via microsyringe. The solution was stirred for 1 h, whereupon it was reduced to dryness. The solid was recrystallized from THF and pentane to afford a dark brown solid (71 % yield). **Method ii)** To a solution of **49** was added a CO purge at a rate of 1 cm³/sec. After 15 min, the CO purge was replaced by a brief argon purge to remove excess carbon monoxide. **(50-BAr^F₄):** To a solution of compound **45** (100 mg, 0.131 mmol) in 30 mL of CH₂Cl₂ was slowly added a solution of [H(Et₂O)₂][B(3,5-(CF₃)₂C₆H₃)₄] (170 mg, 0.170 mmol) in 10 mL of CH₂Cl₂. The resulting mixture was stirred for 1 h whereupon it was reduced to dryness. The solid was recrystallized from ether and pentane affording a dark brown solid, which, after isolation and further washing with pentane (2 x 10 mL), was dried under vacuum (75 % yield). HRMS *m/z* calcd for RhIrP₄O₃C₂₁H₄₅: 913.6678. Found: 913.6676. ¹H NMR (400 MHz, CD₂Cl₂, 27 °C): δ = 2.85 (quin., 4H, depm), -11.32 (m, ¹J_{RhH} =

21.1 Hz, $^2J_{HP} = 9.8$ Hz, Ir–H–Rh); $^{13}\text{C}\{^1\text{H}\}$ NMR (101 MHz, CD_2Cl_2 , 27 °C): $\delta = 187.2$ (dt, 1C, $^1J_{CRh} = 74.6$ Hz, $^2J_{CP} = 16.2$ Hz, Rh–CO), 180.3 (t, 2C, $^2J_{CP} = 9.3$ Hz, Ir–CO); $^{31}\text{P}\{^1\text{H}\}$ NMR (162 MHz, CD_2Cl_2 , 27 °C): $\delta = 27.7$ (dt, 2P, $^1J_{RhP} = 106.9$ Hz, $^2J_{PP} = 45.5$ Hz), -5.5 (t, 2P, $^2J_{PP} = 45.5$ Hz), Elemental analysis calcd (%) for $\text{IrRhSP}_4\text{F}_3\text{O}_6\text{C}_{22}\text{H}_{45}$ (913.67): C 28.92, H 4.96; found: C 29.14, H, 4.97.

- (z) **$[\text{Ir}_2(\text{H})_2(\text{CO})_2(\mu\text{-H})(\mu\text{-C}=\text{CH}_2)(\text{depM})_2][\text{BAr}^{\text{F}}_4]$ (51).** **Method i)** In an NMR tube containing **34** (38 mg, 0.022 mmol) dissolved in 0.8 mL of CD_2Cl_2 , was added ethylene (5 mL, 0.219 mmol) via a gas-tight syringe to the head-space. The solution was mixed and the reaction was monitored by multinuclear NMR. After 2 h, complete conversion to **51** was observed. **Method ii)** In an NMR tube containing **34** (42 mg, 0.024 mmol) dissolved in 0.6 mL CD_2Cl_2 was added TMNO (2 mg, 0.027) dissolved in 0.2 mL CD_2Cl_2 , followed by the addition of ethylene (5 mL, 0.219 mmol) to the head-space. The reaction was mixed and monitored by multinuclear NMR, which showed complete conversion after 15 min. Attempts to isolate the product as a solid for crystallization were unsuccessful due to its solubility in both polar and non-polar solvents. HRMS m/z calcd for $\text{IrP}_4\text{O}_2\text{C}_{22}\text{H}_{49}$: 855.1936. Found: 855.1901. ^1H NMR (498 MHz, CD_2Cl_2 , 27 °C): $\delta = 6.57$ (s, 2H, C=CH₂), 2.85 (m, 2H, depm), 1.75 (m, 2H, depm), -12.66 (m, 2H, Ir–H), -14.69 (m, 1H, Ir–H–Ir); $^{13}\text{C}\{^1\text{H}\}$ NMR (125 MHz, CD_2Cl_2 , 27 °C): $\delta = 172.4$ (m, 2C, Ir–CO); $^{31}\text{P}\{^1\text{H}\}$ NMR (202 MHz, CD_2Cl_2 , 27 °C): $\delta = -6.9$ (s, 4P).
- (aa) **$[\text{Ir}_2(\text{H})_2(\text{CO})_2(\mu\text{-H})(\mu\text{-C}=\text{CHF})(\text{depM})_2][\text{BAr}^{\text{F}}_4]$ (52).** In an NMR tube containing **34** (43 mg, 0.025 mmol) dissolved in 0.5 mL of CD_2Cl_2 , was added TMNO (2 mg, 0.027 mmol) in 0.3 mL of CD_2Cl_2 , along with 5 mL of vinylfluoride (0.0219 mmol) via a gas-tight syringe to the head-space. The solution was mixed and the reaction was monitored by multinuclear NMR. After 30 min, complete conversion to **52** was observed. Attempts

to isolate the product as a solid for crystallization were unsuccessful due to its solubility in both polar and non-polar solvents. Performing the same reaction in the absence of TMNO still produced **52**, however the yield was <10% based on NMR integration after 2 h. ^1H NMR (498 MHz, CD_2Cl_2 , 27 °C): δ = 6.61 (d, 1H, $^2J_{\text{HF}}$ = 108.2 Hz, C=CHF), 2.77 (m, 2H, depm), 1.67 (m, 2H, depm), -12.54 (m, 1H, Ir-H), -13.09 (m, 1H, Ir-H), -15.48 (m, 1H, Ir-H-Ir); $^{13}\text{C}\{^1\text{H}\}$ NMR (125 MHz, CD_2Cl_2 , 27 °C): δ = 171.1 (m, 2C, Ir-CO); ^{19}F NMR (469 MHz, CD_2Cl_2 , 27 °C): δ = -72.1 (d, 1F, $^2J_{\text{HF}}$ = 108.2 Hz); $^{31}\text{P}\{^1\text{H}\}$ NMR (202 MHz, CD_2Cl_2 , 27 °C): δ = -7.1 (m, 2P), -9.1 (m, 2P).

(bb) $[\text{Ir}_2(\text{H})_2(\text{CO})_2(\mu\text{-H})(\mu\text{-C}=\text{C}(\text{H})\text{CH}_3)(\text{dep}_m)_2][\text{BAr}^{\text{F}}_4]$ (53**). Method i)**

In an NMR tube containing **34** (24 mg, 0.014 mmol) dissolved in 0.8 mL of CD_2Cl_2 , was added 5 mL of propylene (0.0219 mmol) via a gas-tight syringe. The solution was mixed and the reaction was monitored by multinuclear NMR. After 2.5 h, complete conversion to **53** was observed.

Method ii) In an NMR tube containing **34** (33 mg, 0.019 mmol) dissolved in 0.6 mL CD_2Cl_2 was added TMNO (1 mg, 0.014) dissolved in 0.2 mL CD_2Cl_2 , followed by the addition of propylene (5 mL, 0.219 mmol). The reaction was mixed and monitored by multinuclear NMR, which showed complete conversion after 15 min. Attempts to isolate the product as a solid for crystallization were unsuccessful due to its solubility in both polar and non-polar solvents. HRMS m/z calcd for $\text{IrP}_4\text{O}_2\text{C}_{23}\text{H}_{51}$: 869.2092. Found: 869.2082. ^1H NMR (498 MHz, CD_2Cl_2 , 27 °C): δ = 6.00 (m, 2H, C=C(H)CH₃), 2.58 (m, 2H, depm), 1.88 (m, 3H, C=C(H)CH₃), 1.63 (m, 2H, depm), -12.37 (m, 1H, $^4J_{\text{HH}}$ = 8.2 Hz, Ir-H), -12.63 (m, 1H, $^4J_{\text{HH}}$ = 8.2 Hz, Ir-H), -14.80 (m, 1H, Ir-H-Ir); $^{13}\text{C}\{^1\text{H}\}$ NMR (125 MHz, CD_2Cl_2 , 27 °C): δ = 171.9 (m, 2C, Ir-CO); $^{31}\text{P}\{^1\text{H}\}$ NMR (202 MHz, CD_2Cl_2 , 27 °C): δ = -6.2 (m, 2P), -7.5 (m, 2P).

(cc) [Ir₂(H)₂(CO)₂(μ-H)(μ-C=C(H)CF₃)(depm)₂][BAr^F₄] (54). Method i)

In an NMR tube containing **34** (42 mg, 0.025 mmol) dissolved in 0.8 mL of CD₂Cl₂, was added 5 mL of 3,3,3-trifluoroethylene (0.0219 mmol) via a gas-tight syringe. The solution was mixed and the reaction was monitored by multinuclear NMR. After 2 h, complete conversion to **54** was observed. **Method ii)** In an NMR tube containing **34** (39 mg, 0.024 mmol) dissolved in 0.6 mL of CD₂Cl₂ was added TMNO (2 mg, 0.027) dissolved in 0.2 mL of CD₂Cl₂, followed by the addition of 3,3,3-trifluoropropylene (5 mL, 0.219 mmol) to the head-space via a gas-tight syringe. The reaction was mixed and monitored by multinuclear NMR, which showed complete conversion after 15 min. Attempts to isolate the product as a solid for crystallization were unsuccessful due to its solubility in both polar and non-polar solvents. ¹H NMR (498 MHz, CD₂Cl₂, 27 °C): δ = 6.70 (s, 1H, C=C(H)CF₃), 2.08 (m, 2H, depm), 1.74 (m, 2H, depm), -12.33 (m, 1H, Ir-H), -12.61 (m, 1H, Ir-H), -14.84 (m, 1H, Ir-H-Ir); ¹³C{¹H} NMR (125 MHz, CD₂Cl₂, 27 °C): δ = 172.3 (t, 1C, ²J_{CP} = 8.7 Hz, Ir-CO), 171.7 (t, 1C, ²J_{CP} = 8.2 Hz, Ir-CO); ¹⁹F NMR (469 MHz, CD₂Cl₂, 27 °C): δ = -59.9 (s, 3F); ³¹P{¹H} NMR (202 MHz, CD₂Cl₂, 27 °C): δ = -8.6 (t, 2P, ²J_{PP} = 28.4 Hz), -9.4 (t, 2P, ²J_{PP} = 28.4 Hz).

(dd) [Ir₂(H)₂(CO)₂(μ-H)(μ-C=C(H)C(H)=CH₂)(depm)₂][BAr^F₄] (55).

Method i) In an NMR tube containing **34** (46 mg, 0.027 mmol) dissolved in 0.8 mL of CD₂Cl₂, was added 5 mL of 1,3-butadiene (0.0219 mmol) via a gas-tight syringe to the head-space. The solution was mixed and the reaction was monitored by multinuclear NMR. After 5 h, complete conversion to **55** was observed. **Method ii)** In an NMR tube containing **34** (51 mg, 0.030 mmol) dissolved in 0.6 mL of CD₂Cl₂ was added TMNO (2 mg, 0.027) dissolved in 0.2 mL of CD₂Cl₂, followed by the addition of 1,3-butadiene (5 mL, 0.219 mmol) via a gas-tight syringe to the head-space. The reaction was mixed and monitored by multinuclear NMR, which showed complete conversion after 15 min. Attempts to isolate the

product as a solid for crystallization were unsuccessful due to its solubility in both polar and non-polar solvents. HRMS m/z calcd for $\text{IrP}_4\text{O}_2\text{C}_{24}\text{H}_{51}$: 881.2092. Found: 881.2084. ^1H NMR (498 MHz, CD_2Cl_2 , 27 °C): δ = 6.82 (d, 1H, $^3J_{\text{HH}} = 9.9$ Hz, $\text{C}=\text{C}(\text{H})\text{C}(\text{H})=\text{C}(\text{H})\text{H}$), 6.28 (ddd, 1H, $^3J_{\text{HH}} = 17.1$ Hz, $^3J_{\text{HH}} = 9.9$ Hz, $^3J_{\text{HH}} = 9.9$ Hz, $\text{C}=\text{C}(\text{H})\text{C}(\text{H})=\text{C}(\text{H})\text{H}$), 4.93 (d, 1H, $^3J_{\text{HH}} = 17.1$ Hz, $\text{C}=\text{C}(\text{H})\text{C}(\text{H})=\text{C}(\text{H})\text{H}$), 4.82 (d, 1H, $^3J_{\text{HH}} = 9.9$ Hz, $\text{C}=\text{C}(\text{H})\text{C}(\text{H})=\text{C}(\text{H})\text{H}$), 2.57 (m, 2H, depm), 1.65 (m, 2H, depm), -12.31 (m, 1H, Ir-*H*), -12.56 (m, 1H, Ir-*H*), -14.70 (m, 1H, Ir-*H*-Ir); $^{13}\text{C}\{^1\text{H}\}$ NMR (125 MHz, CD_2Cl_2 , 27 °C): δ = 171.5 (t, 1C, $^2J_{\text{CP}} = 7.9$ Hz, Ir-CO), 171.3 (t, 1C, $^2J_{\text{CP}} = 7.8$ Hz, Ir-CO); $^{31}\text{P}\{^1\text{H}\}$ NMR (202 MHz, CD_2Cl_2 , 27 °C): δ = -6.6 (m, 2P), -7.1 (m, 2P).

- (ee) **[Ir₂(H)₂(CO)₂(μ -H)(μ -C=C(H)Ph)(depm)₂][BAr^F₄] (56). Method (i)** In a round-bottom flask containing **34** (89 mg, 0.052 mmol) dissolved in 15 mL of CH_2Cl_2 , was added neat styrene (200 μL , 1.746 mmol). The solution was brought to reflux for 48 h, after which the solution was cooled to ambient temperature. The solvent was removed and the yellow residue was dried under reduced pressure. **Method (ii)** In an NMR tube charged with **34** (44 mg, 0.025 mmol) dissolved in 0.6 mL of CD_2Cl_2 was added neat styrene (100 μL , 0.873 mmol), followed immediately by TMNO (2.5 mg, 0.033 mmol) dissolved in 0.2 mL of CD_2Cl_2 . The solution was mixed and the reaction monitored by NMR, after which quantitative conversion to **56** was observed after 10 min. Attempts to isolate the product as a solid for crystallization were unsuccessful due to its solubility in both polar and non-polar solvents. ^1H NMR (498 MHz, CD_2Cl_2 , 27 °C): δ = 7.67 (d, 2H, $^3J_{\text{HH}} = 7.9$ Hz, *-ortho*), 7.66 (s, 1H, $\text{C}=\text{C}(\text{H})\text{Ph}$), 7.28 (t, 2H, $^3J_{\text{HH}} = 7.9$ Hz, *-meta*), 7.17 (t, 1H, $^3J_{\text{HH}} = 7.9$ Hz, *-para*), 2.26 (m, 2H, depm), 1.65 (m, 2H, depm), -11.90 (dt, 1H, $^2J_{\text{HP}} = 15.7$ Hz, $^4J_{\text{HH}} = 9.0$ Hz, Ir-*H*), -12.36 (dt, 1H, $^2J_{\text{HP}} = 14.9$ Hz, $^4J_{\text{HH}} = 9.0$ Hz, Ir-*H*), -14.64 (m, 1H, Ir-*H*-Ir); $^{13}\text{C}\{^1\text{H}\}$ NMR (125 MHz, CD_2Cl_2 , 27

$^{\circ}\text{C}$): $\delta = 171.2$ (m, 2C, Ir–CO); $^{31}\text{P}\{\text{H}\}$ NMR (202 MHz, CD_2Cl_2 , $27\text{ }^{\circ}\text{C}$): $\delta = -8.7$ (m, 2P), -9.2 (m, 2P).

(ff) **$[\text{Ir}_2(\text{H})_2(\text{CO})_2(\mu\text{-H})(\mu\text{-C}=\text{C}(\text{CH}_3)_2)(\text{depm})_2][\text{BAr}^{\text{F}}_4]$ (57)**. In an NMR tube containing **34** (52 mg, 0.030 mmol) dissolved in 0.8 mL of CD_2Cl_2 and cooled to $-80\text{ }^{\circ}\text{C}$, was added TMNO (2.5 mg, 0.033 mmol) followed by isobutylene (25 μL , 0.262 mmol) which had also been cooled to $-80\text{ }^{\circ}\text{C}$. The solution was mixed and slowly allowed to warm to ambient temperature. Once ambient temperature was reached, the reaction was monitored by multinuclear NMR. Attempts to isolate the product as a solid for crystallization were unsuccessful due to its solubility in both polar and non-polar solvents. ^1H NMR (400 MHz, CD_2Cl_2 , $27\text{ }^{\circ}\text{C}$): $\delta = 2.42$ (m, 2H, depm), 1.52 (m, 2H, depm), 1.40 (s, 6H, $\text{C}=\text{C}(\text{CH}_3)_2$), -13.73 (m, 3H, Ir–H), -15.88 (m, 1H, Ir–H–Ir); $^{13}\text{C}\{\text{H}\}$ NMR (101 MHz, CD_2Cl_2 , $27\text{ }^{\circ}\text{C}$): $\delta = 167.6$ (m, 2C, Ir–CO); $^{31}\text{P}\{\text{H}\}$ NMR (162 MHz, CD_2Cl_2 , $27\text{ }^{\circ}\text{C}$): $\delta = -6.2$ (m, 4P).

(gg) **Reaction of 25 with ethylene**. In an NMR tube containing **50-OTf** (36 mg, 0.039 mmol) dissolved in 0.8 mL of CD_2Cl_2 and cooled to $-80\text{ }^{\circ}\text{C}$, was added TMNO (3 mg, 0.040 mmol) followed by ethylene (5 mL, 0.219 mmol). The solution was mixed and slowly allowed to warm to ambient temperature. Once ambient temperature was reached, the reaction was monitored by multinuclear NMR. Decomposition of **50-OTf** was observed, leading to multiple unidentified products.

4.4.3 X-ray Structure Determinations

4.4.3.1 General. Crystals were grown via slow diffusion using the following solvent combinations: $\text{CH}_2\text{Cl}_2/\text{Et}_2\text{O}$ (**26**, **43**); THF/*n*-pentane (**29**); THF/ Et_2O (**36**); $\text{Et}_2\text{O}/n$ -pentane (**41**); $\text{CH}_2\text{Cl}_2/n$ -pentane (**47**). Data were collected using a Bruker SMART 1000 CCD detector/PLATFORM diffractometer with the crystals cooled to $-80\text{ }^{\circ}\text{C}$ (**26**, **29**, **36**, **43**, **47**) or with a Bruker APEX II CCD detector/D8 diffractometer⁸¹ with the crystal cooled to $-100\text{ }^{\circ}\text{C}$ (**41**); all data were collected

using Mo K α radiation ($\lambda = 0.71073 \text{ \AA}$). The data were corrected for absorption via a multi-scan method (**26**, **36**, **43**, **47**) or through Gaussian integration from indexing of the crystal faces (**29**, **41**). Structures were solved using direct methods (*SHELXS-97*⁸² for **26**, **29**, **36**, **43**, and **47**) or Patterson search/structure expansion (*DIRDIF-2008*⁸³ for **41**). Refinements were completed using the program *SHELXL-97*.⁸² Non-hydridic hydrogen atoms were assigned positions based on the sp^2 or sp^3 hybridization geometries of their attached carbon atoms, and were given isotropic displacement parameters 20% greater than those of their parent atoms. See supporting information for a listing of crystallographic experimental data.

4.4.3.2 Special refinement conditions. (i) **26**: The chloro and carbonyl ligands attached to iridium were disordered, thus refined as two sets of positions (Cl(A), C(1A), O(1A) with an occupancy factor of 0.6, and Cl(B), C(1B), O(1B) with an occupancy factor of 0.4). (ii) **29**: The Ir(2)–H(2) distance was restrained to be 1.65(1) \AA . The C(25)–C(26A) and C(25)–C(26B) distances (within a disordered phosphine ethyl group) were restrained to be 1.53(1) \AA . (iii) **36**: The chloro and carbonyl ligands attached to rhodium were disordered, thus refined as two sets of positions ($\{\text{Cl(A), C(1A), O(1A)}\}$ and $\{\text{Cl(B), C(1B), O(1B)}\}$, each with an occupancy factor of 0.5). (iv) **41**: The atomic coordinates and isotropic displacement parameter for the bridging hydrido ligand (H(1)) were allowed to refine without restraints. (v) **47**: Bond distances and angles within the minor (40%) component of the disordered RhIr(CO)₃(CH₃) fragment (Ir(B), Rh(B), O(1B), O(2B), O(3B), C(1B), C(2B), C(3B), C(4B)) were restrained to have the same values as the corresponding ones for the major orientation, as shown in Figure 4.6.

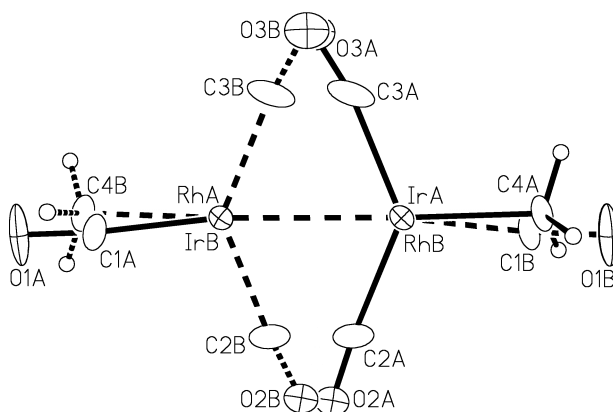


Figure 4.6 – *Perspective view of the disordered IrRhMe(CO)₃ fragment (47). The depm atoms have been omitted for clarity. The atoms of one disordered form are connected by solid bonds, while the others are connected by dashed bonds.*

4.5 Acknowledgements

We thank the Natural Sciences and Engineering Research Council of Canada (NSERC) and the University of Alberta for financial support for this research and NSERC for funding the Bruker D8/APEX II CCD diffractometer. We thank the Chemistry Department's NMR Spectroscopy and Analytical and Instrumentation Laboratories. Finally, we thank NSERC and Alberta Innovates–Technology (formerly Alberta Ingenuity Fund) for scholarships to M.E.S.

4.6 References

- (1) Ritleng, V.; Chetcuti, M. J. *Chem. Rev.* **2007**, *107*, 797.
- (2) Kubiak, C. P.; Eisenberg, R. *J. Am. Chem. Soc.* **1980**, *120*, 3637
- (3) Kubiak, C. P.; Woodcock, C.; Eisenberg, R. *Inorg. Chem.* **1982**, *21*, 2119.
- (4) Woodcock, C., Eisenberg, R. *Inorg. Chem.* **1984**, *23*, 4207.
- (5) Sutherland, B. R.; Cowie, M. *Inorg. Chem.* **1984**, *23*, 2324.
- (6) Sutherland, B. R.; Cowie, M. *Organometallics* **1985**, *4*, 1801.
- (7) Sutherland, B. R.; Cowie, M. *Organometallics* **1985**, *4*, 1637.
- (8) Woodcock, C.; Eisenberg, R. *Inorg. Chem.* **1985**, *24*, 1285.
- (9) McDonald, R.; Sutherland, B. R.; Cowie, M. *Inorg. Chem.* **1987**, *26*, 3333.
- (10) Jenkins, J. A.; Ennett, J. P.; Cowie, M. *Organometallics* **1988**, *7*, 1845.
- (11) Reinking, M. K.; Fanwick, P. E.; Kubiak, C. P. *Angew. Chem. Int. Ed.* **1989**, *28*, 1377.
- (12) Reinking, M. K.; Ni, J. F.; Fanwick, P. E.; Kubiak, C. P. *J. Am. Chem. Soc.* **1989**, *111*, 6459.
- (13) Jenkins, J. A.; Cowie, M. *Organometallics* **1992**, *11*, 2774.
- (14) Jenkins, J. A.; Cowie, M. *Organometallics* **1992**, *11*, 2767.
- (15) Shafiq, F.; Kramarz, K. W.; Eisenberg, R. *Inorg. Chim. Acta* **1993**, *213*, 111.
- (16) Shafiq, F. E., R. *Inorg. Chem.* **1993**, *32*, 3287.
- (17) Torkelson, J. R.; McDonald, R.; Cowie, M. *J. Am. Chem. Soc.* **1998**, *120*, 4047.
- (18) Torkelson, J. R.; Antwi-Nsiah, F. H.; McDonald, R.; Cowie, M.; Pruis, J. G.; Jalkanen, K. J.; DeKock, R. L. *J. Am. Chem. Soc.* **1999**, *121*, 3666.
- (19) Hutton, A. T.; Pringle, P. G.; Shaw, B. L. *Organometallics* **1983**, *2*, 1889.
- (20) Antonelli, D. M.; Cowie, M. *Organometallics* **1990**, *9*, 1818.
- (21) Elliot, D. J.; Ferguson, G.; Holah, D. G.; Hughes, A. N.; Jennings, M. C.; Magnuson, V. R.; Potter, D.; Puddephatt, R. J. *Organometallics* **1990**, *9*, 1336.
- (22) McDonald, R.; Cowie, M. *Inorg. Chem.* **1990**, *29*, 1564.
- (23) Antwi-Nsiah, F.; Cowie, M. *Organometallics* **1992**, *11*, 3157.

- (24) Antwi-Nsiah, F. H.; Oke, O.; Cowie, M. *Organometallics* **1996**, *15*, 1042.
- (25) Oke, O.; McDonald, R.; Cowie, M. *Organometallics* **1999**, *18*, 1629.
- (26) Trepanier, S. J.; Sterenberg, B. T.; McDonald, R.; Cowie, M. *J. Am. Chem. Soc.* **1999**, *121*, 2613.
- (27) Dell'Anna, M. M.; Trepanier, S. J.; McDonald, R.; Cowie, M. *Organometallics* **2001**, *20*, 88.
- (28) Rowsell, B. D.; Trepanier, S. J.; Lam, R.; McDonald, R.; Cowie, M. *Organometallics* **2002**, *21*, 3228.
- (29) Trepanier, S. J.; McDonald, R.; Cowie, M. *Organometallics* **2003**, *22*, 2638.
- (30) Chokshi, A.; Rowsell, B. D.; Trepanier, S. J.; Ferguson, M. J.; Cowie, M. *Organometallics* **2004**, *23*, 4759.
- (31) Trepanier, S. J.; Dennett, J. N. L.; Sterenberg, B. T.; McDonald, R.; Cowie, M. *J. Am. Chem. Soc.* **2004**, *126*, 8046.
- (32) Wigginton, J. R.; Trepanier, S. J.; McDonald, R.; Ferguson, M. J.; Cowie, M. *Organometallics* **2005**, *24*, 6194.
- (33) Hounjet, L. J.; Bierenstiel, M.; Ferguson, M. J.; McDonald, R.; Cowie, M. *Dalton Trans.* **2009**, 4213.
- (34) Broussard, M. E.; Juma, B.; Train, S. G.; Peng, W.-J.; Laneman, S. A.; Stanley, G. G. *Science* **1993**, *260*, 1784.
- (35) Samant, R. G.; Trepanier, S. J.; Wigginton, J. R.; Xu, L.; Bierenstiel, M.; McDonald, R.; Ferguson, M. J.; Cowie, M. *Organometallics* **2009**, *28*, 3407.
- (36) Slaney, M. E.; Anderson, D. J.; Ferguson, M. J.; McDonald, R.; Cowie, M. *J. Am. Chem. Soc.* **2010**, *132*, 16544.
- (37) Chouzier, S.; Gruber, M.; Djakovitch, L. *J. Mol. Catal. A: Chem.* **2004**, *212*, 43.
- (38) Hansen, J.; Li, B.; Dikarev, E.; Autschbach, J.; Davies, H. M. L. *J. Org. Chem.* **2009**, *74*, 6564.
- (39) Peris, E.; Zanardi, A.; Mata, J. A. *J. Am. Chem. Soc.* **2009**, *131*, 14531.
- (40) Zanardi, A.; Mata, J. A.; Peris, E. *J. Am. Chem. Soc.* **2009**, *131*, 14531.

- (41) Gu, S. J.; Xu, D. C.; Chen, W. Z. *Dalton Trans.* **2011**, *40*, 1576.
- (42) Ristic-Petrovic, D.; Torkelson, J. R.; Hilts, R. W.; McDonald, R.; Cowie, M. *Organometallics* **2000**, *19*, 4432.
- (43) Ristic-Petrovic, D.; Anderson, D. J.; Torkelson, J. R.; Ferguson, M. J.; McDonald, R.; Cowie, M. *Organometallics* **2005**, *24*, 3711.
- (44) Anderson, D. J.; McDonald, R.; Cowie, M. *Angew. Chem. Int. Ed.* **2007**, *46*, 3741.
- (45) Slaney, M. E.; Anderson, D. J.; Ristic-Petrovic, D.; McDonald, R.; Cowie, M. *Accepted, Chem. Eur. J.*, Nov. 8, 2011.
- (46) Stoutland, P. O.; Bergman, R. G. *J. Am. Chem. Soc.* **1985**, *107*, 4581.
- (47) Haddleton, D. M.; Perutz, R. N. *J. Chem. Soc., Chem. Commun.* **1986**, 1734.
- (48) Silvestre, J.; Calhorda, M. J.; Hoffmann, R.; Stoutland, P. O.; Bergman, R. G. *Organometallics* **1986**, *5*, 1841.
- (49) Wenzel, T. T.; Bergman, R. G. *J. Am. Chem. Soc.* **1986**, *108*, 4856.
- (50) Ghosh, C. K.; Rodgers, D. P. S.; Graham, W. A. G. *J. Chem. Soc., Chem. Commun.* **1988**, 1511.
- (51) Stoutland, P. O.; Bergman, R. G. *J. Am. Chem. Soc.* **1988**, *110*, 5732.
- (52) Ghosh, C. K.; Graham, W. A. G. *J. Am. Chem. Soc.* **1989**, *111*, 375.
- (53) Ghosh, C. K.; Hoyano, J. K.; Krentz, R.; Graham, W. A. G. *J. Am. Chem. Soc.* **1989**, *111*, 5480.
- (54) Tanke, R. S.; Crabtree, R. H. *Inorg. Chem.* **1989**, *28*, 3444.
- (55) Boutry, O.; Gutierrez, E.; Monge, A.; Nicasio, M. C.; Perez, P. J.; Carmona, E. *J. Am. Chem. Soc.* **1992**, *114*, 7288.
- (56) Bell, T. W.; Brough, S. A.; Partridge, M. G.; Perutz, R. N.; Rooney, A. D. *Organometallics* **1993**, *12*, 2933.
- (57) Deeming, A. J.; Underhill, M. *J. Organomet. Chem.* **1972**, *42*, C60.
- (58) Deeming, A. J.; Underhill, M. *J. Chem. Soc., Chem. Commun.* **1973**, 277.
- (59) Deeming, A. J.; Hasso, S.; Underhill, M.; Canty, A. J.; Johnson, B. F. G.; Jackson, W. G.; Lewis, J.; Matheson, T. W. *J. Chem. Soc., Chem. Commun.* **1974**, 807.

- (60) Deeming, A. J.; Underhill, M. J. *Chem. Soc., Dalton Trans.* **1974**, 1415.
- (61) Boncella, J. M.; Green, M. L. H.; O'Hare, D. J. *Chem. Soc., Chem. Commun.* **1986**, 618.
- (62) Boncella, J. M.; Green, M. L. H. *J. Organomet. Chem.* **1987**, 325, 217.
- (63) Bell, T. W.; Haddleton, D. M.; McCamley, A.; Partridge, M. G.; Perutz, R. N.; Willner, H. *J. Am. Chem. Soc.* **1990**, 112, 9212.
- (64) Suzuki, H.; Omori, H.; Lee, D. H.; Yoshida, Y.; Fukushima, M.; Tanaka, M.; Moro-oka, Y. *Organometallics* **1994**, 13, 1129.
- (65) Ristic-Petrovic, D., Ph.D. Thesis, University of Alberta, 2002.
- (66) Reinking, M. K., Ph.D Thesis, Purdue University, 1989.
- (67) Cordaro, J. G.; Bergman, R. G. *J. Am. Chem. Soc.* **2004**, 126, 3432.
- (68) Soderquist, J. A.; Anderson, C. L. *Tetrahedron Lett.* **1986**, 27, 3961.
- (69) Sterenberg, B. T.; McDonald, R.; Cowie, M. *Organometallics* **1997**, 16, 2297.
- (70) Slaney, M. E.; Anderson, D. J.; Ferguson, M. J.; McDonald, R.; Cowie, M. *Accepted, Organometallics, Jan. 16, 2012.*
- (71) Fryzuk, M. D.; Jones, T.; Einstein, F. W. B. *Organometallics* **1984**, 3, 185.
- (72) MacDougall, T. J.; Llamazares, A.; Kuhnert, O.; Ferguson, M. J.; McDonald, R.; Cowie, M. *Organometallics* **2011**, 30, 952.
- (73) MacDougall, T. J.; Trepanier, S. J.; Dutton, J. L.; Ferguson, M. J.; McDonald, R.; Cowie, M. *Organometallics* **2011**, 30, 5882
- (74) Novikova, Z. S.; Prishchenko, A. A.; Lutsenko, I. F. *Zh. Obshch. Khim.* **1977**, 47, 775.
- (75) Prishchenko, A. A.; Nifantex, N. E.; Novikova, Z. S.; Lutsenko, I. F. *Zh. Obshch. Khim.* **1980**, 50, 1881.
- (76) Vaska, L.; Diluzio, J. W. *J. Am. Chem. Soc.* **1961**, 83, 2784.
- (77) Vrieze, K.; Collman, J. P.; Sears, C. T.; Kubota, M.; Davison, A.; Shawl, E. T. *Inorg. Synth.* **1968**, 11, 101.
- (78) Giordano, G.; Crabtree, R. H.; Heintz, R. M.; Forster, D.; Morris, D. E. *Inorg. Synth.* **1979**, 19, 218.

- (79) McCleverty, J. A.; Wilkinson, G.; Lipson, J. G.; Maddox, M. L.; Kaesz, H. D. *Inorg. Synth.* **1990**, *28*, 84.
- (80) Brookhart, M.; Grant, B.; Volpe Jr., A. F. *Organometallics* **1992**, *11*, 3920.
- (81) Programs for diffractometer operation, unit cell indexing, data collection, data reduction and absorption correction were those supplied by Bruker.
- (82) Sheldrick, G. M. *Acta Crystallogr.* **2008**, *A64*, 112.
- (83) Beurskens, P. T.; Beurskens, G.; de Gelder, R.; Smits, J. M. M.; Garcia-Granda, S.; Gould, R. O. (2008). The DIRDIF-2008 program system. Crystallography Laboratory, Radboud University Nijmegen, The Netherlands.

Chapter 5 – Tandem C–F and C–H Bond Activation in Fluoroolefins Promoted by a *Bis*(diethylphosphino)-methane-Bridged Diiridium Complex: Role of Water in the Activation Processes[†]

5.1 Introduction

The activation of C–F bonds in fluorocarbons represents an important ongoing challenge in organometallic chemistry as new, more effective routes are sought for the synthesis of fluorine-containing compounds, having applications as surfactants,¹⁻³ polymers,^{4,5} pharmaceuticals,⁶⁻¹⁰ agrochemicals,^{11,12} and for the removal of persistent fluorine-containing atmospheric pollutants.^{13,14} Transition-metal hydride complexes have been successfully utilized to effect the carbon-fluorine bond activation in a range of fluorine-containing organic substrates,¹⁵⁻³⁵ often under very mild conditions and in a few cases these reactions have been shown to be catalytic.³¹⁻³⁵ In all these transformations, the hydride ligands have been shown or proposed to fulfill a number of different roles.¹⁵⁻³⁵

Although the majority of C–F bond activation studies have focused on the cleavage of aromatic C–F bonds,³⁶⁻⁴⁴ there has been growing interest in the activation of olefinic C–F bonds.^{18-25,30,45-63} Varying degrees of selectivity have been observed in the hydrodefluorination of fluoroolefins using metal-hydride complexes. For example, Jones *et al.* have demonstrated the efficacy of [Cp*₂ZrH₂] in the hydrodefluorination of 1,1-difluoroethylene, 1,1-difluoromethylenecyclohexane and perfluoropropene to ethylene, methylcyclohexane and propane, respectively,^{18,21,23} while Whittlesey and coworkers have shown conversion of hexafluoropropene to mixtures of *Z*- and *E*-1,2,3,3,3-pentafluoropropene and 2,3,3,3-tetrafluoropropene by *cis*-[Ru(dmpe)₂H₂].¹⁹ In the reactions of [Rh(H)(PEt₃)₃] with hexafluoropropene, Braun *et al.* found that only the olefinic C–F bonds are activated, producing 1,1,1-

[†] The work presented in this chapter has been accepted to *Organometallics* as an invited publication. Slaney, M.E.; Ferguson, M.J.; McDonald, R.; Cowie, M. Accepted, *Organometallics*, Jan. 11, 2012. Manuscript ID: om-2011-011968

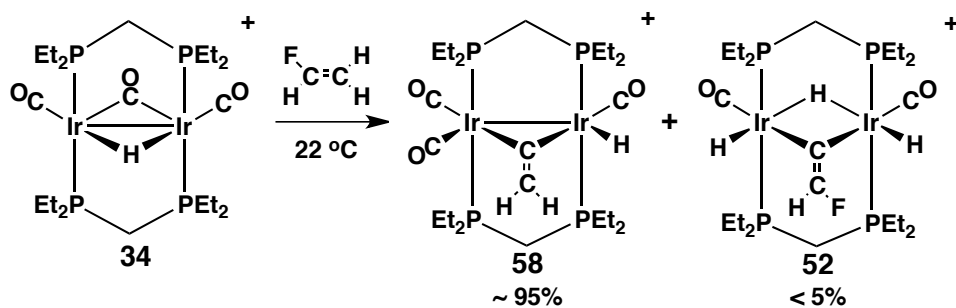
trifluoropropane under a hydrogen atmosphere.^{20,24,30} Also with late metals, Caulton and coworkers reported that the osmium-hydride complex, $[\text{Os}(\text{H})_3\text{Cl}(\text{P}^i\text{Pr}_3)_2]$ reacts with vinyl fluoride and 1,1-difluoroethylene to produce a variety of condition-specific products, including the carbyne complex, $[\text{Os}(\text{H})(\text{F})(\text{Cl})(\equiv\text{CCH}_3)(\text{P}^i\text{Pr}_3)_2]$,²² while a similar complex, namely $[\text{Os}(\text{H})_2(\text{CO})(\text{P}^t\text{Bu}_2\text{Me})_2]$, converts vinylfluoride to ethylene in the presence of a tertiary silane.²⁵

Our approach in bringing about C–F activation in fluoroolefins has involved the use of pairs of metals for the cooperative and selective activation of these substrates. The bridging fluoroolefins in $[\text{Ir}_2(\text{CH}_3)(\text{CO})_2(\mu\text{-olefin})(\text{dppm})_2]^+$ (dppm = $\mu\text{-Ph}_2\text{PCH}_2\text{PPh}_2$; olefin = C_2F_4 , $\text{C}_2\text{F}_3\text{H}$ or $1,1\text{-C}_2\text{F}_2\text{H}_2$) undergo facile fluoride-ion abstraction by Lewis or Brønsted acids, including water,⁶⁴⁻⁶⁶ and in one exceptional case the activation of 1,1-difluoroethylene was promoted under a CO atmosphere leading to complete dehydrofluorination of this group.⁶⁶ Following C–F bond activation in these fluoroolefins, a series of C–C and C–H bond-forming reactions have allowed the conversion of tetrafluoroethylene to trifluoroethylene, the conversion of trifluoroethylene into *cis*-difluoroethylene, 1,2-difluoropropene, 2,3-difluoropropene and 1,1,1-trifluoroethane, and the conversion of 1,1-difluoroethylene to 2-fluoropropene.^{65,66}

In an attempt to extend the scope of cooperative C–F activation by binuclear complexes we have made two key modifications. First, we have replaced the bridging dppm groups by the smaller, more basic depm (*bis*(diethylphosphino)methane, $\text{Et}_2\text{PCH}_2\text{PEt}_2$), in order to improve access of the fluoroolefins to the metals and to utilize the ligand basicity as an aid in stabilizing the cationic products of fluoride-ion removal. In addition, we have replaced the methyl ligand in the above complex by a hydride ligand in order to determine what role this ligand might play in the C–F activation process and in the replacement of fluorines in fluoroolefin substrates. The initial results of this study are reported herein.

5.2 Results

5.2.1 Activation of vinyl fluoride. The reaction of $[\text{Ir}(\text{CO})_3(\mu\text{-H})(\text{dep}m)_2][\text{BAr}^{\text{F}}_4]$ ($\text{BAr}^{\text{F}}_4^- = [\text{B}(3,5\text{-}(\text{CF}_3)_2\text{C}_6\text{H}_3)_4]^-$) (**34**) with vinyl fluoride at ambient temperature results in the formation of $[\text{Ir}_2(\text{H})(\text{CO})_3(\mu\text{-C}=\text{CH}_2)(\text{dep}m)_2][\text{BAr}^{\text{F}}_4]$ (**58**) and $[\text{Ir}_2(\text{H})_2(\text{CO})_2(\mu\text{-H})(\mu\text{-C}=\text{CHF})(\text{dep}m)_2][\text{BAr}^{\text{F}}_4]$ (**52**) in an approximate 20:1 ratio after 30 min, as shown in Scheme 5.1. The major product, compound **58**, a vinylidene-bridged compound, is the apparent result of simultaneous C–F and C–H activation of the geminal hydrogen/fluorine pair in vinyl fluoride, while the minor product **52**, a fluorovinylidene compound, is the result of double C–H activation of the geminal hydrogens, accompanied by CO loss. Repeating the reaction of **34** with vinyl fluoride in the presence of trimethylamine-*N*-oxide (TMNO) results in the exclusive formation of **34** after 10 min, indicating that CO loss is the rate-determining step in the double geminal C–H bond activation process, while performing the reaction in the presence of added water (*ca.* 5 equiv) results in the exclusive formation of **58**, again in only 10 minutes, indicating that water is involved in the C–F activation pathway. Much of the chemistry reported herein was carried out using the $[\text{BAr}^{\text{F}}_4]^-$ anion since it gave the best results for obtaining solid samples. However, as noted in the Experimental section, even with this anion, we were often unsuccessful in obtaining solid samples; our inability to obtain crystalline samples remains one of the disadvantages of *dep*m in this study.



Scheme 5.1 – Reaction of compound **34** with vinyl fluoride.

Compound **58** displays two multiplets (appearing as pseudo-triplets) in the $^{31}\text{P}\{^1\text{H}\}$ NMR spectrum at δ -8.1 and -16.9 , consistent with the chemical inequivalence of the metal centres and the resulting inequivalence of the different ends of the bridging diphosphines. The ^1H NMR spectrum shows two vinylidene protons as singlets at δ 6.33 and 6.29 , two multiplets corresponding to the methylene groups linking the two PEt_2 moieties of each depm ligand at δ 2.71 and 2.09 , an upfield triplet at δ -11.95 with coupling to the pair of neighboring phosphines ($^2J_{\text{HP}} = 16.2$ Hz), and the ethyl resonances in their expected positions (all having the appropriate integrations). The ^1H NMR spectrum also displays a broad singlet at δ 12.0 , indicating the formation of HF as a byproduct, which also appears in the ^{19}F NMR spectrum as a broad singlet at δ -160 ; both signals are sufficiently broad (*ca.* 220 Hz at half height) to mask the H–F coupling, which can vary between 120 and 520 Hz, depending upon the solution species present.^{67,68} The $^{13}\text{C}\{^1\text{H}\}$ NMR spectrum of **58** displays three equal intensity carbonyl resonances at δ 179.3 , 179.0 and 164.8 , all appearing as triplets owing to coupling to the adjacent pairs of ^{31}P nuclei, and selective ^{31}P decoupling experiments establish that the hydride and the carbonyl at δ 179.0 are on one metal with the remaining pair of carbonyls bound to the other metal.

An X-ray structure determination of compound **58**, shown for the complex cation in Figure 1, is fully consistent with the structure proposed based upon NMR spectroscopy. The Ir(1) – Ir(2) separation of $2.7960(4)$ Å confirms a metal-metal interaction, while the bridging vinylidene displays a C(4) – C(5) distance ($1.330(4)$ Å) consistent with a double bond, and is unsymmetrically bridged, being closer to Ir(1) than to Ir(2) ($2.031(3)$ vs. $2.126(3)$ Å), presumably a result of greater crowding at the metal having two carbonyls attached (Ir(2)).

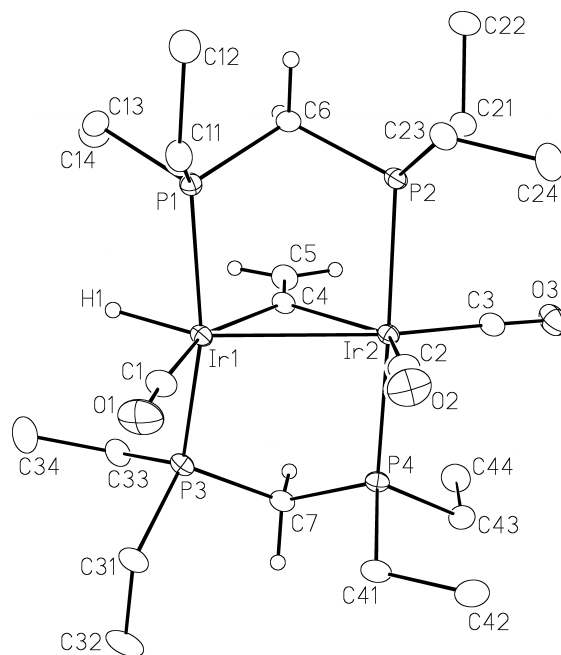


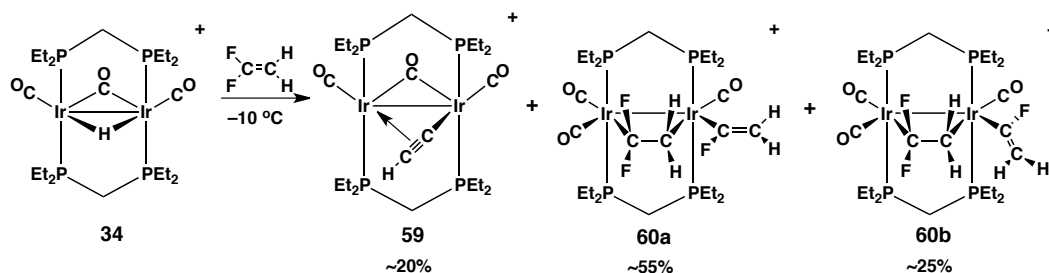
Figure 5.1 – Perspective view of the complex cation of $[\text{Ir}_2(\text{H})(\text{CO})_3(\mu\text{-C}=\text{CH}_2)(\text{depm})_2][\text{BAR}^{\text{F}}_4]$ (**58**) showing the atom labelling scheme. Non-hydrogen atoms are represented by Gaussian ellipsoids at the 20% probability level. Hydrogen atoms are shown with arbitrarily small thermal parameters except for *depm* ethyl hydrogens, which are not shown. Relevant bond distances (Å) and angles (°): $\text{Ir}(1) - \text{Ir}(2) = 2.7960(4)$; $\text{Ir}(1) - \text{C}(4) = 2.031(3)$; $\text{Ir}(2) - \text{C}(4) = 2.126(3)$; $\text{C}(4) - \text{C}(5) = 1.330(4)$; $\text{C}(1) - \text{Ir}(1) - \text{C}(4) = 158.0(1)$; $\text{C}(2) - \text{Ir}(2) - \text{C}(4) = 136.0(1)$; $\text{Ir}(1) - \text{C}(4) - \text{Ir}(2) = 84.5(1)$; $\text{C}(2) - \text{Ir}(2) - \text{C}(3) = 116.1(1)$; $\text{C}(3) - \text{Ir}(2) - \text{C}(4) = 107.8(1)$; $\text{Ir}(1) - \text{C}(4) - \text{C}(5) = 143.6(2)$; $\text{Ir}(2) - \text{C}(4) - \text{C}(5) = 131.9(2)$.

Attempts to investigate the possible role of the hydride ligand in the C–F activation of vinyl fluoride by substituting the hydride ligand by deuterium (**34-D**) proved to be challenging owing to the propensity of **34** to undergo H/D exchange with adventitious water. However, labelling was achieved by the deliberate addition of 15 equiv of D_2O to a solution of **34**, forming a 4:1 mixture of **34-D** and **34** within 24 h. This mixture of isotopologues reacts with vinyl fluoride to produce a protonated version of **58**, in which the deuterium label is lost, indicating that the terminal hydride in the product originates from vinyl fluoride, and not from the original hydride or water. The substantial acceleration of the reaction upon the addition of water identifies that it plays a key role in the C–F activation process, but the role of the hydride ligand is not clear. The mechanism

of C–F activation and the role of water in these processes will be addressed for this and other fluoroolefins later in the manuscript.

The fluorovinylidene-bridged trihydride compound (**52**), the product of double C–H activation, displays two equal intensity multiplets at δ –7.1 and 9.1 in the $^{31}\text{P}\{^1\text{H}\}$ NMR spectrum, again indicating the chemical inequivalence of each end of the diphosphines. A doublet at δ 6.61 in the ^1H NMR spectrum, representing the vinylidene proton displays geminal fluorine coupling of 108.2 Hz. Three upfield signals are observed at δ –12.54, –13.09 and –15.48 (all as multiplets), in which the first two correspond to the terminal hydrides while the upfield signal corresponds to the bridging hydride. The $^{13}\text{C}\{^1\text{H}\}$ NMR spectrum of a ^{13}CO -enriched sample displays only a single broad resonance at δ 171.1; however, integration relative to compound **58** indicates that this broad signal results from the coincidental overlap of two carbonyls. The lone vinylidene fluorine appears as a doublet at δ –72.1 in the ^{19}F NMR spectrum, displaying the same geminal coupling as observed in the vinylidene proton signal. This process of double C–H activation was described in Chapter 4.⁶⁹

5.2.2 Activation of 1,1-difluoroethylene. The reaction of **34** with 1,1-difluoroethylene at –10 °C over 6 h gives three products in an approximate 1:2:1 ratio, and as noted above, water is again found to enhance the rate of reaction, in which all three products are formed within minutes when the reaction is repeated with the deliberate addition of *ca.* 15 equiv of water. One product, $[\text{Ir}_2(\text{CO})_3(\kappa^1:\eta^2\text{-C}\equiv\text{CH})(\text{depM})_2][\text{BAR}^{\text{F}}_4]$ (**59**), results from the apparent elimination of two equivalents of HF from a 1,1-difluoroethylene adduct, while the remaining 2:1 mixture consists of two isomers of $[\text{Ir}_2(\text{C}(\text{F})=\text{CH}_2)(\text{CO})_2(\mu\text{-CF}_2\text{CH}_2)(\text{depM})_2][\text{BAR}^{\text{F}}_4]$ (**60a** and **60b**), differing only in the orientation of the fluorovinyl group, as shown in Scheme 5.2. Compounds **60a** and **60b** contain *two* fluorocarbyl units, and although we were unable to observe the stepwise incorporation of the two difluoroethylene molecules, we have successfully achieved this with trifluoroethylene, as will be discussed in what follows.



Scheme 5.2 – Reaction of compound **34** with 1,1-difluoroethylene at $-10\text{ }^\circ\text{C}$.

The acetylide-bridged product (**59**) is highly reminiscent of the propynyl-bridged analogue, observed in the activation of 1,1-difluoroethylene by a dppm-bridged methyl complex.⁶⁶ Complex **59** displays a broad singlet in the $^{31}\text{P}\{^1\text{H}\}$ NMR spectrum, which changes little upon cooling to $-80\text{ }^\circ\text{C}$, while the quintet at δ 181.6 ($^2J_{\text{CP}} = 5.6\text{ Hz}$) in the $^{13}\text{C}\{^1\text{H}\}$ NMR spectrum of a ^{13}CO -enriched sample broadens slightly upon cooling. The static structure proposed should display two ^{31}P resonances, owing to the chemical inequivalence of both metals, and should also display three carbonyl resonances. We propose a fluxional process whereby the bridging acetylide group is undergoing a “windshield-wiper” process in which it migrates between the two metals as observed in other alkynyl-bridged compounds.^{66,70-74} The acetylide proton appears at δ 5.04, typical for such a group,⁷¹ and in the presence of D_2O undergoes H/D exchange to produce the deuterio-acetylide analogue, indicative of the acidic nature of acetylides. Unfortunately, this rapid H/D exchange does not allow us to obtain information regarding the role of the hydride ligand in the formation of **59** by use of deuterium labelling of **34**.

Compound **60a**, the major product formed, displays a broad multiplet at δ -23.1 and a pseudo-triplet at δ -26.9 in the $^{31}\text{P}\{^1\text{H}\}$ NMR spectrum. The breadth of the downfield signal results from additional ^{19}F -coupling involving the μ - CF_2CH_2 group, as verified by $^{31}\text{P}\{^1\text{H}, ^{19}\text{F}\}$ NMR experiments. In the ^1H NMR spectrum the two fluorovinyl protons appear at δ 5.55 and 4.45, with cis ($^3J_{\text{HF}} = 28.1\text{ Hz}$) and trans coupling ($^3J_{\text{HF}} = 62.1\text{ Hz}$) respectively, to the single fluoro substituent, which appears in the ^{19}F NMR spectrum as a doublet of doublets at δ

–53.4 (^{31}P coupling is not observed for this signal), as shown in Figure 5.2. Selective ^{31}P decoupling experiments show minor, unresolved coupling between the fluorovinyl protons and the upfield phosphorus signal, indicating that the fluorovinyl moiety is bound to the same metal as the “CH₂” end of the $\mu\text{-C}_2\text{F}_2\text{H}_2$

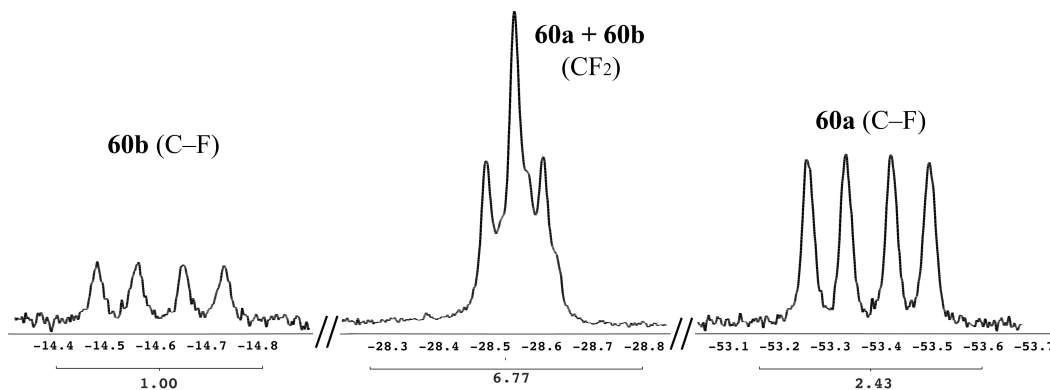


Figure 5.2 – The $^{19}\text{F}\{^{31}\text{P}\}$ NMR spectrum (376 MHz) of a mixture of compounds **60a** and **60b**. The bridging olefin appears as a pair of overlapping triplets for **60a** and **60b**, with the latter slightly offset, resulting in the upfield shoulder feature at δ –28.6. Integrations are shown underneath.

group. Similarly, the methylene protons of the bridging $\text{C}_2\text{F}_2\text{H}_2$ group appear as a multiplet in the ^1H NMR spectrum, which upon selective decoupling of the upfield ^{31}P signal collapses to a pseudo-triplet at δ 1.58 due to coupling to the adjacent CF_2 fluorines (21.1 Hz). The single resonance for the bridging difluoroethylene unit at δ –28.6 in the ^{19}F NMR is consistent with "top/bottom" mirror symmetry about the equatorial plane of the metals and displays coupling to the pair of olefin protons. Three carbonyl resonances appear in the $^{13}\text{C}\{^1\text{H}\}$ NMR spectrum at δ 177.1, 174.6 and 151.6 (the downfield signal as a multiplet while the other signals are broad singlets), and selective ^{31}P -decoupling experiments confirm that the upfield and downfield carbonyls are found on one metal, while also defining the orientation of the fluoroolefin as having the pair of fluorines adjacent to these carbonyls, as shown by the collapse of the signal at δ 177.1 to a triplet ($^3J_{\text{CF}} = 17.7$ Hz) upon ^{31}P -decoupling, displaying residual coupling to the pair of fluorines.

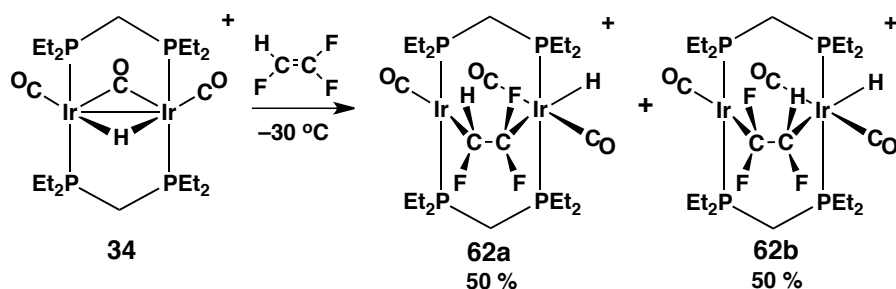
The minor isomer **60b** displays similar spectroscopic parameters to **60a**, with two signals in the $^{31}\text{P}\{^1\text{H}\}$ NMR spectrum at δ –24.2 and –28.7; the former

is again broad owing to coupling to the adjacent “CF₂” fragment of the bridging C₂F₂H₂ unit, while the latter appears as a pseudo-triplet. The ¹H NMR spectrum displays two vinyl protons, each as doublets at δ 5.01 and 3.77, cis (³J_{HF} = 29.8 Hz) and trans (³J_{HF} = 64.1 Hz) coupling, respectively, to the vinylic fluorine, together with minor unresolved coupling to the upfield ³¹P signal, indicating that the fluorovinyl group is again adjacent to the “CH₂” portion of the bridging 1,1-difluoroethylene unit, as for compound **60a**. The methylene protons of the bridging C₂F₂H₂ unit appear as a multiplet at δ 1.31, which upon ³¹P-decoupling (either broadband or selective at δ -28.7) collapses to a pseudo-triplet (³J_{HF} = 21.2 Hz) in which coupling to the adjacent fluorines remains. The ¹⁹F NMR spectrum displays two signals (Figure 2), a doublet of doublets at δ -14.6 due to the vinylic fluorine, with couplings matching those observed in with the vinylic proton resonances, while the “CF₂” unit of the bridging olefin overlaps with the equivalent signal from **60a**. Phosphorus decoupling simplifies the overlapping signals to triplets, with the resonance from **60b** appearing as a slightly upfield-shifted shoulder on the signal for **60a**; integration confirms that the CF₂ resonance for **60b** is overlapping with the signal for **60a**. Three carbonyl resonances are observed in the ¹³C{¹H} NMR spectrum at similar shifts to those of **60a**. The similarities in all spectral parameters of **60a** and **60b**, *except* for the chemical shifts of the vinyl fluorines, which indicates significantly different environments for these substituents, suggest that their difference is a result of rotation of this fluorovinyl group around the Ir–C bond. Presumably the crowded octahedral environment at Ir results in a significant barrier to rotation. Consistent with this interpretation, a spin-saturation transfer experiment at 0 °C, in which saturation of the vinyl proton signal at δ 5.01 of compound **60b** results in the disappearance of the corresponding signal at δ 5.55 for compound **60a**, demonstrating exchange between these isomers

Increasing the temperature above 0 °C results in the conversion of both **60a** and **60b** to an initial vinylidene-bridged product, which slowly converts to a second vinylidene-bridged product after 12 h; both products are the result of C–F activation of the fluorovinyl moiety and accompanying loss of difluoroethylene.

The only signals evident in the ^{19}F NMR spectrum after these transformations are those of the free olefin, $\text{BAr}_4^{\text{F}-}$ and “HF”. This transformation is the result of adventitious water, as confirmed by the rate enhancement upon the deliberate addition of water. Both products appear to have the formulation $[\text{Ir}(\text{OH})(\text{CO})_3(\mu\text{-C}=\text{CH}_2)(\text{dep}_m)_2]^+$ (**61a** and **61b**; possibly also having coordinated H_2O), as confirmed by three distinct carbonyl resonances in the ^{13}C NMR spectrum; however our inability to identify the coordination modes of the presumed hydroxido ligands owing to our inability to identify the ^1H NMR resonances of this group (in the presence of H_2O) and our inability to separate these species does not allow their structural characterization. Identification of the vinylidene ligands is unambiguous in the ^1H NMR spectrum, with **61a** displaying two doublets at δ 6.32 and 5.81 ($^2J_{\text{HH}} = 3.8$ Hz), while **61b** shows two resonances at δ 6.05 and 6.00 ($^2J_{\text{HH}} = 4.6$ Hz).

5.2.3 Activation of trifluoroethylene. Compound **34** reacts with trifluoroethylene (*ca.* 5 equiv) over 2 h at -30 °C to give a 1:1 mixture of two isomers of $[\text{Ir}_2(\text{H})(\text{CO})_3(\mu\text{-CFHCF}_2)(\text{dep}_m)_2][\text{BAr}_4^{\text{F}}]$ (**62a** and **62b**), both the result of trifluoroethylene coordination in the position bridging the two metal centres; these isomers differ only in the orientation of this bridging trifluoroethylene group (Scheme 5.3), as explained below.



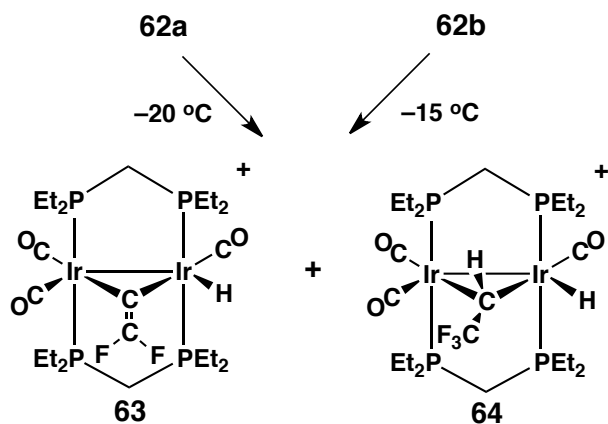
Scheme 5.3 – The addition of trifluoroethylene to compound **34** at -30 °C.

The $^{31}\text{P}\{^1\text{H}\}$ spectrum for **62a** shows two broad multiplets at δ -13.8 (2P) and -15.9 (2P), while **62b** displays three broad signals at δ -13.1 (1P), -14.6 (1P)

and -15.9 (2P). Although for each isomer all four phosphorus nuclei are chemically inequivalent and are expected to produce four signals each, as a result of the top/bottom asymmetry and the inequivalence of both metals, the slight top/bottom asymmetry resulting from the orientation of the C_2F_3H ligand, leads to coincidental overlaps in some resonances, as previously reported for the trifluoroethylene-bridged complex $[Ir_2(CH_3)(CO)_2(\mu-C_2F_3H)(dppm)_2]^+$.⁶⁵ However, the 1H NMR spectrum confirms the loss of both "top/bottom" and "front/back" symmetry with the appearance of eight unique signals corresponding to the methylene protons for the depm backbone of both isomers. The bridging trifluoroethylene proton for **62a** appears at δ 5.50, showing geminal fluorine coupling ($^2J_{HF} = 65.6$ Hz), while for **62b** this signal appears at δ 5.13, ($^2J_{HF} = 64.5$ Hz); however, the breadth of both signals mask other fluorine couplings. The terminal hydride resonances for **62a** and **62b** appear as pseudo-triplets at δ -8.77 and -8.42 , respectively, displaying coupling to the adjacent ^{31}P nuclei. TROSEY NMR experiments confirm the bridging orientation of trifluoroethylene, with the olefinic proton showing correlation to one methylene resonance of the depm backbone for each compound. The ^{19}F NMR spectrum of **62a** and **62b** displays six fluorine signals – three belonging to the bridging fluoroolefins of each isomer (**62a**: δ -108.7 , -118.7 and -195.9); (**62b**: δ -93.5 , -104.2 and -216.5). The distinct geminal F–F couplings for **62a** and **62b** ($^2J_{FF} = 198.3$, 155.3 Hz, respectively) confirms rehybridization of the bridging group towards sp^3 , with the large geminal coupling exceeding that of sp^2 -hybridized fluoroolefins.^{75,76} The $^{13}C\{^1H\}$ NMR spectrum displays three terminal carbonyl resonances for each compound (**62a**: δ 188.1 , 183.7 and 182.2); (**62b**: δ 187.6 , 185.8 and 182.3). In the case of **62a**, the upfield and downfield carbonyl signals show mutual trans coupling ($^2J_{CC} = 42.9$ Hz), while the remaining signal appears as a broad doublet ($^3J_{CF} = 15.8$ Hz), confirming its location opposite the "CFH" end of the olefin. For compound **62b**, a mutual trans carbonyl coupling ($^2J_{CC} = 41.8$ Hz) is again evident, this time between two downfield resonances, while the remaining signal appears as a broad triplet ($^3J_{CF} = 12.4$ Hz), indicating its location trans to the "CF₂" end of the olefin. Further support for the proposed ligand arrangement in

62a and **62b** is evident in the HMBC NMR spectrum, in which exclusive correlation between the hydride ligand and the two mutually trans carbonyls is observed for each compound. Interestingly, compounds **62a** and **62b** are the only ones in this study to assume the geometries in which one metal is square planar and coordinatively unsaturated, while the other is octahedral and saturated. Most others have a pseudo-symmetrical ligand arrangement having two terminal and one bridging ligand (omitting depm) at each metal.

Warming the mixture of the trifluoroethylene-bridged isomers (**62a** and **62b**) to $-20\text{ }^{\circ}\text{C}$ results in the conversion of **62a** to a 1:1 mixture of $[\text{Ir}_2(\text{H})(\text{CO})_3(\mu\text{-C}=\text{CF}_2)(\text{dep}_m)_2][\text{BAR}^{\text{F}}_4]$ (**63**) and $[\text{Ir}_2(\text{H})(\text{CO})_3(\mu\text{-CHCF}_3)(\text{dep}_m)_2][\text{BAR}^{\text{F}}_4]$ (**64**) after 5 h, while leaving **62b** intact at this temperature. Warming slightly to $-15\text{ }^{\circ}\text{C}$ results in the disappearance of **62b** after 5 h and a corresponding increase in the concentrations of **63** and **64**, which remain in a 1:1 ratio, as shown in Scheme 5.4. Compound **63**, the difluorovinylidene analogue to **58**, results from geminal C–H/C–F activation of the bridging trifluoroethylene ligand, while the 2,2,2-trifluoroethylidene-bridged compound **64** is a result of a [1,2]-fluoride shift within the bridging trifluoroethylene units of **62a** and **62b**. Performing this reaction in the presence of added water greatly enhances the rate of conversion to both products (1 h vs. 5 h), again suggesting that water is playing a pivotal role in the activation processes.



Scheme 5.4 – Warming compounds **62a** and **62b** to form a mixture of **63** and **64**.

Compound **63** displays NMR parameters nearly identical to those of **58**, with the exception of two mutually coupled doublets in the ^{19}F NMR spectrum at $\delta -68.4$ and -77.2 ($^2J_{\text{FF}} = 98.6$ Hz). The terminal hydride appears at $\delta -12.46$ in the ^1H NMR spectrum as a triplet of doublets, the doublet resulting from long-range coupling to a fluorine of the bridging difluorovinylidene unit ($^4J_{\text{HF}} = 7.7$ Hz).

An X-ray structure determination of **63** confirms the formulation noted above, revealing a bridged difluorovinylidene group adjacent to the hydride ligand, as shown in Figure 5.2. The iridium/iridium separation ($\text{Ir}(1) - \text{Ir}(2) = 2.7914(5)$ Å) is consistent with a metal/metal interaction, and much like compound **2**, the vinylidene unit is bound more strongly to the hydride-containing iridium ($\text{Ir}(1) - \text{C}(4) = 2.08(1)$ Å, $\text{Ir}(2) - \text{C}(4) = 2.03(1)$ Å, presumably a consequence of less crowding at this metal. All other crystallographic parameters are as expected, and are in close agreement to those of compound **58**.

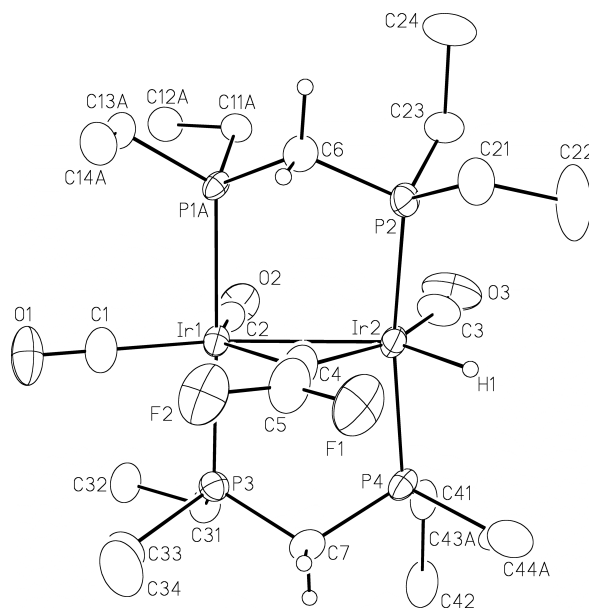
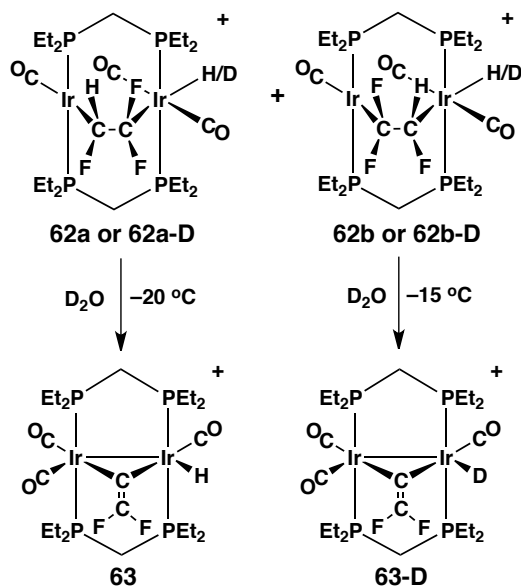


Figure 5.3 – Perspective view of the complex cation of $[\text{Ir}_2(\text{H})(\text{CO})_3(\mu\text{-C}=\text{CF}_2)(\text{depm})_2][\text{BARF}_4]$ (**63**) showing the atom labelling scheme. Thermal parameters are as described in Figure 5.1. Relevant bond distances (Å) and angles ($^\circ$): $\text{Ir}(1) - \text{Ir}(2) = 2.7914(5)$; $\text{Ir}(1) - \text{C}(4) = 2.08(1)$; $\text{Ir}(2) - \text{C}(4) = 2.03(1)$; $\text{C}(4) - \text{C}(5) = 1.28(2)$; $\text{C}(1) - \text{Ir}(1) - \text{C}(2) = 114.9(5)$; $\text{C}(1) - \text{Ir}(1) - \text{C}(4) = 108.4(5)$; $\text{C}(2) - \text{Ir}(1) - \text{C}(4) = 136.7(5)$; $\text{C}(3) - \text{Ir}(2) - \text{C}(4) = 158.7(7)$; $\text{Ir}(1) - \text{C}(4) - \text{Ir}(2) = 85.5(5)$, $\text{F}(1) - \text{C}(5) - \text{F}(2) = 106(1)$.

Deuterium labelling of the terminal hydride of **62a** and **62b** (by starting with **34-D**), in conjunction with the differing reaction rates of **62a** and **62b** enables us to obtain some mechanistic information regarding their conversion to compound **63**. Compound **64** forms from a [1,2]-fluoride shift with the deuterium incorporation found exclusively at the terminal hydride position, with no deuterium incorporation into the trifluoroethylidene unit. As shown in Scheme 5.5, reaction of either **62a** or its deuterio analogue (**62a-D**) with D₂O yields **63**, in which the terminal hydride position is completely protonated, indicating that trifluoroethylene is the source of this hydride ligand. However, compound **62b** or **62b-D** reacts with D₂O to produce **63-D**, in which the hydride is completely deuterated, and therefore originating from D₂O. The significance of this study will be addressed later.



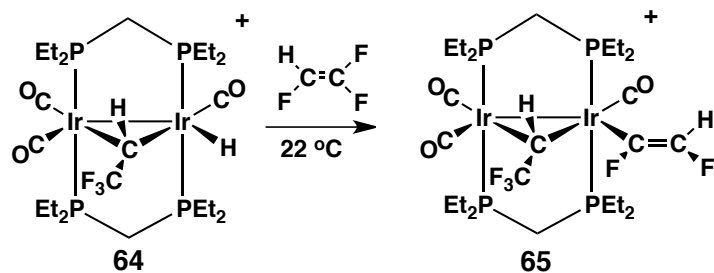
Scheme 5.5 – Deuterium labelling of **62a** and **62b** and subsequent warming to form **63**.

The 2,2,2-trifluoroethylidene-bridged species (**64**) displays four signals in the ³¹P{¹H} spectrum, indicative of four inequivalent phosphorus environments, with pairs of signals displaying large mutual coupling of (351.9 and 302.9 Hz) consistent with a mutually trans arrangement of the diphosphines at both metals. The proton of the bridging 2,2,2-trifluoroethylidene group appears as a broad

multiplet at δ 4.94 in the ^1H NMR spectrum resulting from coupling to four phosphorus and three fluorine nuclei, and broad-band ^{31}P -decoupling results in collapse of this signal to a quartet ($^3J_{\text{HF}} = 17.0$ Hz), while the hydride signal appears at δ -10.52 as a broad multiplet. Three terminal carbonyl signals were found in the $^{13}\text{C}\{^1\text{H}\}$ NMR, all appearing as multiplets, while the ^{19}F NMR spectrum displays a doublet at δ -46.6 ($^3J_{\text{FH}} = 17.0$ Hz) – a shift typical for a bridging trifluoroethylidene group.^{46,47,65}

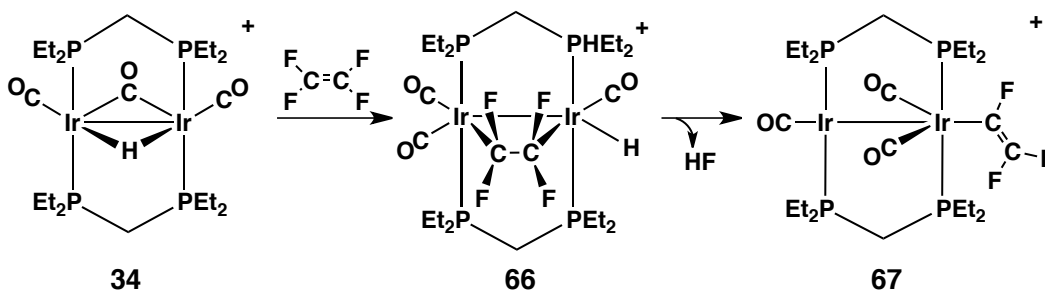
Interestingly, in the presence of excess trifluoroethylene, compound **64** converts to $[\text{Ir}_2(\text{C}(\text{F})=\text{CFH})(\text{CO})_3(\mu\text{-CHCF}_3)(\text{depn})_2][\text{BAR}^{\text{F}}_4]$ (**65**) overnight at ambient temperatures, the result of C–F bond activation of a second equivalent of trifluoroethylene, as outlined in Scheme 5.6. Again, the deliberate addition of water results in an order-of-magnitude rate increase. The NMR spectral parameters for **65** are similar to those of **64**, apart from the additional resonances of the *cis*-difluorovinyl proton group and the disappearance of the hydride resonance. The difluorovinyl proton appears as a doublet of doublets at δ 5.75 in the ^1H NMR spectrum with geminal (81.6 Hz) and trans (24.1 Hz) fluorine coupling, while the two additional fluorine resonances at δ -84.4 and -138.1 each appear as doublets in the ^{19}F NMR spectrum, with the former showing trans proton coupling and the latter displaying geminal proton coupling. Surprisingly, no *cis* coupling is observed between the two fluorine resonances, however the chemical shifts of the two ^{19}F signals, in conjunction with the coupling values observed with the vinylic proton, lead us to assign the *cis* arrangement. The stepwise transformations of **34** through **64** followed by the conversion of **64** to **65** are reminiscent of the reaction of **34** with 1,1-difluoroethylene, in which two equivalents of fluoroolefin were again incorporated, except that incorporation of the second equivalent of trifluoroethylene, did not occur until after isomerization of the first equivalent to a bridging trifluoroethylidene group (**64**). Although for 1,1-difluoroethylene we were unable to observe intermediates involving the first equivalent of $\text{C}_2\text{F}_2\text{H}_2$, the reaction of **34** with trifluoroethylene demonstrates the *stepwise* C–F activation of two fluoroolefins units. It is curious that the

structurally similar difluorovinylidene-bridged species does not also incorporate a second C_2F_3H unit.



Scheme 5.6 – Reaction of compound **64** with a second equivalent of trifluoroethylene.

5.2.4 Activation of tetrafluoroethylene. Compound **34** reacts with tetrafluoroethylene at 0 °C over 1 h to produce the tetrafluoroethylene-bridged complex, $[Ir_2(H)(CO)_3(\mu-CF_2CF_2)(depm)_2][BAR^F_4]$ (**66**) in ~60 % yield based upon $^{31}P\{^1H\}$ NMR integrations (Scheme 5.7) together with unidentified decomposition products. Compound **66** has resulted from C_2F_4 -coordination in the bridging site, accompanied by movement of the hydride ligand from a bridging to a terminal position. As such, compound **66** very much resembles the trifluoroethylidene-bridged species (**64**), while having a surprisingly different structure from those of the trifluoroethylene adducts **62a** and **62b**. This product gives rise to two broad resonances in the $^{31}P\{^1H\}$ NMR spectrum, the breadth of which is a consequence of ^{19}F coupling from the adjacent “ CF_2 ” units of the bridging tetrafluoroethylene ligand. The terminal hydride appears in the 1H NMR spectrum at $\delta -12.63$ as a triplet of triplets, displaying coupling to the adjacent pair of ^{31}P nuclei and to two fluorines from one end of the bridging tetrafluoroethylene moiety ($^2J_{HP} = 17.3$ Hz, $^3J_{HF} = 17.3$ Hz). The ^{19}F NMR spectrum displays a triplet at $\delta -74.4$ and a doublet of triplets $\delta -80.7$, with each displaying coupling to different pairs of phosphorus nuclei as well as coupling to the terminal hydride ($^3J_{FH} = 17.3$ Hz) for the second signal. Surprisingly, no F–F coupling was observed in either signal.



Scheme 5.7 – Reaction of compound **34** with tetrafluoroethylene.

Monitoring the reaction for longer periods (> 12 h) shows the formation of two other products, namely $[\text{Ir}_2(\text{C}(\text{F})=\text{CF}_2)(\text{CO})_3(\text{dep}_m)_2][\text{BAR}^{\text{F}}_4]$ (**67**) (*ca.* 20 %), the result of C–F activation of the bridging tetrafluoroethylene unit with concomitant loss of the hydride ligand and $[\text{Ir}_2(\text{C}_2\text{F}_3)(\text{CO})_x(\mu\text{-C}_2\text{F}_4)(\text{dep}_m)_2][\text{BAR}^{\text{F}}_4]$ (**68**) (< 5%) containing an intact tetrafluoroethylene and a trifluorovinyl group. The incomplete characterization of this minor species has not allowed us to determine its origin. The rate of this transformation is again enhanced upon the addition of 5 equiv of water, increasing the yield of **67** to *ca.* 40 % after 2 h, but with no appreciable change in the quantity of **68** produced. Attempts to favour the formation of **68** by increasing the temperature to 40 °C or increasing the pressure of tetrafluoroethylene had no result.

Compound **67** displays two resonances in the $^{31}\text{P}\{^1\text{H}\}$ NMR spectrum indicating the inequivalence of the two metals. In the ^1H NMR spectrum only *dep*_m resonances appear, with the bridging methylene protons of the *dep*_m backbone appearing as a single resonance, indicative of front/back symmetry about the Ir_2P_4 plane. The ^{19}F NMR spectrum displays three signals for the trifluorovinyl moiety at δ –93.8, –123.9 and –136.1, each appearing as a doublet of doublets ($^3J_{\text{FFtrans}} = 111.6$ Hz, $^2J_{\text{FF}} = 93.0$ Hz, and $^3J_{\text{FFcis}} = 39.7$ Hz). The 2:1 ratio of carbonyl resonances in the $^{13}\text{C}\{^1\text{H}\}$ NMR spectrum and the apparent "front/back" symmetry leads us to suggest the structure shown in Scheme 7, with a terminal trifluorovinyl group on the metal containing two carbonyls, while the other metal has the remaining carbonyl.

As noted above, compound **68** is never obtained in an appreciable yield, even after extended periods (2 days) or upon heating (40 °C) and has only been identified by ^{19}F NMR spectra owing to our inability to locate its $^{31}\text{P}\{\text{H}\}$ and $^{13}\text{C}\{\text{H}\}$ resonances. Nevertheless, the five signals in a 2:2:1:1:1 ratio in the ^{19}F NMR identifies that two fluorocarbyl groups are present; two signals appear for each set of olefinic CF_2 -units ($\delta -76.3$ and -80.4), with three signals at $\delta -94.3$, -121.3 and -132.4 , showing mutual coupling ($^3J_{\text{FFtrans}} = 110.8$ Hz, $^2J_{\text{FF}} = 92.9$ Hz, $^3J_{\text{FFcis}} = 33.4$ Hz), identifying the trifluorovinyl group.

5.3 Discussion

We initiated our current investigation into the C–F bond activation in fluoroolefins, promoted by a pair of adjacent metals, using depm (*bis*(diethylphosphino)methane) as an ancillary bridging ligand, on the assumption that this smaller and more basic diphosphine would result in enhanced reactivity over our previously studied dpmm-bridged complexes. This has certainly proven to be the case in a number of ways. First, a comparison of $[\text{Ir}_2(\text{CO})_3(\mu\text{-H})(\text{depmm})_2]^+$ (**34**) and its dpmm analogue has shown that while the latter is unreactive to all fluoroolefins studied in this report the depm compound (**34**) reacts readily with all of them. Second, although we had observed water-promoted C–F activation in some of the previous dpmm chemistry,^{65,66} this involvement was not nearly as extensive as it has proven to be in the current depm system, as will be discussed. Furthermore, in much of the chemistry reported herein, the smaller size of depm (and possibly its greater basicity) has allowed the incorporation of two fluoroolefin-derived fragments, whereas with dpmm only a single fluorocarbyl unit was incorporated. The facile incorporation of two fluoroolefins was most prevalent with 1,1-difluoroethylene, occurring readily, even at low temperature.

5.3.1 Trifluoroethylene Activation. Of the four fluoroolefins investigated (vinyl fluoride, 1,1-difluoroethylene, trifluoroethylene and tetrafluoroethylene) we initiate our discussion with trifluoroethylene, since this fluoroolefin is the best behaved, in the sense that the stepwise transformations could be easily followed

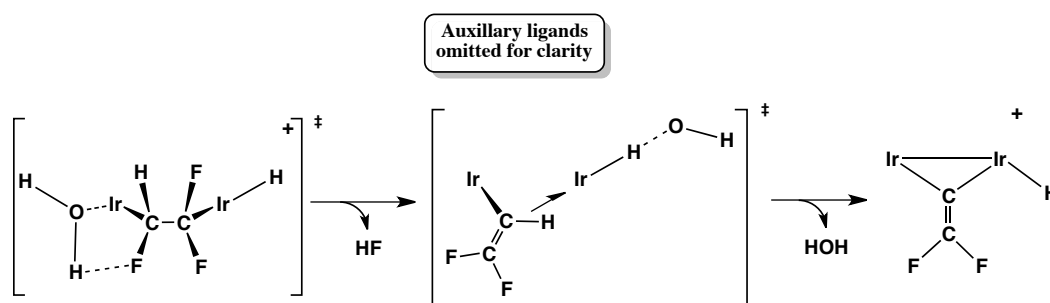
in which the reactions first yielded an olefin adduct, followed by its C–F activation, and (for one C–F activation product) the incorporation of a second fluoroolefin, accompanied by its C–F activation.

As shown earlier in Scheme 5.3, reaction of **34** with trifluoroethylene yields two isomeric adducts in which the fluoroolefin unit bridges the pair of metals, differing only in its orientation with respect to the chemically inequivalent metal centres. Both isomers react further to yield the same two final products, although the isomer having the “CHF” end of the olefin adjacent to the Ir^(I) centre (**62a**) reacts at slightly lower temperature than the isomer having this end of the olefin adjacent to the Ir^(III) centre (**62b**). It appears that the slower conversion of **62b** to subsequent products cannot be rationalized on the basis of its prior isomerization to **62a**, since spin-saturation transfer experiments failed to detect isomerization between these isomers at –20 °C. Furthermore, the conversion of **62a** to **63** and **64** at –20 °C is sufficiently slow (1 h) that the isomerization of **62b** to **62a** should be visible upon warming, which is not observed. Finally, the different H/D labelling studies for the two isomers indicate that **62a** cannot be a common intermediate.

Both products in the conversion of **62a** and **62b** are the result of fluoride-ion loss; in one case fluoride-ion recoordination at the β -carbon of the resulting 2,2-difluorovinyl group occurs (formally a 1,2-fluoride shift) to give a 2,2,2-trifluoroethylidene-bridged product (**64**), while in the second case the fluoride ion is eliminated as HF, accompanied by subsequent C–H activation, yielding the difluorovinylidene-bridged product (**63**). Formation of **64** is not surprising, having been previously observed in the dpmm system, and being favoured by the increase in C–F bond strengths that occurs upon increasing the fluorine substitution at carbon.⁶⁵ The acceleration of this 1,2-fluoride shift in the presence of water leads us to suggest that fluoride-ion transfer is water assisted. Given that this 1,2-shift involves loss of fluoride ion from the “CHF” end of the olefin and recoordination at the “CF₂” end, the somewhat more facile transfer involving **62a** can be rationalized by greater π -back donation from the Ir^(I) centre into the adjacent C–F σ^* orbital in this isomer. In isomer **62b**, the “CHF” end is bound to

the Ir^(III) centre from which π -back donation and the resulting labilization of the fluoride ion should be less (see Scheme 3 for the structures of **62a** and **62b**).

In the transformation of isomers **62a** and **62b** to **63**, formally by HF loss, water again plays a role, as seen by acceleration upon H₂O addition. Labelling studies have proved useful in allowing us to propose a mechanism for the C–F and C–H activation steps in converting the trifluoroethylene ligand in **62a** to the difluorovinylidene ligand in **63**. In the reactions of **62a** and the deuteride analogue (**62a-D**), carried out in the presence of D₂O, compound **63** is observed exclusively as the hydride, with no deuterium incorporation. This hydride can only come from the trifluoroethylene ligand. We propose that HF loss occurs first through protonation by water, yielding the 2,2-difluorovinyl group as shown in Scheme 5.8. Presumably, H₂O coordination at the vacant site on the unsaturated metal adjacent to the “CHF” end of the olefin increases its acidity allowing protonation of the nearby fluorine substituent, much as observed in a previous study on trifluoroethylene.⁶⁵ Water-assisted fluoride-ion abstraction involving the α -fluorines of fluoroalkyl groups has been well documented by Hughes and coworkers.^{29,51,77,78} Subsequent deprotonation of the acidic Ir–H in the dicationic intermediate can then give rise to oxidative addition of the fluorovinyl C–H bond to give the observed cis arrangement of difluorovinylidene and hydride ligands.

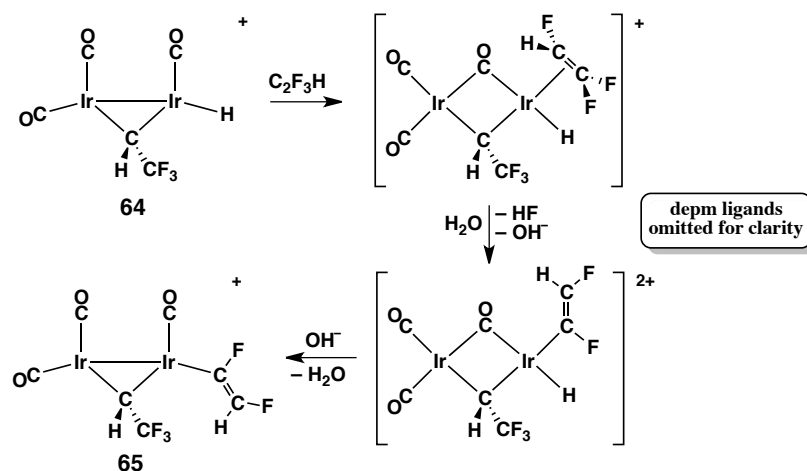


Scheme 5.8 – Proposed mechanism for C–F bond activation of trifluoroethylene in **62a** by water.

The mechanism for C–F and C–H activation in the isomer **62b** is not so easily rationalized since the same deuterium labelling experiments with this isomer give the deuteride (**63-D**) exclusively. We assume that since the rates of

reactions of **62a** and **62b**, although not identical, are very similar, the mechanisms differ only slightly, giving an isomer of **63** in which the hydride ligand migrates to its final location in **63** by a water-assisted deprotonation/reprotonation sequence, as has been observed in related dppm chemistry.⁶⁶ Proton transfer in the presence of D₂O would give predominately the deuteride (**63-D**). Activation of the C–F bond of the “CHF” end of the olefin is favoured over those at the “CF₂” end owing to the greater C–F bond strengths involving the more substituted carbon. Certainly, the isomerization of **62b** to the 2,2,2-trifluoroethylidene-bridged complex (**63**), noted above, already demonstrates the lability of this isolated fluorine.

Although the difluorovinylidene-bridged product (**63**) is unreactive towards additional trifluoroethylene, the related 2,2,2-trifluoroethylidene-bridged product (**64**) reacts with this olefin, resulting in HF loss and replacement of the hydride ligand by a *cis*-difluorovinyl group in the product (**65**; see Scheme 5.9). Acceleration of this reaction by added water again suggests water-assisted fluoride-ion loss, which would give a dicationic vinyl/hydride species, which upon deprotonation yields **65**. In Scheme 5.9 we show the trifluoroethylene group as η^2 -bound to one metal since it seems improbable that it could attain a bridging geometry in a structure already having the trifluoroethylidene group bridging on one face of the complex. However, we cannot rule out the possibility of reversible CO loss in this transformation. The exclusive formation of the *cis*-difluorovinyl group is consistent with the stability gained in this *cis* geometry through hyperconjugation,^{79,80} although it is surprising that fluoride-ion loss has not occurred from the “CHF” end of the olefin.



Scheme 5.9 – Proposed mechanism for C–F bond activation of a second equivalent of trifluoroethylene to form **64**.

5.3.2 1,1-Difluoroethylene Activation. Although, as noted earlier, no intermediates are observed in the reaction of **34** with 1,1-difluoroethylene, the formation of two of the products (isomers **60a** and **60b**; see Scheme 5.2) is reminiscent of compound **65**, in which two equivalents of the fluoroolefin have been incorporated. It is tempting, therefore, to rationalize the formation of **60a** and **60b** as occurring in a sequence paralleling that of **65**. However, we feel that this is unlikely, since we have previously shown that fluoroolefins are more susceptible to fluoride-ion loss when bridging than when terminally bound. Consistent with this idea, activation of the bridging trifluoroethylene ligand in **62** first occurs to give the trifluoroethylidene-bridged product (**64**), which subsequently reacts with the second equiv of the olefin at a slower rate. Although we have no data to support our proposal beyond the acceleration of the reaction by water, we propose water-promoted fluoride-ion loss from a 1,1-difluoroethylene-bridged intermediate, followed by deprotonation of the hydrido ligand to yield a 1-fluorovinyl complex, which subsequently coordinates the additional difluoroethylene ligand. Consistent with the idea that the second difluoroethylene ligand in **60a** and **60b** coordinates after conversion of the first to the fluorovinyl group, warming a mixture of these isomers to above 0 °C results in loss of the fluoroolefin, confirming that it was weakly bound. Fluoroolefin loss is accompanied by removal of the remaining fluorine substituent on the fluorovinyl

group yielding the two incompletely characterized vinylidene products (**61a** and **61b**) as described earlier. This is the only example in this study in which sequential activation of a pair of geminal C–F bonds occurs; for the more highly substituted fluoroolefins (C₂F₃H and C₂F₄) the stronger C–F bonds presumably inhibits loss of a second fluoride. We have previously observed double geminal C–F activation in tri- and tetrafluoroethylene;^{65,66} however, fluoride-ion removal in these cases required the very strong fluorophile, Me₃Si⁺ (as the triflate salt).

Possibly the most fascinating transformation in the chemistry reported herein, is the complete loss of both equivalents of HF from the presumed 1,1-difluoroethylene adduct of **34** to yield the acetylide-bridged product [Ir₂(CO)₃(μ–C≡CH)(depm)₂]⁺ (**59**). As noted earlier, this reactivity parallels that of the dpdm-bridged species, [Ir₂(CH₃)(CO)₂(μ–C₂F₂H₂)(dpdm)₂]⁺, which in the presence of CO slowly yielded the propynyl-bridged product [Ir(CO)₃(μ–C≡CCH₃)(dpdm)₂]⁺, again by loss of both equivalents of HF.⁶⁶ In this previous case the source of the propynyl methyl group was clearly the methyl ligand in the precursor. However, in the present case, neither the source of the acetylide hydrogen, nor the role of the hydrido ligand in the precursor could be ascertained, owing to facile H/D scrambling. How the loss of both equivalents of HF occurs remains a mystery. We considered the possibility that loss of a second fluoride ion could be catalyzed by HF generated in the first abstraction, as has already been shown by Caulton and coworkers;²² however, the addition of triethylamine, in attempts to trap the HF produced, has no effect on the product distribution shown in Scheme 5.2.

5.3.3 Tetrafluoroethylene Activation. The sequence, proposed above, for the reaction of **34** with 1,1-difluoroethylene finds support in the reactivity of compound **34** with tetrafluoroethylene, in which the tetrafluoroethylene-bridged complex (**66**) is initially formed, followed by the subsequent C–F activation of the bridging unit to produce a trifluorovinyl complex **67** (refer to Scheme 5.7). Although there is evidence for a bridging-tetrafluoroethylene/trifluorovinyl complex (**68**) that is analogous to the 1,1-difluoroethylene adducts **60a** and **60b**, its origin is uncertain, owing to its low abundance and consequent incomplete characterization.

As with all previous olefin adducts in this study, fluoride-ion removal from the tetrafluoroethylene-bridged **66** is accelerated by the addition of water. The failure of a related C₂F₄-bridged complex of dpmm, namely [Ir₂(CH₃)(CO)₂(μ-C₂F₄)(dpmm)₂]⁺, to react with water is certainly a further reflection of the influence of the more basic depm ligand on the reactivity. However, the absence of a vacant site on the saturated metals in **66**, which does not allow coordination of water, combined with the accompanying loss of the hydrido ligand, suggests a possible role of this ligand in the overall dehydrofluorination of **66**, in which water could be simultaneously involved in hydrogen bonding with a fluorine substituent and the hydrido ligand as shown in Chart 5.1, leading to loss of HF. So although the hydrido ligand is not directly involved in fluoride-ion abstraction from the fluoroolefin, this proposed hydrogen-bonding interaction should increase water's acidity, promoting HF loss.

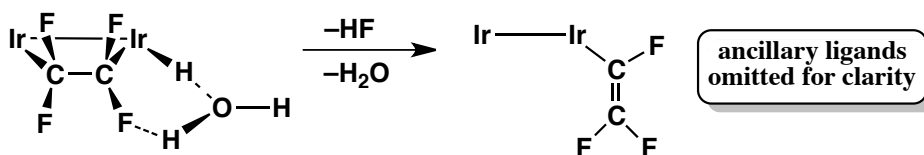


Chart 5.1 – Proposed mechanism for C–F bond activation by water.

5.3.4 Vinyl Fluoride Activation. Finally, the fluoroolefin activation about which we have the least information involves vinyl fluoride, for which no olefin adduct is observed. On the basis of our previous work and the observations discussed above we suggest that this olefin also binds in the bridging site between the metals. As for the trifluoroethylene adduct **62a**, deuterium-labelling studies indicate that the hydrido ligand in the C–H/C–F activation product originates from the fluoroolefin so we suggest a stepwise series of transformations consisting of HF loss upon protonation by water, H⁺ loss from the resulting dicationic hydrido intermediate followed by C–H bond activation of the resulting vinyl group by the adjacent metal, much as outlined in Scheme 5.8.

In summary, the depm complex [Ir₂(CO)₃(μ-H)(depmm)₂]⁺ (**34**) has proven to be much more active towards C–F bond activation than either its dpmm

analogue or the related species $[\text{Ir}_2(\text{CH}_3)(\text{CO})_2(\text{dppm})_2]^+$ (**1**). In all of the chemistry described herein, water plays a pivotal role, being involved in protonation of the coordinated fluoroolefin resulting in subsequent HF loss, and in one case, in the water-assisted 1,2-fluoride migration in trifluoroethylene, yielding a bridging 2,2,2-trifluoroethylidene group. In the two fluoroolefins investigated having a geminal arrangement of H and F substituents (vinyl fluoride and trifluoroethylene), activation of *both* of these bonds occurred in a stepwise manner in which, as described above, water-assisted fluoride-ion loss (as HF) is followed by oxidative addition of the $\alpha\text{-C-H}$ bond of the resulting vinyl or 2,2-difluorovinyl group at the adjacent metal. The hydride ligand in the precursor complex (**34**) appears to play no direct role in the activation processes, and instead appears to be lost as H^+ during the subsequent transformations, replacing the proton lost by water in protonation of a fluorine substituent.

5.4 Experimental

5.4.1 General Comments

All solvents were dried (using appropriate drying agents), distilled before use and stored under dinitrogen. Deuterated solvents used for NMR experiments were freeze-pump-thaw degassed (three cycles) and stored under nitrogen or argon over molecular sieves. Reactions were carried out under argon using standard Schlenk techniques, and compounds that were obtained as solids were purified by recrystallization. Prepurified argon and nitrogen were purchased from Praxair, and carbon-13 enriched CO (99%) was supplied by Isotec Inc. All purchased gases were used as received. Compound **34** was prepared as described.⁶⁹ Trimethylamine-*N*-oxide dihydrate was dried by azeotropic distillation as described in literature.⁸¹ All other reagents were obtained from Aldrich and were used as received (unless otherwise stated).

Proton NMR spectra were recorded on Varian Unity 400 or 500 spectrometers, or on a Bruker AM400 spectrometer. Carbon-13 NMR spectra were recorded on Varian Unity 400 or 500 or Bruker AM300 spectrometers. Phosphorus-31 and fluorine-19 NMR spectra were recorded on Varian Unity 400

or 500 or Bruker AM400 spectrometers. Two-dimensional NMR experiments (COSY, NOESY and ^1H - ^{13}C HMQC) were obtained on Varian Unity 400 or 500 spectrometers.

5.4.2 Preparation of Compounds

(a) Reaction of compound 34 with vinylfluoride. Method i) An NMR tube charged with compound **34** (54 mg, 0.031 mmol) was added 0.8 mL CD_2Cl_2 , resulting in a clear, orange solution. Vinylfluoride gas was then added via a gas-tight syringe (5 mL, 0.219 mmol), and the tube was mixed vigorously. After 30 min., NMR showed complete conversion to a mixture of $[\text{Ir}_2(\text{H})(\text{CO})_3(\mu\text{-C}=\text{CH}_2)(\text{depm})_2][\text{BAr}^{\text{F}}_4]$ (**58**) and $[\text{Ir}_2(\text{H})_2(\text{CO})_2(\mu\text{-H})(\mu\text{-C}=\text{CHF})(\text{depm})_2][\text{BAr}^{\text{F}}_4]$ (**52**) in a 20:1 ratio. The solution was transferred to a Schlenk tube and the solvent was removed under vacuum. The mixture was redissolved in 2 mL diethyl ether and 25 mL of pentane was added to induce precipitation of a yellow solid. (94 % yield of compound **58**). **Method ii)** A round-bottom flask containing compound **34** (78 mg, 0.045 mmol) dissolved in 10 mL CH_2Cl_2 was cooled to $-80\text{ }^\circ\text{C}$ via a dry ice/acetone bath. In a separate round-bottom flask, trimethylamine-*N*-oxide (4 mg, 0.053 mmol) was dissolved in 5 mL CH_2Cl_2 and cooled to $-80\text{ }^\circ\text{C}$. The TMNO solution was transferred, via cannula, to the solution of **34** followed by the addition of vinyl fluoride via a gas tight syringe (10 mL, 0.438 mmol). The solution was slowly warmed to ambient temperature and left to stir for 1 h. The solvent was then removed, leaving a yellow/orange residue. NMR of the residue revealed exclusive formation of compound **52**. Attempts to recrystallize the mixture were unsuccessful due to the high solubility of the product. (83 % yield of compound **52**). **Compound 58:** ^1H NMR (498 MHz, CD_2Cl_2 , $27\text{ }^\circ\text{C}$): δ 6.33 (s, 1H, $\mu\text{-C}=\text{CH}_2$), 6.29 (s, 1H, $\mu\text{-C}=\text{CH}_2$), 2.71 (m, 2H, depm), 2.09 (m, 2H, depm), -11.95 (t, 1H, $^2J_{\text{HP}} = 16.2$ Hz, Ir-*H*); $^{13}\text{C}\{^1\text{H}\}$ NMR (125 MHz, CD_2Cl_2 , $27\text{ }^\circ\text{C}$): δ 179.3 (t, 1C, $^2J_{\text{CP}} = 7.6$ Hz), 179.0 (t, 1C, $^2J_{\text{CP}} = 9.2$ Hz), 164.8 (t, 1C, $^2J_{\text{CP}} = 11.5$ Hz); $^{31}\text{P}\{^1\text{H}\}$ NMR (202 MHz, CD_2Cl_2 , $27\text{ }^\circ\text{C}$): δ -8.1 (t, 2P, $^2J_{\text{PP}} = 34.3$ Hz), -16.9 (t, 2P, $^2J_{\text{PP}} = 34.3$ Hz); elemental analysis

calcd (%) for Ir₂P₄F₂₄O₃C₅₅H₅₉ (1743.2): C 37.90, H 3.41; found: C 38.06, H, 3.68. **Compound 52**: Refer to Chapter 4.

(b) Reaction of compound 1 with 1,1-difluoroethylene. An NMR tube charged with compound **34** (84 mg, 0.049 mmol) was dissolved in 0.8 mL CD₂Cl₂ and cooled to -80 °C via dry ice/acetone bath. 1,1-difluoroethylene (5 mL, 0.219 mmol) was added via a gas-tight syringe and the reaction was monitored by variable temperature, multinuclear NMR spectroscopy. Leaving the mixture at -10 °C for 5 h resulted in the mixture of [Ir₂(CO)₃(μ-κ^l:η²-C≡CH)(depm)₂][BAR^F₄] (**59**), and two isomers of [Ir₂(κ^l-C(F)=CH₂)(CO)₃(μ-C₂F₂H₂)(depm)₂][BAR^F₄] (**60a** and **60b**) in a 1:2:1 ratio, respectively. Warming both **60a** and **60b** to 27 °C resulted in the conversion to [Ir₂(OH)(CO)₃(μ-C=CH₂)(depm)₂][BAR^F₄] (**61a**), and leaving the mixture at this temperature for 12 h converts **61a** to a second vinylidene-bridged product (**61b**). Attempts to isolate any product were unsuccessful due to the high solubility in polar and non-polar solvents. (76% yield of compound **61b**).

Compound 59: ¹H NMR (498 MHz, CD₂Cl₂, 27 °C): δ 5.04 (s, 1H, -C≡CH), 1.99 (m, 2H, depm), 1.72 (m, 2H, depm); ¹³C{¹H} NMR (125 MHz, CD₂Cl₂, 27 °C): δ 181.6 (quin, 3C, ²J_{CP} = 5.6 Hz); ³¹P{¹H} NMR (202 MHz, CD₂Cl₂, 27 °C): δ -6.1 (s, 4P); HRMS *m/z* calc. for [¹⁹³Ir]₂P₄O₃C₂₃H₄₅ [M*]⁺: 879.1586, found 879.1572. **Compound 60a**: ¹H NMR (400 MHz, CD₂Cl₂, -10 °C): δ 5.55 (d, 1H, ³J_{HFcis} = 28.1 Hz, C(F)=CHH), 4.45 (d, 1H, ³J_{HFtrans} = 62.1 Hz, C(F)=CHH), 3.38 (m, 2H, depm), 2.49 (m, 2H, depm), 1.58 (m, 2H, ³J_{HF} = 21.1 Hz, μ-C₂H₂F₂); ¹³C{¹H} NMR (101 MHz, CD₂Cl₂, -10 °C): δ 177.1 (m, 1C, ³J_{CF} = 17.7 Hz), 174.6 (bs, 1C), 151.6 (bs, 1C); ¹⁹F NMR (376 MHz, CD₂Cl₂, -10 °C): δ -28.6 (m, 2F), -53.4 (dd, 1F, ³J_{HFtrans} = 62.1 Hz, ³J_{HFcis} = 28.1 Hz); ³¹P{¹H} NMR (162 MHz, CD₂Cl₂, -10 °C): δ -23.1 (bm, 2P), -26.9 (t, 2P, ²J_{PP} = 38.5 Hz). **Compound 60b**: ¹H NMR (400 MHz, CD₂Cl₂, -10 °C): δ 5.01 (d, 1H, ³J_{HFcis} = 29.8 Hz, C(F)=CHH), 3.77 (d, 1H, ³J_{HFtrans} = 64.1 Hz, C(F)=CHH), 3.36 (m, 2H, depm), 2.48 (m, 2H, depm),

1.31 (m, 2H, $^3J_{\text{HF}} = 21.2$ Hz, $\mu\text{-C}_2\text{F}_2\text{H}_2$); $^{13}\text{C}\{\text{H}\}$ NMR (101 MHz, CD_2Cl_2 , -10 °C): δ 177.6 (m, 1C, $^3J_{\text{CF}} = 16.3$ Hz), 174.6 (bs, 1C), 151.5 (bs, 1C); ^{19}F NMR (376 MHz, CD_2Cl_2 , -10 °C): δ -14.6 (dd, 1F, $^3J_{\text{HFtrans}} = 64.1$ Hz, $^3J_{\text{HFcis}} = 29.8$ Hz), -28.6 (m, 2F); $^{31}\text{P}\{\text{H}\}$ NMR (162 MHz, CD_2Cl_2 , -10 °C): δ -24.2 (bm, 2P), -28.7 (t, 2P, $^2J_{\text{PP}} = 38.5$ Hz). **Compound 61a**: ^1H NMR (498 MHz, CD_2Cl_2 , 27 °C): δ 6.32 (d, 1H, $^2J_{\text{HH}} = 3.8$ Hz, $-\text{C}=\text{CHH}$), 5.81 (d, 1H, $^2J_{\text{HH}} = 3.8$ Hz, $-\text{C}=\text{CHH}$), 2.89 (m, 2H, depm), 1.95 (m, 2H, depm); $^{13}\text{C}\{\text{H}\}$ NMR (125 MHz, CD_2Cl_2 , 27 °C): δ 180.0 (t, 1C, $^3J_{\text{CP}} = 10.2$ Hz), 172.1 (b, 1C), 157.7 (b, 1C); $^{31}\text{P}\{\text{H}\}$ NMR (202 MHz, CD_2Cl_2 , 27 °C): δ -19.3 (bs, 4P). **Compound 61b**: ^1H NMR (498 MHz, CD_2Cl_2 , 27 °C): δ 6.05 (d, 1H, $^2J_{\text{HH}} = 4.6$ Hz, $-\text{C}=\text{CHH}$), 6.00 (d, 1H, $^2J_{\text{HH}} = 4.6$ Hz, $-\text{C}=\text{CHH}$), 2.91 (m, 2H, depm), 2.54 (m, 2H, depm); $^{13}\text{C}\{\text{H}\}$ NMR (125 MHz, CD_2Cl_2 , 27 °C): δ 174.0 (m, 1C), 170.9 (m, 1C), 164.1 (m, 1C); $^{31}\text{P}\{\text{H}\}$ NMR (202 MHz, CD_2Cl_2 , 27 °C): δ -14.7 (t, 2P, $^2J_{\text{PP}} = 35.5$ Hz), -21.8 (t, 2P, $^2J_{\text{PP}} = 35.5$ Hz).

(c) Reaction of compound 34 with trifluoroethylene. In an NMR tube containing compound **34** (64 mg, 0.037 mmol) dissolved in 0.8 mL CD_2Cl_2 , cooled to -80 °C in a dry ice/acetone bath, was added trifluoroethylene (5 mL, 0.219 mmol) via a gas-tight syringe. The mixture was monitored by variable temperature, multinuclear NMR spectroscopy. Keeping the mixture at -30 °C for 2 h resulted in the formation of $[\text{Ir}_2(\text{H})(\text{CO})_3(\mu\text{-CFHCF}_2)(\text{depm})_2][\text{BAr}^{\text{F}}_4]$ (**62a**) and $[\text{Ir}_2(\text{H})(\text{CO})_3(\mu\text{-CF}_2\text{CHF})(\text{depm})_2][\text{BAr}^{\text{F}}_4]$ (**62b**) in a 1:1 ratio. Warming to -20 °C shows the conversion of exclusively **62a** to a 3:1 mixture of $[\text{Ir}_2(\text{H})(\text{CO})_3(\mu\text{-C}=\text{CF}_2)(\text{depm})_2][\text{BAr}^{\text{F}}_4]$ (**63**) and $[\text{Ir}_2(\text{H})(\text{CO})_3(\mu\text{-CHCF}_3)(\text{depm})_2][\text{BAr}^{\text{F}}_4]$ (**64**), while warming to -15 °C lead to the conversion of **62b** to compounds **63** and **64**. Leaving the mixture of **63** and **64** overnight at ambient temperature leads to the conversion of **64** to $[\text{Ir}_2(\kappa^1\text{-C}(\text{F})=\text{CFH})(\text{CO})_3(\mu\text{-CHCF}_3)(\text{depm})_2][\text{BAr}^{\text{F}}_4]$ (**65**), with compound **63** remaining in solution. The mixture was transferred to a Schlenk tube and the solvent was removed under vacuum, giving a yellow resin. The resin was

redissolved in 2 mL of diethyl ether and 25 mL of pentane was added to induce precipitation of a yellow solid. The solid was further washed with 2 x 10 mL pentane and dried to produce a fine, yellow solid. (73 % yield of compound **63**). **Compound 62a**: ^1H NMR (400 MHz, CD_2Cl_2 , $-30\text{ }^\circ\text{C}$): δ 5.50 (bd, 1H, $^2J_{\text{HFgem}} = 65.6$ Hz, $\mu\text{-CF}_2\text{CFH}$), 4.07 (m, 1H, depm), 3.72 (m, 1H, depm), 2.03 (m, 1H, depm), 1.71 (m, 1H, depm), -8.77 (t, 1H, $^2J_{\text{HP}} = 12.9$ Hz, Ir-*H*); $^{13}\text{C}\{^1\text{H}\}$ NMR (101 MHz, CD_2Cl_2 , $-30\text{ }^\circ\text{C}$): δ 188.1 (dm, 1C, $^2J_{\text{CC}} = 42.9$ Hz), 183.7 (bd, 1C, $^3J_{\text{CF}} = 15.8$ Hz), 182.2 (dm, 1C, $^2J_{\text{CC}} = 42.9$ Hz); ^{19}F NMR (376 MHz, CD_2Cl_2 , $-30\text{ }^\circ\text{C}$): δ -108.7 (dd, 1F, $^2J_{\text{FFgem}} = 198.3$ Hz, $^3J_{\text{FFtrans}} = 46.9$ Hz), -118.7 (d, 1F, $^2J_{\text{FFgem}} = 198.3$ Hz), -195.9 (dd, 1F, $^2J_{\text{FHgem}} = 65.6$ Hz, $^3J_{\text{FFtrans}} = 46.9$ Hz); $^{31}\text{P}\{^1\text{H}\}$ NMR (162 MHz, CD_2Cl_2 , $-30\text{ }^\circ\text{C}$): δ -13.8 (bm, 2P), -15.9 (bm, 2P). **Compound 62b**: ^1H NMR (400 MHz, CD_2Cl_2 , $-30\text{ }^\circ\text{C}$): δ 5.13 (bd, 1H, $^2J_{\text{HFgem}} = 64.5$ Hz, $\mu\text{-CHF}_2\text{CF}_2$), 4.20 (m, 1H, depm), 3.68 (m, 1H, depm), 1.95 (m, 1H, depm), 1.86 (m, 1H, depm), -8.42 (t, 1H, $^2J_{\text{HP}} = 12.7$ Hz, Ir-*H*); $^{13}\text{C}\{^1\text{H}\}$ NMR (101 MHz, CD_2Cl_2 , $-30\text{ }^\circ\text{C}$): δ 187.6 (dm, 1C, $^2J_{\text{CC}} = 41.8$ Hz), 185.8 (dm, 1C, $^2J_{\text{CC}} = 41.8$ Hz), 182.3 (bt, 1C, $^3J_{\text{CF}} = 12.4$ Hz); ^{19}F NMR (376 MHz, CD_2Cl_2 , $-30\text{ }^\circ\text{C}$): δ -93.5 (dd, 1F, $^2J_{\text{FFgem}} = 155.3$ Hz, $^3J_{\text{FFtrans}} = 49.7$ Hz), -104.3 (d, 1F, $^2J_{\text{FFgem}} = 155.3$ Hz), -216.5 (dd, 1F, $^2J_{\text{FHgem}} = 64.5$ Hz, $^3J_{\text{FFtrans}} = 49.7$ Hz); $^{31}\text{P}\{^1\text{H}\}$ NMR (162 MHz, CD_2Cl_2 , $-30\text{ }^\circ\text{C}$): δ -13.1 (bm, 1P), -14.6 (bm, 1P), -15.9 (bm, 2P). **Compound 63**: ^1H NMR (498 MHz, CD_2Cl_2 , $27\text{ }^\circ\text{C}$): δ 2.67 (m, 2H, depm), 1.95 (m, 2H, depm), -12.46 (td, 1H, $^2J_{\text{HP}} = 15.7$ Hz, $^4J_{\text{HF}} = 7.7$ Hz, Ir-*H*); $^{13}\text{C}\{^1\text{H}\}$ NMR (125 MHz, CD_2Cl_2 , $27\text{ }^\circ\text{C}$): δ 177.2 (bm, 1C), 169.4 (bm, 1C), 159.7 (bm, 1C); ^{19}F NMR (469 MHz, CD_2Cl_2 , $27\text{ }^\circ\text{C}$): δ -68.4 (d, 1F, $^2J_{\text{FF}} = 98.6$ Hz), -77.2 (d, 1F, $^2J_{\text{FF}} = 98.6$ Hz); $^{31}\text{P}\{^1\text{H}\}$ NMR (202 MHz, CD_2Cl_2 , $27\text{ }^\circ\text{C}$): δ -6.7 (t, 2P, $^2J_{\text{PP}} = 28.5$ Hz), -16.2 (t, 2P, $^2J_{\text{PP}} = 28.5$ Hz); HRMS *m/z* calc. for $[\text{Ir}_2\text{P}_4\text{O}_3\text{C}_{23}\text{H}_{45}\text{F}_2]^{+}$: 917.1540, found 917.1543. **Compound 64**: ^1H NMR (498 MHz, CD_2Cl_2 , $27\text{ }^\circ\text{C}$): δ 4.94 (m, 1H, $^3J_{\text{HF}} = 17.0$ Hz, C(*H*) CF_3), 2.53 (m, 1H, depm), 2.51 (m, 1H, depm), 1.95 (m, 1H, depm), 1.91 (m, 1H, depm), -10.52 (bm, 1H, Ir-*H*); $^{13}\text{C}\{^1\text{H}\}$ NMR (125 MHz, CD_2Cl_2 , 27

°C): δ 177.3 (m, 1C), 176.8 (m, 1C), 159.3 (m, 1C); ^{19}F NMR (469 MHz, CD_2Cl_2 , 27 °C): δ -46.4 (d, 3F, $^3J_{\text{FH}} = 17.0$ Hz); $^{31}\text{P}\{^1\text{H}\}$ NMR (202 MHz, CD_2Cl_2 , 27 °C): δ -11.0 (dm, 1P, $^2J_{\text{PP}} = 351.9$ Hz), -17.9 (dm, 1P, $^2J_{\text{PP}} = 351.9$ Hz), -18.0 (dm, 1P, $^2J_{\text{PP}} = 302.9$ Hz), -31.2 (dm, 1P, $^2J_{\text{PP}} = 302.9$ Hz). **Compound 65:** ^1H NMR (498 MHz, CD_2Cl_2 , 27 °C): δ 5.75 (dd, 1H, $^2J_{\text{HF}} = 81.6$ Hz, $^3J_{\text{HF}} = 24.1$ Hz, -C(F)=CFH), 4.89 (m, 1H, $^3J_{\text{HF}} = 17.4$ Hz, -C(H)CF₃), 3.23 (m, 1H, depm), 3.11 (m, 1H, depm), 2.95 (m, 1H, depm), 2.14 (m, 1H, depm); $^{13}\text{C}\{^1\text{H}\}$ NMR (125 MHz, CD_2Cl_2 , 27 °C): δ 174.7 (m, 1C), 165.3 (m, 1C), 157.1 (m, 1C); ^{19}F NMR (469 MHz, CD_2Cl_2 , 27 °C): δ -47.1 (d, 3F, $^3J_{\text{FH}} = 17.4$ Hz), -84.6 (d, 1F, $^3J_{\text{FH}} = 24.1$ Hz), -138.1 (dm, 1F, $^2J_{\text{FH}} = 81.6$ Hz); $^{31}\text{P}\{^1\text{H}\}$ NMR (202 MHz, CD_2Cl_2 , 27 °C): δ -18.8 (dm, 1P, $^2J_{\text{PP}} = 356.2$ Hz), -22.5 (dm, 1P, $^2J_{\text{PP}} = 285.7$ Hz), -28.7 (dm, 1P, $^2J_{\text{PP}} = 356.2$ Hz), -32.3 (dm, 1P, $^2J_{\text{PP}} = 285.7$ Hz); HRMS m/z calc. for [^{193}Ir]₂P₄O₃C₂₅H₄₆F₅ [M*]⁺: 999.1571, found 999.1571.

(d) Reaction of compound 34 with tetrafluoroethylene. In an NMR tube containing compound **34** (91 mg, 0.053 mmol) dissolved in 0.8 mL CD_2Cl_2 was added tetrafluoroethylene (5 mL, 0.219 mmol) via a gas-tight syringe. The solution was mixed and left at ambient temperature for 1 h. The reaction was verified by multinuclear NMR spectroscopy, confirming the formation of $[\text{Ir}_2(\text{H})(\text{CO})_3(\mu\text{-CF}_2\text{CF}_2)(\text{depm})_2][\text{BAr}^{\text{F}}_4]$ (**66**). Leaving the mixture at ambient temperature for 5 h results in minor amounts of $[\text{Ir}_2(\text{C}(\text{F})=\text{CF}_2)(\text{CO})_3(\text{depm})_2][\text{BAr}^{\text{F}}_4]$ (**67**) (22 % yield), and $[\text{Ir}_2(\text{C}(\text{F})=\text{CF}_2)(\text{CO})_3(\mu\text{-CF}_2\text{CF}_2)(\text{depm})_2][\text{BAr}^{\text{F}}_4]$ (**68**) (<5% yield) as observed in the ^{19}F NMR spectrum. Leaving the mixture for longer periods of time (2 days) or heating to 40 °C results in the decomposition to numerous unidentified products. (63 % yield for compound **66**). **Compound 66:** ^1H NMR (498 MHz, CD_2Cl_2 , 27 °C): δ 3.28 (m, 2H, depm), 2.86 (m, 2H, depm), -12.63 (tt, 1H, $^2J_{\text{HP}} = 17.3$ Hz, $^3J_{\text{HF}} = 17.3$ Hz, Ir-H); $^{13}\text{C}\{^1\text{H}\}$ NMR (125 MHz, CD_2Cl_2 , 27 °C): δ 174.4 (bm, 1C), 164.6 (bm, 1C), 153.9 (bm, 1C); ^{19}F

NMR (469 MHz, CD₂Cl₂, 27 °C): δ -74.4 (t, 2F, $^3J_{\text{FP}} = 17.0$ Hz), -80.7 (dt, 2F, $^2J_{\text{FH}} = 17.3$ Hz, $^3J_{\text{FP}} = 13.4$ Hz); $^{31}\text{P}\{\text{H}\}$ NMR (202 MHz, CD₂Cl₂, 27 °C): δ -15.0 (bt, 2P, $^2J_{\text{PP}} = 48.1$ Hz), -21.9 (bt, 2P, $^2J_{\text{PP}} = 48.1$ Hz). **Compound 67:** ^1H NMR (498 MHz, CD₂Cl₂, 27 °C): δ 2.96 (m, 4H, depm); $^{13}\text{C}\{\text{H}\}$ NMR (125 MHz, CD₂Cl₂, 27 °C): δ 185.6 (t, 2C, $^2J_{\text{CP}} = 13.3$ Hz), 185.2 (bt, 1C, $^2J_{\text{CP}} = 10.4$ Hz); ^{19}F NMR (498 MHz, CD₂Cl₂, 27 °C): δ -93.8 (dd, 1F, $^2J_{\text{FF}} = 93.0$ Hz, $^3J_{\text{FFcis}} = 39.7$ Hz), -123.9 (dd, 1F, $^3J_{\text{FFtrans}} = 111.6$ Hz, $^2J_{\text{FF}} = 93.0$ Hz), -136.1 (dd, $^3J_{\text{FFtrans}} = 111.6$ Hz, $^3J_{\text{FFcis}} = 39.7$ Hz); $^{31}\text{P}\{\text{H}\}$ NMR (202 MHz, CD₂Cl₂, 27 °C): δ -17.4 (t, 2P, $^2J_{\text{PP}} = 24.9$ Hz), -20.5 (bt, 2P, $^2J_{\text{PP}} = 24.9$ Hz). **Compound 68:** ^{19}F NMR (498 MHz, CD₂Cl₂, 27 °C): δ -76.3 (bs, 2F), -80.4 (bs, 2F), -94.3 (dd, 1F, $^2J_{\text{FF}} = 92.9$ Hz, $^3J_{\text{FFcis}} = 33.4$ Hz), -121.3 (dd, 1F, $^3J_{\text{FFtrans}} = 110.8$ Hz, $^2J_{\text{FF}} = 92.9$ Hz), -132.4 (dd, $^3J_{\text{FFtrans}} = 110.8$ Hz, $^3J_{\text{FFcis}} = 33.4$ Hz).

5.4.3 X-ray Structure Determinations

5.4.3.1 General. Crystals were grown via slow diffusion of *n*-pentane into a diethyl ether solution of the compound. Data were collected using a Bruker APEX II CCD detector/D8 diffractometer⁸² with the crystals cooled to -100 °C; all data were collected using Mo *K* α radiation ($\lambda = 0.71073$ Å). The data were corrected for absorption through Gaussian integration from indexing of the crystal faces. Structures were solved using Patterson search/structure expansion (*DIRDIF-2008*⁸³ for **58**) or direct methods (*SHELXS-97*⁸⁴ for **63**). Refinements were completed using the program *SHELXL-97*.⁸⁴ Non-hydridic hydrogen atoms were assigned positions based on the sp^2 or sp^3 hybridization geometries of their attached carbon atoms, and were given isotropic displacement parameters 20% greater than those of their parent atoms. See Supporting Information for a listing of crystallographic experimental data.

5.4.3.2 Special refinement conditions. (i) **58:** The Ir(1)–H(1) distance was constrained to be 1.55(1) Å during refinement. F–C distances within two disordered trifluoromethyl groups (of the [B{C₆H₃-3.5-(CF₃)₂}₄]⁻ ion) were

constrained to be equal (within 0.03 Å) to a common value during refinement:
 $d(\text{F}(71\text{A})\text{--C}(77)) = d(\text{F}(72\text{A})\text{--C}(77)) = d(\text{F}(73\text{A})\text{--C}(77)) = d(\text{F}(71\text{B})\text{--C}(77)) =$
 $d(\text{F}(72\text{B})\text{--C}(77)) = d(\text{F}(73\text{B})\text{--C}(77)) = d(\text{F}(74\text{A})\text{--C}(78)) = d(\text{F}(75\text{A})\text{--C}(78)) =$
 $d(\text{F}(76\text{A})\text{--C}(78)) = d(\text{F}(74\text{B})\text{--C}(78)) = d(\text{F}(75\text{B})\text{--C}(78)) = d(\text{F}(76\text{B})\text{--C}(78))$. (ii)
63: The Ir(2)–H(1) distance was fixed at 1.79 Å during refinement. The C–F and
F···F distances within the disordered CF₃ groups (centred by carbon atoms
C(58A), C(58B) and C(87)) of the anion were restrained to be 1.35(1) and 2.20(1)
Å, respectively. Additionally, the C(43A)–C(44A) distance was restrained to be
1.50(1) Å.

5.5 Acknowledgements

We thank the Natural Sciences and Engineering Research Council of Canada (NSERC) and the University of Alberta for financial support for this research and NSERC for funding the Bruker D8/APEX II CCD diffractometer. We thank the Chemistry Department's NMR Spectroscopy and Analytical and Instrumentation Laboratories. Finally, we thank NSERC and Alberta Innovates–Technology (formerly Alberta Ingenuity Fund) for scholarships to M.E.S.

5.6 References

- (1) Giesy, J. P.; Kannan, K. *Environ. Sci. Technol.* **2002**, *36*, 146A.
- (2) Kennedy, G. L.; Butenhoff, J. L.; Olsen, G. W.; O'Connor, J. C.; Seacat, A. M.; Perkins, R. G.; Biegel, L. B.; Murphy, S. R.; Farrar, D. G. *Crit. Rev. Toxicol.* **2004**, *34*, 351.
- (3) Sweetman, A. J.; Paul, A. G.; Jones, K. C. *Environ. Sci. Technol.* **2009**, *43*, 386.
- (4) Ellis, D. A.; Mabury, S. A.; Martin, J. W.; Muir, D. C. G. *Nature* **2001**, *412*, 321.
- (5) Narita, T. *Polym. J.* **2011**, *43*, 497.
- (6) Park, B. K.; Kitteringham, N. R.; O'Neill, P. M. *Annu. Rev. Pharmacol. Toxicol.* **2001**, *41*, 443.
- (7) Ismail, F. M. D. *J. Fluorine Chem.* **2002**, *118*, 27.
- (8) Isanbor, C.; O'Hagan, D. *J. Fluorine Chem.* **2006**, *127*, 303.
- (9) Kirk, K. L. *J. Fluorine Chem.* **2006**, *127*, 1013.
- (10) O'Hagan, D. *J. Fluorine Chem.* **2010**, *131*, 1071.
- (11) Key, B. D.; Howell, R. D.; Criddle, C. S. *Environ. Sci. Technol.* **1997**, *31*, 2445.
- (12) Theodoridis, G. In *Advances in Fluorine Science*; Alain, T., Ed.; Elsevier: 2006; Vol. 2, p 121.
- (13) Wallington, T. J.; Schneider, W. F.; Worsnop, D. R.; Nielsen, O. J.; Sehested, J.; Debruyne, W. J.; Shorter, J. A. *Environ. Sci. Technol.* **1994**, *28*, A320.
- (14) Metz, B.; Kuijpers, L.; Solomon, S.; Andersen, S. O.; Davidson, O.; Pons, J.; de Jager, D.; Kestin, T.; Manning, M.; Meyer, L. *Safeguarding the Ozone Layer and the Global Climate System: Issues Related to Hydrofluorocarbons and Perfluorocarbons*, 2005.
- (15) Kiplinger, J. L.; Richmond, T. G.; Osterberg, C. E. *Chem. Rev.* **1994**, *94*, 373.
- (16) Burdeniuc, J.; Jedlicka, B.; Crabtree, R. H. *Chem. Ber. Recl.* **1997**, *130*, 145.

- (17) Richmond, T. In *Activation of Unreactive Bonds and Organic Synthesis*; Murai, S., Alper, H., Gossage, R., Grushin, V., Hidai, M., Ito, Y., Jones, W., Kakiuchi, F., van Koten, G., Lin, Y. S., Mizobe, Y., Murai, S., Murakami, M., Richmond, T., Sen, A., Suginome, M., Yamamoto, A., Eds.; Springer Berlin / Heidelberg: 1999; Vol. 3, p 243.
- (18) Kraft, B. M.; Lachicotte, R. J.; Jones, W. D. *J. Am. Chem. Soc.* **2000**, *122*, 8559.
- (19) Kirkham, M. S.; Mahon, M. F.; Whittlesey, M. K. *Chem. Comm.* **2001**, 813.
- (20) Braun, T.; Noveski, D.; Neumann, B.; Stammler, H. G. *Angew. Chem. Int. Ed.* **2002**, *41*, 2745.
- (21) Kraft, B. M.; Jones, W. D. *J. Am. Chem. Soc.* **2002**, *124*, 8681.
- (22) Ferrando-Miguel, G.; Gerard, H.; Eisenstein, O.; Caulton, K. G. *Inorg. Chem.* **2002**, *41*, 6440.
- (23) Jones, W. D. *Dalton Trans.* **2003**, 3991.
- (24) Noveski, D.; Braun, T.; Schulte, M.; Neumann, B.; Stammler, H. G. *Dalton Trans.* **2003**, 4075.
- (25) Renkema, A.; Werner-Zwanziger, U.; Pagel, M. D.; Caulton, K. G. *J. Mol. Catal. A: Chem.* **2004**, *224*, 125.
- (26) Torrens, H. *Coord. Chem. Rev.* **2005**, *249*, 1957.
- (27) Perutz, R. N.; Braun, T. In *Comprehensive Organometallic Chemistry III* 2007; Vol. 1, p 725.
- (28) Amii, H.; Uneyama, K. *Chem. Rev.* **2009**, *109*, 2119.
- (29) Hughes, R. P. *Eur. J. Inorg. Chem.* **2009**, *2009*, 4591.
- (30) Braun, T.; Salomon, M. A.; Altenhoner, K.; Teltewskoi, M.; Hinze, S. *Angew. Chem. Int. Ed.* **2009**, *48*, 1818.
- (31) Aizenberg, M.; Milstein, D. *Science* **1994**, *265*, 359.
- (32) Aizenberg, M.; Milstein, D. *J. Am. Chem. Soc.* **1995**, *117*, 8674.
- (33) Young, R. J.; Grushin, V. V. *Organometallics* **1999**, *18*, 294.
- (34) Braun, T.; Wehmeier, F.; Altenhöner, K. *Angew. Chem. Int. Ed.* **2007**, *46*, 5321.

- (35) Jäger-Fiedler, U.; Klahn, M.; Arndt, P.; Baumann, W.; Spannenberg, A.; Burlakov, V. V.; Rosenthal, U. *J. Mol. Catal. A: Chem.* **2007**, *261*, 184.
- (36) Edelbach, B. L.; Jones, W. D. *J. Am. Chem. Soc.* **1997**, *119*, 7734.
- (37) Schaub, T.; Backes, M.; Radius, U. *J. Am. Chem. Soc.* **2006**, *128*, 15964.
- (38) Camadanli, S.; Beck, R.; Florke, U.; Klein, H. F. *Dalton Trans.* **2008**, 5701.
- (39) Nova, A.; Erhardt, S.; Jasim, N. A.; Perutz, R. N.; Macgregor, S. A.; McGrady, J. E.; Whitwood, A. C. *J. Am. Chem. Soc.* **2008**, *130*, 15499.
- (40) Buckley, H. L.; Wang, T. E.; Tran, O.; Love, J. A. *Organometallics* **2009**, *28*, 2356.
- (41) Johnson, S. A.; Taylor, E. T.; Cruise, S. J. *Organometallics* **2009**, *28*, 3842.
- (42) Reade, S. P.; Mahon, M. F.; Whittlesey, M. K. *J. Am. Chem. Soc.* **2009**, *131*, 1847.
- (43) Zheng, T. T.; Sun, H. J.; Chen, Y.; Li, X. Y.; Durr, S.; Radius, U.; Harms, K. *Organometallics* **2009**, *28*, 5771.
- (44) Clot, E.; Eisenstein, O.; Jasim, N.; Macgregor, S. A.; McGrady, J. E.; Perutz, T. *Acc. Chem. Res.* **2011**, *44*, 333.
- (45) Bonnet, J. J.; Mathieu, R.; Poilblanc, R.; Ibers, J. A. *J. Am. Chem. Soc.* **1979**, *101*, 7487.
- (46) Booth, B. L.; Haszeldine, R. N.; Mitchell, P. R.; Cox, J. J. *Chem. Comm.* **1967**, 529.
- (47) Green, M.; Laguna, A.; Spencer, J. L.; Stone, F. G. A. *J. Chem. Soc., Dalton Trans.* **1977**, 1010.
- (48) Hacker, M. J.; Littlecott, G. W.; Kemmitt, R. D. W. *J. Organomet. Chem.* **1973**, *47*, 189.
- (49) Hudlicky, M. *J. Fluorine Chem.* **1989**, *44*, 345.
- (50) Hughes, R. P.; Laritchev, R. B.; Zakharov, L. N.; Rheingold, A. L. *J. Am. Chem. Soc.* **2004**, *126*, 2308.
- (51) Hughes, R. P.; Rose, P. R.; Rheingold, A. L. *Organometallics* **1993**, *12*, 3109.

- (52) Jones, M. T.; McDonald, R. N. *Organometallics* **1988**, *7*, 1221.
- (53) Kemmitt, R. D. W.; Nichols, D. I. *J. Chem. Soc. A* **1969**, 1577.
- (54) Kuhnel, M. F.; Lentz, D. *Angew. Chem. Int. Ed.* **2010**, *49*, 2933.
- (55) Lentz, D.; Kuhnel, M. F. *Angew. Chem. Int. Ed.* **2010**, *49*, 2933.
- (56) Maples, P. K.; Green, M.; Stone, F. G. A. *J. Chem. Soc., Dalton Trans.* **1973**, 2069.
- (57) Ohashi, M.; Kambara, T.; Hatanaka, T.; Saijo, H.; Doi, R.; Ogoshi, S. *J. Am. Chem. Soc.* **2011**, *133*, 3256.
- (58) Peterson, A. A.; McNeill, K. *Organometallics* **2006**, *25*, 4938.
- (59) Peterson, A. A.; Thoreson, K. A.; McNeill, K. *Organometallics* **2009**, *28*, 5982.
- (60) Rieth, R. D.; Brennessel, W. W.; Jones, W. D. *Eur. J. Inorg. Chem.* **2007**, 2839.
- (61) Ristic-Petrovic, D.; Wang, M.; McDonald, R.; Cowie, M. *Organometallics* **2002**, *21*, 5172.
- (62) Roundhill, D. M.; Lawson, D. N.; Wilkinson, G. *J. Chem. Soc. A* **1968**, 845.
- (63) Roundhill, D. M.; Wilkinson, G. *J. Chem. Soc. A* **1968**, 506.
- (64) Anderson, D. J.; McDonald, R.; Cowie, M. *Angew. Chem. Int. Ed.* **2007**, *46*, 3741.
- (65) Slaney, M. E.; Anderson, D. J.; Ferguson, M. J.; McDonald, R.; Cowie, M. *J. Am. Chem. Soc.* **2010**, *132*, 16544.
- (66) Slaney, M. E.; Anderson, D. J.; Ristic-Petrovic, D.; McDonald, R.; Cowie, M. *Accepted, Chem. Eur. J.*, Nov. 8, 2011.
- (67) Soriano, J.; Shamir, J.; Netzer, A.; Marcus, Y. *Inorg. Nucl. Chem. Letters* **1969**, *5*, 209.
- (68) Gouin, L.; Cousseau, J.; Smith, J. A. S. *J. Chem. Soc., Faraday Trans.* **1977**, *73*, 1878.
- (69) Slaney, M. E.; Anderson, D. J.; Ferguson, M. J.; McDonald, R.; Cowie, M. *Accepted, Organometallics*, Jan. 16, 2012.
- (70) Cowie, M.; Loeb, S. J. *Organometallics* **1985**, *4*, 852.

- (71) Deraniyagala, S. P.; Grundy, K. R. *Organometallics* **1985**, *4*, 424.
- (72) Yam, V. W. W.; Yeung, P. K. Y.; Chan, L. P.; Kwok, W. M.; Phillips, D. L.; Yu, K. L.; Wong, R. W. K.; Yan, H.; Meng, Q. J. *Organometallics* **1998**, *17*, 2590.
- (73) Wong, K. M. C.; Hui, C. K.; Yu, K. L.; Yam, V. W. W. *Coord. Chem. Rev.* **2002**, *229*, 123.
- (74) Lam, W. H.; Yam, V. W. W. *Inorg. Chem.* **2010**, *49*, 10930.
- (75) Ihrig, A. M.; Smith, S. L. *J. Am. Chem. Soc.* **1970**, *94*, 34
- (76) Foris, A. *Magn. Reson. Chem.* **2004**, *42*, 534.
- (77) Hughes, R. P.; Lindner, D. C.; Rheingold, A. L.; LiableSands, L. M. *J. Am. Chem. Soc.* **1997**, *119*, 11544.
- (78) Hughes, R. P.; Lindner, D. C.; Smith, J. M.; Zhang, D. H.; Incarvito, C. D.; Lam, K. C.; Liable-Sands, L. M.; Sommer, R. D.; Rheingold, A. L. *Dalton Trans.* **2001**, 2270.
- (79) Goodman, L.; Gu, H. B.; Pophristic, V. *J. Phys. Chem. A* **2005**, *109*, 1223.
- (80) O'Hagan, D. *Chem. Soc. Rev.* **2008**, *37*, 308.
- (81) Soderquist, J. A.; Anderson, C. L. *Tetrahedron Lett.* **1986**, *27*, 3961.
- (82) Programs for diffractometer operation, unit cell indexing, data collection, data reduction and absorption correction were those supplied by Bruker.
- (83) Beurskens, P. T.; Beurskens, G.; de Gelder, R.; Smits, J. M. M.; Garcia-Granda, S.; Gould, R. O. (2008). The DIRDIF-2008 program system. Crystallography Laboratory, Radboud University Nijmegen, The Netherlands.
- (84) Sheldrick, G. M. *Acta Crystallogr.* **2008**, *A64*, 112.

Chapter 6 – Conclusions

6.1 Project Motivation. At the onset of this project, my goal was to investigate the roles of adjacent metals in the activation of organic substrates and to determine the ways in which these metals can act in a cooperative manner to promote unique reactivity that is either not observed or more difficult to carry out in monometallic systems. Numerous reports from our group have successfully shown the cooperative involvement of metals and their ability to enhance substrate reactivity, including carbon-carbon bond formation through the coupling of methylene units¹, or by the insertion of unsaturated substrates into bridging methylene units,² facile C–H bond activation either of a methyl ligand by an adjacent metal,³ or by geminal C–H activation of 1,3-butadiene,⁴ and in C–F bond activation of fluoroolefins.⁵ At the time I joined the Cowie group the preliminary work on geminal C–H activation and on C–F activation had been reported^{4,5} but required follow-up studies to determine if the scope of olefin and fluoroolefin reactivity was limited to those mentioned, and to determine what improvements could be made to incorporate other substrates or to improve the reported reactivity patterns. All of the processes studied on these topics had been carried out with dppm as the bridging diphosphine group and it was evident that the dppm ligands introduced limitations on the reactivity. Numerous key intermediates were labile at low temperatures, suggesting that more basic diphosphine ligands could help stabilize key intermediates. Furthermore, decreasing the size of the diphosphine substituents could also be an effective modification to favour binding of olefin adducts and to increase the scope of fluoroolefin substrates, which were limited to fluorine-substituted ethylene. As such, my goals were to finish the development of a new, smaller ligand system initiated by Jason Anderson and explore its reactivity with olefins and fluoroolefins and secondly, to continue investigating the role of adjacent metals in the C–F activation of fluoroolefins with the dppm system.

6.2 Synthesis of Depm Precursors. As mentioned above, our group previously reported the double C–H activation involving a pair of geminal hydrogens of 1,3-butadiene promoted by the diiridium complex, $[\text{Ir}_2(\text{CH}_3)(\text{CO})_2(\text{dppm})_2]^+$ (**1**).⁴ Although such geminal C–H activation is unusual, the scope involving this compound was limited since no other α -olefins investigated reacted in this manner. Interestingly, a *transoid* $\eta^2:\eta^2$ -butadiene adduct was observed at low temperature, suggesting that it might be an intermediate in the activation process. Further evidence that this coordination mode is necessary came from the reaction with ethylene, which formed an adduct but failed to give any C–H activated products. Furthermore, substitution at one of the olefinic units of butadiene, with aims of inhibiting coordination of this olefinic moiety, gave neither an observed adduct nor C–H activation, supporting the idea that the involvement of both metals was necessary. Even with 1,3-butadiene, the C–H activation process was extremely slow and the diolefin was very weakly bound.

This report, in part, was the motivation behind the synthesis of a smaller, more basic diphosphine ligand system that would be analogous to the above dppm system based on the reasoning that the smaller diphosphines would allow for easier and stronger substrate access to the metals, while the greater basicity would also help stabilize coordination complexes due to the enhanced back-donation from the metal to the olefin, while also promoting the oxidative addition of the C–H bonds.

Although the obvious choice of diphosphine was *bis(dimethylphosphino)methane* (dmpm), which was expected to impart the required changes outlined above, previous studies had found that its chemistry deviated significantly from that of the analogous dppm systems,^{6,7} and as such, developing the targeted bimetallic dmpm complexes proved to be difficult. However, the chemistry involving *bis(diethylphosphino)methane* (dep_m) seemed to closely resemble that of the well-documented dppm systems, and allowed for both the rational synthesis of precursors and the direct comparison to the previously reported chemistry.

An unfortunate result of switching to the smaller, more basic depm ligands was the increased propensity of several of our target complexes to react with water – reactivity that was not observed with the dppm analogues. The formation of the methyl dicarbonyl complexes, namely $[MM'(CH_3)(CO)_2(depm)_2]^+$ ($M = M' = Ir$ (**32**); $M = Ir, M' = Rh$ (**48**)), proved to be extremely challenging due to their subsequent reactivity with water, resulting in the elimination of methane and formation of the unspectacular hydroxide complexes. This remains a challenge of the depm chemistry and requires careful examination into other methods for synthesizing these targeted systems or other ways to remove water beyond those examined in this dissertation.

6.3 Carbon–Hydrogen Bond Activation. Although the original goal was to directly compare the chemistry of $[Ir_2(CH_3)(CO)_2(depm)_2]^+$ (**32**) to its dppm analogue (**1**), its inherent susceptibility to adventitious water made it extremely difficult to study. However, the diiridium hydride complex, $[Ir_2(CO)_3(\mu-H)(depm)_2]^+$ (**34**), the dppm analogue of which was rather unreactive, proved to be surprisingly reactive towards a variety of α -olefins, yielding vinylidene-trihydride complexes of the form $[Ir_2(H)_2(CO)_2(\mu-H)(\mu-C=CRR')](depm)_2]^+$ (**51 – 57**), similar to that noted above in the reaction of compound **1** with 1,3-butadiene.⁴ The propensity of this complex to activate both geminal C–H bonds of α -olefins is unique to this system – the analogous dppm compound does not react with olefins.

It appears that the greater basicity, combined with the smaller size of the bridging depm ligands, enhances the coordination chemistry and allows for a greater range of α -olefins capable of undergoing double C–H activation, including *styrene* and *isobutylene*, two sterically encumbered α -olefins. In the presence of TMNO, all olefins examined gave the double C–H bond activation products within minutes, while in the absence of TMNO, the expected products were formed; however, the rates were found to vary depending upon the size of the α -olefin studied, and in the case of *isobutylene*, the reaction did not proceed in the absence of TMNO.

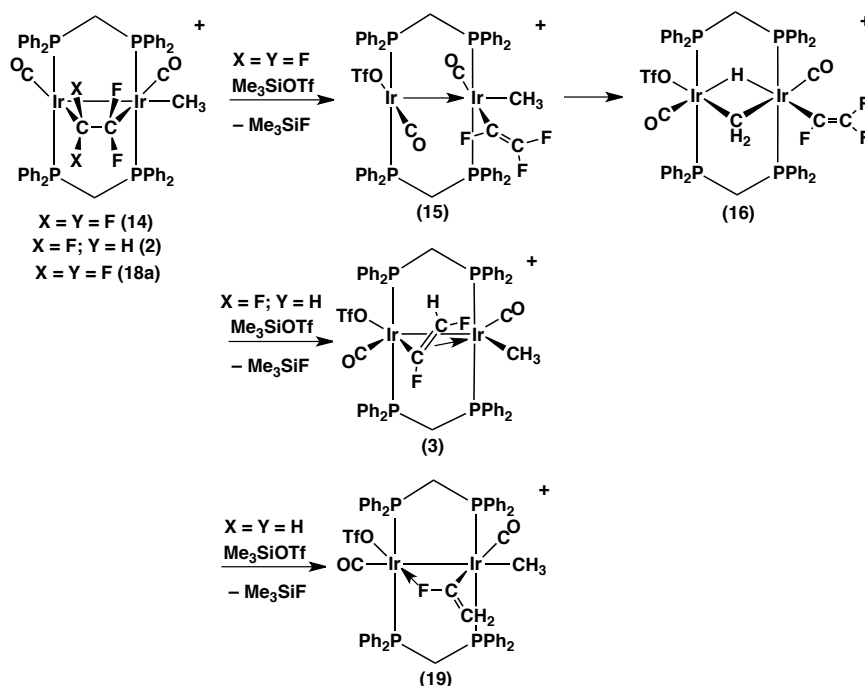
Labeling studies also indicate a different mechanism is occurring compared to the dppm example. Whereas the product from the reaction of **1** with 1,3-butadiene, namely $[\text{Ir}_2(\text{CH}_3)(\text{H})(\text{CO})_2(\mu\text{-H})(\mu\text{-C}=\text{C}(\text{H})\text{C}(\text{H})=\text{CH}_2)(\text{dep}m)_2]^+$, has mutually trans hydride ligands located on opposite faces of the Ir_2P_4 plane, the products in the olefin activation by the depm complex have the hydride ligands originating from C–H activation processes in a cis arrangement, adjacent to the resulting vinylidene fragment – all on the same face of the Ir_2P_4 core. Although low temperature NMR studies did not reveal any intermediates preceding geminal activation, it is clear that the second metal plays a pivotal role in the second C–H activation step.

6.4 Carbon-Fluorine Bond Activation. Jason Anderson also began studies investigating the role of adjacent metals in the activation of C–F bonds of fluoroolefins. During his final years as a Ph.D. candidate, he found preliminary results suggesting that fluoroolefins bound in the bridging mode between a pair of adjacent metals are more susceptible to C–F activation than fluoroolefins bound in the traditional η^2 -coordination mode to a single metal.⁵ This communication, which also focused on the synergistic involvement of metals to induce reactivity unique to bimetallic systems, acted as a starting point for my second project. My objectives for this research involved: (a) investigating the details associated with Jason’s preliminary findings, including unambiguous characterization of products and intermediates, (b) expanding the chemistry to perform C–F bond activation with other fluorophilic reagents beyond strong acids and (c) functionalization of the newly activated fluorocarbyl fragments.

It is evident that fluoroolefins bound in a bridging position between a pair of metals are more susceptible to fluoride-ion abstraction than η^2 -bound analogues, by virtue of the more extensive olefin rehybridization that occurs when bridging.⁵ In particular, this was demonstrated in the work involving the competitive experiment in which fluoride-ion removal from a bridging 1,1-difluoroethylene ligand of $[\text{Ir}_2(\text{CH}_3)(\text{CO})_2(\mu\text{-C}_2\text{F}_2\text{H}_2)(\text{dpp}m)_2]^+$ (**18a**) occurs

readily at $-40\text{ }^{\circ}\text{C}$ while the isomeric η^2 -bound olefin, $[\text{Ir}_2(\text{CH}_3)(\text{CO})_2(\eta^2\text{-C}_2\text{F}_2\text{H}_2)(\text{dppm})_2]^+$ (**18b**), is resistant to fluoride-ion loss up to $0\text{ }^{\circ}\text{C}$.

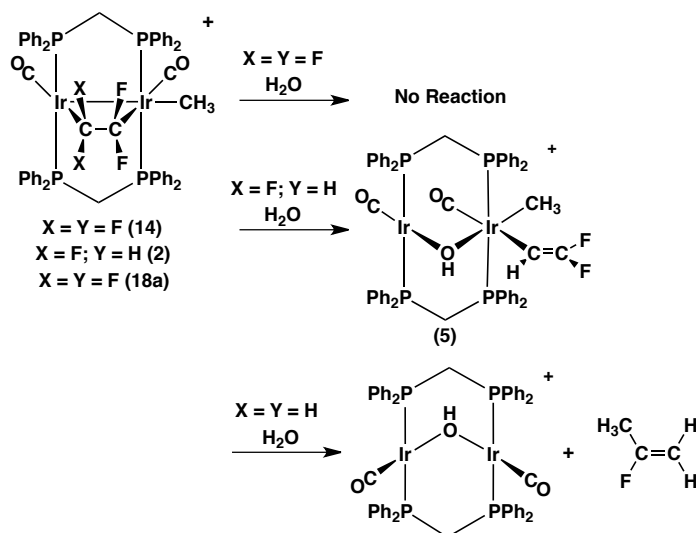
For each of the tetrafluoroethylene-, trifluoroethylene- and 1,1-difluoroethylene-bridged species, $[\text{Ir}_2(\text{CH}_3)(\text{CO})_2(\mu\text{-olefin})(\text{dppm})_2]^+$ (olefin = C_2F_4 (**14**), $\text{C}_2\text{F}_3\text{H}$ (**2**), $\text{C}_2\text{F}_2\text{H}_2$ (**18a**)), abstraction of a fluoride ion was readily achieved upon the reaction with Me_3SiOTf or HOTf . Interestingly, the fluorovinyl products that resulted were quite different in the three cases, as diagrammed in Scheme 6.1. In the case of the trifluorovinyl product, the kinetic isomer rearranged above $0\text{ }^{\circ}\text{C}$ to the thermodynamic product, with both having the same κ^1 -vinyl binding mode. Fluoride-ion removal from the $\text{C}_2\text{F}_3\text{H}$ adduct yielded a *cis*-difluorovinyl group that is σ -bound to one metal and interacting with the second by a π -interaction.⁸ This presents the first example of this coordination mode for a fluorovinyl group. The monofluorovinyl group in **19**, obtained from fluoride-ion abstraction from the bridging $\text{C}_2\text{F}_2\text{H}_3$ adduct, is bound in an unusual $\mu\text{-}\kappa^1\text{:}\kappa^1$ -mode, through the vinyl carbon at one metal and the adjacent fluorine at



Scheme 6.1 – A comparison of the three different fluorovinyl binding modes upon C–F activation of the respective fluoroolefin-bridged adducts.

the other;⁹ again, there is no precedent for this coordination mode. The observation that the trifluorovinyl group is terminally bound in both isomers is possibly a reflection of its larger bulk, disfavoring both bridging geometries, owing to interactions with the dppm phenyl groups, although it is also likely that the additional fluorines on this group lower the ability of the α -fluorine to function as an effective donor to the adjacent metal, as seen for the monofluorovinyl product (**19**). Conversely, the failure of the monofluorovinyl group to interact with the second metal in an η^2 -binding mode, as seen for the *cis*-difluorovinyl analogue (**3**),⁸ parallels the very poor η^2 -binding ability of monofluoroethylene, which has been attributed to the large reorganizational energy required upon coordination, making η^2 -coordination unfavourable in the case of lower fluorine substitution.^{10,11}

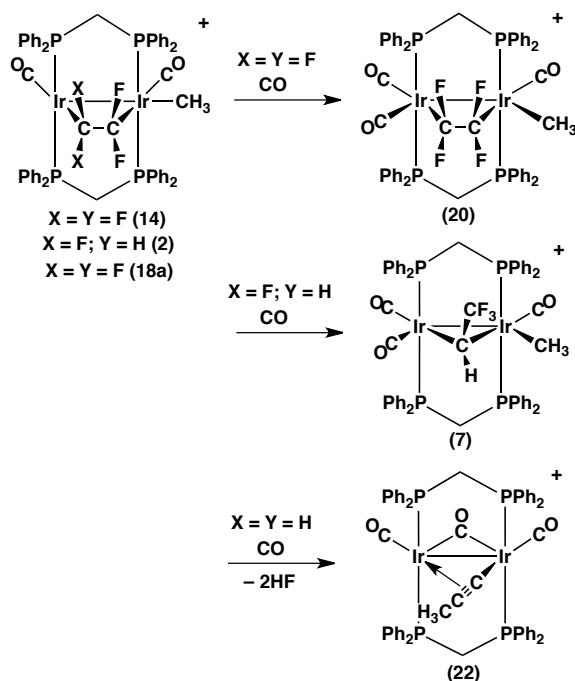
The three fluoroolefin-bridged products display a progression in reactivity with changing fluorine content, as is evident in their reactions with either water or carbon monoxide. As shown in Scheme 6.2, the tetrafluoroethylene adduct (**14**) is unreactive towards water, even at elevated temperature, whereas the trifluoroethylene analogue (**2**) reacts at ambient temperature to give the hydroxido-bridged difluorovinyl product shown, and the 1,1-difluoroethylene



Scheme 6.2 – A comparison of the reactivities of the three different fluoroolefins-bridged adducts with water.

adduct (**18a**) reacts at $-20\text{ }^{\circ}\text{C}$ to give 2-fluoropropene by reductive elimination of the resulting monofluorovinyl and the methyl groups. Although there are obvious parallels in the reactivity of the 1,1-difluoroethylene and the trifluoroethylene adducts with H_2O , I assume that they proceed by subtly different mechanisms for the reasons noted in Chapter 3.

The reactions of these three fluoroolefin adducts with CO also vary substantially, as shown in Scheme 6.3; whereas the C_2F_4 adduct (**14**) gives only the unexceptional carbonyl adduct, the other two yield much more interesting results. In the case of the trifluoroethylene adduct (**2**), reaction with CO results in isomerization of the olefin moiety to a bridging 2,2,2-trifluoroethylidene group (**7**) – reactivity that has precedent,^{8,12-14} while the 1,1-difluoroethylene adduct (**18a**) results in the unprecedented loss of both equivalents of HF, accompanied by migration of the methyl ligand to the resulting acetylide (C_2^{2-}) moiety to yield a propynyl group (**22**). How this last transformation proceeds remains a mystery, but is nevertheless a clear demonstration of the unusual reactivity that can be imparted by the pair of adjacent metals.



Scheme 6.3 – A comparison of the reactivities of the three different fluoroolefin-bridged adducts with carbon monoxide.

Functionalization of the fluorovinyl groups that results from activation of one C–F bond in the three fluoroolefin adducts has been carried out by either hydrogenolysis to give the corresponding fluoroolefins, in which one fluorine in the original fluoroolefin has been replaced by hydrogen, or by reductive elimination of the fluorovinyl and methyl groups to give the corresponding fluoropropenes. Two exceptions were observed in these functionalizations: reductive elimination does not occur for the trifluorovinyl group, presumably owing to a strong Ir–C₂F₃ bond – a result of the high fluorine content, and hydrogenolysis of the monofluorovinyl group, owing to decomposition of the unstable fluorovinyl compound. Nonetheless, I was able to successfully convert tetrafluoroethylene to trifluoroethylene, trifluoroethylene to *cis*-difluoroethylene, 1,1,1-trifluoroethane, and to mixture of difluoropropenes, while 1,1-difluoroethylene was readily converted to 2-fluoropropene.

The success observed with the C–F activation of fluoroolefins bound in the bridging mode in the dppm system led us to also explore their reactivity with the depm systems. Recall that my motivation behind exploring depm as ancillary diphosphine ligands was due to its smaller size, which should allow for richer coordination chemistry and its greater basicity, which should enhance the reactivity of substrates while also increasing the stability of cationic products. Although the original goal was again to directly compare the two methyl-dicarbonyl systems (**1** and **32**), the diiridium-hydride complex (**34**), having already displayed chemistry similar to that of compound **1** with α -olefins, again was used as the precursor for the reactions with fluoroolefins.

Noticeable differences regarding fluoroolefin reactivity with the depm system (**34**) are observed compared to the dppm chemistry. One difference is the incorporation of up to two fluoroolefin units, as observed with the 1,1-difluoroethylene adduct $[\text{Ir}_2(\text{C}(\text{F})=\text{CH}_2)(\text{CO})_3(\mu\text{-CF}_2\text{CH}_2)(\text{dep}_m)_2]^+$ (**60a/60b**), and the 2,2,2-trifluoroethylidene-bridged complex $[\text{Ir}_2(\text{C}(\text{F})=\text{CFH})(\text{CO})_3(\mu\text{-CHCF}_3)(\text{dep}_m)_2]^+$ (**65**). Although there was also evidence for the coordination of multiple units of tetrafluoroethylene (**68**), the structure of this product is

undetermined due to my inability to obtain it in appreciable yields. The coordination of multiple fluoroolefin units was not observed with dppm, and appears to be the result of the smaller size of the ethyl substituents; the steric demand of the phenyl substituents in dppm prohibited the coordination of multiple fluoroolefin moieties.

Another difference is the formation of the bridging vinylidene and difluorovinylidene products (**58** and **63**), both the result of geminal C–F *and* C–H activation of the respective fluoroolefin. The C–H bond activation of fluoroolefins is more common with the depm complexes, with the only example observed with the dppm chemistry involving the double HF elimination from 1,1-difluoroethylene to give a bridging propynyl group (**22**), a reaction that is also observed with the depm diphosphine system. The propensity for the depm complexes to activate C–H bonds of fluoroolefins is presumably due to the greater basicity of the ethyl substituents, which promotes the oxidative addition by inductively increasing π -back donation into the C–H antibonding orbital, and stabilizes the higher oxidation states in the products.

The greater basicity of depm is evident in the susceptibility of the fluoroolefins to undergo facile C–F bond cleavage by water. Although the activation of 1,1-difluoro- and trifluoroethylene by water was observed in the dppm cases, increasing the fluorine substitution was found to dramatically decrease the susceptibility for C–F activation. In the case of depm, there is a minor decrease in the ability of water to cleave the C–F bonds of bridging fluoroolefins as fluorine substitution increases, however, the tetrafluoroethylene complex, $[\text{Ir}_2(\text{H})(\text{CO})_3(\mu\text{-CF}_2\text{CF}_2)(\text{depm})_2]^+$ (**66**), undergoes C–F activation in the presence of water. Interestingly, the hydride ligand in the hydride-bridged precursor is not directly involved in the cleavage of carbon-fluorine bonds. Instead, I found that water was solely responsible for the C–F bond cleavage processes, as confirmed by the dramatic increase in reaction rates upon the deliberate addition of water.

Finally, the reactivity of the hydride complex (**34**) with fluoroolefins reiterates the importance of the bridging coordination mode as a new, facile

method for the *selective* C–F bond activation of fluoroolefins. Although vinylfluoride and 1,1-difluoroethylene showed no evidence of coordination in the bridging mode prior to C–F activation (recall the bridging coordination mode was observed after initial C–F activation of 1,1-difluoroethylene), the trifluoroethylene- and tetrafluoroethylene-bridged adducts are both observed as precursors to C–F activation.

6.5 Final Remarks and Future Directions. As stated in the section 6.1 of this chapter, my goal was to investigate the role of adjacent metals in promoting reactivity not observed in monometallic systems, with particular emphasis on the C–H bond activation of α -olefins and the C–F bond activation of fluoroolefins. My ‘two-pronged’ approach involved first looking at a diiridium system bridged by the bulky dpmm diphosphine, while the other involved investigating the depm ligand system, with its smaller size and greater basicity expected to play a role in the reactivity. While the dpmm system was successful in performing the C–H activation of 1,3-butadiene⁴ and C–F bond activation of fluoroolefins,^{8,9} the size and electronic characteristics of the phenyl-substituted dpmm ligands limits the scope of substrates studied. For example, the coordination of fluoroolefins was limited to tetrafluoroethylene and smaller, while larger fluoroolefins did not coordinate. Conversely, the depm ligand system showed promising results regarding both the C–H activation of larger α -olefins and the C–F (and C–H) bond activation of fluoroolefins, with the incorporation of multiple fluoroolefin units. Unfortunately, the substitution of phenyl for ethyl groups has also had detrimental effects.

Despite the fact that depm dramatically increased reactivity, one caveat of this ligand system is its increased solubility in both polar and non-polar solvents, making the isolation and purification of these compounds extremely difficult. Numerous attempts to modify the solubility of these compounds by altering the anion proved to be futile, with the most promising anion, $\text{BAr}^{\text{F}}_4^-$, only producing a couple of crystalline samples.

Another drawback of this system is its ability to undergo both C–F *and* C–H activation of fluoroolefins. Although the formation of the bridging vinylidene and difluorovinylidene compounds (**58** and **63**) are interesting, their subsequent functionalization, work that still needs to be explored, may prove to be challenging due to the tendency of bridging-vinylidenes in these systems to be unreactive. Nonetheless, further studies need to be done to explore the potential of functionalizing these activated fragments, with the primary focus involving hydrogenolysis. The added advantage with this system is the potential to reform the hydride starting material upon the addition of hydrogen, closing the catalytic cycle to produce the hydrodefluorinated products. Alternatively, the sequential addition of H^+ and H^- could also be effective, if hydrogen is found to be unreactive with these compounds.

Finally, the incorporation of multiple fluoroolefin units in the depm chemistry, while interesting, could also have a negative impact on the functionalization of these compounds, due to their coordinative saturation. One way to avoid the coordination of multiple fluoroolefin units is to modify the diphosphine backbone to slightly increase the steric bulk while simultaneously maintaining the electron-donating properties of depm. The substitution of the ethyl by isopropyl groups is one potential solution; however, the problem of increased solubility could again give rise to issues related to product isolation and characterization.

6.6 References

- (1) Trepanier, S. J.; Dennett, J. N. L.; Sterenberg, B. T.; McDonald, R.; Cowie, M. *J. Am. Chem. Soc.* **2004**, *126*, 8046.
- (2) Rowsell, B. D.; McDonald, R.; Ferguson, M. J.; Cowie, M. *Organometallics* **2003**, *22*, 2944.
- (3) Torkelson, J. R.; Antwi-Nsiah, F. H.; McDonald, R.; Cowie, M.; Pruis, J. G.; Jalkanen, K. J.; DeKock, R. L. *J. Am. Chem. Soc.* **1999**, *121*, 3666.
- (4) Ristic-Petrovic, D.; Torkelson, J. R.; Hiltz, R. W.; McDonald, R.; Cowie, M. *Organometallics* **2000**, *19*, 4432.
- (5) Anderson, D. J.; McDonald, R.; Cowie, M. *Angew. Chem. Int. Ed.* **2007**, *46*, 3741.
- (6) Reinking, M. K., Ph.D Thesis, Purdue University, 1989.
- (7) Reinking, M. K.; Fanwick, P. E.; Kubiak, C. P. *Angew. Chem. Int. Ed.* **1989**, *28*, 1377.
- (8) Slaney, M. E.; Anderson, D. J.; Ferguson, M. J.; McDonald, R.; Cowie, M. *J. Am. Chem. Soc.* **2010**, *132*, 16544.
- (9) Slaney, M. E.; Anderson, D. J.; Ristic-Petrovic, D.; McDonald, R.; Cowie, M. *Accepted by Chem. Eur. J.*, Nov. 8, 2011.
- (10) Cedeño, D. L.; Weitz, E.; Berces, A. *J. Phys. Chem. A* **2001**, *105*, 8077.
- (11) Schlappi, D. N.; Cedeño, D. L. *J. Phys. Chem. A* **2003**, *107*, 8763.
- (12) Booth, B. L.; Haszeldine, R. N.; Mitchell, P. R.; Cox, J. J. *Chem. Comm.* **1967**, 529.
- (13) Green, M.; Laguna, A.; Spencer, J. L.; Stone, F. G. A. *J. Chem. Soc., Dalton Trans.* **1977**, 1010.
- (14) Bonnet, J. J.; Mathieu, R.; Poilblanc, R.; Ibers, J. A. *J. Am. Chem. Soc.* **1979**, *101*, 7487.

Appendices

Appendix I – Contributions from Co-Authors

Chapter 1

Dr. Martin Cowie assisted with editing.

Chapter 2

Dr. Jason Anderson initiated the project and reported preliminary results as a communication and his thesis.^{† ‡}

Dr. Michael Ferguson and Dr. Robert MacDonald performed all crystallographic structure determinations.

Dr. Martin Cowie assisted with editing.

Chapter 3

Dr. Jason Anderson initiated the project and reported preliminary results as a communication and his thesis.^{† ‡}

Dr. Dusan Ristic-Petrovic grew crystals of compound **22** suitable for an X-ray diffraction study.

Dr. Michael Ferguson and Dr. Robert MacDonald performed all crystallographic structure determinations.

Dr. Martin Cowie assisted with editing.

Chapter 4

Dr. Jason Anderson initiated studies on the diiridium and dirhodium systems and reported preliminary results in his thesis.[‡]

Dr. Michael Ferguson and Dr. Robert MacDonald performed all crystallographic structure determinations.

Dr. Martin Cowie assisted with editing.

Chapter 5

Dr. Michael Ferguson and Dr. Robert MacDonald performed all crystallographic structure determinations.

Dr. Martin Cowie assisted with editing.

Chapter 6

Dr. Martin Cowie assisted with editing.

[†] Anderson, D. J.; MacDonald, R.; Cowie, M. *Angew. Chem. Int. Ed.* **2007**, *46*, 3741.

[‡] Anderson, D. J., Ph.D. Thesis, University of Alberta, 2007.

Appendix II – Drying Agents for Solvents

| Solvent | Drying Agent |
|--------------------|---|
| acetone | calcium chloride (CaCl ₂)/benzophenone |
| acetonitrile | calcium hydride (CaH ₂) |
| benzene | sodium metal (Na) /benzophenone |
| dichloromethane | phosphorus pentoxide (P ₂ O ₅) |
| diethyl ether | sodium metal (Na) /benzophenone |
| dimethylsulphoxide | type 4A molecular sieves |
| methanol | magnesium sulphate (MgSO ₄) |
| nitromethane | calcium hydride (CaH ₂) |
| <i>n</i> -pentane | sodium metal (Na) |
| tetrahydrofuran | sodium metal (Na) /benzophenone |

Appendix III – Crystallographic Experimental Details

Table A.1. Crystallographic Experimental Details for Compound **3**.

| | |
|---|---|
| <i>A. Crystal Data</i> | |
| formula | C _{62.5} H _{60.5} Cl _{3.5} F ₈ Ir ₂ O ₈ P ₄ S ₂ |
| formula weight | 1788.08 |
| crystal dimensions (mm) | 0.31 x 0.31 x 0.10 |
| crystal system | triclinic |
| space group | P $\bar{1}$ (No. 2) |
| unit cell parameters ^a | |
| <i>a</i> (Å) | 17.096 (2) |
| <i>b</i> (Å) | 17.193 (2) |
| <i>c</i> (Å) | 23.436 (3) |
| α (deg) | 92.1030 (18) |
| β (deg) | 93.6893 (18) |
| γ (deg) | 98.6202 (18) |
| <i>V</i> (Å ³) | 6789.1 (15) |
| <i>Z</i> | 4 |
| <i>r</i> _{calcd} (g cm ⁻³) | 1.749 |
| μ (mm ⁻¹) | 4.284 |
| <i>B. Data Collection and Refinement Conditions</i> | |
| diffractometer | Bruker D8/APEX II CCD ^b |
| radiation (λ [Å]) | graphite-monochromated Mo K α (0.71073) |
| temperature (°C) | -100 |
| scan type | ω scans (0.3°) (25 s exposures) |
| data collection 2θ limit (deg) | 54.44 |
| total data collected | 46603 (-21 $\leq h \leq$ 21, -22 $\leq k \leq$ 22, 0 $\leq l \leq$ 30) |
| independent reflections | 46603 ($R_{\text{int}} = 0.0000$) |
| number of observed reflections (<i>NO</i>) | 33992 [$F_0^2 \geq 2\sigma(F_0^2)$] |
| structure solution method | Patterson/structure expansion (<i>DIRDIF-2008</i> ^c) |
| refinement method | full-matrix least-squares on F^2 (<i>SHELXL-97</i> ^d) |
| absorption correction method | multi-scan (<i>TWINABS</i>) |
| range of transmission factors | 0.6839–0.3493 |
| data/restraints/parameters | 46603 / 17 ^e / 1572 |
| goodness-of-fit (<i>S</i>) ^f [all data] | 1.062 |
| final <i>R</i> indices ^g | |
| <i>R</i> ₁ [$F_0^2 \geq 2\sigma(F_0^2)$] | 0.0783 |
| <i>wR</i> ₂ [all data] | 0.1939 |
| largest difference peak and hole | 5.109 and -2.900 e Å ⁻³ |

^aObtained from least-squares refinement of 9840 reflections with $4.64^\circ < 2\theta < 50.80^\circ$.

^bPrograms for diffractometer operation, data collection, data reduction and absorption correction were those supplied by Bruker. The crystal used for data collection was found to display non-merohedral twinning. Both components of the twin were indexed with the program *CELL_NOW* (Bruker AXS Inc., Madison, WI, 2004). The second twin component can be

related to the first component by 180° rotation about the $[1 \ 1/8 \ -1/2]$ axis in real space and about the $[1 \ 0 \ -1]$ axis in reciprocal space. Integrated intensities for the reflections from the two components were written into a *SHELXL-97* HKLF 5 reflection file with the data integration program *SAINTE* (version 7.53A), using all reflection data (exactly overlapped, partially overlapped and non-overlapped).

^cBeurskens, P. T.; Beurskens, G.; de Gelder, R.; Smits, J. M. M.; Garcia-Granda, S.; Gould, R. O. (2008). The *DIRDIF-2008* program system. Crystallography Laboratory, Radboud University Nijmegen, The Netherlands.

^dSheldrick, G. M. *Acta Crystallogr.* **2008**, *A64*, 112–122.

^eDistance restraints were applied to some of the solvent CH₂Cl₂ and *n*-pentane molecules:

$d(\text{Cl}(7\text{S})-\text{C}(4\text{S})) = d(\text{Cl}(8\text{S})-\text{C}(4\text{S})) = 1.80(1) \text{ \AA}$; $d(\text{Cl}(7\text{S})\cdots\text{Cl}(8\text{S})) = 2.95(1) \text{ \AA}$; $d(\text{C}(11\text{S})-\text{C}(12\text{S})) = d(\text{C}(12\text{S})-\text{C}(13\text{S})) = d(\text{C}(13\text{S})-\text{C}(14\text{S})) = d(\text{C}(14\text{S})-\text{C}(15\text{S})) = d(\text{C}(21\text{S})-\text{C}(22\text{S})) = d(\text{C}(22\text{S})-\text{C}(23\text{S})) = d(\text{C}(23\text{S})-\text{C}(24\text{S})) = d(\text{C}(24\text{S})-\text{C}(25\text{S})) = 1.54(1) \text{ \AA}$;
 $d(\text{C}(11\text{S})\cdots\text{C}(13\text{S})) = d(\text{C}(12\text{S})\cdots\text{C}(14\text{S})) = d(\text{C}(13\text{S})\cdots\text{C}(15\text{S})) = d(\text{C}(21\text{S})\cdots\text{C}(23\text{S})) = d(\text{C}(22\text{S})\cdots\text{C}(24\text{S})) = d(\text{C}(23\text{S})\cdots\text{C}(25\text{S})) = 2.52(1) \text{ \AA}$.

$fS = [\Sigma w(F_o^2 - F_c^2)^2 / (n - p)]^{1/2}$ (n = number of data; p = number of parameters varied; $w = [\sigma^2(F_o^2) + (0.0482P)^2 + 154.6786P]^{-1}$ where $P = [\text{Max}(F_o^2, 0) + 2F_c^2]/3$).

$gR_1 = \Sigma ||F_o| - |F_c|| / \Sigma |F_o|$; $wR_2 = [\Sigma w(F_o^2 - F_c^2)^2 / \Sigma w(F_o^4)]^{1/2}$.

Table A.2. Crystallographic Experimental Details for Compound 5.

A. Crystal Data

| | |
|---|---|
| formula | C ₅₉ H ₅₆ Cl ₂ F ₅ Ir ₂ O ₆ .50P ₄ S |
| formula weight | 1575.28 |
| crystal dimensions (mm) | 0.51 x 0.16 x 0.12 |
| crystal system | monoclinic |
| space group | <i>P2</i> ₁ / <i>n</i> (an alternate setting of <i>P2</i> ₁ / <i>c</i> [No. 14]) |
| unit cell parameters ^a | |
| <i>a</i> (Å) | 13.0038 (4) |
| <i>b</i> (Å) | 24.7743 (8) |
| <i>c</i> (Å) | 18.3417 (6) |
| β (deg) | 94.3755 (4) |
| <i>V</i> (Å ³) | 5891.7 (3) |
| <i>Z</i> | 4 |
| <i>r</i> _{calcd} (g cm ⁻³) | 1.776 |
| μ (mm ⁻¹) | 4.814 |

B. Data Collection and Refinement Conditions

| | |
|--|--|
| diffractometer | Bruker D8/APEX II CCD ^b |
| radiation (λ[Å]) | graphite-monochromated Mo Kα (0.71073) |
| temperature (°C) | -100 |
| scan type | ω scans (0.3°) (20 s exposures) |
| data collection 2θ limit (deg) | 55.14 |
| total data collected | 51801 (-16 ≤ <i>h</i> ≤ 16, -32 ≤ <i>k</i> ≤ 32, -23 ≤ <i>l</i> ≤ 23) |
| independent reflections | 13582 (<i>R</i> _{int} = 0.0202) |
| number of observed reflections (<i>NO</i>) | 12235 [<i>F</i> _o ² ≥ 2σ(<i>F</i> _o ²)] |

| | |
|---|--|
| structure solution method | direct methods (<i>SIR97</i> ^c) |
| refinement method | full-matrix least-squares on F^2 (<i>SHELXL-97</i> ^d) |
| absorption correction method | Gaussian integration (face-indexed) |
| range of transmission factors | 0.6051–0.1910 |
| data/restraints/parameters | 13582 [$F_0^2 \geq -3\sigma(F_0^2)$] / 20 ^e / 744 |
| goodness-of-fit (S) ^f | 1.017 [$F_0^2 \geq -3\sigma(F_0^2)$] |
| final R indices ^g | |
| R_1 [$F_0^2 \geq 2\sigma(F_0^2)$] | 0.0225 |
| wR_2 [$F_0^2 \geq -3\sigma(F_0^2)$] | 0.0611 |
| largest difference peak and hole | 1.287 and –0.793 e Å ⁻³ |

^aObtained from least-squares refinement of 9686 reflections with $4.74^\circ < 2\theta < 55.10^\circ$.

^bPrograms for diffractometer operation, data collection, data reduction and absorption correction were those supplied by Bruker.

^cAltomare, A.; Burla, M. C.; Camalli, M.; Cascarano, G. L.; Giacovazzo, C.; Guagliardi, A.; Moliterni, A. G. G.; Polidori, G.; Spagna, R. *J. Appl. Cryst.* **1999**, *32*, 115–119.

^dSheldrick, G. M. *Acta Crystallogr.* **2008**, *A64*, 112–122.

^eThe disordered/partially occupied solvent molecules had the following distance restraints applied: for dichloromethane, C–Cl, 1.800(2) Å, Cl⋯Cl, 2.870(2) Å; for diethylether, C–C 1.530(2) Å, C–O, 1.430(2) Å, C⋯O, 2.420(2) Å, C⋯C, 2.340(2) Å.

$\int S = [\sum w(F_0^2 - F_c^2)^2 / (n - p)]^{1/2}$ (n = number of data; p = number of parameters varied; $w = [\sigma^2(F_0^2) + (0.0349P)^2 + 6.5481P]^{-1}$ where $P = [\text{Max}(F_0^2, 0) + 2F_c^2]/3$).

$gR_1 = \sum ||F_0| - |F_c|| / \sum |F_0|$; $wR_2 = [\sum w(F_0^2 - F_c^2)^2 / \sum w(F_0^4)]^{1/2}$.

Table A.3. Crystallographic Experimental Details for Compound **13**.

A. Crystal Data

| | |
|--|---|
| formula | C ₅₈ H ₅₀ Cl ₄ F ₆ Ir ₂ O ₉ P ₄ S ₂ |
| formula weight | 1719.18 |
| crystal dimensions (mm) | 0.19 x 0.19 x 0.13 |
| crystal system | orthorhombic |
| space group | <i>Pbca</i> (No. 61) |
| unit cell parameters ^a | |
| a (Å) | 20.9533 (10) |
| b (Å) | 23.2733 (11) |
| c (Å) | 54.433 (3) |
| V (Å ³) | 26544 (2) |
| Z | 16 |
| r_{calcd} (g cm ⁻³) | 1.721 |
| μ (mm ⁻¹) | 4.395 |

B. Data Collection and Refinement Conditions

| | |
|----------------------------|---|
| diffractometer | Bruker D8/APEX II CCD ^b |
| radiation (λ [Å]) | graphite-monochromated Mo $K\alpha$ (0.71073) |

| | |
|---|---|
| temperature (°C) | −100 |
| scan type | ω scans (0.3°) (20 s exposures) |
| data collection 2θ limit (deg) | 52.88 |
| total data collected | 207019 ($-26 \leq h \leq 26$, $-29 \leq k \leq 29$, $-68 \leq l \leq 68$) |
| independent reflections | 27266 ($R_{\text{int}} = 0.0995$) |
| number of observed reflections (NO) | 19998 [$F_o^2 \geq 2\sigma(F_o^2)$] |
| structure solution method | direct methods (<i>SHELXS-97</i> ^c) |
| refinement method | full-matrix least-squares on F^2 (<i>SHELXL-97c, d</i>) |
| absorption correction method | Gaussian integration (face-indexed) |
| range of transmission factors | 0.5988–0.4858 |
| data/restraints/parameters | 27266 / 0 / 1450 |
| goodness-of-fit (S) ^e [all data] | 1.088 |
| final R indices ^f | |
| R_1 [$F_o^2 \geq 2\sigma(F_o^2)$] | 0.0580 |
| wR_2 [all data] | 0.1165 |
| largest difference peak and hole | 2.857 and $-1.794 \text{ e } \text{\AA}^{-3}$ |

^aObtained from least-squares refinement of 9974 reflections with $4.32^\circ < 2\theta < 47.68^\circ$.

^bPrograms for diffractometer operation, data collection, data reduction and absorption correction were those supplied by Bruker.

^cSheldrick, G. M. *Acta Crystallogr.* **2008**, *A64*, 112–122.

^dAttempts to refine peaks of residual electron density as disordered or partial-occupancy solvent dichloromethane or diethylether carbon, chlorine or oxygen atoms were unsuccessful. The data were corrected for disordered electron density through use of the SQUEEZE procedure (Sluis, P. van der; Spek, A. L. *Acta Crystallogr.* **1990**, *A46*, 194–201) as implemented in *PLATON* (Spek, A. L. *Acta Crystallogr.* **1990**, *A46*, C34; Spek, A. L. *J. Appl. Cryst.* **2003**, *36*, 7–13. *PLATON* - a multipurpose crystallographic tool. Utrecht University, Utrecht, The Netherlands). A total solvent-accessible void volume of 4905 \AA^3 with a total electron count of 982 (consistent with 24 molecules of solvent dichloromethane, or 3 molecules per asymmetric unit, or 1.5 molecules formula unit of the $[\text{Ir}_2(\text{CO})_3(\text{CH}_2)(\text{O}_3\text{SCF}_3)(\text{dppm})_2][\text{CF}_3\text{SO}_3]$ molecule) was found in the unit cell.

^e $S = [\sum w(F_o^2 - F_c^2)^2 / (n - p)]^{1/2}$ (n = number of data; p = number of parameters varied; $w = [\sigma^2(F_o^2) + (0.0277P)^2 + 215.5532P]^{-1}$ where $P = [\text{Max}(F_o^2, 0) + 2F_c^2] / 3$).

^f $R_1 = \sum ||F_o| - |F_c|| / \sum |F_o|$; $wR_2 = [\sum w(F_o^2 - F_c^2)^2 / \sum w(F_o^4)]^{1/2}$.

Table A.4. Crystallographic Experimental Details for Compound **14**.

| | |
|-----------------------------------|---|
| <i>A. Crystal Data</i> | |
| formula | C _{59.25} H _{54.5} Cl _{2.5} F ₇ Ir ₂ O _{5.5} P ₄ S |
| formula weight | 1616.49 |
| crystal dimensions (mm) | 0.33 x 0.26 x 0.24 |
| crystal system | triclinic |
| space group | $P\bar{1}$ (No. 2) |
| unit cell parameters ^a | |
| a (Å) | 24.5658 (7) |

| | |
|---|---|
| b (Å) | 24.9915 (7) |
| c (Å) | 32.7022 (10) |
| α (deg) | 103.4967 (4) |
| β (deg) | 94.4410 (4) |
| γ (deg) | 105.4840 (4) |
| V (Å ³) | 18603.7 (9) |
| Z | 12 |
| r_{calcd} (g cm ⁻³) | 1.731 |
| μ (mm ⁻¹) | 4.600 |
| <i>B. Data Collection and Refinement Conditions</i> | |
| diffractometer | Bruker D8/APEX II CCD ^b |
| radiation (λ [Å]) | graphite-monochromated Mo K α (0.71073) |
| temperature (°C) | -100 |
| scan type | ω scans (0.3°) (20 s exposures) |
| data collection 2θ limit (deg) | 51.34 |
| total data collected | 138979 ($-29 \leq h \leq 29$, $-30 \leq k \leq 30$, $-39 \leq l \leq 39$) |
| independent reflections | 70337 ($R_{\text{int}} = 0.0413$) |
| number of observed reflections (NO) | 52990 [$F_0^2 \geq 2\sigma(F_0^2)$] |
| structure solution method | direct methods (<i>SHELXS-97</i> ^c) |
| refinement method | full-matrix least-squares on F^2 (<i>SHELXL-97</i> ^{c,d}) |
| absorption correction method | Gaussian integration (face-indexed) |
| range of transmission factors | 0.4011–0.3087 |
| data/restraints/parameters | 70337 / 39 ^e / 4244 |
| goodness-of-fit (S) ^f [all data] | 1.000 |
| final R indices ^g | |
| R_1 [$F_0^2 \geq 2\sigma(F_0^2)$] | 0.0364 |
| wR_2 [all data] | 0.1148 |
| largest difference peak and hole | 2.794 and $-1.510 \text{ e } \text{Å}^{-3}$ |

^aObtained from least-squares refinement of 9913 reflections with $4.46^\circ < 2\theta < 47.84^\circ$.

^bPrograms for diffractometer operation, data collection, data reduction and absorption correction were those supplied by Bruker.

^cSheldrick, G. M. *Acta Crystallogr.* **2008**, *A64*, 112–122.

^dAttempts to refine peaks of residual electron density as disordered or partial-occupancy solvent dichloromethane chlorine or carbon atoms were unsuccessful. The data were corrected for disordered electron density through use of the SQUEEZE procedure (Sluis, P. van der; Spek, A. L. *Acta Crystallogr.* **1990**, *A46*, 194–201) as implemented in *PLATON* (Spek, A. L. *Acta Crystallogr.* **1990**, *A46*, C34; Spek, A. L. *J. Appl. Cryst.* **2003**, *36*, 7–13. *PLATON* - a multipurpose crystallographic tool. Utrecht University, Utrecht, The Netherlands). A total solvent-accessible void volume of 662.4 Å³ with a total electron count of 94 (consistent with two molecules of solvent dichloromethane, or 1/6 molecule of CH₂Cl₂ per formula unit of the diiridium complex ion) was found in the unit cell.

^eWithin the disordered triflate ion: $d(\text{S}(6\text{A})-\text{O}(601)) = d(\text{S}(6\text{A})-\text{O}(602)) = d(\text{S}(6\text{A})-\text{O}(603)) =$

$d(\text{S}(6\text{B})-\text{O}(604)) = d(\text{S}(6\text{B})-\text{O}(605)) = d(\text{S}(6\text{B})-\text{O}(606)) = 1.45(1) \text{ \AA}$; $d(\text{S}(6\text{A})-\text{C}(601)) = d(\text{S}(6\text{B})-\text{C}(602)) = 1.80(1) \text{ \AA}$; $d(\text{F}(601)-\text{C}(601)) = d(\text{F}(601)-\text{C}(601)) = d(\text{F}(601)-\text{C}(601)) = d(\text{F}(601)-\text{C}(601)) = 1.35(1) \text{ \AA}$; $d(\text{S}(6\text{B})\cdots\text{F}(604)) = d(\text{S}(6\text{B})\cdots\text{F}(605)) = d(\text{S}(6\text{B})\cdots\text{F}(606)) = 2.56(1) \text{ \AA}$; $d(\text{F}(604)\cdots\text{F}(605)) = d(\text{F}(604)\cdots\text{F}(606)) = d(\text{F}(605)\cdots\text{F}(606)) = 2.15(1) \text{ \AA}$. Within the solvent dichloromethane molecules: $d(\text{Cl}(11)-\text{C}(6\text{S})) = d(\text{Cl}(12)-\text{C}(6\text{S})) = d(\text{Cl}(13)-\text{C}(7\text{S})) = d(\text{Cl}(14)-\text{C}(7\text{S})) = d(\text{Cl}(15)-\text{C}(8\text{S})) = d(\text{Cl}(16)-\text{C}(8\text{S})) = d(\text{Cl}(17)-\text{C}(9\text{S})) = d(\text{Cl}(18)-\text{C}(9\text{S})) = 1.75(1) \text{ \AA}$; $d(\text{Cl}(11)\cdots\text{Cl}(12)) = d(\text{Cl}(13)\cdots\text{Cl}(14)) = d(\text{Cl}(15)\cdots\text{Cl}(16)) = d(\text{Cl}(17)\cdots\text{Cl}(18)) = 2.85(1) \text{ \AA}$. Within the solvent diethyl ether molecules: $d(\text{O}(30\text{S})-\text{C}(31\text{S})) = d(\text{O}(30\text{S})-\text{C}(33\text{S})) = 1.46(1) \text{ \AA}$; $d(\text{C}(31\text{S})-\text{C}(32\text{S})) = d(\text{C}(33\text{S})-\text{C}(34\text{S})) = 1.52(1) \text{ \AA}$; $d(\text{O}(30\text{S})\cdots\text{C}(32\text{S})) = d(\text{O}(30\text{S})\cdots\text{C}(34\text{S})) = 2.43(1) \text{ \AA}$; $d(\text{C}(31\text{S})\cdots\text{C}(33\text{S})) = 2.38(1) \text{ \AA}$.
 $\int S = [\sum w(F_o^2 - F_c^2)^2 / (n - p)]^{1/2}$ (n = number of data; p = number of parameters varied; $w = [\sigma^2(F_o^2) + (0.0657P)^2]^{-1}$ where $P = [\text{Max}(F_o^2, 0) + 2F_c^2]/3$).
 $\mathcal{R}_1 = \sum ||F_o| - |F_c|| / \sum |F_o|$; $wR_2 = [\sum w(F_o^2 - F_c^2)^2 / \sum w(F_o^4)]^{1/2}$.

Table A.5. Crystallographic Experimental Details for Compound **16**.

| | |
|---|---|
| <i>A. Crystal Data</i> | |
| formula | C ₆₀ H ₅₃ Cl ₆ F ₉ Ir ₂ O ₈ P ₄ S ₂ |
| formula weight | 1858.12 |
| crystal dimensions (mm) | 0.58 x 0.56 x 0.19 |
| crystal system | orthorhombic |
| space group | <i>Pca</i> 2 ₁ (No. 29) |
| unit cell parameters ^a | |
| <i>a</i> (Å) | 24.2849 (14) |
| <i>b</i> (Å) | 11.9699 (7) |
| <i>c</i> (Å) | 23.3578 (13) |
| <i>V</i> (Å ³) | 6789.8 (7) |
| <i>Z</i> | 4 |
| <i>r</i> _{calcd} (g cm ⁻³) | 1.818 |
| μ (mm ⁻¹) | 4.384 |
| <i>B. Data Collection and Refinement Conditions</i> | |
| diffractometer | Bruker PLATFORM/SMART 1000 CCD ^b |
| radiation (λ [Å]) | graphite-monochromated Mo <i>K</i> α (0.71073) |
| temperature (°C) | -80 |
| scan type | ω scans (0.3°) (20 s exposures) |
| data collection 2 θ limit (deg) | 55.00 |
| total data collected | 57536 ($-31 \leq h \leq 31, -15 \leq k \leq 15, -30 \leq l \leq 30$) |
| independent reflections | 15502 ($R_{\text{int}} = 0.0298$) |
| number of observed reflections (<i>NO</i>) | 14629 [$F_o^2 \geq 2\sigma(F_o^2)$] |
| structure solution method | direct methods (<i>SHELXS-97</i> ^c) |
| refinement method | full-matrix least-squares on F^2 (<i>SHELXL-97c, d</i>) |
| absorption correction method | multi-scan (<i>SADABS</i>) |
| range of transmission factors | 0.4897–0.1853 |
| data/restraints/parameters | 15502 / 18 ^e / 777 |

| | |
|---|------------------------------------|
| Flack absolute structure parameter ^f | 0.013(4) |
| goodness-of-fit (S) ^g [all data] | 1.055 |
| final R indices ^h | |
| R ₁ [$F_o^2 \geq 2\sigma(F_o^2)$] | 0.0266 |
| wR ₂ [all data] | 0.0682 |
| largest difference peak and hole | 1.575 and -1.258 e Å ⁻³ |

^aObtained from least-squares refinement of 6745 reflections with $4.78^\circ < 2\theta < 54.40^\circ$.

^bPrograms for diffractometer operation, data collection, data reduction and absorption correction were those supplied by Bruker.

^cSheldrick, G. M. *Acta Crystallogr.* **2008**, *A64*, 112–122.

^dAttempts to refine peaks of residual electron density as disordered or partial-occupancy solvent dichloromethane chlorine or carbon atoms were unsuccessful. The data were corrected for disordered electron density through use of the SQUEEZE procedure (Sluis, P. van der; Spek, A. L. *Acta Crystallogr.* **1990**, *A46*, 194–201) as implemented in PLATON (Spek, A. L. *Acta Crystallogr.* **1990**, *A46*, C34; Spek, A. L. *J. Appl. Cryst.* **2003**, *36*, 7–13. PLATON - a multipurpose crystallographic tool. Utrecht University, Utrecht, The Netherlands). A total solvent-accessible void volume of 1320.7 Å³ with a total electron count of 544 (consistent with 12 molecules of solvent dichloromethane, or 3 molecules per formula unit of the diiridium complex cation) was found in the unit cell.

^e(i) The Ir(1)–C(4A) and Ir(1)–C(4B) distances (involving the disordered trifluorovinyl group) were constrained to be equal (within 0.03 Å) during refinement. (ii) The F–C distances within the minor conformer of the disordered trifluorovinyl group were restrained during refinement: d(F(1B)–C(4B)) = d(F(2B)–C(5B)) = d(F(3B)–C(5B)) = 1.35(1) Å. (iii) Restraints were applied during refinement to distances within the disordered noncoordinated triflate ion: d(S(2A)–O(91A)) = d(S(2A)–O(92A)) = d(S(2A)–O(93A)) = d(S(2B)–O(91B)) = d(S(2B)–O(92B)) = d(S(2B)–O(93B)) = 1.45(1) Å; d(S(2A)–C(91A)) = d(S(2B)–C(91B)) = 1.80(1) Å; d(F(91A)–C(91A)) = d(F(92A)–C(91A)) = d(F(93A)–C(91A)) = d(F(91B)–C(91B)) = d(F(92B)–C(91B)) = d(F(93B)–C(91B)) = 1.35(1) Å.

^fFlack, H. D. *Acta Crystallogr.* **1983**, *A39*, 876–881; Flack, H. D.; Bernardinelli, G. *Acta Crystallogr.* **1999**, *A55*, 908–915; Flack, H. D.; Bernardinelli, G. *J. Appl. Cryst.* **2000**, *33*, 1143–1148. The Flack parameter will refine to a value near zero if the structure is in the correct configuration and will refine to a value near one for the inverted configuration.

^g $S = [\sum w(F_o^2 - F_c^2)^2 / (n - p)]^{1/2}$ (n = number of data; p = number of parameters varied; $w = [\sigma^2(F_o^2) + (0.0392P)^2 + 1.4447P]^{-1}$ where $P = [\text{Max}(F_o^2, 0) + 2F_c^2]/3$).

^h $R_1 = \sum ||F_o| - |F_c|| / \sum |F_o|$; $wR_2 = [\sum w(F_o^2 - F_c^2)^2 / \sum w(F_o^4)]^{1/2}$.

Table A.6. Crystallographic Experimental Details for Compound **21**.

A. Crystal Data

| | |
|-----------------------------------|---|
| formula | C ₅₈ H ₄₇ F ₉ Ir ₂ O ₉ P ₄ S ₂ |
| formula weight | 1631.36 |
| crystal dimensions (mm) | 0.56 x 0.16 x 0.10 |
| crystal system | orthorhombic |
| space group | <i>Pca</i> 2 ₁ (No. 29) |
| unit cell parameters ^a | |
| <i>a</i> (Å) | 22.5843 (9) |
| <i>b</i> (Å) | 11.5088 (4) |
| <i>c</i> (Å) | 22.4724 (9) |

| | |
|---|--|
| V (Å ³) | 5841.0 (4) |
| Z | 4 |
| r_{calcd} (g cm ⁻³) | 1.855 |
| μ (mm ⁻¹) | 4.818 |
| <i>B. Data Collection and Refinement Conditions</i> | |
| diffractometer | Bruker D8/APEX II CCD ^b |
| radiation (λ [Å]) | graphite-monochromated Mo $K\alpha$ (0.71073) |
| temperature (°C) | -100 |
| scan type | ω scans (0.3°) (15 s exposures) |
| data collection 2θ limit (deg) | 55.04 |
| total data collected | 50235 ($-29 \leq h \leq 29$, $-14 \leq k \leq 14$, $-29 \leq l \leq 29$) |
| independent reflections | 13385 ($R_{\text{int}} = 0.0274$) |
| number of observed reflections (NO) | 12893 [$F_0^2 \geq 2\sigma(F_0^2)$] |
| structure solution method | Patterson/structure expansion (<i>DIRDIF-2008</i> ^c) |
| refinement method | full-matrix least-squares on F^2 (<i>SHELXL-97</i> ^d) |
| absorption correction method | Gaussian integration (face-indexed) |
| range of transmission factors | 0.6444–0.1733 |
| data/restraints/parameters | 13385 / 0 / 756 |
| Flack absolute structure parameter ^e | 0.434(8) |
| goodness-of-fit (S) ^f [all data] | 1.041 |
| final R indices ^g | |
| R_1 [$F_0^2 \geq 2\sigma(F_0^2)$] | 0.0471 |
| wR_2 [all data] | 0.1157 |
| largest difference peak and hole | 8.189 and $-4.435 \text{ e } \text{Å}^{-3}$ |

^aObtained from least-squares refinement of 9920 reflections with $4.36^\circ < 2\theta < 44.60^\circ$.

^bPrograms for diffractometer operation, data collection, data reduction and absorption correction were those supplied by Bruker.

^cBeurskens, P. T.; Beurskens, G.; de Gelder, R.; Smits, J. M. M.; Garcia-Granda, S.; Gould, R. O. (2008). The *DIRDIF-2008* program system. Crystallography Laboratory, Radboud University Nijmegen, The Netherlands.

^dSheldrick, G. M. *Acta Crystallogr.* **2008**, *A64*, 112–122.

^eFlack, H. D. *Acta Crystallogr.* **1983**, *A39*, 876–881; Flack, H. D.; Bernardinelli, G. *Acta Crystallogr.* **1999**, *A55*, 908–915; Flack, H. D.; Bernardinelli, G. *J. Appl. Cryst.* **2000**, *33*, 1143–1148. The Flack parameter will refine to a value near zero if the structure is in the correct configuration and will refine to a value near one for the inverted configuration. The value observed herein is indicative of racemic twinning, and was accommodated during the refinement (using the *SHELXL-93* TWIN instruction [see reference *d*]).

^f $S = [\sum w(F_0^2 - F_c^2)^2 / (n - p)]^{1/2}$ (n = number of data; p = number of parameters varied; $w = [\sigma^2(F_0^2) + (0.0429P)^2 + 63.5787P]^{-1}$ where $P = [\text{Max}(F_0^2, 0) + 2F_c^2]/3$).

^g $R_1 = \sum |F_0| - |F_c| / \sum |F_0|$; $wR_2 = [\sum w(F_0^2 - F_c^2)^2 / \sum w(F_0^4)]^{1/2}$.

Table A.7. Crystallographic Experimental Details for Compound **22**.

| | |
|---|--|
| <i>A. Crystal Data</i> | |
| formula | C ₅₈ H ₄₉ Cl ₂ F ₃ Ir ₂ O ₆ P ₄ S |
| formula weight | 1510.21 |
| crystal dimensions (mm) | 0.28 x 0.13 x 0.07 |
| crystal system | triclinic |
| space group | <i>P</i> $\bar{1}$ (No. 2) |
| unit cell parameters ^a | |
| <i>a</i> (Å) | 12.8269 (6) |
| <i>b</i> (Å) | 15.1227 (7) |
| <i>c</i> (Å) | 16.0743 (7) |
| α (deg) | 103.7580 (9) |
| β (deg) | 95.1235 (9) |
| γ (deg) | 107.4610 (9) |
| <i>V</i> (Å ³) | 2845.3 (2) |
| <i>Z</i> | 2 |
| <i>r</i> _{calcd} (g cm ⁻³) | 1.763 |
| μ (mm ⁻¹) | 4.975 |
| <i>B. Data Collection and Refinement Conditions</i> | |
| diffractometer | Bruker PLATFORM/SMART 1000 CCD ^b |
| radiation (λ [Å]) | graphite-monochromated Mo K α (0.71073) |
| temperature (°C) | -80 |
| scan type | ω scans (0.2°) (25 s exposures) |
| data collection 2θ limit (deg) | 52.76 |
| total data collected | 15475 ($-15 \leq h \leq 16$, $-18 \leq k \leq 12$, $-20 \leq l \leq 20$) |
| independent reflections | 11416 ($R_{\text{int}} = 0.0299$) |
| number of observed reflections (<i>NO</i>) | 8457 [$F_0^2 \geq 2\sigma(F_0^2)$] |
| structure solution method | Patterson/structure expansion (<i>DIRDIF-99</i> ^c) |
| refinement method | full-matrix least-squares on F^2 (<i>SHELXL-97d,e</i>) |
| absorption correction method | Gaussian integration (face-indexed) |
| range of transmission factors | 0.7221–0.3364 |
| data/restraints/parameters | 11416 / 26 ^f / 562 |
| goodness-of-fit (<i>S</i>) ^g [all data] | 1.027 |
| final <i>R</i> indices ^h | |
| <i>R</i> ₁ [$F_0^2 \geq 2\sigma(F_0^2)$] | 0.0419 |
| <i>wR</i> ₂ [all data] | 0.1077 |
| largest difference peak and hole | 1.775 and -1.309 e Å ⁻³ |

^aObtained from least-squares refinement of 7798 reflections with $4.64^\circ < 2\theta < 52.74^\circ$.

^bPrograms for diffractometer operation, data collection, data reduction and absorption correction were those supplied by Bruker.

^cBeurskens, P. T.; Beurskens, G.; de Gelder, R.; Garcia-Granda, S.; Israel, R.; Gould, R. O.; Smits, J. M. M. (1999). The *DIRDIF-99* program system. Crystallography Laboratory, University of Nijmegen, The Netherlands.

^dSheldrick, G. M. *Acta Crystallogr.* **2008**, *A64*, 112–122.

^eAttempts to refine peaks of residual electron density as disordered or partial-occupancy solvent dichloromethane chlorine or carbon atoms were unsuccessful. The data were corrected for disordered electron density through use of the SQUEEZE procedure (Sluis, P. van der; Spek, A. L. *Acta Crystallogr.* **1990**, *A46*, 194–201) as implemented in *PLATON* (Spek, A. L. *Acta Crystallogr.* **1990**, *A46*, C34; Spek, A. L. *J. Appl. Cryst.* **2003**, *36*, 7–13. *PLATON* - a multipurpose crystallographic tool. Utrecht University, Utrecht, The Netherlands). A total solvent-accessible void volume of 300.8 Å³ with a total electron count of 99 (consistent with 2 molecules of solvent dichloromethane, or one molecule per formula unit of the diiridium complex molecule) was found in the unit cell.

^fAn idealized geometry was imposed upon the disordered triflate anion through use of the following distance restraints: d(S(1A)–C(91A)) = d(S(1B)–C(91B)) = 1.75(1) Å; d(S(1A)–O(91A)) = d(S(1A)–O(92A)) = d(S(1A)–O(93A)) = d(S(1B)–O(91B)) = d(S(1B)–O(92B)) = d(S(1B)–O(93B)) = 1.45(1) Å; d(F(91A)–C(91A)) = d(F(92A)–C(91A)) = d(F(93A)–C(91A)) = d(F(91B)–C(91B)) = d(F(92B)–C(91B)) = d(F(93B)–C(91B)) = 1.35(1) Å; d(F(91A)···F(92A)) = d(F(91A)···F(93A)) = d(F(91A)···F(93A)) = d(F(91B)···F(92B)) = d(F(91B)···F(93B)) = d(F(92B)···F(93B)) = 2.20(1) Å; d(O(91A)···O(92A)) = d(O(91A)···O(93A)) = d(O(91A)···O(93A)) = d(O(91B)···O(92B)) = d(O(91B)···O(93B)) = d(O(92B)···O(93B)) = 2.37(1) Å.

$gS = [\sum w(F_o^2 - F_c^2)^2 / (n - p)]^{1/2}$ (n = number of data; p = number of parameters varied; $w = [\sigma^2(F_o^2) + (0.0558P)^2]^{-1}$ where $P = [\text{Max}(F_o^2, 0) + 2F_c^2]/3$).

$hR_1 = \sum ||F_o| - |F_c|| / \sum |F_o|$; $wR_2 = [\sum w(F_o^2 - F_c^2)^2 / \sum w(F_o^4)]^{1/2}$.

Table A.8. Crystallographic Experimental Details for Compound **26**.

| | |
|---|--|
| <i>A. Crystal Data</i> | |
| formula | C ₂₀ H ₄₄ Cl ₂ Ir ₂ O ₂ P ₄ |
| formula weight | 895.73 |
| crystal dimensions (mm) | 0.54 x 0.52 x 0.43 |
| crystal system | monoclinic |
| space group | <i>P2</i> ₁ / <i>n</i> (an alternate setting of <i>P2</i> ₁ / <i>c</i> [No. 14]) |
| unit cell parameters ^a | |
| <i>a</i> (Å) | 10.5127 (5) |
| <i>b</i> (Å) | 11.6941 (6) |
| <i>c</i> (Å) | 11.9926 (6) |
| β (deg) | 103.8544 (9) |
| <i>V</i> (Å ³) | 1431.44 (12) |
| <i>Z</i> | 2 |
| <i>r</i> _{calcd} (g cm ⁻³) | 2.078 |
| μ (mm ⁻¹) | 9.713 |
| <i>B. Data Collection and Refinement Conditions</i> | |
| diffractometer | Bruker PLATFORM/SMART 1000 CCD ^b |
| radiation (λ [Å]) | graphite-monochromated Mo <i>K</i> α (0.71073) |
| temperature (°C) | –80 |

| | |
|---|---|
| scan type | ω scans (0.2°) (20 s exposures) |
| data collection 2θ limit (deg) | 52.80 |
| total data collected | 7929 ($-12 \leq h \leq 13$, $-14 \leq k \leq 14$, $-14 \leq l \leq 14$) |
| independent reflections | 2908 ($R_{\text{int}} = 0.0248$) |
| number of observed reflections (NO) | 2836 [$F_0^2 \geq 2\sigma(F_0^2)$] |
| structure solution method | direct methods (<i>SHELXS-86</i> ^c) |
| refinement method | full-matrix least-squares on F^2 (<i>SHELXL-93</i> ^d) |
| absorption correction method | empirical (<i>SADABS</i>) |
| range of transmission factors | 0.1027–0.0773 |
| data/restraints/parameters | 2908 [$F_0^2 \geq -3\sigma(F_0^2)$] / 0 / 139 |
| extinction coefficient (x) ^e | 0.0029 (2) |
| goodness-of-fit (S) ^f | 1.226 [$F_0^2 \geq -3\sigma(F_0^2)$] |
| final R indices ^g | |
| R_1 [$F_0^2 \geq 2\sigma(F_0^2)$] | 0.0265 |
| wR_2 [$F_0^2 \geq -3\sigma(F_0^2)$] | 0.0725 |
| largest difference peak and hole | 2.075 and $-3.059 \text{ e } \text{\AA}^{-3}$ |

^aObtained from least-squares refinement of 8106 reflections with $4.63^\circ < 2\theta < 52.75^\circ$.

^bPrograms for diffractometer operation, data collection, data reduction and absorption correction were those supplied by Bruker.

^cSheldrick, G. M. *Acta Crystallogr.* **1990**, *A46*, 467–473.

^dSheldrick, G. M. *SHELXL-93*. Program for crystal structure determination. University of Göttingen, Germany, 1993. Refinement on F_0^2 for all reflections (all of these having $F_0^2 \geq -3\sigma(F_0^2)$). Weighted R -factors wR_2 and all goodnesses of fit S are based on F_0^2 ; conventional R -factors R_1 are based on F_0 , with F_0 set to zero for negative F_0^2 . The observed criterion of $F_0^2 > 2\sigma(F_0^2)$ is used only for calculating R_1 , and is not relevant to the choice of reflections for refinement. R -factors based on F_0^2 are statistically about twice as large as those based on F_0 , and R -factors based on ALL data will be even larger.

^e $F_c^* = kF_c[1 + x\{0.001F_c^2I^3/\sin(2q)\}]^{-1/4}$ where k is the overall scale factor.

^f $S = [\sum w(F_0^2 - F_c^2)^2/(n - p)]^{1/2}$ (n = number of data; p = number of parameters varied; $w = [\sigma^2(F_0^2) + (0.0335P)^2 + 4.6571P]^{-1}$ where $P = [\text{Max}(F_0^2, 0) + 2F_c^2]/3$).

^g $R_1 = \sum ||F_0| - |F_c||/\sum |F_0|$; $wR_2 = [\sum w(F_0^2 - F_c^2)^2/\sum w(F_0^4)]^{1/2}$.

Table A.9. Crystallographic Experimental Details for Compound **29**.

A. Crystal Data

| | |
|-----------------------------------|--|
| formula | C ₂₃ H ₄₇ F ₃ Ir ₂ O ₆ P ₄ S |
| formula weight | 1016.95 |
| crystal dimensions (mm) | 0.32 x 0.23 x 0.19 |
| crystal system | triclinic |
| space group | $P\bar{1}$ (no.2) |
| unit cell parameters ^a | |
| a (Å) | 10.6784 (7) |
| b (Å) | 12.5837 (9) |

| | |
|---|--|
| c (Å) | 14.9169 (10) |
| α (deg) | 111.4041 (10) |
| β (deg) | 96.2866 (11) |
| γ (deg) | 107.8398 (11) |
| V (Å ³) | 1720.2 (2) |
| Z | 2 |
| r_{caled} (g cm ⁻³) | 1.963 |
| μ (mm ⁻¹) | 8.024 |
| B. Data Collection and Refinement Conditions | |
| diffractometer | Bruker PLATFORM/SMART 1000 CCD ^b |
| radiation (λ [Å]) | graphite-monochromated Mo K α (0.71073) |
| temperature (°C) | -80 |
| scan type | ω scans (0.3°) (20 s exposures) |
| data collection 2θ limit (deg) | 52.78 |
| total data collected | 13362 ($-13 \leq h \leq 13, -15 \leq k \leq 15, -18 \leq l \leq 18$) |
| independent reflections | 6992 ($R_{\text{int}} = 0.0224$) |
| number of observed reflections (NO) | 6039 [$F_0^2 \geq 2\sigma(F_0^2)$] |
| structure solution method | direct methods (<i>SHELXS-86</i> ^c) |
| refinement method | full-matrix least-squares on F^2 (<i>SHELXL-93</i> ^d) |
| absorption correction method | Gaussian integration (face-indexed) |
| range of transmission factors | 0.3109–0.1833 |
| data/restraints/parameters | 6992 [$F_0^2 \geq -3\sigma(F_0^2)$] / 3 ^e / 354 |
| goodness-of-fit (S) ^f | 1.050 [$F_0^2 \geq -3\sigma(F_0^2)$] |
| final R indices ^g | |
| R_1 [$F_0^2 \geq 2\sigma(F_0^2)$] | 0.0308 |
| wR_2 [$F_0^2 \geq -3\sigma(F_0^2)$] | 0.0811 |
| largest difference peak and hole | 2.273 and -0.746 e Å ⁻³ |

^aObtained from least-squares refinement of 4949 reflections with $4.48^\circ < 2\theta < 52.79^\circ$.

^bPrograms for diffractometer operation, data collection, data reduction and absorption correction were those supplied by Bruker.

^cSheldrick, G. M. *Acta Crystallogr.* **1990**, *A46*, 467–473.

^dSheldrick, G. M. *SHELXL-93*. Program for crystal structure determination. University of Göttingen, Germany, 1993. Refinement on F_0^2 for all reflections (all of these having $F_0^2 \geq -3\sigma(F_0^2)$). Weighted R -factors wR_2 and all goodnesses of fit S are based on F_0^2 ; conventional R -factors R_1 are based on F_0 , with F_0 set to zero for negative F_0^2 . The observed criterion of $F_0^2 > 2\sigma(F_0^2)$ is used only for calculating R_1 , and is not relevant to the choice of reflections for refinement. R -factors based on F_0^2 are statistically about twice as large as those based on F_0 , and R -factors based on ALL data will be even larger.

^eThe Ir(2)–H(2) distance was restrained to be 1.65(1) Å. The C(25)–C(26A) and C(25)–C(26B) distances were restrained to be 1.53(1) Å.

^f $S = [\sum w(F_0^2 - F_c^2)^2 / (n - p)]^{1/2}$ (n = number of data; p = number of parameters varied; $w = [s^2(F_0^2) + (0.0399P)^2 + 3.1190P]^{-1}$ where $P = [\text{Max}(F_0^2, 0) + 2F_c^2] / 3$).

$$gR_1 = \Sigma||F_o| - |F_c||/\Sigma|F_o|; wR_2 = [\Sigma w(F_o^2 - F_c^2)^2/\Sigma w(F_o^4)]^{1/2}.$$

Table A.10. Crystallographic Experimental Details for Compound **36**.

| | |
|--|--|
| <i>A. Crystal Data</i> | |
| formula | C ₂₀ H ₄₄ Cl ₂ O ₂ P ₂ Rh ₂ |
| formula weight | 717.15 |
| crystal dimensions (mm) | 0.37 x 0.32 x 0.28 |
| crystal system | monoclinic |
| space group | <i>P2</i> ₁ / <i>n</i> (an alternate setting of <i>P2</i> ₁ / <i>c</i> [No. 14]) |
| unit cell parameters ^a | |
| <i>a</i> (Å) | 10.4972 (6) |
| <i>b</i> (Å) | 11.6908 (6) |
| <i>c</i> (Å) | 12.0101 (7) |
| β (deg) | 103.7950 (10) |
| <i>V</i> (Å ³) | 1431.37 (14) |
| <i>Z</i> | 2 |
| <i>r</i> _{calcd} (g cm ⁻³) | 1.664 |
| μ (mm ⁻¹) | 1.579 |
| <i>B. Data Collection and Refinement Conditions</i> | |
| diffractometer | Bruker PLATFORM/SMART 1000 CCD ^b |
| radiation (λ [Å]) | graphite-monochromated Mo <i>K</i> α (0.71073) |
| temperature (°C) | -80 |
| scan type | ω scans (0.2°) (25 s exposures) |
| data collection 2θ limit (deg) | 52.78 |
| total data collected | 6899 (-13 \leq h \leq 13, -14 \leq k \leq 13, -12 \leq l \leq 15) |
| independent reflections | 2912 (<i>R</i> _{int} = 0.0264) |
| number of observed reflections (<i>NO</i>) | 2749 [<i>F</i> _o ² \geq 2 σ (<i>F</i> _o ²)] |
| structure solution method | direct methods (<i>SHELXS-86</i> ^c) |
| refinement method | full-matrix least-squares on <i>F</i> ² (<i>SHELXL-93</i> ^d) |
| absorption correction method | empirical (<i>SADABS</i>) |
| range of transmission factors | 0.6662–0.5927 |
| data/restraints/parameters | 2912 [<i>F</i> _o ² \geq -3 σ (<i>F</i> _o ²)] / 0 / 163 |
| goodness-of-fit (<i>S</i>) ^e | 1.139 [<i>F</i> _o ² \geq -3 σ (<i>F</i> _o ²)] |
| final <i>R</i> indices ^f | |
| <i>R</i> ₁ [<i>F</i> _o ² \geq 2 σ (<i>F</i> _o ²)] | 0.0231 |
| <i>wR</i> ₂ [<i>F</i> _o ² \geq -3 σ (<i>F</i> _o ²)] | 0.0608 |
| largest difference peak and hole | 0.641 and -0.303 e Å ⁻³ |

^aObtained from least-squares refinement of 6740 reflections with 4.64° < 2 θ < 52.75°.

^bPrograms for diffractometer operation, data collection, data reduction and absorption correction were those supplied by Bruker.

^cSheldrick, G. M. *Acta Crystallogr.* **1990**, *A46*, 467–473.

^dSheldrick, G. M. *SHELXL-93*. Program for crystal structure determination. University of

Göttingen, Germany, 1993. Refinement on F_o^2 for all reflections (all of these having $F_o^2 \geq -3\sigma(F_o^2)$). Weighted R -factors wR_2 and all goodnesses of fit S are based on F_o^2 ; conventional R -factors R_1 are based on F_o , with F_o set to zero for negative F_o^2 . The observed criterion of $F_o^2 > 2\sigma(F_o^2)$ is used only for calculating R_1 , and is not relevant to the choice of reflections for refinement. R -factors based on F_o^2 are statistically about twice as large as those based on F_o , and R -factors based on ALL data will be even larger.

$eS = [\Sigma w(F_o^2 - F_c^2)^2 / (n - p)]^{1/2}$ (n = number of data; p = number of parameters varied; $w = [s^2(F_o^2) + (0.0274P)^2 + 0.5983P]^{-1}$ where $P = [\text{Max}(F_o^2, 0) + 2F_c^2]/3$).

$\int R_1 = \Sigma |F_o| - |F_c| / \Sigma |F_o|$; $wR_2 = [\Sigma w(F_o^2 - F_c^2)^2 / \Sigma w(F_o^4)]^{1/2}$.

Table A.11. Crystallographic Experimental Details for Compound **41**.

| | |
|---|--|
| <i>A. Crystal Data</i> | |
| formula | C ₅₃ H ₅₈ BClF ₂₄ O ₃ P ₄ Rh ₂ |
| formula weight | 1580.96 |
| crystal dimensions (mm) | 0.44 x 0.38 x 0.15 |
| crystal system | monoclinic |
| space group | $P2_1/c$ (No. 14) |
| unit cell parameters ^a | |
| a (Å) | 14.9379 (5) |
| b (Å) | 14.7561 (5) |
| c (Å) | 30.2835 (11) |
| β (deg) | 103.4274 (5) |
| V (Å ³) | 6492.8 (4) |
| Z | 4 |
| r_{calcd} (g cm ⁻³) | 1.617 |
| μ (mm ⁻¹) | 0.757 |
| <i>B. Data Collection and Refinement Conditions</i> | |
| diffractometer | Bruker PLATFORM/APEX II CCD ^b |
| radiation (λ [Å]) | graphite-monochromated Mo $K\alpha$ (0.71073) |
| temperature (°C) | -100 |
| scan type | ω scans (0.3°) (15 s exposures) |
| data collection 2θ limit (deg) | 55.10 |
| total data collected | 57600 ($-19 \leq h \leq 19$, $-19 \leq k \leq 19$, $-39 \leq l \leq 39$) |
| independent reflections | 14977 ($R_{\text{int}} = 0.0217$) |
| number of observed reflections (NO) | 12830 [$F_o^2 \geq 2\sigma(F_o^2)$] |
| structure solution method | Patterson/structure expansion (<i>DIRDIF-2008</i> ^c) |
| refinement method | full-matrix least-squares on F^2 (<i>SHELXL-97</i> ^d) |
| absorption correction method | Gaussian integration (face-indexed) |
| range of transmission factors | 0.8949–0.7298 |
| data/restraints/parameters | 14977 / 0 / 1014 |
| goodness-of-fit (S) ^e [all data] | 1.029 |
| final R indices ^f | |
| R_1 [$F_o^2 \geq 2\sigma(F_o^2)$] | 0.0377 |

| | |
|----------------------------------|---|
| wR_2 [all data] | 0.1013 |
| largest difference peak and hole | 1.363 and $-1.172 \text{ e } \text{\AA}^{-3}$ |

^aObtained from least-squares refinement of 9173 reflections with $4.38^\circ < 2\theta < 41.06^\circ$.

^bPrograms for diffractometer operation, data collection, data reduction and absorption correction were those supplied by Bruker.

^cBeurskens, P. T.; Beurskens, G.; de Gelder, R.; Smits, J. M. M.; Garcia-Granda, S.; Gould, R. O. (2008). The *DIRDIF-2008* program system. Crystallography Laboratory, Radboud University Nijmegen, The Netherlands.

^dSheldrick, G. M. *Acta Crystallogr.* **2008**, *A64*, 112–122.

^e $S = [\sum w(F_o^2 - F_c^2)^2 / (n - p)]^{1/2}$ (n = number of data; p = number of parameters varied; $w = [\sigma^2(F_o^2) + (0.0432P)^2 + 9.2895P]^{-1}$ where $P = [\text{Max}(F_o^2, 0) + 2F_c^2]/3$).

$fR_1 = \sum |F_o| - |F_c| / \sum |F_o|$; $wR_2 = [\sum w(F_o^2 - F_c^2)^2 / \sum w(F_o^4)]^{1/2}$.

Table A.12. Crystallographic Experimental Details for Compound **43**.

A. Crystal Data

| | |
|-----------------------------------|--|
| formula | C ₂₅ H ₄₄ F ₆ O ₁₁ P ₄ Rh ₂ S ₂ |
| formula weight | 1028.42 |
| crystal dimensions (mm) | 0.49 x 0.40 x 0.16 |
| crystal system | monoclinic |
| space group | <i>P2₁/m</i> (No. 11) |
| unit cell parameters ^a | |
| <i>a</i> (Å) | 9.5764 (6) |
| <i>b</i> (Å) | 21.3460 (14) |
| <i>c</i> (Å) | 10.0396 (6) |
| β (deg) | 108.0810 (10) |
| <i>V</i> (Å ³) | 1950.9 (2) |
| <i>Z</i> | 2 |

| | |
|--|-------|
| r_{calcd} (g cm ⁻³) | 1.751 |
| μ (mm ⁻¹) | 1.196 |

B. Data Collection and Refinement Conditions

| | |
|--|---|
| diffractometer | Bruker PLATFORM/SMART 1000 CCD ^b |
| radiation (λ [Å]) | graphite-monochromated Mo K α (0.71073) |
| temperature (°C) | -80 |
| scan type | ω scans (0.2°) (20 s exposures) |
| data collection 2θ limit (deg) | 52.72 |
| total data collected | 11122 ($-8 \leq h \leq 11$, $-26 \leq k \leq 26$, $-12 \leq l \leq 12$) |
| independent reflections | 4079 ($R_{\text{int}} = 0.0200$) |
| number of observed reflections (<i>NO</i>) | 3810 [$F_o^2 \geq 2\sigma(F_o^2)$] |
| structure solution method | direct methods (<i>SHELXS-86</i> ^c) |
| refinement method | full-matrix least-squares on F^2 (<i>SHELXL-93</i> ^d) |
| absorption correction method | multi-scan (<i>SADABS</i>) |
| range of transmission factors | 0.8317–0.5918 |
| data/restraints/parameters | 4079 [$F_o^2 \geq -3\sigma(F_o^2)$] / 0 / 244 |
| goodness-of-fit (<i>S</i>) ^e | 1.040 [$F_o^2 \geq -3\sigma(F_o^2)$] |

| | |
|-------------------------------------|---|
| final R indices ^f | |
| $R_1 [F_0^2 \geq 2\sigma(F_0^2)]$ | 0.0225 |
| $wR_2 [F_0^2 \geq -3\sigma(F_0^2)]$ | 0.0625 |
| largest difference peak and hole | 0.694 and $-0.526 \text{ e } \text{\AA}^{-3}$ |

^aObtained from least-squares refinement of 5433 reflections with $4.86^\circ < 2\theta < 52.72^\circ$.

^bPrograms for diffractometer operation, data collection, data reduction and absorption correction were those supplied by Bruker.

^cSheldrick, G. M. *Acta Crystallogr.* **1990**, *A46*, 467–473.

^dSheldrick, G. M. *SHELXL-93*. Program for crystal structure determination. University of Göttingen, Germany, 1993. Refinement on F_0^2 for all reflections (all of these having $F_0^2 \geq -3\sigma(F_0^2)$). Weighted R -factors wR_2 and all goodnesses of fit S are based on F_0^2 ; conventional R -factors R_1 are based on F_0 , with F_0 set to zero for negative F_0^2 . The observed criterion of $F_0^2 > 2\sigma(F_0^2)$ is used only for calculating R_1 , and is not relevant to the choice of reflections for refinement. R -factors based on F_0^2 are statistically about twice as large as those based on F_0 , and R -factors based on ALL data will be even larger.

^e $S = [\sum w(F_0^2 - F_c^2)^2 / (n - p)]^{1/2}$ (n = number of data; p = number of parameters varied; $w = [\sigma^2(F_0^2) + (0.0344P)^2 + 1.1794P]^{-1}$ where $P = [\text{Max}(F_0^2, 0) + 2F_c^2]/3$).

^f $R_1 = \sum |F_0| - |F_c| / \sum |F_0|$; $wR_2 = [\sum w(F_0^2 - F_c^2)^2 / \sum w(F_0^4)]^{1/2}$.

Table A.13. Crystallographic Experimental Details for Compound **47**.

A. Crystal Data

| | |
|-----------------------------------|--|
| formula | $\text{C}_{23}\text{H}_{47}\text{F}_3\text{IrO}_6\text{P}_4\text{RhS}$ |
| formula weight | 927.66 |
| crystal dimensions (mm) | 0.54 x 0.16 x 0.15 |
| crystal system | monoclinic |
| space group | $P2_1/c$ (No. 14) |
| unit cell parameters ^a | |
| a (Å) | 8.0072 (12) |
| b (Å) | 18.318 (3) |
| c (Å) | 23.367 (4) |
| β (deg) | 90.877 (2) |
| V (Å ³) | 3426.9 (9) |
| Z | 4 |

r_{calcd} (g cm⁻³) 1.798

μ (mm⁻¹) 4.658

B. Data Collection and Refinement Conditions

| | |
|---------------------------------------|---|
| diffractometer | Bruker PLATFORM/SMART 1000 CCD ^b |
| radiation (λ [Å]) | graphite-monochromated Mo $K\alpha$ (0.71073) |
| temperature (°C) | -80 |
| scan type | ω scans (0.3°) (20 s exposures) |
| data collection 2θ limit (deg) | 52.86 |
| total data collected | 25673 ($-9 \leq h \leq 10$, $-22 \leq k \leq 22$, $-29 \leq l \leq 29$) |

| | |
|---|---|
| independent reflections | 6971 ($R_{\text{int}} = 0.0346$) |
| number of observed reflections (NO) | 6224 [$F_0^2 \geq 2\sigma(F_0^2)$] |
| structure solution method | direct methods (<i>SHELXS-97^c</i>) |
| refinement method | full-matrix least-squares on F^2 (<i>SHELXL-97^d</i>) |
| absorption correction method | multi-scan (<i>SADABS</i>) |
| range of transmission factors | 0.5417–0.1876 |
| data/restraints/parameters | 6971 [$F_0^2 \geq -3\sigma(F_0^2)$] / 18 ^e / 384 |
| goodness-of-fit (S) ^f | 1.182 [$F_0^2 \geq -3\sigma(F_0^2)$] |
| final R indices ^g | |
| R_1 [$F_0^2 \geq 2\sigma(F_0^2)$] | 0.0526 |
| wR_2 [$F_0^2 \geq -3\sigma(F_0^2)$] | 0.1334 |
| largest difference peak and hole | 3.100 and $-1.649 \text{ e } \text{\AA}^{-3}$ |

^aObtained from least-squares refinement of 6215 reflections with $5.56^\circ < 2\theta < 52.86^\circ$.

^bPrograms for diffractometer operation, data collection, data reduction and absorption correction were those supplied by Bruker.

^cSheldrick, G. M. *Acta Crystallogr.* **1990**, *A46*, 467–473.

^dSheldrick, G. M. *SHELXL-97*. Program for crystal structure determination. University of Göttingen, Germany, 1997.

^eThe minor (40%) component of the disordered $\text{RhIr}(\text{CO})_3(\text{CH}_3)$ fragment (IrB, RhB, O1B, O2B, O3B, C1B, C2B, C3B, C4B) was restrained to have the same bond lengths and angles as the major orientation.

^f $S = [\sum w(F_0^2 - F_c^2)^2 / (n - p)]^{1/2}$ (n = number of data; p = number of parameters varied; $w = [\sigma^2(F_0^2) + (0.0304P)^2 + 46.1634P]^{-1}$ where $P = [\text{Max}(F_0^2, 0) + 2F_c^2]/3$).

^g $R_1 = \sum ||F_0| - |F_c|| / \sum |F_0|$; $wR_2 = [\sum w(F_0^2 - F_c^2)^2 / \sum w(F_0^4)]^{1/2}$.

Table A.14. Crystallographic Experimental Details for Compound **58**.

A. Crystal Data

| | |
|--|---|
| formula | $\text{C}_{55}\text{H}_{59}\text{BF}_{24}\text{Ir}_2\text{O}_3\text{P}_4$ |
| formula weight | 1743.11 |
| crystal dimensions (mm) | 0.41 x 0.29 x 0.18 |
| crystal system | triclinic |
| space group | $P\bar{1}$ (No. 2) |
| unit cell parameters ^a | |
| a (Å) | 12.5007 (16) |
| b (Å) | 14.6611 (18) |
| c (Å) | 18.491 (2) |
| α (deg) | 76.3985 (15) |
| β (deg) | 84.0521 (16) |
| γ (deg) | 86.3437 (16) |
| V (Å ³) | 3273.5 (7) |
| Z | 2 |
| r_{calcd} (g cm ⁻³) | 1.768 |
| μ (mm ⁻¹) | 4.268 |

B. Data Collection and Refinement Conditions

| | |
|---|--|
| diffractometer | Bruker PLATFORM/APEX II CCD ^b |
| radiation (λ [Å]) | graphite-monochromated Mo K α (0.71073) |
| temperature (°C) | –100 |
| scan type | ω scans (0.3°) (15 s exposures) |
| data collection 2θ limit (deg) | 55.08 |
| total data collected | 29059 ($-16 \leq h \leq 16$, $-19 \leq k \leq 19$, $-23 \leq l \leq 24$) |
| independent reflections | 14991 ($R_{\text{int}} = 0.0144$) |
| number of observed reflections (<i>NO</i>) | 13501 [$F_o^2 \geq 2\sigma(F_o^2)$] |
| structure solution method | Patterson/structure expansion (<i>DIRDIF-2008</i> ^c) |
| refinement method | full-matrix least-squares on F^2 (<i>SHELXL-97</i> ^d) |
| absorption correction method | Gaussian integration (face-indexed) |
| range of transmission factors | 0.5155–0.2729 |
| data/restraints/parameters | 14991 / 13 ^e / 889 |
| goodness-of-fit (S) ^f [all data] | 1.023 |
| final <i>R</i> indices ^g | |
| R_1 [$F_o^2 \geq 2\sigma(F_o^2)$] | 0.0229 |
| wR_2 [all data] | 0.0578 |
| largest difference peak and hole | 3.166 and –1.444 e Å ^{–3} |

^aObtained from least-squares refinement of 7504 reflections with $4.36^\circ < 2\theta < 46.22^\circ$.

^bPrograms for diffractometer operation, data collection, data reduction and absorption correction were those supplied by Bruker.

^cBeurskens, P. T.; Beurskens, G.; de Gelder, R.; Smits, J. M. M.; Garcia-Granda, S.; Gould, R. O. (2008). The *DIRDIF-2008* program system. Crystallography Laboratory, Radboud University Nijmegen, The Netherlands.

^dSheldrick, G. M. *Acta Crystallogr.* **2008**, *A64*, 112–122.

^eThe Ir(1)–H(1) distance was constrained to be 1.55(1) Å during refinement. F–C distances within two disordered trifluoromethyl groups (of the [B{C₆H₃–3.5-(CF₃)₂}]₄[–] ion) were constrained to be equal (within 0.03 Å) to a common value during refinement: d(F(71A)–C(77)) = d(F(72A)–C(77)) = d(F(73A)–C(77)) = d(F(71B)–C(77)) = d(F(72B)–C(77)) = d(F(73B)–C(77)) = d(F(74A)–C(78)) = d(F(75A)–C(78)) = d(F(76A)–C(78)) = d(F(74B)–C(78)) = d(F(75B)–C(78)) = d(F(76B)–C(78)).

$fS = [\sum w(F_o^2 - F_c^2)^2 / (n - p)]^{1/2}$ (n = number of data; p = number of parameters varied; $w = [\sigma^2(F_o^2) + (0.0258P)^2 + 4.3209P]^{-1}$ where $P = [\text{Max}(F_o^2, 0) + 2F_c^2]/3$).

$gR_1 = \sum ||F_o| - |F_c|| / \sum |F_o|$; $wR_2 = [\sum w(F_o^2 - F_c^2)^2 / \sum w(F_o^4)]^{1/2}$.

Table A.15. Crystallographic Experimental Details for Compound **63**.

A. Crystal Data

| | |
|-------------------------|--|
| formula | C ₅₅ H ₅₇ BF ₂₆ Ir ₂ O ₃ P ₄ |
| formula weight | 1779.10 |
| crystal dimensions (mm) | 0.36 x 0.25 x 0.11 |
| crystal system | triclinic |

| | |
|---|--|
| space group | $P\bar{1}$ (No. 2) |
| unit cell parameters ^a | |
| a (Å) | 12.6522 (6) |
| b (Å) | 14.9899 (7) |
| c (Å) | 17.6977 (8) |
| α (deg) | 97.0697 (6) |
| β (deg) | 97.5218 (6) |
| γ (deg) | 92.0058 (6) |
| V (Å ³) | 3297.8 (3) |
| Z | 2 |
| r_{calcd} (g cm ⁻³) | 1.792 |
| μ (mm ⁻¹) | 4.242 |
| <i>B. Data Collection and Refinement Conditions</i> | |
| diffractometer | Bruker PLATFORM/APEX II CCD ^b |
| radiation (λ [Å]) | graphite-monochromated Mo K α (0.71073) |
| temperature (°C) | -100 |
| scan type | ω scans (0.3°) (20 s exposures) |
| data collection 2θ limit (deg) | 53.16 |
| total data collected | 27069 ($-15 \leq h \leq 15$, $-18 \leq k \leq 18$, $-22 \leq l \leq 22$) |
| independent reflections | 13755 ($R_{\text{int}} = 0.0214$) |
| number of observed reflections (NO) | 10661 [$F_o^2 \geq 2\sigma(F_o^2)$] |
| structure solution method | direct methods (<i>SHELXS-97</i> ^c) |
| refinement method | full-matrix least-squares on F^2 (<i>SHELXL-97</i> ^c) |
| absorption correction method | Gaussian integration (face-indexed) |
| range of transmission factors | 0.6457–0.3096 |
| data/restraints/parameters | 13755 / 20 ^d / 963 |
| goodness-of-fit (S) ^e [all data] | 1.071 |
| final R indices ^f | |
| R_1 [$F_o^2 \geq 2\sigma(F_o^2)$] | 0.0645 |
| wR_2 [all data] | 0.1504 |
| largest difference peak and hole | 4.877 and -4.932 e Å ⁻³ |

^aObtained from least-squares refinement of 9886 reflections with $4.36^\circ < 2\theta < 51.62^\circ$.

^bPrograms for diffractometer operation, data collection, data reduction and absorption correction were those supplied by Bruker.

^cSheldrick, G. M. *Acta Crystallogr.* **2008**, *A64*, 112–122.

^dThe C–F and F \cdots F distances within the disordered CF₃ groups (centred by carbon atoms C58A, C58B and C87) of the anion were restrained to be 1.35(1) and 2.20(1) Å, respectively. Additionally, the C43A–C44A distance was restrained to be 1.50(1) Å.

^e $S = [\sum w(F_o^2 - F_c^2)^2 / (n - p)]^{1/2}$ (n = number of data; p = number of parameters varied; $w = [\sigma^2(F_o^2) + (0.0367P)^2 + 34.5136P]^{-1}$ where $P = [\text{Max}(F_o^2, 0) + 2F_c^2]/3$).

^f $R_1 = \sum ||F_o| - |F_c|| / \sum |F_o|$; $wR_2 = [\sum w(F_o^2 - F_c^2)^2 / \sum w(F_o^4)]^{1/2}$.

Appendix IV – Crystallographic Data

Structure reports, crystallographic information files (CIFs) and checkCIF reports for the structures discussed in Chapters 2 – 5 can be obtained free of charge by contacting either Dr. Robert McDonald or Dr. Michael Ferguson at the address below and quoting the internal reference number(s) for the appropriate compound(s) provided below:

X-Ray Crystallography Laboratory (Room E3-13)

Department of Chemistry, University of Alberta

11227 Saskatchewan Drive, NW

Edmonton, AB, Canada, T6G 2G2

Tel.: 1 780 492-2485 Fax.: 1 780 492-8231

E-mail: bob.mcdonald@ualberta.ca

michael.ferguson@ualberta.ca

Table A.16. Crystallographic identification codes.

| CHAPTER 2 | | CHAPTER 4 | |
|-----------------|-------------------------|-----------------|-------------------------|
| Compound Number | Internal Reference Code | Compound Number | Internal Reference Code |
| 3 | COW0840 | 26 | COW0226 |
| 5 | COW0933 | 29 | COW0414 |
| 13 | COW1001 | 36 | COW0237 |
| CHAPTER 3 | | 41 | COW1121 |
| Compound Number | Internal Reference Code | 43 | COW0404 |
| 14 | COW1027 | 47 | COW0513 |
| 16 | COW0801 | CHAPTER 5 | |
| 21 | COW1032 | Compound Number | Internal Reference Code |
| 22 | COW0219 | 58 | COW1111 |
| | | 63 | COW1108 |